COMPOSITE PULSES FOR NQR SPECTROSCOPY

A Thesis Submitted
In Partial Fulfilment of the Requirements
for the Degree of
DOCTOR OF PHILOSOPHY

by

A. RAMAMOORTHY

to the

DEPARTMENT OF CHEMISTRY
INDIAN INSTITUTE OF TECHNOLOGY KANPUR
AUGUST, 1989

Dedicated

to

My Parents

STATEMENT

I hereby declare that the work embodied in this thesis entitled, COMPOSITE PULSES FOR NQR SPECTROSCOPY, originally undertaken under the guidance of Professor P. T. Narasimhan, has been completed after his retirement under the supervision of Professor P. Raghunathan.

In keeping with scientific tradition, wherever work done by others has been utilized, due acknowledgement has been made.

A. Ramamoorthy
Candidate

CERTIFICATE I

Certified that the work presented in this thesis entitled, 'COMPOSITE PULSES FOR NQR SPECTROSCOPY' by Mr. A. Ramamoorthy, Department of Chemistry, I.I.T. Kanpur has been completed under my supervision and has not been submitted elsewhere for a degree.

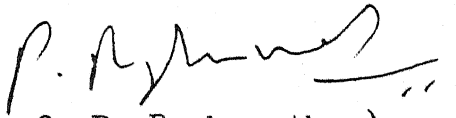

(Prof. P. Raghunathan)
Thesis Supervisor
Department of Chemistry,
I.I.T. Kanpur

Kanpur,
August 1989.

DEPARTMENT OF CHEMISTRY
INDIAN INSTITUTE OF TECHNOLOGY KANPUR, INDIA

CERTIFICATE II

This is to certify that Mr. A. Ramamoorthy has satisfactorily completed all the courses required for the Ph.D. degree programme. These courses include:

Chm 505	Principles of Organic Chemistry
Chm 521	Chemical Binding
Chm 524	Modern Physical Methods in Chemistry
Chm 525	Principles of Physical Chemistry
Chm 545	Principles of Inorganic Chemistry
Chm 626	Solid State Chemistry
Chm 634	Symmetry and Molecular Structure
Chm 800	General Seminar
Chm 801	Special Seminar
Chm 900	Ph.D. Thesis work

Mr. A. Ramamoorthy was admitted to the candidacy of the Ph.D. degree in August 1985, after he successfully completed the written and oral qualifying examinations.

P S Goel

(P. S. Goel)
Professor and Head,
Deptt. of Chemistry,
I.I.T., KANPUR

Javed Iqbal

(Javed Iqbal)
Convener,
Departmental Post-Graduate Committee,
Department of Chemistry,
I.I.T., KANPUR

ACKNOWLEDGEMENTS

I thank,

--- Prof. P. T. Narasimhan for his guidance,

--- Prof. P. Raghunathan for his guidance and constant encouragement,

--- Dr. N. Chandrakumar for his useful discussions on this thesis problem, kind help throughout the experimental work at CLRI, Madras and for his advise during the times of my trouble

--- Mr. Sankarapandi and Dr. Manoharan for their interest in my research work and friendship,

--- my colleagues Drs. Narsimha, Ravinder, and messrs Subbu, Anil, Siddharth, V. G. Ju, Ilango and Kasi for providing an ideal scientific atmosphere in the laboratory and their friendship,

--- Drs. S. Manogaran and V. Ravishakar for their interest in this work,

--- Chemical Physics Group, CLRI, Madras for their help during the experimental work,

--- my friends Messrs Devanand, Sampath, Baski, Pandimani, Mughambu, Victor, Ranjit, Yogi, Pandian, Immi, Usilai, Croco, Uday, Dey, Sanjay, Balki and Drs. Palaniappan, Praveen, Srini, Chiddu and other Hall fourites for making my stay at IIT a pleas one.

--- Mrs. Chandrakumar, Mrs. Visalakshi Vijayaraghavan and Messrs S. Sankarapandi, Params and Sattur (IIT-Madras) for their hospitality at Madras,

--- Mr. R. D. Singh for the efficient typing of the manuscript,

--- Messrs Bhausar, Umesh, Ram Singh and Ram Shankar for their help in the lab,

--- my parents for their unfailing love and encouragement.

A. Ramamoorthy

SYNOPSIS

Pure nuclear quadrupole resonance (NQR) spectroscopy of solids is generally characterised by broad lines with widths of the order of kilohertz, in contrast to high resolution nuclear magnetic resonance (NMR) spectroscopy where the line widths are of the order of a fraction of a hertz. This is mainly because the electric field gradient (efg) inhomogeneity and dipole-dipole interactions between the quadrupolar nucleus and other nuclear dipoles are not averaged out as in fluids. Dislocation, strains, presence of impurities, torsional motions of units in the crystal and fluctuations in the temperature cause a random distribution of the efg at the quadrupole nuclear site. Hence, there will be a distribution of quadrupole frequencies ($\Delta\omega_Q$) aroundthe central frequency (ω_Q) in NQR spectra. In some cases, the presence of chemically inequivalent sites leads to multiple lines in the NQR spectrum.

Uniform excitation of such broadband NQR spectra is not possible by means of a single radio frequency (rf) pulse of finite width and usually limited power. In addition to this, the presence of rf field inhomogeneity ($\Delta\omega_1$) results in poor NQR signal intensity. Similar problems have been overcome to a great extent in NMR spectroscopy using composite pulses. These are a cluster of rectangular rf pulses whose amplitude and phase are piecewise constant and are applied without any time delay between them. Composite pulses consisting of n rf pulses can be completely defined by 2n variables, namely, n flip angles and n rf phases.

This thesis deals with the construction of composite pulses for NQR spectroscopy. No previous reference on composite pulses for NQR spectroscopy exists in the literature.

Unlike in NMR, composite pulses consisting of a large number of rf pulses cannot be used in NQR because of the short quadrupolar, polar spin-spin relaxation times (T_2), which is of the order of milliseconds. Though it is possible, in principle, to design composite pulse sequences with arbitrary flip angles, in NQR two kinds of sequences are important. They are: (1) Composite $\pi/2$ pulse - for uniform excitation over a large range of $\Delta\omega_Q$ and/or $\Delta\omega_1$ with a net flip angle of 90°; $O(2)$. Composite pulses - these are of two kinds: (a) composite inversion or π pulses for uniform population inversion at thermal equilibrium condition and (b) composite refocussing pulse applied to refocus uniformly the transverse magnetization prepared from the thermal equilibrium condition by a 90° pulse, over a larger range of $\Delta\omega_Q$ and/or $\Delta\omega_1$ with a net flip angle 180°.

In the present work, we have examined the Magnus expansion approach in a manner similar to that of coherent averaging theory for designing composite pulses. In this approach, an m-th order composite pulse is defined as one which satisfies the condition $V^{(i)} = 0$; $0 \leq i \leq m$, where $V^{(i)}$ is the i-th-order term in the Magnus expansion. We have limited ourselves to zeroth-order sequences since higher-order sequences generally consist of a large number of rf pulses, which are not suitable for NQR. We have also explored the possibility of synthesizing composite $\pi/2$ pulses using the numerical approach with a view to enhance the NQR

signal intensity from powder specimens.

The thesis consists of seven chapters and five appendices. The first chapter is a brief introduction to NQR spectroscopy, where the possible role of composite pulses in NQR has also been outlined. The necessary quantum mechanical background for studying the spin dynamics in NQR spectroscopy is also presented in this chapter.

Chapter II considers various techniques that have been successful in deriving NMR composite pulse sequences with a view to assessing their suitability for NQR spectroscopy. One cannot use the geometrical approach in NQR since, unlike in NMR of $I = 1/2$ case, one cannot easily visualize the spin trajectories for spin $I \geq 1$ cases. A multidimensional search of a n flip angles and n rf phases defining an n-pulse sequence using a purely numerical analysis approach involves an enormous amount of computer time and hence is not recommended for NQR spectroscopy. Iterative schemes (recursive expansion, reversed nutation pulse and fixed-point methods) yield, in general, sequences with a large number of rf pulses. As pointed out earlier, T_2 values in NQR being shorter than in NMR, it is not desirable to construct larger duration sequences for NQR. Moreover, the mechanism by which composite pulses overcome the limitations of a single rf pulse is not clear with these procedures. The Magnus expansion approach for NMR composite pulses, proposed by Tycko (Phys. Rev. Lett. 51, 775 (1983)), has been adapted here for NQR because it has the following advantages: (1) it reduces the problem of finding composite pulses to that of solving a set of equation, (2) it treats the

composite pulse sequence entirely rather than a pulse-by-pulse analysis, and (3) it can be used for nuclei with any spin I value. A general theoretical procedure for constructing composite pulses using the Magnus expansion technique in the case of NQR spectroscopy is given in Chapter II.

Chapter III presents the design of NQR composite pulses for physically equivalent spin I = 1 nuclei in single crystals using the Magnus expansion approach to compensate for efg and rf field inhomogeneities. The fictitious spin-1/2 operator formalism of Vega and Pines (J. Chem. Phys. 66, 5624 (1977)) has been employed to carry out the spin dynamics calculations. A set of zeroth-order composite pulse sequences consisting of two and three rf pulses has been obtained to overcome efg and rf field inhomogeneities, and the performance of these composite pulses is demonstrated by computer simulations. If one limits oneself to phase-alternating rf pulses in the sequence then the procedure of deriving composite pulses using the Magnus expansion approach is simplified and such sequences are also easy to implement experimentally. A group of phase-alternating composite inversion π and $\pi/2$ pulse sequences, including the "symmetric" ones i.e., symmetric with respect to the centre rf pulse in the sequence, has been derived. Computer simulations show that all the sequences reported here perform much better than a single rf pulse to compensate for $\Delta\omega_Q$ and/or $\Delta\omega_1$. It has been demonstrated through the derivation of symmetric phase-alternating composite pulses that there exists a one-to-one correspondence between the spin I = 1/2 NMR case and pure NQR of spin I = 1 case. Results presented here are shown

to be independent of the asymmetry in efg.

Chapter IV is concerned with the generalization of the applicability of composite pulse sequences to an arbitrary spin I nucleus in NQR spectroscopy. It has been proved that the composite $\pi/2$ and π pulses derived using the Magnus expansion technique to compensate for $\Delta\omega_Q$ and/or $\Delta\omega_1$ for physically equivalent spin I = 3/2 nuclei in single crystals are identical with those of the sequences constructed for spin I = 1 nuclei. Here we have applied the irreducible spherical tensor operator formalism proposed by Bowden et al. (J. Magn. Reson. 67, 415 (1986)) for studying the spin dynamics.

Chapter V develops and exemplifies the procedure for calculating rf pulse responses in powders. A numerical approach has been employed to construct composite $\pi/2$ pulses for powders. Composite $\pi/2$ pulses thus derived have a great potential in NQR spectroscopy since a large number of samples investigated in practical NQR spectroscopy are in the powder form and the use of these sequences should result in better NQR signal intensity in comparison to intensities obtained using single rf pulses.

In Chapter VI, experimental verification of the performance of composite pulses derived using the Magnus expansion technique is presented. The performance of both composite π and $\pi/2$ pulses has been evaluated by measuring the ^{35}Cl NQR signal intensity as a function of resonance offset ($\Delta\omega_Q$) and flip angle errors at room temperature in samples of powdered $HgCl_2$, single crystalline and powder specimen of $NaClO_3$. Experimental results confirm that almost all the composite π pulses function much better than a single π

pulse in all the systems we have tested. But, somewhat surprisingly, the performance of composite $\pi/2$ pulses is markedly excellent in $HgCl_2$ powder, while not being effective in $NaClO_3$. Represanting each pulse of slip angle θ and phase ϕ as $(\theta)_\phi$, the sequence $(45)_{180}$-$(135)_0$ is recommended as a composite $\pi/2$ pulse while sequences $(90)_0$-$(270)_{90}$-$(90)_0$ and $(315)_0$-$(225)_{180}$-$(90)_0$ are recommended as composite π pulses for routine experimental work in NQR.

The last chapter of the thesis summarizes the present work and concludes with a brief outline of the scope for future work in the area of composite pulse NQR spectroscopy.

Appendix A presents the definition of fictitious spin-1/2 operators and their commutation relations, while Appendix B deals with irreducible spherical tensors for spin I = 3/2 case and their commutation relationships. The importances of interaction frames in magnetic resonance have been explained in Appendix C and Appendix D discusses the general rf pulse response evaluations in NQR spectroscopy. Appendix E contains details of the derivation of composite $\pi/2$ pulses for quadrupole echo without phase distortions in the case of NMR of spin I = 1 nuclei using the Magnus expansion method.

LIST OF SYMBOLS AND ABBREVIATIONS

$\mathcal{H}_Q$	Quadrupole Hamiltonian
$\mathcal{H}_{rf}$	RF Hamiltonian
$\mathcal{H}_z$	Zeeman Hamiltonian
V_1	EFG inhomogeneity Hamiltonian
V_2	RF field inhomogeneity Hamiltonian
ω_Q	Quadrupole frequency (Hz)
eQ	Electric Quadrupole moment
eq	Electric field gradient
η	Asymmetry parameter
ω_1	Strength of the rf field (rad sec^{-1})
γ	Gyromagnetic ratio
H_1	Amplitude of the rf field in Gauss
ω_D	Strength of the dipole-dipole interaction (rad sec^{-1})
J	Indirect spin-spin coupling parameter
ω_o	Larmor frequency (rad sec^{-1})
H_o	Strength of the Zeeman field (Gauss)
$\Delta\omega_Q$	Distribution of quadrupole frequencies or quadrupole resonance offset (Hz)
δq	Electric field gradient inhomogeneity
$\Delta\omega_o$	Larmor frequency offset (Hz)
$\Delta\omega_1$	Inhomogeneity in the rf field strength (rad sec^{-1})
$(\theta)_\phi$	RF pulse with a flip angle of θ and phase ϕ.
T_1	Spin lattice relaxation time
T_2	Spin-spin relaxation time
σ	Density matrix
ρ	Reduced density matrix

I	Spin angular momentum operator
I_x, I_y and I_z	Components of I
I_{pi} $(p = X,Y,Z;$ $(i = 1,2,3)$	Fictitious spin-1/2 operators
T_m^l	Irreducible spherical tensor operators with rank 1 and order m
$\mathbb{1}$	Unity matrix
$U(t)$	Time evolution operator or Liouville operator or Dyson expression
$[A,B] = AB-BA$	Commutator of A and B
$[A,B]_+ = AB+BA$	Anti-commutator of A and B
$A^\dagger$	Adjoint of A
A^{-1}	Inverse of A
$\|>$	Ket vector
$<\|$	Bra vector
$<\|\|>$	Matrix element
$\langle Q \rangle$	Expectation value of an operator Q
Tr	Trace
$\sim$	Tilde

AHT	Average Hamiltonian Theory
CW	Continuous Wave
EFG	Electric Field Gradient
FID	Free Induction Decay
FT	Fourier Transform
NMR	Nuclear Magnetic Resonance

NQR	Nuclear Quadrupole Resonance
PACPS	Phase Alternating Composite Pulse Sequence
QIF	Quadrupole Interaction Frame
QPAS	Quadrupole Principal Axis System
RF	Radio Frequency
RFPAS	Radio Frequency Principal Axis System

LIST OF FIGURES

List of Figures (contd.)

List of Figures (contd.)

LIST OF TABLES

List of Tables (contd.)

TABLE OF CONTENTS

Table of contents (contd.)

Tables of contents (contd.)

Table of contents (contd.)

CHAPTER I

INTRODUCTION

I.A Nuclear Quadrupole Resonance (NQR) Spectroscopy

I.A.1 Phenomenon and Detection

The interaction between the electric quadrupole moment, eQ, of a nucleus with spin $I \geq 1$ and eq, the electric field gradient (efg) surrounding it causes the splitting of energy levels even in the absence of magnetic field.[1*] This interaction, defined by the quadrupole Hamiltonian, $\mathcal{H}_Q$, is given by[1,2]

$$\mathcal{H}_Q = \frac{e^2qQ}{4I(2I-1)}\left[3I_z^2 - I^2 + \eta\,(I_x^2 - I_y^2)\right] \qquad .. \text{(I.1)}$$

in terms of the angular momentum operator I. η is the asymmetry parameter, defined as

$$\eta = \left|\frac{V_{xx} - V_{yy}}{V_{zz}}\right| \qquad .. \text{(I.2)}$$

V_{ii} are the components of efg tensor defined such that $|V_{zz}| \geq |V_{yy}| \geq |V_{xx}|$. Since the electric field surrounding the nucleus is produced only by charges external to the nucleus the

---

*References appear at the end of each chapter.

Laplace equation, given below, holds.

$$V_{xx} + V_{yy} + V_{zz} = 0 \qquad .. \text{(I.3)}$$

Thus η ranges from 0 to 1. If $\eta = 0$, then the efg is axially symmetric. The term e^2qQ in Eqn. (I.1), where $eq = V_{zz}$, is referred to as the nuclear quadrupole coupling constant.

In a representation where $\mathcal{H}_Q$ is diagonal and $\eta = 0$, the quadrupolar energy levels are expressed as[1]

$$E_m = \frac{e^2qQ}{4I(2I-1)} [3m^2 - I(I+1)] , \qquad .. \text{(I.4)}$$

where m is the z-component of the nuclear spin I. The energy levels are doubly degenerate in m except for the m = 0 energy level in the case of integral spins. The presence of η mixes states corresponding to $\Delta m = \pm 2$ and the m's are no longer 'good' quantum numbers. In addition, η lifts the degeneracy of $\pm m$ energy levels in the case of integral spins. For various values of the nuclear spin I, the secular equations and corresponding eigenvalues are available in the literature.[1,3,4] Transition between the energy levels established by $\mathcal{H}_Q$ can be produced by the application of an oscillating radio frequency (rf) field which interacts with the magnetic dipole moment of the nucleus. The NQR phenomenon has been observed by various techniques including continuous wave (CW) and pulsed Fourier Transform (FT) methods,[5,6] as in Nuclear Magnetic Resonance (NMR) spectroscopy. In this thesis, we shall be concerned with only pulsed NQR.

If one applies an rf pulse of a frequency ω_Q, to the system under study for a short time, t_w, (known as rf pulse width), with an rf field strength $\omega_1 = \gamma H_1$ (rad/sec) (where γ = gyromagnetic ratio; H_1 = rf field amplitude in Gauss) and detects the following NQR signal in time domain, the observed response of the system decays with a time constant (T_2) known as spin-spin relaxation time. This response is called Free Induction Decay (FID). By Fourier -transforming this FID, one gets the NQR signal in the frequency domain.[6] Generally broad (line width of the order of kiloHertz) and multiple lines are observed in the NQR spectrum because of various internal interactions present in the system.[1] Hence, using a single rf pulse with finite power, it is not possible to excite these broad spectra uniformly. Exactly with this problem in view, we have undertaken the task of constructing broadband excitation rf pulse sequences for NQR spectroscopy in zero dc magnetic field, which forms the bulk of the subject matter contained in this Thesis.

For a better understanding of the problem we present, in Section I.A.2, various line broadening mechanisms which characterize NQR spectroscopy. The need for broadband excitation in NQR will also be illustrated in Section I.B. A powerful theoretical tool for studying the pulsed response of quadrupolar systems is the density matrix approach, and we present the background for such spin dynamics calculations in Section I.C. Finally, this chapter ends with an outline of the present thesis in Section I.D.

I.A.2 Line Broadening Effects in NQR

In pure NQR spectroscopy (i.e., zero applied magnetic field), line broadening originates from two main sources; these are the (i) electric and (ii) magnetic interactions present in the solid material. In this section, a brief discussion of these interactions is given.

I.A.2(i) Electrical Sources of Line Broadening

NQR frequency corresponding to the coherence between any two energy levels in a spin I quadrupole nucleus is given by $\omega_Q \alpha e^2qQ$,[1] where q is the efg component. Effects which cause a change in efg-s of quadrupole nuclei lead to a distribution of NQR frequencies $(\omega_Q \pm \Delta\omega_Q)$. For example, strains and dislocations in the crystal or in powder grains create a random distortion of intermolecular interactions and a corresponding random distribution of efg is evidenced at quadrupole nuclear sites. Strains which result from the crystal growth process[7-9] and the presence of impurities in the crystal lattice[1,10] have been found to broaden NQR lines. In NQR literature, the effects of molecular motion upon quadrupole frequencies have been studied.[1] There are two kinds of molecular motions, namely, torsional and the hindered rotational motions of the molecule about some axes in the crystal.[1] Baeyer[11] has shown that torsional motions of units constituting the crystal lattice lead to (a) a shift in the resonance frequency, due to fluctuations in efg and (b) a change in the relaxation process affecting quadrupole resonance. Both

of these are, of course, temperature dependent. As such, NQR frequencies are highly sensitive to changes in temperature which affects the random motions of units in the crystal lattice.[12] Generally, the temperature coefficient of the NQR frequency, $\frac{d\omega_Q}{dT}$, is negative. This effect has been explored in the construction of NQR thermometers which can measure temperatures accurately.[12,13] Overall, these abovementioned effects are responsible for experimentally observed line widths (often they are of the order of a few kiloHertz to a few megaHertz). This means that the spin-spin relaxation time T_2 and spin-lattice relaxation time, T_1 (which play very important roles in determining NQR line widths), are much shorter.[1]

Apart from the inhomogeneous broadening[14] of NQR lines, electrical interactions create multiple spectral lines in an NQR spectrum.[8,15-17] Often, the presence of chemically inequivalent sites[1] in the crystal specimen leads to multiple lines in the pure quadrupole resonance spectrum itself. Here, two or more quadrupole nuclei with spin $I \geqslant 1$ are said to be chemically inequivalent when they have different chemical environments or different efg-s in the crystal lattice. Two chemically inequivalent sites cannot be related by any kind of symmetry operation. Chemical inequivalence may arise due to the occupation of atoms with quadrupole nuclei, at chemically different environments in the free molecule itself or it may also originate even in cases where the atoms are in equivalent positions in the free molecule but the interactions between neighbouring molecule in the solid destroy

their equivalence.[1] The splittings produced by the presence of chemically inequivalent atoms in the free molecule are much larger than those produced in the latter case, because of the comparative weakness of intermolecular forces relative to that of the forces that exist inside the molecule. In NQR literature, multiple lines for a given quadrupolar nuclear species have been observed in many systems and has been attributed to chemical inequivalence.[16,17] For example, at 77 K, sixteen lines have been detected in the ^{35}Cl NQR spectrum of solid CCl_4 with a spectral width of $\sim$350 kHz.[8]

I.A.2(ii) Magnetic Interactions

There are two kinds of magnetic interactions between a resonant nucleus and other non-resonant nuclei of the same or different species.[17] They are, namely, (a) direct magnetic dipole-dipole interactions, and (b) indirect spin-spin interaction, also called J-coupling.[1,19] The spin-spin coupling is usually much smaller than the dipole-dipole interaction and is not of interest to us in the present work. Hence we consider only the dipole-dipole interaction here.

(a) Dipole-dipole interactions: Dipole-dipole interaction is the interaction between the magnetic moment of a resonant nucleus with the dipolar field due to the magnetic moments of all other spins in a rigid lattice. This depends on the magnitude, orientations of the magnetic moments and also the lengths and orientations of the vectors describing their relative positions. When the quadrupole nucleus has one very close neighbour, then the dipolar interaction with it predominates over that of distant neighbours and

fine splitting may be observed in NQR spectrum, similar to the 'Pake doublet' in NMR.[20] Slow beats in the spin echo envelope have been observed in solid N_2,[22] because of the intramolecular dipolar interactions. In the chlorine NQR spectrum of solid chlorine ($\eta \neq 0$),[21] due to ^{35}Cl-^{35}Cl and ^{37}Cl-^{37}Cl homonuclear dipolar interaction a doublet has been detected. Heteronuclear dipole-dipole interaction has been observed by Mackowiak and Brookeman[22] for HCl as fine splittings in the ^{35}Cl quadrupole line. Other typical examples may also be found in the NQR literature.[23]

I.B Necessity for Broadband Excitation in NQR

As pointed out in the previous section, NQR spectral lines are inherently broad and the presence of multiple lines leads to a broadband NQR frequency spectrum. Usually, in FT NQR, a single rf pulse with a constant frequency and power is used to excite the whole wide spread spin populations so as to obtain the entire NQR frequency spectrum.[6] However, it is often not possible to excite the broadband NQR spectrum uniformly by a single rf pulse. Spins which are off-resonant with respect to the rf pulse frequency are poorly excited and hence their resultant signal intensity will be poor. This problem can be partly overcome by applying high rf power. But, because of difficulties in the experimental technique, the production of high power rf pulses is limited.

In addition to this, the response of a single rf pulse is highly sensitive to rf field inhomogeneity ($\Delta\omega_1$) across the NQR

sample placed in an rf coil. Because of this $\omega_1 \pm \Delta\omega_1$ distribution in the system, spins in different parts of the sample feel different flip angles ($\theta \pm \Delta\theta$) which are directly proportional to the strength and time duration of an applied rf pulse. Thus, the observed signal intensity is poor and, in powder specimens particularly, it is difficult to find out the exact $\pi/2$ and π rf pulse time durations in an experiment. So it is essential to find a suitable replacement for single rf pulse in FT NQR experiments. Somewhat similar problems, such as resonance offset and rf field inhomogeneity, have been overcome by the use of 'composite pulses'[24] instead of single rf pulses in NMR spectroscopy. A 'composite pulse' is a sequence of phase shifted, constant amplitude rectangular rf pulses, without any time delay between them, to excite the spin populations over a larger range of some experimental parameters compared to a single rf pulse. To the best of our knowledge, no attempt has so far been made in the realm of NQR spectroscopy to design 'composite pulses'. Therefore, a programme of designing composite pulses that compensate for efg inhomogeneity or resonance offset ($\Delta\omega_Q$) and rf field inhomogeneity ($\Delta\omega_1$) in NQR spectroscopy seems worthwhile. To construct such rf pulse sequences different routes[24] have been analysed from the NQR point of view. These will be presented in Chapter II of this thesis.

As a convenient background for understanding the theoretical procedures involved in this work, we present the spin dynamics studies using the density matrix approach in the next section.

I.C Spin Dynamics Studies

I.C.1 A Brief Survey of Theoretical Procedures Employed in NQR Spectroscopy for Spin Dynamics Studies

In this subsection, we briefly survey the different procedures used in NQR literature to follow the time evolution of the spin system. In 1955, Bloom et al.[25] used the time dependent perturbation theory to evaluate the state of the spin system in the presence and absence of rf pulses. Later, Das et al.[26] developed the density matrix mathod for calculating the FID and spin echo signal for a general spin I in the case of single crystals. Pratt et al. have investigated the response of a spin 3/2 system in NQR to (i) a long off-resonant rf pulse[27] and (ii) two-pulse sequence.[28] In these cases, the response of the quadrupolar nucleus has been proved to be similar to that of spin 1/2 nuclei in NMR experiments. In 1977, Pratt[29] has introduced an interaction representation approach to analyse the Slichter-Holton and Lee-Goldburg pulse sequences in spin 3/2 NQR spectroscopy. A common difficulty with these methods is in obtaining complete solutions for differential equations at different times. Using these methods one cannot explain the experimental results of many newer pulse techniques in NQR. Furthermore, it is not necessary to consider the entire form of the density matrix. This problem can be simplified by defining the density matrix of a system containing spin I nuclei in terms of properly selected $(2I+1)^2-1$ traceless independent Hermitian operators. Such a set of operators, which give rise to the very useful 'fictitious spin-1/2' operator formalism,[30] has been proposed by

Vega and Pines[31] for the use of multiple quantum studies in spin I = 1, NMR spectroscopy. This has been effectively used later in spin 1 NQR spectroscopy to study the Overhauser effect by Vega[32] and also for analysing the effect of various pulse sequences.[33] Provotorov et al.[34] have used this formalism along with the procedure of canonical transformation to analyse the line narrowing effect of multiple pulse sequences in NQR spectroscopy. Due to the simple commutation relationship of these operators, we have adapted this formalism in our procedure for designing composite pulses for application to spin 1 cases.[35] A detailed description of the fictitious spin-1/2 formalism is presented in Appendix A of this thesis. This formalism has been generalised in recent years for higher spin cases by Vega[36] and Wokaun and Ernst[37] independently. A generalised version of this formalism has been applied for studying the behaviour of multiple pulse sequences in spin 3/2 case.[38] Projection operators have been employed in a theoretical study of multiple pulse sequences in NQR spectroscopy.[39] Recently, Singh and Armstrong have employed SU(3) group generators for investigation of the zero-time resolution technique[40] and Jeener-Broekart pulse sequence[41] in spin 3/2 NQR spectroscopy. Irreducible spherical tensor operators[42] have been used by Sanctuary et al. to solve the Liouville equation directly for the cases of I = 1, 3/2 and 5/2 [4] and to study the selective excitation in pulsed NQR spectroscopy.[43] Somewhat similar approach has been used in a theoretical argument questioning the existence of the phenomenon 'quadrupole precession' in spin I = 1 and 3/2 cases[44] in the absence of Zeeman field.

A modified version of spherical tensors, proposed by Bowden and Hutchison,[45] has been used for multiple quantum NQR studies in I = 5/2 case.[46] Since spherical tensors form a complete basis set and their commutation relations are well established, we have employed them in the procedure for constructing composite pulses for spin 3/2 case in this thesis. In Appendix B, we have presented an introduction to irreducible spherical tensors, their commutation relationships and their matrix representations. Since the present work employs the density matrix method, it is felt that a brief discussion about this method is essential, and this has been done in the following section.

I.C.2 Density Matrix Method

I.C.2(i) Density Matrix

We consider a multilevel spin system with a complete set of eigen states $|\phi_k\rangle$. The state of the system can be written as $|\psi\rangle = \Sigma_k c_k |\phi_k\rangle$. A mixture of independently prepared states $|\psi_n\rangle$ (n = 1,2,...) with statistical weights w_n can be completely described by an operator, σ, as

$$\sigma = \sum_n w_n |\psi_n\rangle\langle\psi_n| \qquad .. (I.5)$$

The operator σ is generally called the 'density matrix' or 'statistical operator'.[47] σ may also be viewed as a vector in Liouville space.[48] σ is Hermitian, that is, $\langle\phi_i|\sigma|\phi_j\rangle = \langle\phi_j|\sigma|\phi_i\rangle^*$. The diagonal element ($\sigma_{mm}$) of the density matrix corresponds to the probability of finding the system in the state

$|\phi_m\rangle$. Trace of σ, $Tr(\sigma)$, is equal to 1, showing that it is independent of the choice of the representation. The main advantage of using the density operator is that all information on the behaviour of a given system can be expressed in terms of expectation values of suitably chosen operators. For example, the expectation value of any operator Q is given by

$$\langle Q \rangle = Tr(\sigma Q) \qquad .. (I.6)$$

This approach has been introduced by Fano in 1957.[49] Since then, it has been effectively used for the spin dynamics studies in magnetic resonance.[50-52]

Thermal equilibrium density matrix, $\sigma(0)$, can be given according to the Boltzmann distribution of populations among the energy levels. In our case, an ensemble of quadrupole nuclei with spin $I \geq 1$ in the absence of a magnetic field can be defined as

$$\sigma(0) = \exp\left(\frac{-\mathcal{H}_Q}{kT}\right)\left\{Tr[\exp(-\mathcal{H}_Q/kT)]\right\}^{-1} \qquad .. (I.7)$$

Using the high temperature approximation,[50] we write

$$\sigma(0) \approx [Tr(\mathbb{1})]^{-1}\,(1 - \mathcal{H}_Q/kT) \qquad .. (I.8)$$

where $\mathcal{H}_Q$ is the quadrupole Hamiltonian given by Eqn. (I.1), k is the Boltzmann constant and T is the temperature. Off-diagonal elements of $\sigma(0)$ can be taken to be zero according to the random

phase approximation.[53] The first term in Eqn. (I.8) is unaffected by an evolution of the system, so we need to follow only the evolution of the second term. For simplicity, we write

$$\sigma(0) \approx [\mathrm{Tr}(\mathbb{1})]^{-1} \left[1 - \frac{\rho(0)}{kT}\right] \qquad .. \text{(I.9)}$$

where $\rho(0)$ is the reduced thermal equilibrium density matrix defined as

$$\rho(0) = \mathcal{H}_Q \qquad .. \text{(I.10)}$$

I.C.2(ii) Time Evolution of the Spin System

The time development of the spin system under various interactions defined by the Hamiltonian, $\mathcal{H}$, can be studied using the equation of motion of the density matrix, written as

$$\frac{i\, d\rho(t)}{dt} = [\mathcal{H}, \rho(t)] \qquad .. \text{(I.11)}$$

This can be derived from the time dependent Schrödinger equation in the Hilbert space.[47] This differential equation is often called the von Neumann equation or Liouville equation (because it assumes the same form as the equation of motion for the phase space probability distribution in classical mechanics).[48] The solution of Liouville-von Neumann equation is given as

$$\rho(t) = U(t)\, \rho(0)\, U(t)^{-1} \qquad .. \text{(I.12)}$$

$$\text{where } U(t) = T \exp\left[-i \int_0^t \mathcal{H}(t')\, dt'\right] \qquad .. \text{(I.13)}$$

is called the Liouville operator or Dyson expression[47] or the time evolution operator corresponding to the interactions given by $\mathcal{H}$. T is the Dyson time-ordering operator, which orders operators of longer time arguments in the expanded exponential to the left. For example,

$$T\left\{\mathcal{H}(t')\,\mathcal{H}(t'')\right\} = \begin{cases} \mathcal{H}(t')\,\mathcal{H}(t'') & \text{if } t' > t'' \\ \mathcal{H}(t'')\,\mathcal{H}(t') & \text{if } t'' > t' \end{cases} \qquad .. \text{ (I.14)}$$

During such an evolution of the density matrix:
(a) the eigen values of the density matrix are time independent;
(b) the diagonal elements of the density matrix will not change with time and (c) its off-diagonal elements, which correspond to the coherence between different energy levels, oscillate with time.

In magnetic resonance, the time evolution of spin population can be thought of as rotations of spin vectors in a $(2I + 1)$ dimensional space. Commonly, exponential operators are used to explain such time evolution and their properties are as follows:[54]

(a) Evolution operator $U(t)$ unitary, i.e., $UU^{\dagger} = \mathbb{1}$ .. (I.15)

(b) $e^{A} = 1 + A + \frac{A^2}{2!} + \frac{A^3}{3!} + \ldots$ .. (I.16)

(c) $e^{A}\, e^{B} = e^{A+B} = e^{B}\, e^{A}$ if and only if $[A,B] = 0$ .. (I.17)

where A and B must be anti-Hermition so that e^{A} and e^{B} will be unitary.

(d) Baker-Campbell-Hausdorff (BCH)[55] formula to second order is given for $[A,B] \neq 0$ case as

$$e^{A}\, e^{B} = \exp\Big\{ A + B + 1/2\,(A+B) + 1/12\,[A,(A+B)] + 1/12\,[[A,B],B] + \ldots \Big\} \quad .. \text{(I.18)}$$

Using the BCH formula, one can write,

$$e^{iA\alpha}\, B\, e^{-iA\alpha} = B, \text{ if } [A,B] = 0 \quad .. \text{(I.19)}$$

This explains the constant of motion of B under the effect of A and

$$e^{iA\alpha}\, B\, e^{-iA\alpha} = B\cos(\alpha) - C\sin(\alpha), \text{ if } [A,B] = iC; \text{ cyclic} \ldots \text{(I.20)}$$

One may also independently derive the above result using the following nested commutation relationship[56]

$$e^{iA\alpha}\, B\, e^{-iA\alpha} = B + i\alpha\,[A,B] + \frac{(i\alpha)^2}{2!}[A,[A,B]] + \frac{(i\alpha)^3}{3!}[A,[A,[A,B]]] + \ldots \quad .. \text{(I.21)}$$

In some cases, evaluating such a time evolution becomes a difficult task. For this purpose, computer programs have been developed in NMR literature for the automatic generation of the commutator algebra.[57] However, in solving time dependent equation of motion, one has to make approximations to get time independent solutions. In the next subsection, we review the different strategies that have been used in magnetic resonance for studying time dependent perturbations.

I.C.3 Methods for Solving Time dependent von Neumann Equation

Evolution of the spin systems under the effect of a time dependent Hamiltonian can be brought out by

$$\frac{i\, d\rho(t)}{dt} = [\mathcal{H}(t), \rho(t)] \qquad .. \text{(I.22)}$$

In magnetic resonance, the applied rf radiation is time dependent and in some cases we often make the line broadening interactions time dependent by transfering into a suitable interaction frame. For example, in average Hamiltonian theory (AHT)[51,52] which is used to explain the multiple pulse effects, one uses the rf interaction frame to induce a time dependence on the internal interactions called $\mathcal{H}_{int}(t)$ and it is time-averaged out to achieve line narrowed spectrum. Similar is the case with the construction of composite pulses.[58] In general, however, an exact solution of Eqn. (I.22) is not possible. Often, the interaction $\mathcal{H}(t)$ is a small perturbation and Eqn. (I.22) can be solved by approximation. Some of the methods applied in the literature are presented below.

I.C.3(i) Time dependent Perturbation Theory

In this theory, one gets an iterated solution given by[47]

$$U(t) = 1 - \frac{i}{\hbar} \int_0^t dt_1\, \mathcal{H}(t_1) + \left(\frac{i}{\hbar}\right)^2 \int_0^t dt_1 \int_0^{t_1} dt_2\, \mathcal{H}(t_1)\, \mathcal{H}(t_2) + \ldots \qquad .. \text{(I.23)}$$

The disadvantage with this solution is that it is not unitary.

But in magnetic resonance, unitary operators in the exponential form are needed because they do not change tr(ρ) and they correspond to rotations in a (2I+1) dimensional space for spin I case. Moreover, this solution is expected to be accurate only for small $\mathcal{H}(t)$.

I.C.3(ii) Magnus Expansion Approximation

In 1954, Magnus[59] solved the time dependent differential equation with a procedure which is essentially a rearrangement of the perturbation series. In this procedure, the major assumption is that $\mathcal{H}(t)$ is constant in smaller intervals of time t_1, t_2, ... t_n with $t = t_1 + t_2 + \ldots + t_n$. $\mathcal{H}(t)$ is expanded to an infinite series as

$$\mathcal{H}(t) = \mathcal{H}^{(0)} + \mathcal{H}^{(1)} + \mathcal{H}^{(2)} + \ldots \mathcal{H}^{(n)} + \ldots \quad .. \text{(I.24)}$$

where $\mathcal{H}^{(n)}$ is the nth-order term in the series. The zeroth- and first-order terms are expressed as[47]

$$\mathcal{H}^{(0)} = \frac{1}{t} \int_0^t \mathcal{H}(t')\, dt' \quad .. \text{(I.25)}$$

and $$\mathcal{H}^{(1)} = \frac{-i}{2t} \int_0^t dt_2 \int_0^{t_2} dt_1 [\mathcal{H}(t_2), \mathcal{H}(t_1)] \quad .. \text{(I.26)}$$

Similarly, an nth-order term is given by (n+1) integrals with n commutators of $\mathcal{H}(t)$. Here, each term is a Hermitian operator and the infinite series can be limited to any order so as to get a unitary solution. In this series, $\mathcal{H}^{(0)}$ is the main term and other higher order terms are quantum corrections to the classical

solution $\mathcal{H}^{(0)}$. Hamiltonians corresponding to different time intervals do not commute with each other. As Magnus has pointed out,[59] the Magnus formula is the extention of BCH formula,[55] which is for $\mathcal{H}(t)$ with only two different time intervals. The exponential solutions for a time dependent differential equation has been also derived independently by Robinson in 1963[60] and by Pechukas and Light in 1965.[61]

Magnus expansion has been effectively used to synthesize multiple pulse[51,52] and composite pulse[58] sequences. Warren and Zewail[62] have extended these techniques into the optical region. Cady[63] has used it in the theory of spectral line broadening and Sheck et al.[64] have applied Magnus expansion in the theory of multiphoton absorption. Cross[65] used it in his formulation of scattering theory, while Saxon and Light[66] have applied it in the treatment of various problems in molecular scattering and energy transfer. It has even been used in the formulation of the Born-Oppenheimer approximation.[67] It suffices to say here that the present literature is extensive on the applications of the Magnus expansion technique. However, several groups have reported that the application of the Magnus expansion in the Schrödinger representation to explain the observed experimental results was less than satisfactory.[68-70] The reason for this could be due to the possible errors in the forms of the Magnus expansion terms used. It may be mentioned here that there exists a number of derivations of the Magnus expansion terms[60,61] and there are variations in the resulting definitions of different order terms between authors. Later, in 1985, Salzman[71] developed an

alternative to the Magnus expansion and he notes that it is easier to use than the original Magnus expansion itself. His procedure leads to a straightforward derivation of unique higher-order Magnus expansion terms. Salzman concludes that the problems with Magnus expansion more likely arise from a lack of the convergence of the series.

Magnus expansion approach has been successful in predicting the behaviour of the spin system at relatively short times; however, because of the convergence problem which is called as 'Magnus paradox',[68] it fails to account properly for the long time behaviour.[70,72] This is the case regarding its use in the analysis of multiple pulse spin-locking experiments[70] on dipole-coupled many-body spin systems. In the literature, the convergence of Magnus expansion for a two-level case has been studied in detail and even the radius of convergence has been extended considerably.[72] The criterion proposed as a lower limit to the convergence radius of the Magnus series is given by

$$\int_0^{\tau} |\omega(t)|\, dt < 2\pi \qquad .. \text{(I.27)}$$

where $\pm\omega(t)/2$ are the time-dependent eigen values of the Hamiltonian $\mathcal{H}(t)$.

Furthermore, the equilibrium properties of the system can not be determined in the Magnus expansion procedure by statistical mechanical techniques analogous to those for time independent systems. In AHT[51,52] based on the use of Magnus expansion,

the observation of the system are possible only at the end of a cycle ($U_{rf}(t_c) = \pm \mathbb{1}$), where the rf interaction frame and the observation frame coincide. These problems have been to some extent overcome by the application of Krylov, Bogolijubov and Mitropolskij approach (KBM)[73] and Floquet theory[74] which are suitable alternatives to the Magnus expansion. KBM averaging method has been used to observe theoretically the slow motion evolution of the spin density matrix during the applied multiple pulse sequences.[75] Using the Floquet theory, Maricq[76,77] analysed pulsed spin-locking phenomenon resulting with the application of multiple pulse sequences in magnetic resonance. Equilibrium properties of a model time dependent Hamiltonian in an interaction reference frame have been extensively studied with the help of Floquet theorem.[76] For further details about spin dynamics in magnetic resonance, one is referred to the literature.[51,52,56,78]

It should be mentioned here that, as far as the construction of composite pulses is concerned, the use of Magnus expansion approximation is the suitable one and this has been completely successful in NMR spectroscopy.[24,58] In this thesis, we have applied the Magnus expansion technique, for designing composite pulses suitable to NQR spectroscopy, and this has been detailed in Chapter II.

I.D Scope of the Present Work

Uniform excitation of broad quadrupole frequency spectrum in zero dc magnetic field is necessary (i) to improve the NQR signal intensity and (ii) while searching for chemically

inequivalent sites present in the crystal system by observing the multiple lines of NQR spectrum. This would be of greater importance in investigating high temperature superconductivity materials whose NQR line widths are of the order of a few MHz.[79] It will be also useful in improving the T_1 and T_2 measurements with better inversion and refocussing of spin populations over wider ranges of $\Delta\omega_Q$ in spin inversion recovery and spin echo methods, respectively. Similarly, excitation over a larger range of $\Delta\omega_1$ would compensate for flip angle errors of rf pulses employed in pulsed techniques of NQR. For this purpose, in the present work, we propose composite π and $\pi/2$ pulses for the replacement of single rf pulses in compensating efg and rf field inhomogeneities in NQR spectroscopy.

In Chapter II, various routes used in NMR spectroscopy for designing composite pulses have been analyzed from the NQR point of view and a general theoretical procedure based on the Magnus approximation is given for NQR of spin I nuclei.

Chapter III deals with the design of composite pulses using the Magnus approach for spin I = 1 nuclei. Fictitious spin-1/2 operator formalism is employed for the spin dynamics calculations. In Chapter IV, this procedure is extended for a general spin I nucleus by applying spherical tensors. Composite $\pi/2$ pulses that can enhance the NQR signal intensity in polycrystalline samples have been designed using a purely numerical approach in Chapter V. Experimental verification of composite pulses designed using the Magnus expansion method, on powder specimens of sodium chlorate ($NaClO_3$) and mercuric chloride ($HgCl_2$) have been presented in Chapter VI.

In the last chapter of the thesis important conclusions and points for further work in this area of research have been given. Five Appendices have been included to clarify some aspects of the present work.

Summary

In this chapter, a brief introduction to the phenomenon of NQR and its detection as well as a discussion of various line broadening mechanisms in NQR have been given. However, no attempt has been made to cover the full literature of NQR spectroscopy. The need for designing composite pulses to overcome resonance offset and rf field inhomogeneity problems in NQR has been emphasized. This chapter also presents an introduction to the density matrix approach to the study of spin dynamics in NQR spectroscopy. The density matrix approach is of great value in understanding magnetic resonance phenomena in general and NQR spectroscopy, in particular. In this context, the Magnus expansion approach to the solution of time dependent problems has been critically examined.

REFERENCES

1. T. P. Das and E. L. Hahn, 'Nuclear Quadrupole Resonance Spectroscopy,' Academic Press, New York (1958).
2. A. Abragam, 'Principles of Nuclear Magnetism,' Oxford University Press, Oxford (1961), Chapter VII.
3. (a) R. Bersohn, J. Chem. Phys. 20, 1505 (1952).
   (b) C. Dean, Phys. Rev. 96, 1053 (1954).
   (c) R. B. Creel, H. R. Brooker and R. G. Barnes, J. Magn. Reson. 41, 146 (1980);
   R. B. Creel, J. Magn. Reson. 52, 515 (1983);
   R. B. Creel and D. A. Drabold, J. Molec. Struct. 111, 85 (1983).
   (d) Y. Morino and M. Toyama, J. Chem. Phys. 35, 1289 (1961).
   (e) M. H.Cohen, Phys. Rev. 96, 1278 (1954).
   (f) G. M. Muha, J. Magn. Reson. 53, 85 (1983).
4. M. S. Krishnan and B. C. Sanctuary, Z. Naturforsch. 41a, 353 (1986).
5. T. P. Das and A. K. Saha, 'Theory and Applications of Nuclear Induction,' Saha Institute of Nuclear Physics, Calcutta, India (1957).
6. Ref. 1, Chapter II.
7. G. D. Watkins and R. V. Pound, Phys. Rev. 85, 1062 (1951).
8. R. Livingston, J. Phys. Chem. 57, 496 (1953).
9. T. C. Wang, Phys. Rev. 99, 566 (1955).
10. Y. Imaeda, J. Sci. Hiroshima Univ. Ser. A 24, 239 (1960); H. Vargas, A. Chappe, J. Pelzl and D. Dautreppe, J. Phys. Chem. Solids 3, 2021 (1973).
11. H. Baeyer, Z. Physik 130, 227 (1951).

12. D. Nakamura, R. Ikeda and M. Kubo, Coord. Chem. Rev. 17, 281 (1975).

13. (a) D. B. Utton and J. B. Vannier, Instrum. Technol. 23, 47 (1976).
(b) A. Ohte and I. Iwakawa, IEEE Trans. Instrum. Measu. IM25, 357 (1976).

14. J. D. Macomber, 'The Dynamics of Spectroscopic Transitions,' John Wiley and Sons, New York (1976), Chapter 6 (Homogeneous and inhomogeneous line broadenings are clearly explained).

15. E. A. C. Lucken, 'Nuclear Quadrupole Coupling Constants,' Academic Press, New York (1969).

16. G. K. Semin, T. A. Babushkina and G. G. Yakobson, 'Nuclear Quadrupole Resonance in Chemistry,' John Wiley, New York (1975).

17. L. Ramakrishnan, S. Soundararajan, V. S. S. Sastry and J. Ramakrishna, Coord. Chem. Rev. 22, 123 (1977).

18. G. E. Pake, 'Nuclear Magnetic Resonance,' Solid State Physics, Academic Press, New York (1956), Vol. 2, p. 24.

19. N. E. Ainbinder and I. G. Shaposhnikov, in 'Advances in Nuclear Quadrupole Resonance,' Vol. 3, Ed. J. A. S. Smith, Heyden and Son, London (1978), p. 101.

20. J. R. Brookeman, P. C. Canepa and A. S. De Reggi, Phys. Lett. 39A, 415 (1972).

21. A. A. V. Gibson, J. R. Brookeman and T. A. Scott, Phys. Lett. 50A, 31 (1974).

22. M. Mackowiak and J. R. Brookeman, Acta. Phys. Pol. 52A, 281 (1977).

23. I. J. F. Poplett, in 'Advances in Nuclear Quadrupole Resonance,' Vol. 4, Ed. J. A. S. Smith, Heydon and Son, London, (1980), p. 115.

24. M. H. Levitt, Prog. NMR Spectrosc. 18, 61 (1986) and references cited therein.

25. M. Bloom, E. L. Hahn and B. Herzog, Phys. Rev. 97, 1699 (1955).

26. T. P. Das, A. K. Saha and D. K. Roy, Proc. Roy. Soc. (London) 227A, 407 (1955);
T. P. Das and A. K. Saha, Phys. Rev. 98, 516 (1955);
Ref. 5, Chapter VI,

27. J. C. Pratt, P. Raghunathan and C. A. McDowell, J. Chem. Phys. 61, 1016 (1974).

28. J. C. Pratt, P. Raghunathan and C. A. McDowell, J. Magn. Reson. 20, 313 (1975).

29. J. C. Pratt, Mol. Phys. 34, 539 (1977).

30. Ref. 2, Chapter II.

31. S. Vega and A. Pines, J. Chem. Phys. 66, 5624 (1977).

32. S. Vega, J. Chem. Phys. 63, 3769 (1975).

33.(a)R. S. Cantor and J. S. Waugh, J. Chem. Phys. 73, 1054 (1980).
(b)D. Ya. Osokin, Phys. Stat. Sol. 102(b), 681 (1980);
D. Ya. Osokin, Phys. Stat. Sol. 109(b), K7 (1982);
D. Ya. Osokin, J. Molec. Struct. 83, 343 (1982);
V. L. Ermakov and D. Ya. Osokin, Mol. Phys. 53, 1335 (1984).

34. B. N. Provotorov and A. K. Khitrin, JETP Lett. 34, 157 (1981);
A. K. Hitrin, G. E. Karnaukh and B. N. Provotorov, J. Mol. Struct. 83, 269 (1982);
G.E. Karnaukh, B. N. Provotorov and A. K. Khitrin, Sov. Phys. JETP 57, 93 (1983).

35. A. Ramamoorthy and P. T. Narasimhan, J. Molec. Struct. 192, 333 (1989).

36. S. Vega, J. Chem. Phys. 68, 5518 (1978).

37. A. Wokaun and R. R. Ernst, J. Chem. Phys. 67, 1752 (1977).

38. A. K. Dubey and P. T. Narasimhan, J. Molec. Struct. 192, 321 (1989).

39. O. S. Zueva and A. R. Kessel, Sov. Phys. Solid State 19, 408 (1977);
O. S. Zueva and A. R. Kessel, Sov. Phys. JETP 46, 1136 (1977);
A. Kessel and O. Zueva, Physica 90B, 205 (1977);
A. R. Kessel and O. S. Zueva, Phys. Lett. 68A, 347 (1978);
O. S. Zueva and A. R. Kessel, Sov. Phys. Solid State, 21, 2032 (1979);
O. S. Zueva and A. R. Kessel, J. Molec. Struct. 83, 383 (1982);
O. S. Zueva, J. Molec. Struct. 83, 379 (1982).

40. M. A. Singh and R. L. Armstrong, J. Magn. Reson. 78, 538 (1988).

41. M. A. Singh and R. L. Armstrong, Phys. Rev. 38B, 50 (1988).

42. (a) U. Fano and G. Racah, 'Irreducible Tensorial Sets,' Academic Press, New York (1959).
(b) H. A. Buckmaster, Can. J. Phys. 40, 1670 (1962);
H. A. Buckmaster, R. Chatterjee and Y. H. Shing, Phys. Status Solidi, 13, 9 (1972).

43. B. C. Sanctuary and F. P. Temme, J. Molec. Struct. 111, 97 (1983).

44. V. Ravishankar, Mol. Phys. 62, 1409 (1987).

45. G. J. Bowden and W. D. Butchison, J. Magn. Reson. 67, 403 (1986);
G. J. Bowden, W. D. Hutchison and J. Khachan, J. Magn. Reson.

G. J. Bowden and W. D. Hutchison, J. Magn. Reson. 70, 361 (1986);

G.J. Bowden and W.D. Hutchison, J. Magn. Reson. 71, 1 (1987);

G.J. Bowden and W.D. Hutchison, J. Magn. Reson. 72, 61 (1987);

G. J. Bowden, W. D. Hutchison and F. Separovic, J. Magn. Reson. 79, 413 (1988);

G. J. Bowden, J. Khachan and J. P. D. Martin, J. Magn. Reson. 83, 79 (1989);

W. D. Hutchison, Ph.D. Thesis, University of New South Wales, NSW, Australia (1987).

46. R. Reddy and P. T. Narasimhan, J. Molec. Struct. 192, 309 (1989).

47. K. Blum, 'Density Matrix Theory and Applications,' Plenum Press, New York (1937).

48. J. Jeener, Adv. Magn. Reson. 10, 1 (1982).

49. U. Fano, Rev. Mod. Phys. 29, 74 (1957).

50. M. Goldman, 'Spin Temperature and Nuclear Magnetic Resonance in Solids,' Oxford University Press, Oxford (1970).

51. U. Haeberlen, 'High Resolution NMR in Solids: Selective Averaging,' Academic Press, New York (1976).

52. M. Mehring, 'Principles of High Resolution NMR in Solids,' second, revised and enlarged edition, Springer-Verlag, New York (1983).

53. C. P. Slichter, 'Principles of Magnetic Resonance,' 2nd revised edition, Springer-Verlag, New York (1980), Chapter 5.

54. P. L. Corio, 'Structure of High-Resolution NMR Spectra,' Academic Press, New York (1966), Appendix III.

55. (a) J. E. Campbell, Proc. London Math. Soc. 29, 14 (1898).
(b) H. F. Baker, Proc. London Math. Soc. 34, 347 (1902); H. F. Baker, Proc. London Math. Soc. 35, 333 (1903); H. F. Baker, Proc. London Math. Soc. (second series) 2, 293 (1904); H. F. Baker, Proc. London Math. Soc. (second series) 3 24 (1904).
(c) F. Hausdorff, Ber. Verhandl, Saechs. Akad. Wiss. Leipzig. Math. Naturw. kl. 58, 19 (1906).

56. B. C. Gerstein and C. R. Dybowski, 'Transient Techniques in NMR of Solids,' Academic Press, London (1985), Chapter 2.

57. (a) G. V. Visalakshi and N. Chandrakumar, J. Magn. Reson. 75, 1 (1987).
(b) W. Studer, J. Magn. Reson. 77, 424 (1988).

58. R. Tycko, Phys. Rev. Lett. 51, 775 (1983).

59. W. Magnus, Commun. Pure Appl. Math. 7, 649 (1954).

60. D. W. Robinson, Helv. Phys. Acta 36, 140 (1963).

61. P. Pechukas and J. C. Light, J. Chem. Phys. 44, 3897 (1966).

62. W. S. Warren and A. H. Zewail, J. Chem. Phys. 78, 3583 (1978).

63. W. A. Cady, J. Chem. Phys. 60, 3318 (1974).

64. I. Schek,J. Jortner and M. L. Sage, Chem. Phys. 59, 11 (1981).

65. R. J. Cross, J. Chem. Phys. 79, 1272 (1983).

66. R. P. Saxon and J. C. Light, J. Chem. Phys. 56, 3874 (1972).

67. J. C. Y. Chen and J. D. Kelly, J. Chem. Phys. 43, 1429 (1965).

68. A. Abragam and M. Goldman, 'Nuclear Magnetism: Order and Disorder,' Oxford University Press, New York (1982).

69. (a) I. Schek, M. L. Sage and J. Jortner, Chem. Phys. Lett. 63, 230 (1979).

(b) D. Suwelack and J. S. Waugh, Phys. Rev. 22B, 5110 (1980).

(c) B. N. Provotorov and E. B. Feldman, Sov. Phys. JETP 52, 1116 (1980);

E. B. Feldman, Phys. Lett. 104A, 479 (1984).

(d) S. C. Leasure, K. F. Milfeld and R. E. Wyatt, J. Chem. Phys. 74, 6197 (1981);

K. F. Milfeld and R. E. Wyatt, Phys. Rev. 27A,72 (1983).

70. R. S. Cantor, Ph.D. Thesis, Massachusetts Institute of Technology, Cambridge, Massachusetts (1979).

71. W. R. Salzman, J. Chem. Phys. 82, 822 (1985);

W. R. Salzman, J. Chem. Phys. 85, 4605 (1986);

W. R. Salzman, Chem. Phys. Lett. 124, 531 (1986).

72. M. M. Maricq, J. Chem. Phys. 86, 5647 (1987).

73. (a) N. N. Bogolubov and Y. A. Mitropolsky, 'Asymptotic Methods in the Theory of Non-Linear Oscillations,' Gorden and Breach, New York (1961).

(b) L. L. Buishvili and M. G. Menabde, Sov. Phys. JETP 50, 1176 (1979);

L. L. Buishvili, G. V. Kobakhidze and M. G. Menabde, Sov. Phys. JETP 57, 80 (1983).

(c) Ref. 52, Appendix G.

74. (a) J. H. Shirley, Phys. Rev. 138, B979 (1965).

(b) S. R. Barone and B. A. Narcowich, Phys. Rev. 15A, 1109 (1977).

75. N. E. Ainbinder and G. B. Furman, Sov. Phys. JETP, 58, 575 (1983).

76. M. M. Maricq, Phys. Rev. 25B, 6622 (1982);

M. M. Maricq, Phys. Rev. 31B, 127 (1985);

M. M. Maricq, Phys. Rev. 33B, 4501 (1986);

M. M. Maricq, Phys. Rev. Lett. 56, 1433 (1986).

77. M. M. Maricq, J. Chem. Phys. 85, 5167 (1986).

78.(a) R. R. Ernst, G. Bodenhausen and A. Wokaun, 'Principles of Nuclear Magnetic Resonance in one and two Dimensions,' Clarendon Press, Oxford (1987), Chapters 2 and 3.

(b) N. Chandrakumar and S. Subramanian, 'Modern Techniques in High-Resolution FT-NMR,' Springer-Verlag, New York (1987), Chapters 1 and 6.

(c) M. Goldman, 'Quantum Description of High-Resolution NMR in Liquids,' Clarendon Press, Oxford (1988), Chapters 2 - 5.

79. I. Furo, A. Janossy, L. Mihaly, P. Banki, Pocsik, I. Bakonyi, I. Heinmaa, E. Joon and E. Lippmaa, Phys. Rev. 36B, 5690 (1987);

R. E. Walstedt, W. W. Warren Jr., R. F. Bell, G. L. Brennert, G. P. Espinosa, J. P. Remeika, R. J. Cava and I. A. Rietman, Phys. Rev. 36B, 5727 (1987);

I. Watanabe, K. Kumagi, Y. Nakamura and H. Nakajma, J. Magn. Magn. Mater. 76-7, 599 (1988);

S. V. Verkhovskii, Yu. I. Zhdanov, B. A. Aleksashin, K. N. Mikhalev, V. V. Serikov, A. M. Bogdanovich, V. L. Kozhevnikov and S. M. Cheshnitskii, JETP Lett. 47, 448 (1988);

V. V. Serikov, A. M. Bogdanovich, S. V. Verkhovskhii, Yu. I. Zhdanov, B. A. Aleksashin, K. N. Mikhalev, V. L. Kozhevnikov and S. M. Cheshnitstii, JETP Lett. 47, 533 (1988);

W. W. Warren, R. E. Walstedt, G. F. Brennert, R. F. Bell, R. J. Cava and G. P. Espinosa , J. Appl. Phys. 64, 6081 (1988).

CHAPTER II

TECHNIQUES FOR THE DESIGN OF COMPOSITE PULSES FOR BROADBAND EXCITATION IN NQR SPECTROSCOPY

There are various ways of designing broadband excitation composite pulses and they have been used effectively in NMR spectroscopy. The purpose of this chapter is to discuss these methods briefly, especially in relation to NQR spectroscopy and to outline a thoretical procedure for constructing composite pulses for NQR spectroscopy using the Magnus expansion approach. This chapter is organised as follows. In Section II.A, the geometrical approach of deriving composite pulses has been outlined. Different iterative schemes have been considered in Section II.B, while in Section II.C, we deal with the 'coherent averaging' approach. Section II.D presents the details of the use of Magnus expansion in coherent averaging approach to construct composite pulses for NQR spectroscopy.

II.A Geometrical Approach

It is well known that the state of an isolated spin 1/2 nucleus can be represented by a vector in three dimensional space and the dynamics of the spin can be understood in terms of the rotation of the vector in an appropriate coordinate space which is the Bloch-vector model.[1] In this model, the thermal

equilibrium spin system in NMR can be defined by a vector along the magnetic field direction (z-axis). Now in the rotating coordinate a 90° rf pulse applied along the x-axis (90°_{x}) rotates the magnetization vector from z- to y-axis. Similarly a 180°_{x} pulse will leave the vector along -z-axis. The Bloch-vector model has been very useful in NMR to visualize the spin dynamics in many experiments and has in fact been employed to follow the spin trajectories under multiple pulse sequences.[2,3]

In 1979, Levitt and Freeman[4] used this Bloch-vector model to design composite pulses that compensate for resonance offset ($\Delta\omega_0$) and rf field inhomogeneity ($\Delta\omega_1$). They have examined Bloch-vector trajectories as a function of $\Delta\omega_0$ and $\Delta\omega_1$. From the geometrical pictures, the conclusion emerges that combinations of various flip angles and rf phases constituting the composite pulse have to be carefully chosen such that it cancels out the defects of a single rf pulse. Relaxation of spins is neglected while considering the motion of the nuclear magnetization subjected to a composite pulse in the Bloch-vector model. In this method the overall effect of a composite pulse is obtained by the solution of a simple problem in spherical geometry. Instead of seeking an analytical solution for this problem which is geometrically complicated, computer simulated trajectories have been used. The geometrical method has been successful in developing composite pulse sequences[5-7] which are widely used in NMR today.

The disadvantages of the geometrical approach are given below. The variety of composite pulses, and their degree of compensation achieved, have been restricted by the limits of

human ability in visualizing a set of three dimensional rotations, each subject to errors. Though the extent of compensation can be increased by increasing the number of rf pulses in a composite pulse, no easy method has been proposed to construct such sequences. Increasing the number of pulses in a composite pulse complicates the geometrical picture also. At a time, one can construct a composite pulse to compensate only one parameter and the assumption that the initial condition is always defined by a vector along the z-axis limits its applicability. Moreover, it is not valid for coupled spin systems.

From the NQR point of view, the geometrical method is not as attractive as in NMR for constructing composite pulses. The simple vector model is not possible for spin $I > 1/2$ cases, unlike in spin 1/2 case. Imagination of a vector representing a spin I nucleus in a $(2I+1)^2-1$ dimensional space is necessary, if one wishes to use the geometrical method for a spin $I > 1/2$ quadrupolar nucleus.

II.B Iterative Schemes

In this approach,[6-13] rather than attempting to construct a sequence with the desired propagator directly, a set of operations is defined that will be applied repetitively to an initial pulse sequence, thus generating a series of iterative sequences. The procedure of using iterative schemes is depicted in Fig. II.1.

The aim of iterative procedure is to construct the operations in such a way that the propagators for iterative sequences converge to a desired form. Constructing higher iterative

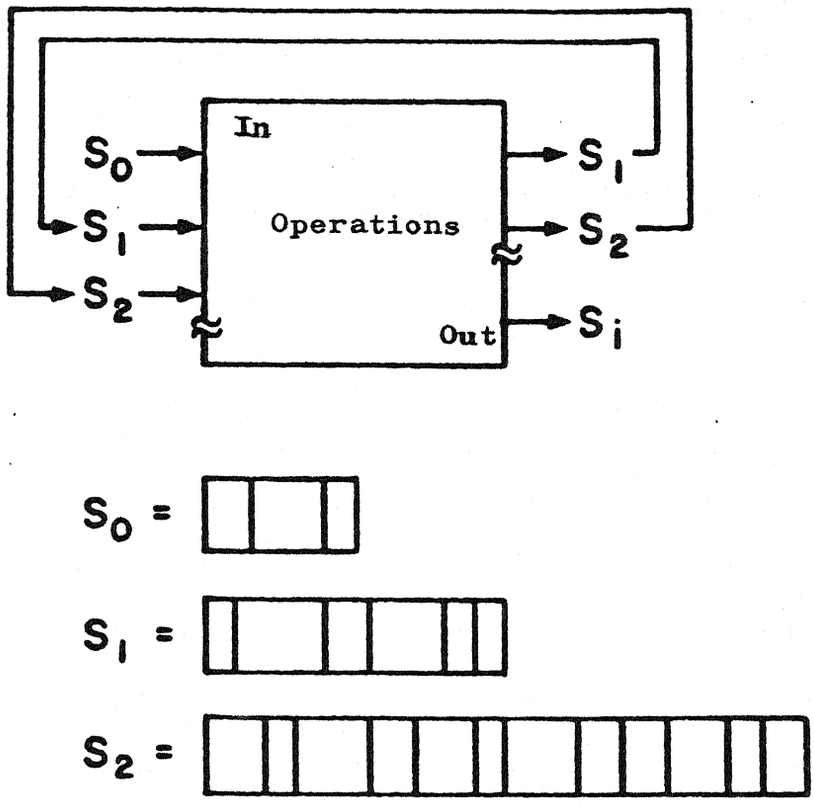

Fig. II.1 Schematic illustration of an iterative scheme.[11] Operations are applied repetitively to an initial pulse sequence S_o, and generating a series of iterative schemes S_1, S_2 etc.

sequences becomes increasingly complex and it will be composed of increasing number of individual pulses. The higher the iterate sequence the better the performance will be. Iterative sequences perform independent of the choice of the initial sequence, For example, regardless of S_o, S_3 may be a broadband excitation sequence. Therefore, the development and evaluation of an iterative scheme must focus on the operations that comprise the sequence rather than on the specific sequences that the scheme generates.

In NMR literature, operations treated include phase shifting of rf pulses,[8-11] concatenation of sequences[8-11] permutation of rf pulses,[6] fixed-point theory,[11,12] formation of inversion sequences[8] and pure numerical analysis.[14,15] It is beyond the scope of this dissertation to explain all these procedures in detail but for the sake of completeness, a brief presentation is given here.

II.B.1 Recursive Expansion Procedure

This is an iterative scheme[8,13] for constructing composite pulses of arbitrary flip angles, not necessarily $\pi/2$ or π radians, to achieve higher degree of compensation for resonance offset and rf field inhomogeneity in NMR. The procedure for generating a better composite $\pi/2$ pulse is as follows:

(i) Choose a composite $\pi/2$ pulse, P_o^m; m is the order of iteration.

(ii) Find out the inverse sequence $(P_o^m)^{-1}$ by phase inversion and time reversal.

(iii) Phase shift the inverse sequence in phase by $\pm\pi/2$ to get $(P_{\pm\pi/2}^m)^{-1}$.

(iv) Concatenate with the original sequence P_o^m, in any order, to get an improved sequence like $P_o^{m+1} = (P_{\pm\pi/2}^m)^{-1} P_o^m$.

(v) Steps (i) to (iv) may be applied in turn to P_o^{m+1} and the process repeated to get a desired sequence.

(vi) At any stage, the composite $\pi/2$ pulse P_o^m may be converted into a composite pulse of flip angle β (arbitrary) by forming

$(P_\beta^m)^{-1}\ P_\beta^m$; for example, if $\beta = 135^o$, then $P_o^{m+1} = (P_{3\pi/4}^m)^{-1}\ P_o^m$ is a composite 135^o pulse. If $P_o^o = (\pi/2)_y$, a single $\pi/2$ pulse applied along the y-axis of the rotating frame.

$$(P_{\pi/2}^o)^{-1} = (\pi/2)_x$$

$$P_o^1 = (\pi/2)_x(\pi/2)_y \ .$$

This is a composite $\pi/2$ pulse which compensates for the rf field inhomogeneity effects.

Starting from P_o^1 , we can construct a composite inversion pulse as follows:

$$R_o^1 = (P_\pi^1)^{-1}\ P_o^1$$

$$= (\pi/2)_y(\pi/2)_x(\pi/2)_x(\pi/2)_y$$

$$= (\pi/2)_y(\pi)_x(\pi/2)_y \ .$$

Sequences constructed by this procedure have been effectively used in high resolution NMR, NMR imaging and broadband decoupling experiments.[6,7,13,16]

II.B.2 Reversed Nutation Sequences

Following the recursive expansion procedure, Shaka and Freeman[9] constructed a set of composite inversion π pulses using a method which is similar to the recursive expansion approach. In this method, called the reversed nutation method,[9,13] starting from a single π pulse, composite inversion pulses are obtained by the following procedure:

$$P^m \longrightarrow P^m (P^m)^{-1} P^m = P^{m+1}$$

Let $P^o = \pi_x$

then $P^1 = \pi_x \pi_y \pi_x$, is a composite inversion π pulse. Similarly, starting from the sequence P^1 with $(P^1)^{-1} = \pi_y \pi_{-x} \pi_y$, we get

$$P^2 = P^1 (P^1)^{-1} P^1 \text{ as}$$

$$P^2 = \pi_x \pi_y \pi_x \pi_y \pi_{-x} \pi_y \pi_x \pi_y \pi_x$$

P^2 is also a composite π pulse, whose performance is better than P^1.

II.B.3 Phase Shifting and Catenation Operation Scheme

In this procedure, a class of iterative scheme[10] is defined by the following operations:

(i) Consider an rf pulse sequence S_i and form N phase shifted versions of S_i with phase shifts ϕ_1, ϕ_2, ... ϕ_N (where N is an odd integer).

(ii) A new sequence S_{i+1} is obtained by concatenating the N phase shifted versions in order from 1 to N as explained in an example below. Thus S_{i+1} is N times longer than S_i.

An example of constructing a composite π pulse is given here. We assume that S_i is acting on an isolated spin to produce a rotation R_i, given by

$$R_i = \exp[-i(I_x \cos\phi_o + I_y \sin\phi_o)\pi]\exp(-i\delta I) \quad .. (II.1)$$

where ϕ_o is the rf phase and δ has a z-component of zero. R_i is

in fact the propagator for S_i i.e., $R_i = U_i(t)$. If the inversion is nearly complete then δ is small. Applying the iterative scheme, a new sequence S_{i+1} is generated to first order in $|\delta|$. The propagator R_{i+1} is given by

$$R_{i+1} = \exp[-i(I_x \cos\phi_T + I_y \sin\phi_T)\pi]\exp(-i\delta_T I) \quad .. \text{(II.2)}$$

where $$\phi_T = \phi_o + \sum_{n=1}^{N} (-1)^{n+1} \phi_n \quad .. \text{(II.3)}$$

and $$\delta_T = \sum_{n=1}^{N} \{\delta_x \cos\beta_n - \delta_y \sin\beta_n, (-1)^{n+1}\delta_y \cos\beta_n + (-1)^{n+1}\delta_x \sin\beta_n, 0\} \quad .. \text{(II.4)}$$

β_n is given by

$$\beta_n = \phi_n + \sum_{m=1}^{n-1} (-1)^{m+1}\, 2\phi_m \text{ for odd } n \quad .. \text{(II.5a)}$$

$$\beta_n = \phi_n - 2\phi_o + \sum_{m=1}^{n-1} (-1)^{m}\, 2\phi_m \text{ for even } n \quad .. \text{(II.5b)}$$

If δ_T can be made to vanish by properly selecting phase shifts, the first-order deviation from complete inversion in S_i will be nullified in S_{i+1}. Thus, it is possible to generate composite π pulse sequences S_1, S_2, S_3 etc. starting from S_o for broadband spin inversion over large ranges of $\Delta\omega_1$ and $\Delta\omega$. One of the composite inversion π pulse thus achieved is

$$S_1 : (\pi)_o(\pi)_o(\pi)_{120}(\pi)_{60}(\pi)_{120} \cdot$$

II.B.4 Fixed Point Theory

The propagator that corresponds to any rf pulse sequence can be represented by a point in the propagator space, which is a subset of Liouville space. For example, the propagator space for a quadrupolar spin $I = 1$ nucleus is an eight dimensional space but if the quadrupole interaction vanishes then the dimension of the propagator space reduces to three. The purpose of this method[12] is to find a proper function (F) which generates the higher iterative sequences ($U_{i+1} = FU_i$) in such a way that (i) the higher iterates U_1, U_2, etc. should be determined by the initial one (U_o) and (ii) for a given U_i there should be only one U_{i+1}.

When there is only one sequence given by the propagator $\bar{U}$ describing the desired response, that is, $U_n = \bar{U}$ if $U_o = \bar{U}$ and

$$\bar{U} = F\bar{U} \quad \text{or} \quad \bar{U} = F^n \bar{U} \qquad .. \text{(II.6)}$$

where F^n is the n iteration of the function F, $\bar{U}$ is then said to be a fixed point of F. In general, there may be a set of propagators which give the desired results,

$$\{\bar{U}^{(k)}\} = F\{\bar{U}^{(j)}\} \qquad .. \text{(II.7)}$$

Then both $\{\bar{U}^{(k)}\}$ and $\{\bar{U}^{(j)}\}$ are said to be invariant sets of F.

An iterative sequence with a stable fixed point (shown in Figure II.2(a)) will generate broadband excitation sequences whereas F with unstable fixed point (shown in Figure II.2(b)) generates narrowband excitation sequences.[12] A range of initial

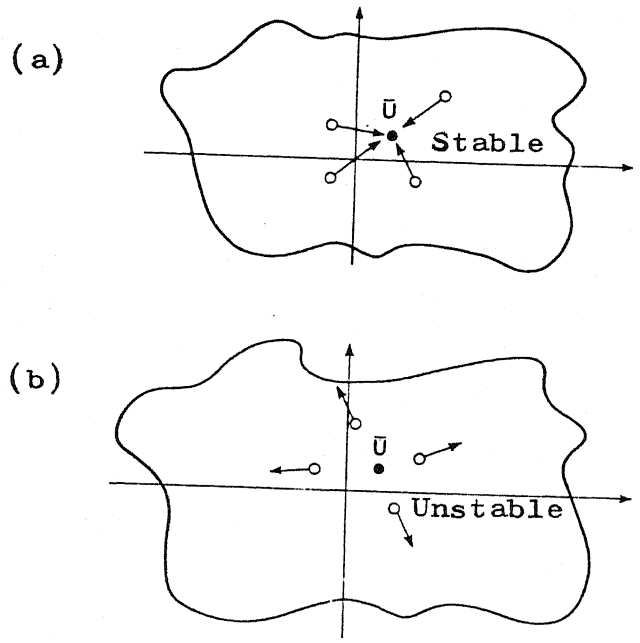

Figure II.2 (a) Points near a stable fixed point converge to the fixed point with successive iterations of F. (b) Points near an unstable fixed point diverge. The axes are along directions in a multi-dimensional space.

pulse sequence propagators, arising from a range of experimental parameters, converges to the desired propagators upon iteration in the case of stable fixed point. Generally, a simple expression for F is not possible. For this, basins must be mapped with a computer program. These basin images define the dynamics of F, superstable fixed points. Basin images will have regions shaded according to the number of iterations required for an initial point in a given region to converge to a fixed point. Basin images can be used to guide the selection of an initial pulse sequence so as to

get better composite pulses. An initial sequence is selected for which the locus of the initial points conforms to the basin of the desired fixed point.

For example, the composite inversion π pulse 300 $\overline{120}$ is obtained by a computer search conducted over possible two pulse sequences with phases 0 and 180. Rotation in three dimensional space can be represented by matrices which are elements of a spherical subspace belonging to the group called SO(3).[17] The points in SO(3) space have been calculated for each possible sequence with the variation $\Delta\omega$ from $-1.4\ \omega_1^{\circ}$ to $+1.4\ \omega_1^{\circ}$. Similarly, $(165)_0$-$(165)_{105}$-$(165)_0$ and many other sequences have been generated by this procedure.[11,12]

The advantages of this approach[11,12] are the following: A unified set of concepts and the accompanying geometrical picture allow visualizations, comparisons of scheme and explanations of their essential features to be made. Dynamical concepts allow a clear treatment of schemes that will be normally difficult to consider. However, in higher dimensions, or in problems with arbitrary dimension, the basins are more difficult to be generated by computer programs.

II.B.5 Numerical Approach

This procedure[14] removes restrictions on the pulse parameters and allows the design of composite pulses with fewer components and shorter duration. The efficiency of a composite pulse sequence can be defined by the function[14]

$$F(x) = \sum_p \sum_q \alpha_{pq}[I(a_p,b_q) - S(x,a_p,b_q)]^2 \qquad .. (II.8)$$

where (ap,bq) is a point on the $\Delta\omega/\omega_1^o - \Delta\omega_1/\omega_1^o$ plane at which the desired response is I(ap,bq), α_{pq} determines the relative contribution of each point to F(x). Minimising F(x) with respect to the parameters x will give an optimum composite pulse sequence. This is carried out by a multi-dimensional search of the global minimum corresponding to the best set of parameter values. Some of the composite pulse sequences have been verified by this procedure and newer ones have been constructed.[14] This method does not provide insight into the mechanism of error compensation. Though it generates efficient pulses, each iteration increases the number of pulses in the required sequence.

Shaka[15] has applied a numerical non-linear optimization procedure and obtained several phase alternated composite pulses for ultra broadband spin inversion in NMR spectroscopy. These phase alternated pulses have a phase of either 0^o or 180^o only. In principle, it is possible to consider arbitrary phases also for the pulses.

Generally, iterative schemes and pure numerical approaches demand larger computer time for generating composite pulses and they yield mostly longer duration pulse sequences, which will not be useful in NQR spectroscopy because of the shorter spin-spin relaxation time, T_2. The composite $\pi/2$ pulse derived from recursive expansion[8,13] approach, namely, $(90)_0-(90)_{90}$[8] is not a better pulse sequence to compensate for efg inhomogeneity in NQR. Moreover, the mechanism by which these sequences compensate

for different effects so as to give broadband excitation is not yet clearly understood.

II.C Magnus Expansion Approach

In Chapter I, we have discussed the importance of Magnus approximation in magnetic resonance. Pulse sequences have been discovered for line narrowing, time-reversal and other such experiments[2,3] using the AHT which employs the Magnus approximation.[18] The basic idea behind this theory is to get a pulse sequence, under which a particular line broadening interaction is averaged out. In AHT, Magnus expansion is used to solve the time dependent von Neumann equation defining the evolution of spin population under a desired rf pulse sequence. The solution obtained by Magnus expansion is expressed with a time independent Hamiltonian called average Hamiltonian or effective Hamiltonian[19] which is effective during the desired pulse sequence. AHT concept has been used to construct broadband decoupling composite pulse sequences in NMR.[6,7,13,16,17] In a similar manner, Magnus expansion has been used in the construction of composite pulses for broadband excitation in NMR spectroscopy.[11,20,21] The purpose of broadband excitation problem is to find a pulse sequence, whose net propagator will have a desired form and independent of a particular effect which causes the broadening of the frequency spectrum.

In this approach, only a certain part of AHT is applicable. The important and common idea behind AHT and broadband

excitation problem is the use of 'toggling frame'[19] (or the rf interaction frame) to impart a time dependence to the internal Hamiltonian of the spin system. Spin evolution under a constant time independent effective Hamiltonian derived using the Magnus expansion is also common for both the cases. Otherwise, the requirement that $U_{rf}(t) = \mathbb{1}$ [19] (for a cyclic rf pulse sequence) of AHT is not at all a necessary condition for broadband excitation problem; rather, $U_{rf}(t)$ has to be a rotation that creates transverse magnetization. Since composite pulses are not applied repetitively like multiple pulse sequences, the condition of stroboscopic observation (or the so called 'window' in AHT)[19] is not needed for the broadband excitation problem.

Advantages of Magnus expansion approach are as follows. This technique[20] of finding out composite pulses is valid for a general spin I case. This method can be used for constructing sequences to overcome all kinds of interactions and at a time more than one effect can be considered. Here, the task of achieving broadband excitation sequences boils down to solving a set of analytical equations. This method treats composite pulses entirely rather than pulse-by-pulse analysis and, therefore, the results are independent of the initial state of the system. Pulse sequences obtained by this procedure are equivalent to constant, pure rotations produced by single rf pulses. In addition to this, the mechanism by which different sequences are developed is easy to understand and to improve further. Hence, this method has a general applicability to many areas. Especially for NQR spectroscopy, it would be possible to derive shorter time

duration ($<< T_2$) sequences. Therefore, we have chosen this particular approach in the present work.

Before concluding this section on different approaches employed in the design of NMR composite pulses, we would like to survey the following important recent literature. Counsell et al.[22] have proposed an analytical theory using the quaternion formalism[23,24] for the analysis of several NMR composite pulses. In 1987, Sanctuary and Cole[25] showed that the analytical expressions generated by the multiple theory[26] agree with other theoretical approaches and experimental results. Alternative approaches like continuous phase modulation,[27] amplitude modulation[28,29] and frequency switching[29,30] of rf pulses have been used to devise composite pulse sequences in the NMR literature. Recently, Zax and Vega[31] have used a perturbation treatment with Floquet formalism to derive broadband excitation pulses of arbitrary flip angle for two-level systems. In what follows, a general Magnus expansion technique for designing composite pulses in spin I NQR spectroscopy is discussed.

II.D Magnus Expansion Approach for the Construction of Composite Pulses in NQR

We consider an ensemble of physically equivalent spin $I > 1/2$ nuclei at the sites of a single crystal in the absence of Zeeman field. Defining a common quadrupole principal axis system (QPAS) for all physically equivalent spin systems and assuming that QPAS coincides with the laboratory frame, the total Hamiltonian, $\mathcal{H}$, of the system in QPAS is given by

$$\mathcal{H} = \mathcal{H}_Q + \mathcal{H}_{rf}(t) + V \qquad .. \text{(II.9)}$$

where $\mathcal{H}_Q$ is the quadrupolar Hamiltonian[32] and it is explicitly given in terms of Cartesian coordinate angular momentum operators (I_x, I_y, I_z and I) in Chapter I (see Eqn. (I.1)). The Hamiltonian $\mathcal{H}_{rf}(t)$ in Eqn. (II.9) defines the interaction between the spins and an applied rf radiation of strength ω_1 (rad/sec) with phase $\phi(t)$ which is piecewise constant. Typically, the rf radiation is applied in the form of pulses that are ideally square, so that ω_1 is piecewise constant having values either 0 or ω_1 only. It can be expressed in QPAS as

$$\mathcal{H}_{rf}(t) = -2\omega_1(t) \cos(\omega_Q t + \phi(t))\, I_x \qquad .. \text{(II.10)}$$

where ω_Q is the quadrupole frequency. In writing Eqn. (II.10), we have made the assumption that the x-axis of QPAS is aligned along the rf coil axis. Unlike in NMR, here both components of the linearly polarized rf radiation (i.e., two circularly polarized rf components with strength ω_1 and rotating in opposite direction at a frequency ω_Q) interact with the spin magnetization in zero magnetic field.[33]

In general, the Hamiltonian V in Eqn. (II.9) may include any other interactions in the spin assembly. In NQR, these can be different effects that lead to the efg inhomogeneity (δq) which in turn create a quadrupole frequency distribution ($\Delta\omega_Q$), dipole-dipole interactions (ω_D), spin-spin coupling, resonance offset and rf field inhomogeneity ($\Delta\omega_1$). The mechanisms

responsible for these interactions[32] have been described in Chapter I. Here, resonance offset is the frequency difference between the applied rf radiation and the quadrupole frequency. Since Hamiltonians corresponding to the effects of resonance offset and efg inhomogeneity transform in the same way under unitary transformations, we denote both of them by $\Delta\omega_Q$ in this thesis. The various terms of the Hamiltonians in Eqn. (II.9) may then be arranged in an order, namely, $\mathcal{H}_Q \gg \mathcal{H}_{rf}(t) \gg V$. Therefore, in QPAS, the time evolution of the spin system is largely brought about by the quadrupole Hamiltonian, $\mathcal{H}_Q$ which is already well-characterized and therefore contributes little new information. But usually in NQR one is interested in studying the effect of rf radiation on the spin system. So, it is necessary to suppress $\mathcal{H}_Q$. Furthermore, in QPAS, $\mathcal{H}_{rf}(t)$ is itself time-dependent and it would be highly cumbersome to carry out the theoretical analysis of NQR experiments. These difficulties can be overcome by a transformation of $\mathcal{H}$ to a new frame called 'quadrupole interaction frame' (QIF) defined by the unitary operator U_Q.[34] This frame is somewhat similar to that of the 'rotating frame' used in NMR;[35] however, QIF cannot be visualized by a simple geometrical picture.

Now in QIF, $\mathcal{H}$ becomes

$$\tilde{\mathcal{H}} = U_Q^{-1}\mathcal{H}\,U_Q = \tilde{\mathcal{H}}_{rf}(t) + \tilde{V} \qquad .. \text{(II.11)}$$

QIF is represented by a tilde ($\sim$) over the Hamiltonians,

where $U_Q = \exp(-i\mathcal{H}_Q t)$ .. (II.12)

Derivation of Eqn. (II.11) from Eqn. (II.9) can be easily understood with the help of Appendix C. In QIF, the transformed rf Hamiltonian $\tilde{\mathcal{H}}_{rf}(t)$ is time dependent and it possesses rapidly oscillating terms such as $\cos(n\omega_Q t)$ and $\sin(n\omega_Q t)$. Effects corresponding to these high frequency terms are similar to the Bloch-Siegert effect in NMR[36] and in NQR, this has not been extensively studied because of its limited chemical applications. However, in 1984, Furman[37] reported the first observation of Bloch-Siegert effect in NQR. To a first order approximation these high frequency terms can be dropped, and the resultant rf Hamiltonian $\tilde{\mathcal{H}}_{rf}$, is time independent in QIF. Furthermore, the main interaction $\mathcal{H}_Q$ may also be suppressed, and Eqn. (II.11) may be written as

$$\tilde{\mathcal{H}} = \tilde{\mathcal{H}}_{rf} + \tilde{V} \qquad .. \text{(II.13)}$$

The procedure of truncation of high frequency terms will be explicitly shown in later chapters for spin I = 1 and 3/2 cases. But it can be generally said that truncation means rejection of all those terms whose operators depend on time in such a way that their time average vanishes.

The concept of QIF is more than a mere mathematical trick. In NQR experiments which employ phase sensitive detection, the observed experimental results correspond to the theoretical response of the spin system in QIF. We can then say that usually NQR experiments are performed in QIF. Now in QIF, the time evolution of the spin system is described by the von Neuman equation[38] as

$$\frac{d\,\tilde{\rho}(0)}{dt} = -i[\tilde{\mathcal{H}},\ \tilde{\rho}(0)] \qquad .. \text{(II.14)}$$

where $\tilde{\rho}(0) = U_Q^{-1}\,\rho(0)\,U_Q \approx \mathcal{H}_Q$ .. (II.15)

Derivation of Eqn. (II.15) for a general case is given in Appendix C. The reduced density matrix $\rho(0)$ has been derived in Chapter I. The solution of Eqn. (II.14) is given by the Dyson expression as

$$U(t) = T \exp\left[-i \int_0^t \tilde{\mathcal{H}}(t')\,dt'\right], \qquad .. \text{(II.16)}$$

where T is the Dyson time-ordering operator (see Chapter I). The density matrix defining the spins at time 't' in QIF is given by

$$\tilde{\rho}(t) = U(t)\,\tilde{\rho}(0)\,U(t)^{-1} \qquad .. \text{(II.17)}$$

where $U(t)$ defines the evolution of the spin system under the simultaneous effects of $\tilde{\mathcal{H}}_{rf}$ and $\tilde{V}$. Here, $\tilde{\mathcal{H}}_{rf} \gg \tilde{V}$. Therefore, the main time dependence of $\tilde{\rho}(t)$ comes from $\tilde{\mathcal{H}}_{rf}$. Since we would like to design composite pulses that reduce the effects of the interaction $\tilde{V}$, it is necessary to understand further the evolution of the system under $\tilde{V}$ alone. The important parts of $\tilde{V}$ can be made apparent by a transformation to a new frame called the 'toggling frame' (i.e., the rf interaction frame). The concept of this new frame is similar to the one that has been implemented in AHT.[19] The frame is so called because it toggles with respect to QIF, according to the rhythm of rf pulses in the applied composite pulse sequence. Toggling frame and QIF coincide in the

absence of rf pulses in the present problem, but in the case of AHT the toggling frame and QIF coincide only at windows. In the toggling frame, the net Hamiltonian is expressed as

$$\tilde{\tilde{\mathcal{H}}} = U_{rf}^{-1}(t)\,\tilde{\mathcal{H}}\,U_{rf}(t) = \tilde{\tilde{V}}(t) \qquad .. \text{(II.18)}$$

Throughout this thesis we represent the toggling frame by double tildes ($\approx$). It should be noted that the transformed Hamiltonian, namely, $\tilde{\tilde{V}}(t)$, is time dependent. Alternatively, we may say that the internal Hamiltonian is deliberately made time dependent. Now, the equation of motion becomes (Appendix C)

$$\frac{d\,\tilde{\tilde{\rho}}(0)}{dt} = -i\left[\,\tilde{\tilde{V}}(t),\ \tilde{\tilde{\rho}}(0)\,\right] \qquad .. \text{(II.19)}$$

where $$\tilde{\tilde{\rho}}(0) = \rho(0) \qquad .. \text{(II.20)}$$

The solution to this differential equation is derived to be

$$U_v(t) = T\exp\left[\,-i\int_0^t \tilde{\tilde{V}}(t')\,dt'\,\right] \qquad .. \text{(II.21)}$$

In QIF, the complete evolution operator, i.e., Eqn. (II.16), becomes

$$U(t) = U_{rf}(t)\,U_v(t)\ . \qquad .. \text{(II.22)}$$

One can notice the importance of the toggling frame in separating the simultaneous time evolution under $\tilde{\mathcal{H}}_{rf}$ and $\tilde{V}$. From

Eqn. (II.19), it can be stated that in the absence of internal interactions represented by the Hamiltonian V, the spin system in the toggling frame denoted by $\tilde{\tilde{\rho}}(t)$ remains stationary (or it is said to be a constant of the motion). Since $\tilde{\tilde{V}}(t)$ is time dependent, $U_v(t)$ is time dependent. Therefore the problem now is to solve a time dependent differential equation, i.e., Eqn. (II.19). As has been discussed in Chapter I, we use the Magnus approximation for this purpose in a manner similar to that of AHT, to write

$$\tilde{\tilde{V}} = V^{(0)} + V^{(1)} + V^{(2)} + ... + V^{(i)} + ... \quad .. (II.23)$$

In Chapter I, the different terms in the above mentioned Magnus expansion have been separately explained (Eqns. (I.25) and (I.26)). These terms can be derived for various spin values and they can be expressed in terms of rf pulse phases (ϕ_n) and flip angles (θ_n). For example, considering a composite pulse containing N-pulses, it can be completely defined by 2N parameters, namely, the N-flip angles and N-phases. Schematically, a N pulse composite pulse has been represented in Figure II.3. Now $V^{(i)}$ can be written in terms of these 2N variables (or unknowns). At this point, if we can make $\tilde{\tilde{V}}(t) = 0$ by adjusting the 2N unknowns in such a way that $V^{(i)}$ goes to zero, then the propagator $U_v(t) = \mathbb{1}$. This means that the spin populations would not feel the effect of different internal interactions. Therefore, the applied composite pulse sequence excites the spin system uniformly irrespective of the strength of the interaction V. This can be

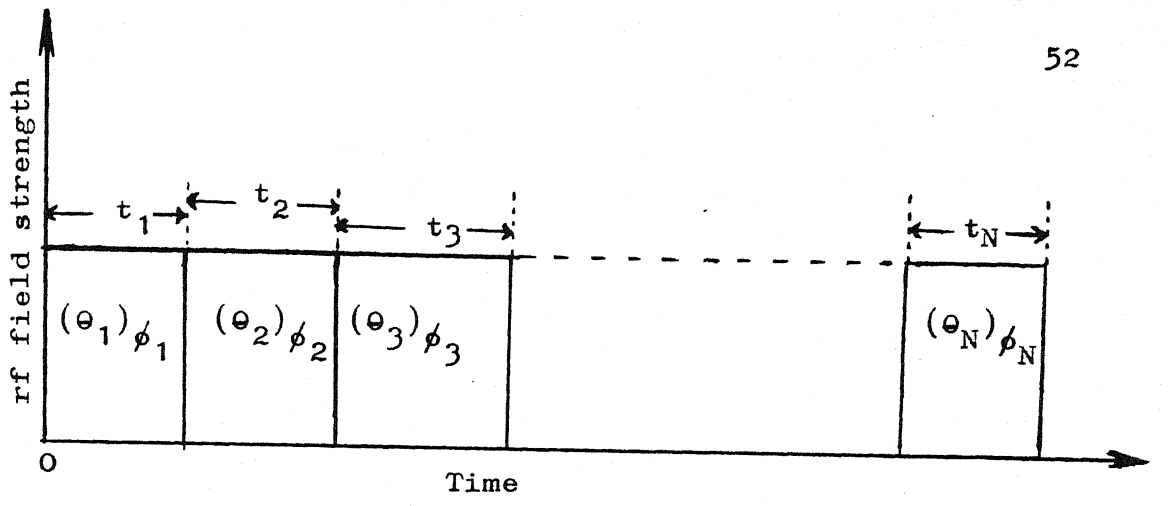

Figure II.3 Schematic representation of a composite pulse consisting of N rf pulses with individual time durations denoted as t_1, t_2, t_3, ...t_N.

achieved by selecting an mth-order composite pulse which satisfies the following conditions:[39]

(i) all the Magnus terms should be equal to zero, i.e.,

$$V^{(n)} = 0 \text{ for } 0 \leq n \leq m \qquad .. \text{ (II.24)}$$

As m increases, the degree of compensation increases. So, an mth-order composite pulse will produce better broadband excitation than an (m-1)th-order composite pulse. However, commonly higher order sequences will be of longer time duration.

(ii) The composite pulse that satisfies the above condition should behave like a single rf pulse. For example, a composite $\pi/2$ pulse is defined by the maximum spin magnetization in the transverse plane of QPAS[39] i.e.,

$$\mathrm{Tr}\left[\tilde{M}_x,\ U_{rf}(t)\ \rho(0)\ U_{rf}(t)^{-1}\right] = \langle I_x \rangle_{\text{maximum}} \qquad .. \text{ (II.25)}$$

where M_x is the observable operator in QIF. The derivation of M_x is given in Appendix D for I = 1 and 3/2 cases. Similarly, a composite inversion π pulse is given by the minimum expectation value of I_z and by zero transverse spin magnetization. It can be expressed as

$$\mathrm{Tr}\left[\tilde{M}_z,\ U_{rf}(t)\,\rho(0)\,U_{rf}(t)^{-1}\right] = \langle I_z\rangle_{\text{minimum}} = -\langle I_z\rangle_{\text{maximum}}$$

and $\langle I_x\rangle = \langle I_y\rangle = 0$ . .. (II.26)

Therefore, an mth-order composite pulse consisting of N rf pulses can be derived by solving (m+1) equations, namely, Eqn. (II.24) and Eqn. (II.25) or Eqn. (II.26) simultaneously so as to get 2N variables which define the complete sequence. The efficiency of these composite pulses can be examined by evaluating the response of the spin system (refer Appendix D) as a function of a parameter which defines the interaction V. For example, for a composite $\pi/2$ pulse, the signal amplitude, W_1, should be evaluated by the following expression[39]:

$$W_1 = \frac{\mathrm{Tr}\left[\tilde{M}_x,\ \tilde{\rho}(t)\right]}{\mathrm{Tr}\left[I_x^2\right]} \qquad \text{.. (II.27)}$$

Similarly, the extent of spin inversion by a composite π pulse is given by

$$W_2 = \frac{-\mathrm{Tr}\left[\tilde{M}_z,\ \tilde{\rho}(t)\right]}{\mathrm{Tr}\left[I_z^2\right]} \,. \qquad \text{.. (II.28)}$$

Using this approach composite pulses with any arbitrary net flip angle can be designed. But as far as NQR spectroscopy is concerned, only composite $\pi/2$ and composite π pulses are important.

The main goal of this thesis is to design shorter time duration ($\ll T_2$) composite pulses ($\pi/2$ and π) with broadband ($\omega_Q \pm \Delta\omega_Q$ and $\omega_1 \pm \Delta\omega_1$) excitation performance that would be applicable in any kind of FT NQR spectroscopy. In the present work, we limit ourselves to zeroth order composite pulses because usually higher order sequences are of longer time duration and therefore they may not be of much importance in NQR spectroscopy. In this approach, composite pulses compensating simultaneously, for different effects can be derived. But for the sake of simplicity we have considered different effects separately. This procedure applied for spin 1^{39} and spin 3/2 cases have been presented in Chapters III and IV, respectively.

Summary

In this chapter, the various procedures for designing composite pulse sequences reported in the recent NMR literature have been briefly reviewed in the light of their applicability/adaptation to NQR spectroscopy. The merits of using the Magnus expansion approach have been pointed out. The purpose of the Magnus expansion employed in both AHT and broadband excitation problems has been clearly brought out. A general theoretical treatment of designing composite pulses for an arbitrary spin I (≥ 1) nuclei for use in NQR spectroscopy has been developed.

REFERENCES

1. A. Abragam, 'The Principles of Nuclear Magnetism,' Oxford University Press, Oxford (1961).
2. U. Haeberlen, 'High Resolution NMR in Solids: Selective Averaging,' Academic Press, New York (1976).
3. M. Mehring, 'Principles of High Resolution NMR Spectroscopy in Solids,' Second, revised and enlarged edition, Springer-Verlag, Heidelberg (1983).
4. M. H. Levitt and R. Freeman, J. Magn. Reson. 33, 473 (1979).
5. (a) R. Freeman, S. P. Kempsell and M. H. Levitt, J. Magn. Reson. 38, 453 (1980);
   M. H. Levitt and R. Freeman, J. Magn. Reson. 43, 65 (1981).
   (b) M. H. Levitt, J. Magn. Reson. 48, 234 (1982);
   M. H. Levitt, J. Magn. Reson. 50, 95 (1982).
6. M. H. Levitt, R. Freeman and T. Frenkiel, Adv. Magn. Reson. 11, 47 (1983).
7. M. H. Levitt, Prog. NMR Spectrosc. 18, 61 (1986) and references cited therein.
8. M. H. Levitt and R. R. Ernst, J. Magn. Reson. 55, 247 (1983).
9. A. J. Shaka and R. Freeman, J. Magn. Reson. 55, 487 (1983);
   A. J. Shaka and R. Freeman, J. Magn. Reson. 60, 169 (1984).
10. R. Tycko and A. Pines, Chem. Phys. Lett. 111, 462 (1984);
    W. S. Warren, D. P. Weitekamp and A. Pines, J. Chem. Phys. 73, 2084 (1980).
11. R. Tycko, Ph.D. Thesis, University of California, Berkeley (1984).

12. R. Tycko, A. Pines and J. Guckenheimer, J. Chem. Phys. 83, 2775 (1985);
H. Cho and A. Pines, J. Chem. Phys. 86, 6591 (1987).

13. R. R. Ernst, G. Bodenhausen and A. Wokaun, 'Principles of Nuclear Magnetic Resonance in one and two Dimensions,' Clarendon Press, Oxford (1987), Chapter 4.

14. D. J. Lurie, Magn. Reson. Imaging 3, 235 (1985);
D. J. Lurie, J. Magn. Reson. 70, 11 (1986).

15. A. J. Shaka, Chem. Phys. Lett. 120, 201 (1985).

16. (a) M. H. Levitt and R. Freeman, J. Magn. Reson. 43, 502 (1981);
M. H. Levitt, R. Freeman and T. Frenkiel, J. Magn. Reson. 47, 328 (1982);
M. H. Levitt, R. Freeman and T. Frenkiel, J. Magn. Reson. 50, 157 (1982);
R. Freeman, T. Frenkiel and M. H. Levitt, J. Magn. Reson. 50, 345 (1982);
A. J. Shaka, J. Keeler, T. Frenkiel and R. Freeman, J. Magn. Reson. 52, 335 (1983);
A. J. Shaka, J. Keeler and R. Freeman, J. Magn. Reson. 53, 313 (1983);
A. J. Shaka, P. B. Barker and R. Freeman, J. Magn. Reson. 71, 520 (1987).

(b) J. S. Waugh, J. Magn. Reson. 49, 517 (1982);
J. S. Waugh, J. Magn. Reson. 50, 30 (1982).

(c) D. Suter, K. V. Schenker and A. Pines, J. Magn. Reson. 73, 90 (1987);

K. V. Schenker, D. Suter and A. Pines, J. Magn. Reson. 73, 99 (1987);

A. J. Shaka, C. J. Lee and A. Pines, J. Magn. Reson. 77, 274 (1988).

(d) A. J. Shaka and J. Keeler, Prog. NMR Spectrosc. 19, 47 (1987).

17. (a) J. F. Cornwell, 'Group Theory in Physics,' Vol. II, Academic Press, London (1984), Chapter 12.

(b) A. W. Joshi, 'Elements of Group Theory for Physicists,' third edition, Wiley Eastern Limited, New Delhi (1985), Chapter 4.

18. W. Magnus, Commun. Pure Appl. Math. 7, 649 (1954).

19. (a) U. Haeberlen and J. S. Waugh, Phys. Rev. 175, 453 (1968); Ref. 2, Chapters IV and V.

(b) Ref. 3, Chapter 3.

20. R. Tycko, Phys. Rev. Lett. 51, 775 (1983).

21. R. Tycko, E. Schneider and A. Pines, J. Chem. Phys. 81, 680 (1984);

R. Tycko, H. M. Cho, E. Schneider and A. Pines, J. Magn. Reson. 61, 90 (1985);

A. J. Shaka and A. Pines, J. Magn. Reson. 71, 495 (1987).

22. C. Counsell, M. H. Levitt and R. R. Earnst, J. Magn. Reson. 63, 133 (1985).

23. W. R. Hamilton, Proc. Roy. Irish. Acad. 2, 424 (1944), in W. R. Hamilton, 'Mathematical Papers,' Vol. 3, Cambridge University Press, London (1967).

24. B. Blümich and H. Spiess, J. Magn. Reson. 61, 356 (1985).

25. B. C. Sanctuary and H. B. R. Cole, J. Magn. Reson. 71, 106 (1987).

26. B. C. Sanctuary, T.K. Halstead, P.A. Osment, Mol. Phys. 49, 753 (1983);
G. Campolieti, N. Lee and B. C. Sanctuary, Mol. Phys. 55, 1033 (1985).

27. J. Baum, R. Tycko and A. Pines, J. Chem. Phys. 79, 4643 (1983); J. Baum, R. Tycko and A. Pines, Phys. Rev. 32A, 3435 (1985).

28. (a) C. J. Bauer, R. Freeman, T. Frenkiel, J. Keeler and A. J. Shaka, J. Magn. Reson. 58, 442 (1984).
(b) W. S. Warren, J. Chem. Phys. 81, 5437 (1984).
(c) J. H. Gutow, M. McCoy, F. Spano and W. S. Warren, Phys. Rev. Lett. 55, 1090 (1985).

29. K. Ugurbill, M. Garwood and M. R. Bendall, J. Magn. Reson. 72, 177 (1987).

30. (a) T. Fujiwara and K. Nagayama, J. Magn. Reson. 77, 53 (1988).
(b) A. Bielecki, A. C. Kolbert and M. H. Levitt, Chem. Phys. Lett. 155, 341 (1989).

31. D. B. Zax and S. Vega, Phys. Rev. Lett. 62, 1840 (1989).

32. T. P. Das and E. L. Hahn, 'Nuclear Quadrupole Resonance Spectroscopy,' Academic Press, New York (1958).

33. M. Bloom, E. L. Hahn and B. Herzog, Phys. Rev. 97, 1699 (1955).

34. M. Goldman, 'Spin Temperature and Nuclear Magnetic Resonance in Solids,' Oxford University Press, Oxford (1970), Chapter 1.

35. (a) Ref. 1, Chapter II.
(b) Ref. 2, p. 49-50.

36. (a) Ref. 1, Chapter II.

(b) Ref. 3, Appendix H.

37. G. B. Furman, Izv. Vyssh. Vchebn. Zaved, Radiofiz, 27, 667 (1984).

38. K. Blum, 'Density Matrix Theory and Applications,' Plenum Press, New York (1937).

39. A. Ramamoorthy and P. T. Narasimhan, J. Molec. Struct. 192, 333 (1989).

CHAPTER III

DERIVATION OF NQR COMPOSITE PULSES USING THE MAGNUS EXPANSION APPROACH FOR SPIN I = 1 NUCLEI IN SINGLE CRYSTAL SPECIMENS*

In the previous chapter, we have developed a general theoretical procedure based on Magnus expansion approach for the construction of composite pulses in NQR spectroscopy. This chapter deals with the procedure for deriving composite $\pi/2$ and composite π pulses that can compensate for efg and rf field inhomogeneities in pure NQR spectroscopy of single crystals containing spin I = 1 nuclei.

This chapter is organized as follows. Section III.A presents the Hamiltonians that represent the various interactions present in the model system assumed for our theoretical study and they have been expressed in terms of fictitious spin-1/2 operators. Construction of composite pulses that overcome the problems of efg and rf field inhomogeneities through the Magnus expansion technique and the examination of composite pulses have been presented in Section III.B. Section III.C covers the derivation of phase alternating composite pulse sequences (PACPS) and their performance with respect to offset or efg inhomogeneity effects.

---

*Part of the material in this chapter has been published in J. Molec. Struct. 192, 333 (1989).

III.A Hamiltonian of the Spin System

We consider an assembly of non-interacting, physically equivalent spin I = 1 quadrupole nuclei in the absence of a Zeeman field. Only the following interactions are taken into account in the model system assumed here, quadrupole interaction, $\mathcal{H}_Q$, various interactions as defined in Chapter I which lead to efg inhomogeneity, rf interaction, the inhomogeneity in the applied rf field. Since only physically equivalent spins are considered, we can define a common quadrupole principal axis system (QPAS)[1] for the total spin system. For simplicity, coincidence of QPAS and laboratory frames is assumed. Although it would seem to be a crude approximation to consider the spins as an ensemble of isolated non-interacting single spins, it is a good starting point for constructing composite pulses for NQR spectroscopy. In what follows, spin Hamiltonians are explained in detail.

III.A.1 Quadrupole Hamiltonian

A general form of the quadrupole Hamiltonian, $\mathcal{H}_Q$, for a spin I nucleus in terms of cartesian angular momentum operators is given in Chapter I (vide Eqn. (I.1)). For spin I = 1 nucleus, $\mathcal{H}_Q$, can be written as[1]

$$\mathcal{H}_Q = \frac{e^2qQ}{4} \left(3I_z^2 - I^2 + \eta(I_x^2 - I_y^2)\right) \qquad .. \text{(III.1)}$$

In the present spin 1 theoretical analysis, we use the fictitious spin-1/2 operator formalism of Vega and Pines[2] as a basic mathematical tool. This formalism is explained in Appendix A. Using

fictitious spin-1/2 operators, $\mathcal{H}_Q$ is expressed in QPAS by

$$\mathcal{H}_Q = \frac{e^2qQ}{2} \left(I_{X3} - I_{Y3} - I_{Z3}\right) . \qquad .. \text{(III.2)}$$

Following Cantor and Waugh,[3] we write

$$\mathcal{H}_Q = \omega_p I_{p3} + \omega_p' I_{p4} \; ; \quad p = X, Y, Z \qquad .. \text{(III.3)}$$

where
$$\omega_X = \frac{e^2qQ}{4} (\eta + 3) \; ; \quad \omega_X' = \frac{e^2qQ}{4} (\eta - 1) \qquad .. \text{(III.4a)}$$

$$\omega_Y = \frac{e^2qQ}{4} (\eta - 3) \; ; \quad \omega_Y' = \frac{-e^2qQ}{4} (\eta + 1) \qquad .. \text{(III.4b)}$$

$$\omega_Z = \frac{-e^2qQ}{2} \eta \; ; \quad \omega_Z' = \frac{e^2qQ}{2} \qquad .. \text{(III.4c)}$$

The energy level diagrams along with energies, transition frequencies and wave functions for a quadrupole nucleus of spin I = 1 in zero magnetic field are given in Figure III.1 for $\eta = 0$ and $\eta \neq 0$ cases. ω_X, ω_Y and ω_Z are the three pure quadrupole resonance frequencies indicated in Figure III.1. In FT NQR, at a time one deals with only one transition,[3] we consider here the transition with frequency ω_X (see Figure III.1) and let $\omega_X = \omega_Q$; $\omega_X' = \omega_Q'$. Now Eqn. (III.3) becomes

$$\mathcal{H}_Q = \omega_Q I_{X3} + \omega_Q' I_{X4} . \qquad .. \text{(III.5)}$$

III.A.2 <u>EFG Inhomogeneity Hamiltonian</u>

Various mechanisms which lead to efg inhomogeneity and broadening of NQR lines have been discussed in Chapter I. We

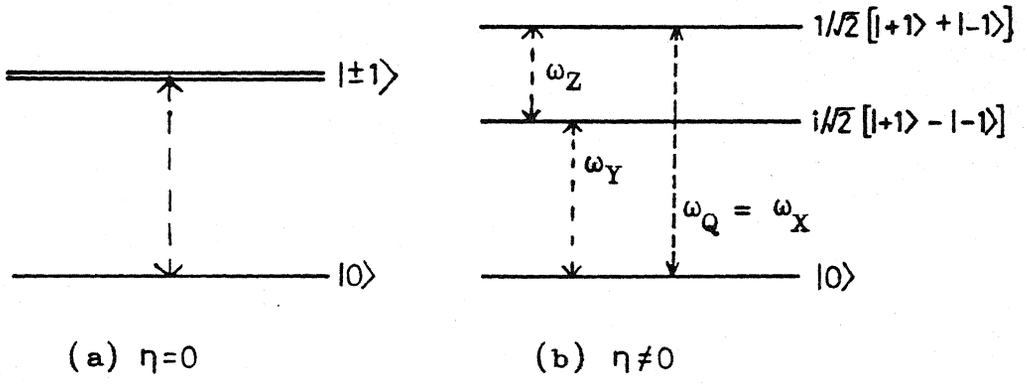

(a) $\eta=0$ (b) $\eta\neq0$

Figure III.1 Energy levels and wave functions for a quadrupole nucleus of spin I = 1 in the absence of a Zeeman field, (a) $\eta = 0$ and (b) $\eta \neq 0$ cases.

represent δq to be the spread in efg and $\Delta\omega_p$ to be the frequency distribution or resonance offset parameter. Now, the efg inhomogeneity Hamiltonian, V_1, in QPAS is given by

$$V_1 = \Delta\omega_p I_{X3} + \Delta\omega'_p I_{X4} \quad ; \; p = X, Y, Z \; . \qquad .. \text{(III.6)}$$

Substitution of δq for q in ω_p and ω'_p gives expressions for $\Delta\omega_p$ and $\Delta\omega'_p$, respectively. As it has been explained in Chapter II, QIF[4] is the reference frame in NQR spectroscopy and in QIF, the transformed efg inhomogeneity Hamiltonian V_1 is

$$\tilde{V}_1 = U_Q^{-1} V_1 U_Q = V_1 \quad ; [U_Q, V_1] = 0 \; . \qquad .. \text{(III.7)}$$

A more explicit expression for U_Q is given in Eqn. (II.12).

III.A.3 RF Hamiltonian

Writing the rf Hamiltonian (Eqn. (II.10)) in terms of fictitious spin-1/2 operators in QPAS we get,

$$\mathcal{H}_{rf} = -4\omega_1 \cos(\omega_p t + \phi(t))\, I_{p1} \qquad .. \text{(III.8)}$$

where $\omega_1 = \gamma H_1$ (rad/sec). γ is the gyromagnetic ratio of the nucleus and H_1 is the rf field magnitude in units of Gauss. In QIF,

$$\tilde{\mathcal{H}}_{rf} = U_Q^{-1}\, \mathcal{H}_{rf}\, U_Q$$

$$= -4\omega_1 \cos(\omega_p t + \phi(t)) \exp[(i\mathcal{H}_Q t)\, I_{p1} \exp(-i\mathcal{H}_Q t)] \qquad .. \text{(III.9)}$$

where $\exp(-i\mathcal{H}_Q t) = \exp(-i\omega_p I_{X3} t) \exp(-i\omega_p' I_{X4} t)$ . .. (III.10)

In writing this expression, we have used the property $[I_{p3}, I_{p4}] = 0$. To evaluate the transformation property of I_{p1} under $\mathcal{H}_Q$, we use the commutation relationships given in Appendix A. Applying the nested commutation relationship (Eqn. (I.21)), $\tilde{\mathcal{H}}_{rf}$ becomes

$$\tilde{\mathcal{H}}_{rf} = -4\omega_1 \cos(\omega_p t + \phi(t))[I_{p1} \cos\omega_p t - I_{p2} \sin\omega_p t]. \qquad .. \text{(III.11)}$$

Selecting only one frequency i.e., $\omega_p = \omega_Q$,

$$\tilde{\mathcal{H}}_{rf} = -4\omega_1 \Big\{ I_{X1}\Big[\cos^2\omega_Q t - \frac{\sin(2\omega_Q t)}{2}\Big] \cos\phi(t) - I_{X2}\Big[\frac{\sin(2\omega_Q t)}{2} + \sin^2\omega_Q t\Big] \sin\phi(t) \Big\}. \qquad .. \text{(III.12)}$$

Now, truncating high frequency terms, we obtain

$$\tilde{\mathcal{H}}_{rf} = -2\omega_1[I_{X1} \cos\phi(t) - I_{X2} \sin\phi(t)] \; . \qquad .. \text{(III.13)}$$

III.A.4 RF Field Inhomogeneity Hamiltonian

Denoting $\Delta\omega_1 = \gamma \Delta H_1$ to be the inhomogeneity in rf field strength, the rf field inhomogeneity Hamiltonian, V_2, in QPAS can be written as

$$V_2 = -4 \Delta\omega_1 \cos[\omega_p t + \phi(t)] I_{p1} \quad .. \text{(III.14)}$$

In QIF,

$$\tilde{V}_2 = -2 \Delta\omega_1 [I_{X1} \cos\phi(t) - I_{X2} \sin\phi(t)] . \quad .. \text{(III.15)}$$

The total Hamiltonian of the spin system in QIF is (refer Appendix C)

$$\tilde{\mathcal{H}} = \tilde{\mathcal{H}}_{rf} + \tilde{V}_1 + \tilde{V}_2 . \quad .. \text{(III.16)}$$

After thus representing spin Hamiltonians in terms of fictitious spin-1/2 operators[2] in the observation frame (QIF), in the next section, we shall design composite pulses based on Magnus expansion approximation[5] for spin 1 NQR spectroscopy.[6]

III.B Composite Pulses for Spin 1 NQR

The importance of composite pulses in NQR spectroscopy has been highlighted in Chapter I. Various routes[7-9] of designing composite pulses for NQR have been analyzed in Chapter II. In the area of NMR one already has, at present, composite pulses starting with a minimum of two pulses going upto several pulses, typically nine pulses.[8] But in NQR, the application of such

longer time duration composite pulses is limited by shorter T_2. Therefore, we confine ourselves to construct two and three pulse composite pulse sequences. We denote the composite pulse sequence as $(\theta_1)\phi_1$-$(\theta_2)\phi_2$-$(\theta_3)\phi_3$, where $(\theta_n)\phi_n$ represents nth-rf pulse in the sequence with flip angle θ_n and phase ϕ_n.

III.B.1 Composite Pulses for the Compensation of efg Inhomogeneity

Since the inclusion of higher-order Magnus terms usually results in a longer time duration composite pulse,[9] we consider only the main term, namely, zeroth-order term in the Magnus series. In the next subsection, we present zeroth-order composite pulses for overcoming efg inhomogeneity.

III.B.1(i) Design of Zeroth-Order Composite Pulses

In QIF, the net Hamiltonian is given by

$$\tilde{\mathcal{H}} = \tilde{\mathcal{H}}_{rf} + \tilde{V}_1 \ . \qquad .. \ (II.17)$$

Using the idea of 'toggling frame',[10] we arrive at (Chapter II)

$$U = U_{rf}(t)\ U_{V_1}(t) \ . \qquad .. \ (II.18)$$

The rf propagator corresponding to different time intervals for a three pulse sequence is given below:

$$U_{rf}(t) = \begin{cases} \exp(2i\omega_1 t_1 I_{X1}), & \ldots \quad 0 \le t_1 \le \frac{\theta_1}{2\omega_1} \\ \exp(i\phi_2 I_{X3})\ \exp(2i\omega_1 t_2 I_{X1})\ \exp(-i\phi_2 I_{X3})\ \exp(i\theta_1 I_{X1}), & \ldots \quad 0 \le t_2 \le \frac{\theta_2}{2\omega_1} \\ \exp(i\phi_3 I_{X3})\ \exp(2i\omega_1 t_3 I_{X1})\ \exp(-i\phi_3 I_{X3})\ \exp(i\phi_2 I_{X3})\ \exp(i\theta_2 I_{X1})\ \exp(-i\phi_2 I_{X3})\ \exp(i\theta_1 I_{X1}), & \ldots \quad 0 \le t_3 \le \frac{\theta_3}{2\omega_1} \end{cases}$$

where t_n denotes the nth-rf pulse width.

In writing the above equation, we have made use of the following points:

(a) phase of the first rf pulse in the composite pulse sequence is assumed to be a reference rf phase of the sequence and it has been set to zero i.e., $\phi_1 = 0$. Alternatively, one can assume the phase of any one of the rf pulses to be the reference-phase.

(b) In the presence of non-zero phase ($\phi_n \neq 0$), the rf Hamiltonian, $\tilde{\mathcal{H}}_{rf}$ (Eqn.III.13) contains two operators, namely, I_{X1} and I_{X2}. Since $[I_{X1}, I_{X2}] \neq 0$, we make a transformation to a new frame defined by the unitary operator, $U = \exp(i\phi_n I_{X3})$. In the new frame, the transformed rf Hamiltonian is $\tilde{\mathcal{H}}'_{rf} = -2\omega_1 I_{X1}$. During each rf pulse, we take the spin system to this new frame which depend on the phase of the corresponding rf pulse and we bring back the spin system to QIF after the effect of $\tilde{\mathcal{H}}'_{rf}$ interaction. This procedure simplfies

the evolution of the spin dynamics under the action of $U_{rf}(t)$. Note that when the rf phase $\phi_n = 0$, the new frame and QIF coincide.

(c) The flip angle of an rf pulse is stated as

θ_n = effective rf field strength multiplied by the pulse width

$$= 2\omega_1 t_n \qquad .. \text{(III.20)}$$

θ_n is commonly given in radians.

The net evolution of the spin system in the toggling frame is given by

$$U_{V_1}(t) = T \exp\left[-i \int_o^t dt' \tilde{\tilde{V}}_1(t')\right] \qquad .. \text{(III.21)}$$

$\tilde{\tilde{V}}_1(t)$ is the complete Hamiltonian or the transformed efg inhomogeneity Hamiltonian in the toggling frame and clearly, it is time dependent. $\tilde{\tilde{V}}_1(t)$ has been derived using the rf propagator in Eqn. (III.19) to be[6]

$$\tilde{\tilde{V}}_1(t) = \Delta\omega_Q \left[a(t)I_{X1} + b(t)I_{X2} + C(t)I_{X3}\right] + \Delta\omega_Q' I_{X4} \qquad .. \text{(III.22)}$$

Since $[I_{X4}, \rho(0)] = 0$, the last term in the above equation does not effect the spin system. Therefore, we write

$$\tilde{\tilde{V}}_1(t) = \Delta\omega_Q\left[(a(t)I_{X1} + b(t)I_{X2} + c(t)I_{X3})\right] \qquad .. \text{(III.23)}$$

where the coefficients a(t), b(t) and c(t) are time dependent and they can be given in terms of θ_n and ϕ_n at different time intervals of the pulse sequence as

$$a(t) = \begin{cases} 0, & .. \; 0 \le t_1 \le \dfrac{\theta_1}{2\omega_1} \\ -\sin(2\omega_1 t_2)\sin\phi_2, & .. \; 0 \le t_2 \le \dfrac{\theta_2}{2\omega_1} \\ \sin(2\omega_1 t_3)\,[\frac{1}{2}\sin(2\phi_2)\cos\phi_3\,(1-\cos\theta_2) & \\ \quad -\sin\phi_3(\cos^2\phi_2 + \sin^2\phi_2\cos\theta_2)] & .. \; 0 \le t_3 \le \dfrac{\theta_3}{2\omega_1} \\ \quad -\cos(2\omega_1 t_3)\sin\theta_2\sin\phi_2 & \end{cases}$$

.. (III.24)

$$b(t) = \begin{cases} -\sin(2\omega_1 t_1), & .. \; 0 \le t_1 \le \dfrac{\theta_1}{2\omega_1} \\ -\cos(2\omega_1 t_2)\sin\theta_1 - \sin(2\omega_1 t_2)\cos\phi_2\cos\theta_1, & .. \; 0 \le t_2 \le \dfrac{\theta_2}{2\omega_1} \\ \cos\theta_1[-\cos\phi_2\sin\theta_2\cos(2\omega_1 t_3) & \\ \quad -\cos^2\phi_2\cos\theta_2\sin(2\omega_1 t_3)\cos\phi_3 & \\ \quad -\frac{1}{2}\sin(2\phi_2)\cos\theta_2\sin(2\omega_1 t_3)\sin\phi_3 & \\ \quad -\sin^2\phi_2\sin(2\omega_1 t_3)\cos\phi_3 & .. \; 0 \le t_3 \le \dfrac{\theta_3}{2\omega_1} \\ \quad +\frac{1}{2}\sin(2\phi_2)\sin(2\omega_1 t_3)\sin\phi_3] & \\ -\sin\theta_1[\cos\theta_2\cos(2\omega_1 t_3) - \sin\theta_2\sin(2\omega_1 t_3). & \\ \qquad .\cos(\phi_2+\phi_3)] & \end{cases}$$

.. (III.25)

and

$$C(t) = \begin{cases} \cos(2\omega_1 t_1), & .. \; 0 \le t_1 \le \dfrac{\theta_1}{2\omega_1} \\ \cos(2\omega_1 t_2)\cos\theta_1 - \sin(2\omega_1 t_2)\cos\phi_2 \sin\theta_1, & .. \; 0 \le t_2 \le \dfrac{\theta_2}{2\omega_1} \\ \left.\begin{aligned} &-\sin\theta_1 \cos\phi_2[\sin\theta_2 \cos(2\omega_1 t_3) \\ &\quad +\cos\theta_2 \sin(2\omega_1 t_3)\cos(\phi_2+\phi_3)] \\ &\quad -\sin\theta_1\sin\phi_2\sin(2\omega_1 t_3)\sin(\phi_2-\phi_3) \\ &\quad +\cos\theta_1\cos\theta_2\cos(2\omega_1 t_3) \\ &\quad -\cos\theta_1\sin\theta_2\sin(2\omega_1 t_3)\cos(\phi_2+\phi_3) \end{aligned}\right\} & .. \; 0 \le t_3 \le \dfrac{\theta_3}{2\omega_1} \end{cases}$$

.. (III.26)

As it has been discussed in Chapter II, we apply the Magnus expansion approximation[5] to get an effective time independent efg Hamiltonian in the toggling frame. $\tilde{\tilde{V}}_1(t)$ can be expanded into an infinite series

$$\tilde{\tilde{V}}_1(t) = V_1^{(0)} + V_1^{(1)} + V_1^{(2)} + ... \qquad .. \text{(III.27)}$$

where $V_1^{(n)}$ is the nth-order term in the Magnus expansion. The explicit expression for the zeroth- and first-order terms are given in Chapter I (Eqns. (I.25) and (I.26)) and higher order terms are also available in literature.[5,11] Now, according to the Magnus expansion approach[9] (Chapter II), a zeroth-order composite pulse is one which has $V_1^{(0)} = 0$. In this zeroth-order approximation, we truncate the higher order terms whose contribution would be negligibly small when compared with the main term $V_1^{(0)}$. $V_1^{(0)}$ for a three pulse composite pulse sequence can be obtained

by integrating equations (III.24), (III.25) and (III.26) with respective time intervals of the sequence. $V_1^{(0)}$ on integration or, alternatively, 'time-averaged' in the language of AHT,[10] turns out to be[6]

$$V_1^{(0)} = \frac{\Delta\omega_Q}{2\omega_1}\left[a\, I_{X1} + b\, I_{X2} + c\, I_{X3}\right] \qquad .. \text{(III.28)}$$

Now the coefficients are time independent constants for a given rf pulse sequence; otherwise, they are dependent on θ_n and ϕ_n for an arbitrary pulse sequence. Explicit expressions for a, b and c have been derived and are presented below.

$$\begin{aligned} a = {} & \sin\phi_2\,(\cos\theta_2 - \sin\theta_2\sin\theta_3 - 1) \\ & + (\cos\theta_3 - 1)\left[\cos^2\phi_2\sin\phi_3 + \tfrac{1}{2}\cos\theta_2\,\sin 2\phi_2\,\cos\phi_3 + \right. \\ & \left. + \cos\theta_2\sin\phi_3\sin^2\phi_2 - \tfrac{1}{2}\cos\phi_3\,\sin 2\phi_2\right] \end{aligned} \qquad .. \text{(III.29)}$$

$$\begin{aligned} b = {} & \cos\theta_1 - 1 - \sin\theta_1(\sin\theta_2 + \cos\theta_2\sin\theta_3) \\ & + \cos\theta_1\cos\phi_2(\cos\theta_2 - 1 - \sin\theta_2\sin\theta_3) \\ & + (\cos\theta_3 - 1)\left[-\sin\theta_1\sin\theta_2\cos(\phi_2+\phi_3)\right. \\ & \qquad + \cos\theta_1\cos\phi_3(\cos\theta_2\cos^2\phi_2 + \sin^2\phi_2) \\ & \qquad \left. + \tfrac{1}{2}\cos\theta_1\sin 2\phi_2\sin\phi_3\,(\cos\theta_2 + 1)\right] \end{aligned} \qquad .. \text{(III.30)}$$

and

$$\begin{aligned} c = {} & \cos\theta_1(\sin\theta_2 + \cos\theta_2\sin\theta_3) + \sin\theta_1 \\ & + \sin\theta_1\cos\phi_2(\cos\theta_2 - \sin\theta_2\sin\theta_3 - 1) \\ & + (\cos\theta_3 - 1)\left[\sin\theta_1\sin\phi_2\sin(\phi_2-\phi_3)\right. \\ & \qquad + \sin\theta_1\cos\theta_2\cos\phi_2\cos(\phi_2-\phi_3) \\ & \qquad \left. + \cos\theta_1\sin\theta_2\cos(\phi_2-\phi_3)\right] \end{aligned} \qquad .. \text{(III.31)}$$

For a zeroth-order composite pulse sequence with $V_1^{(0)} = 0$, a, b, and c should vanish identically. We have optimized θ_n and ϕ_n for a three-pulse sequence to get $V_1^{(0)} = 0$ and we have arrived at a composite inversion π pulse, namely, $(90)_0$-$(270)_{90}$-$(90)_0$. However, it is a difficult task to get sequences with $V_1^{(0)} = 0$ by varying θ_n and ϕ_n. To reduce this complexity, we have relaxed the condition from $V_1^{(0)} = 0$ to

$$[V_1^{(0)}, \rho(0)] = 0 \qquad .. \text{(III.32)}$$

According to this new condition[6] $V_1^{(0)}$ does not necessarily have to be zero but if $V_1^{(0)}$ or $U_{V_1}(t)$ commutes with the thermal equilibrium density matrix, $\rho(0)$, then the spin system will not evolve under the efg inhomogeneity Hamiltonian. Hence, a uniform broadband excitation would be achieved. This condition demands only a and b to be zero independently. However, it is felt, even at this stage, it is not easy to derive many better sequences for our purpose. So, we have obtained sequences with even smaller terms of a and b as composite pulses.[6] Thus, we could arrive at the following sequences: $(90)_0$-$(225)_{180}$-$(315)_0$ has been found to be a composite inversion π pulse. $(90)_0$-$(300)_{90}$ and $(385)_0$-$(320)_{180}$-$(25)_0$ are derived for composite $\pi/2$ pulses.[6] A summary of zeroth-order terms in the Magnus expansion associated with these pulse sequences is presented in Table III.1. In what follows, we test the behaviour of the abovementioned composite pulses.

Table III.1 Zeroth-Order Magnus Expansion term for different NQR Composite Pulse Sequences that Compensate efg Inhomogeneity in the Spin I = 1 Case

Composite pulse	Zeroth-order Magnus expansion term, $V_1^{(0)}$
(a) Composite $\pi/2$ pulses:	
i) $(90)_0-(300)_{90}$	$\Delta\omega_Q [-0.0734\ I_{X_1} - 0.0197\ I_{X_2} + 0.1469\ I_{X_3}]$
ii) $(385)_0-(320)_{180}-(25)_0$	$\Delta\omega_Q [-0.0026\ I_{X_2} + 0.0026\ I_{X_3}]$
(b) Composite π pulses:	
i) $(90)_0-(270)_{90}-(90)_0$	0
ii) $(90)_0-(225)_{180}-(315)_0$	$\Delta\omega_Q [-0.0533\ I_{X_2} + 0.3105\ I_{X_3}]$

III.B.1(ii) Evaluation of the Performance of Composite Pulses as a Function of EFG Inhomogeneity

It is necessary to know the extent of compensation against efg inhomogeneity for a given composite pulse sequence. It can be obtained by evaluating the time evolution of the thermal equilibrium density matrix $\rho(0)$, under the simultaneous effect of the rf pulse in the sequence and the efg inhomogeneity.[6] The complete Hamiltonian of the spin ensemble in QIF can be written as

$$\tilde{\mathcal{H}} = -2\omega_1[I_{X1}\cos\phi_n - I_{X2}\sin\phi_n] + \Delta\omega_Q I_{X3} + \Delta\omega_Q' I_{X4} \quad .. \text{(III.33)}$$

$$\text{since } [I_{X4}, I_{Xi}] = [I_{X4}, \rho(0)] = 0 \; ; \; i = 1, 2, 3 . \quad .. \text{(III.34)}$$

We drop the I_{X4} term which is not effective in the spin evolution. Now, $\tilde{\mathcal{H}}$ is given by

$$\tilde{\mathcal{H}} = -2\omega_1[I_{X1}\cos\phi_n - I_{X2}\sin\phi_n] + \Delta\omega_Q I_{X3} . \quad .. \text{(III.35)}$$

Since the two terms in the above equation do not commute, to simplify our calculations we diagonalise $\tilde{\mathcal{H}}$. This is done in two steps.[6] First, a transformation by a unitary operator, namely, $\exp(-i\phi_n I_{X3})$, followed by a transformation with $\exp(-i\beta I_{X2})$, where $\beta = \tan^{-1}(2\omega_1/\Delta\omega_Q)$. Now, the diagonalised Hamiltonian is

$$\tilde{\mathcal{H}}^d = \exp(-i\beta I_{X2})\exp(-i\phi_n I_{X3})\,\tilde{\mathcal{H}}\exp(i\phi_n I_{X3})\exp(i\beta I_{X2})$$

$$= [2\omega_1\sin\beta + \Delta\omega_Q\cos\beta]I_{X3} = \frac{\alpha_n I_{X3}}{t_n} , \quad .. \text{(III.36)}$$

where

$$\alpha_n = t_n(2\omega_1 \sin\beta + \Delta\omega_Q \cos\beta) \quad .. \text{(III.37)}$$

is the effective flip angle of an rf pulse in the presence of efg inhomogeneity. In deriving $\tilde{\mathcal{H}}^d$, we have used the commutation relationships given in Appendix A. Essentially, the Hamiltonian $\tilde{\mathcal{H}}$ is transferred to a diagonal frame and back to QIF during each rf pulse in the sequence. The net propagator given by Eqn. (II.16) becomes, for an rf pulse in the sequence,

$$U_n(t) = \exp(i\phi_n I_{X3}) \exp(i\beta I_{X2}) \exp(-i\alpha_n I_{X3}) \exp(-i\beta I_{X2}) \exp(-i\phi_n I_{X3}) \quad .. \text{(III.38)}$$

The complete propagator representing a N-pulse composite pulse sequence is given by the product of individual rf pulse propagators time-ordered by the Dyson operator[10] as

$$U(t) = U_N\, U_{N-1} \ldots U_n \ldots U_3\, U_2\, U_1 \quad .. \text{(III.39)}$$

For a three-pulse sequence that has been considered in the present work of the type $(\theta_1)_{\phi_1}\text{-}(\theta_2)_{\phi_2}\text{-}(\theta_3)_{\phi_3}$, we write

$$\begin{aligned} U(t) = {} & \exp(i\phi_3 I_{X3}) \exp(i\beta I_{X2}) \exp(i\alpha_3 I_{X3}) \exp(-i\beta I_{X2}) \\ & \exp[\, i(\phi_2-\phi_3)\, I_{X3}] \exp(i\beta I_{X2}) \exp(-i\alpha_2 I_{X3}) \\ & \exp(-i\beta I_{X2}) \exp[\, i(\phi_1-\phi_2) I_{X3}\,] \exp(i\beta I_{X2}) \\ & \exp(i\alpha_1 I_{X3}) \exp(-i\beta I_{X2}) \exp(-i\phi_1 I_{X3}) \end{aligned} \quad .. \text{(III.40)}$$

Now using this time evolution propagator, the expression for the density matrix at the end of the composite pulse sequence $\tilde{\rho}(t)$

can be evaluated (Eqn. II.17). Therefore, the performance of a composite $\pi/2$ pulse is given by the intensity of the NQR signal as (Appendix D) (Eqn. II.27),

$$W_1 = \frac{Tr[I_{X2}, \tilde{\rho}(t)]}{Tr[I_{X2}^2]}$$

$$= \cos\phi_3[b_1\sin\alpha_3 + b_2\cos\alpha_3]$$

$$-\sin\phi_3[-b_3\sin\beta + b_1\cos\beta\cos\alpha_3 - b_2\cos\beta\sin\alpha_3] \quad .. \text{(III.41)}$$

where I_{X2} is the observable operator in QIF and this has been derived and explained in Appendix D.

Similarly, the performance of a composite inversion π pulse is given by (Eqn. (II.28))

$$W_2 = \frac{-Tr[I_{X3}, \tilde{\rho}(t)]}{Tr[I_{X3}^2]}$$

$$= b_3\cos\beta + b_1\sin\beta\cos\alpha_3 - b_2\sin\beta\sin\alpha_3 \quad .. \text{(II.42)}$$

where

$$b_1 = \cos\beta\cos(\phi_2-\phi_3)[a_1\cos\beta\cos\alpha_2 - a_2\cos\beta\sin\alpha_2 - a_3\sin\beta]$$

$$+ \cos\beta\sin(\phi_2-\phi_3)[a_1\sin\alpha_2 + a_2\cos\alpha_2]$$

$$+ \sin\beta[a_1\sin\beta\cos\alpha_2 - a_2\sin\beta\sin\alpha_2 + a_3\cos\beta] \quad .. \text{(II.43)}$$

$$b_2 = \cos(\phi_2-\phi_3)[a_1\sin\alpha_2 + a_2\cos\alpha_2]$$

$$+ \sin(\phi_2-\phi_3)[-a_1\cos\beta\cos\alpha_2 + a_2\cos\beta\sin\alpha_2 + a_3\sin\beta]$$

$$.. \text{(II.44)}$$

$$b_3 = \sin\beta\cos(\phi_2-\phi_3)[-a_1\cos\beta\cos\alpha_2 + a_2\cos\beta\sin\alpha_2 + a_3\sin\beta]$$

$$-\sin\beta\sin(\phi_2-\phi_3)[a_1\sin\alpha_2 + a_2\cos\alpha_2]$$

$$+\cos\beta[a_1\sin\beta\cos\alpha_2 - a_2\sin\beta\sin\alpha_2 + a_3\cos\beta] \quad .. \text{(III.45)}$$

$$a_1 = \frac{1}{2}\sin 2\beta[\sin\alpha_1\sin(\phi_1-\phi_2) + \cos\beta\cos(\phi_1-\phi_2)(\cos\alpha_1-1)]$$

$$+ \sin^2\beta[\cos^2\beta + \cos\alpha_1\sin^2\beta] \quad .. \text{(III.46)}$$

$$a_2 = \sin\beta[\sin\alpha_1\cos(\phi_1-\phi_2) + \cos\beta\sin(\phi_1-\phi_2)(1-\cos\alpha_1)]$$

.. (III.47)

and

$$a_3 = -\sin^2\beta[\sin\alpha_1\sin(\phi_1-\phi_2) + \cos\beta\cos(\phi_1-\phi_2)(\cos\alpha_1-1)]$$

$$+\cos\beta[\cos^2\beta + \cos\alpha_1\sin^2\beta] \quad .. \text{(III.48)}$$

The performance of composite $\pi/2$ pulses is compared with that of a single $\pi/2$ pulse with respect to their ability to compensate for efg inhomogeneity. In Figure III.2 the signal response is plotted as a function of $\Delta\omega_Q$ which is expressed in ω_1 units. In Figure III.3, we compare the inversion efficiency of composite inversion π pulses with that of a single π pulse as a function of the efg inhomogeneity parameter.

III.B.2 Composite Pulses for the Compensation of RF Field Inhomogeneity

III.B.2(i) Design of Zeroth-Order Composite Pulses

The net Hamiltonian in QIF is given by

$$\tilde{\mathcal{H}} = \tilde{\mathcal{H}}_{rf} + \tilde{V}_2 \quad .. \text{(III.49)}$$

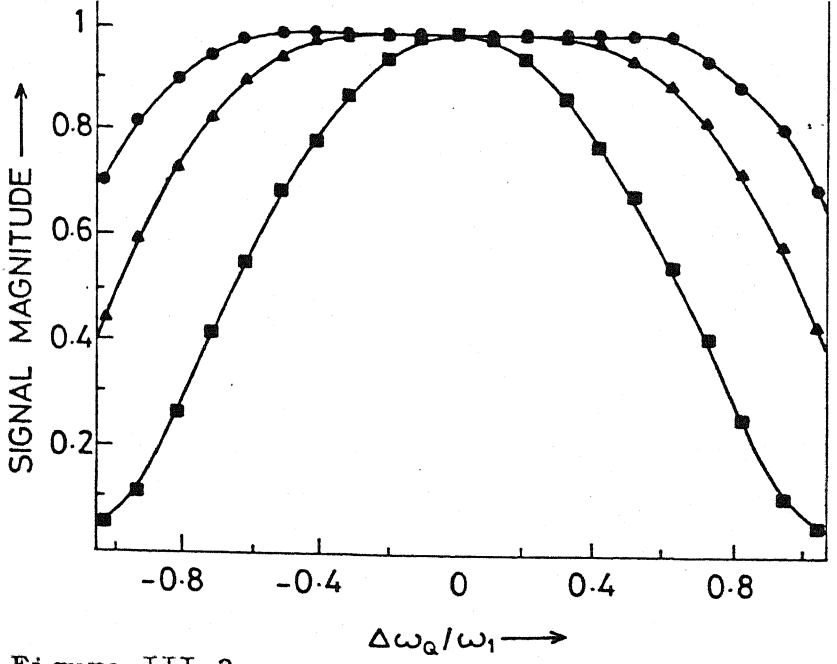

Figure III.3

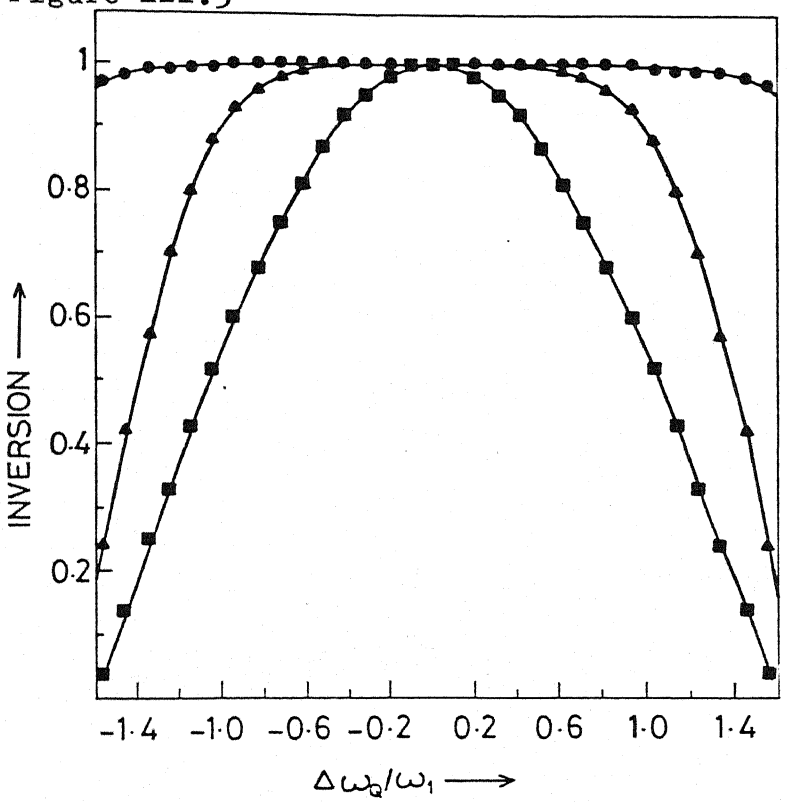

Figure III.2 The signal magnitude as a function of $\Delta\omega_Q/\omega_1$ for a single $\pi/2$ pulse (squares), the zeroth-order composite pulses $(90)_0$-$(300)_{90}$ (circles) and $(385)_0$-$(320)_{180}$-$(25)_0$ (triangles).

Figure III.3 The extent of the inversion of spin population, as a function of $\Delta\omega_Q/\omega_1$ for a single π pulse (squares), the zeroth-order composite pulses $(90)_0$-$(270)_{90}$-$(90)_0$ (triangles) and $(90)_0$-$(225)_{180}$-$(315)_0$ (circles).

In the toggling frame defined by $U_{rf}(t)$ (Eqn. (III.19)), we have

$$\tilde{\tilde{\mathcal{H}}} = \tilde{\tilde{V}}_2(t) \qquad .. \text{(III.50)}$$

The net evolution in QIF is written as

$$U(t) = U_{rf}(t)\, U_{V_2}(t) \qquad .. \text{(III.51)}$$

$$\text{where } U_{V_2}(t) = T \exp\left[-i \int_0^t dt'\, \tilde{\tilde{V}}_2(t')\right] \qquad .. \text{(III.52)}$$

$\tilde{\tilde{V}}_2(t)$ has been derived using the commutation relations given in Appendix A as[6]

$$\tilde{\tilde{V}}_2(t) = -2\Delta\omega_1 [a'(t)\, I_{X1} + b'(t)\, I_{X2} + c'(t)\, I_{X3}] \qquad .. \text{(III.53)}$$

The coefficients in the above equation at respective time intervals are given below:

$$a'(t) = \begin{cases} 1 & , \quad .. \quad 0 \le t_1 \le \dfrac{\theta_1}{2\omega_1} \\ \cos\phi_2 & , \quad .. \quad 0 \le t_2 \le \dfrac{\theta_2}{2\omega_1} \\ (A_1 \cos\phi_2 + A_2 \sin\phi_2) & , \quad .. \quad 0 \le t_3 \le \dfrac{\theta_3}{2\omega_1} \end{cases} \qquad .. \text{(III.54)}$$

$$b'(t) = \begin{cases} 0 & , \quad .. \quad 0 \le t_1 \le \dfrac{\theta_1}{2\omega_1} \\ -\cos\theta_1 \sin\phi_2 & , \quad .. \quad 0 \le t_2 \le \dfrac{\theta_2}{2\omega_1} \\ \cos\theta_1 [A_2 \cos\phi_2 - A_1 \sin\phi_2] - A_3 \sin\theta_1 & , \quad .. \quad 0 \le t_3 \le \dfrac{\theta_3}{2\omega_1} \end{cases} \qquad .. \text{(III.55)}$$

and

$$c'(t) = \begin{cases} 0 & , \quad .. \; 0 \leq t_1 \leq \dfrac{\theta_1}{2\omega_1} \\ -\sin\theta_1 \sin\phi_2 & , \quad .. \; 0 \leq t_2 \leq \dfrac{\theta_2}{2\omega_1} \\ [-A_1 \sin\phi_2 + A_2 \cos\phi_2]\sin\theta_1 + A_3 \cos\theta_1 & , \quad .. \; 0 \leq t_3 \leq \dfrac{\theta_3}{2\omega_1} \end{cases}$$

.. (III.56)

where $A_1 = \cos(\phi_2 - \phi_3)$,

$A_2 = \cos\theta_2 \sin(\phi_2 - \phi_3)$

and $A_3 = \sin\theta_2 \sin(\phi_2 - \phi_3)$.

The time dependent rf field inhomogeneity Hamiltonian, $\approx\!\!\!\!\!\sim \bar{V}_2(t)$ can be expanded using the Magnus expansion approximation[5] as given by

$$\approx\!\!\!\!\!\sim \bar{V}_2(t) = V_2^{(0)} + V_2^{(1)} + V_2^{(2)} + \ldots \qquad .. \text{ (III.57)}$$

To derive zeroth-order composite pulses,[7] $V_2^{(0)}$ (Eqn. (I.25)) has been derived by time-averaging Eqns. (III.54), (III.55) and (III.56) at respective time intervals to get

$$V_2^{(0)} = \frac{-\Delta\omega_1}{\omega_1} \left[a' I_{X1} + b' I_{X2} + c' I_{X3}\right] \qquad .. \text{ (III.58)}$$

Now, $V_2^{(0)}$ is time independent, and the time independent coefficients are given below:

$$a' = \theta_1 + \theta_2 \cos\phi_2 + \theta_3 \cos\phi_2 \cos(\phi_2 - \phi_3) + \theta_3 \cos\theta_2 \sin\phi_2 \sin(\phi_2 - \phi_3) \qquad .. \text{ (III.59)}$$

$$b' = -\theta_2\cos\theta_1\sin\phi_2 + \theta_3\cos\theta_1\cos\theta_2\cos\phi_2\sin(\phi_2-\phi_3)$$
$$-\theta_3\sin\theta_1\sin\theta_2\sin(\phi_2-\phi_3) - \theta_3\cos\theta_1\sin\phi_2\cos(\phi_2-\phi_3) \quad .. \text{(III.60)}$$

and

$$c' = -\theta_2\sin\theta_1\sin\phi_2 - \theta_3\sin\theta_1\sin\phi_2\cos(\phi_2-\phi_3)$$
$$+ \theta_3\sin(\phi_2-\phi_3)\,[\cos\theta_1\sin\theta_2 + \sin\theta_1\cos\theta_2\cos\phi_2] \quad .. \text{(III.61)}$$

Now to satisfy the condition $V_2^{(0)} = 0$, we have varied the unknowns and found that $(180)_0$-$(180)_{120}$-$(180)_0$ is a composite π pulse. Similarly, variables have been chosen to satisfy the condition

$$[V_2^{(0)},\ \rho(0)] = 0 \quad .. \text{(III.62)}$$

This search produced two more sequences, namely, $(90)_0$-$(180)_{90}$-$(90)_0$ and $(90)_0$-$(360)_{120}$-$(90)_0$. Both these sequences are composite inversion π pulses. Zeroth-order Magnus expansion terms are given in Table III.2 for all the composite pulses constructed for compensating rf field inhomogeneity.

III.B.2(ii) Evaluation of the Performance of Composite Pulses as a Function of RF Field Inhomogeneity

Mathematical expressions to analyze the performance of composite pulses, viz., W_1' (Eqn. (II.27) and W_2' (Eqn. (II.28)), have been derived. These analytical expressions are very similar to Eqn. (III.41) and Eqn. (III.42). However, some minor modifications are needed to get W_1' and W_2' for the present case. They are: the effective flip angle α_n in Eqns. (III.41) and (III.42) has to

Table III.2 Zeroth-Order Magnus Expansion Term for Different NQR Composite Pulse Sequences that Compensate rf Field Inhomogeneity in the Spin I = 1 Case

Composite π pulse	Zeroth-order Magnus expansion term, $V_2^{(0)}$
i) $(90)_0-(180)_{90}-(90)_0$	$\Delta\omega_1 I_{X3}$
ii) $(180)_0-(180)_{120}-(180)_0$	0
iii) $(90)_0-(360)_{120}-(90)_0$	$1.1547\ \Delta\omega_1 I_{X3}$

be replaced by

$$\alpha_n = 2\, t_n\, (\omega_1 + \Delta\omega_1)\ , \qquad \text{.. (III.63)}$$

$\beta = 90^{\circ}$ and the efg inhomogeneity must be taken as zero, i.e., $\Delta\omega_Q = 0$. Using these expression, we have computer simulated the performance of composite π pulses given in Table III.2 as a function of rf field inhomogeneity.[6] They are shown in Figure III.4 along with single π pulse response for comparison.

III.B.3 Results and Discussion

Computer simulations presented in Figures III.2 - III.4 illustrate that the composite pulse sequences designed through the Magnus expansion approach to compensate for inhomogeneities of efg and rf field perform significantly better than the corresponding single rf pulse. From the analytical expressions of $V_1^{(0)}$ and $V_2^{(0)}$ given in Tables III.1 and III.2, respectively, one would expect that a pulse sequence with $V_n^{(0)}$ (n = 1 or 2) of smaller size should perform better than a pulse sequence with $V_n^{(0)}$ of larger size.[7] However, in our case, we note the following interesting points.

(i) The performance of the composite $\pi/2$ pulse $(90)_0$-$(300)_{90}$ with larger $V_1^{(0)}$ is better than that of $(385)_0$-$(320)_{180}$-$(25)_0$ with smaller $V_1^{(0)}$ (Figure III.2; Table III.1).

(ii) The composite inversion π pulse sequences $(90)_0$-$(225)_{180}$-$(315)_0$ with $V_1^{(0)} \neq 0$ shows better uniform population inversion than $(90)_0$-$(270)_{90}$-$(90)_0$ sequence with $V_1^{(0)} = 0$ (Figure III.3 ; Table III.1).

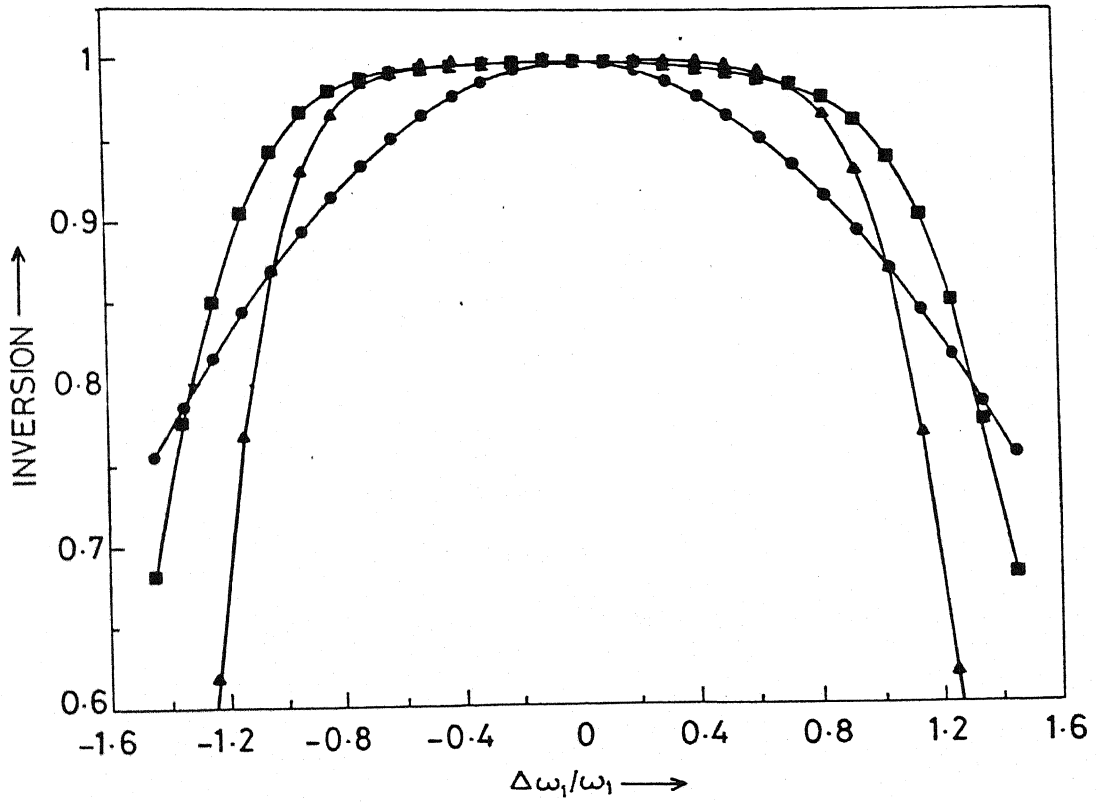

Figure III.4 The extent of the inversion of spin populations, as a function of $\Delta\omega_1/\omega_1$ for a π pulse (circles), the zeroth-order composite pulses $(90)_0$-$(180)_{90}$-$(90)_0$ (triangles) and $(180)_0$-$(180)_{120}$-$(180)_0$ or $(90)_0$-$(360)_{120}$-$(90)_0$ (squares).

(iii) Similarly in the sequence $(90)_0$-$(360)_{120}$-$(90)_0$ with larger $V_2^{(0)}$, the degree of compensation for the rf field inhomogeneity is larger than that of $(90)_0$-$(180)_{90}$-$(90)_0$ whose $V_2^{(0)}$ is of smaller size (Figure III.4; Table III.2). It may be pointed out here that for both these sequences $[V_2^{(0)}, \rho(0)] = 0$.

These results clearly reveal the importance of higher-order terms in the Magnus expansion which are not taken into account. It may be pointed out that the Magnus approximation[5] works well for small perturbations, that is, for $\mathcal{H}_{rf} \gg V_n$.[7,10] Further, Magnus expansion does not converge[12] for larger values of $\frac{\Delta\omega_Q}{\omega_1}$ or $\frac{\Delta\omega_1}{\omega_1}$ and the limitations of perturbation approach are inherent in the Magnus approximation. On the other hand, it is also possible that the presence of a non-zero $V_n^{(0)}$ $(n = 1,2)$ term with the requirement $[V_n^{(0)}, \rho(0)] = 0$ reduces the contribution from the higher order terms in the Magnus expansion. For example, if $V_n^{(0)}$ is much larger than $V_n^{(1)}$, then only those components of $V_n^{(1)}$ that commute with $V_n^{(0)}$ will significantly affect the performance of a pulse sequence. This effect is similar to that of "second averaging"[10] discussed in multiple pulse line narrowing experiments in solid state NMR. Apart from the abovementioned results, we highlight the following interesting points:

(a) The results for $(90)_0$-$(360)_{120}$-$(90)_0$ and $(180)_0$-$(180)_{120}$-$(180)_0$ sequences are exactly the same for a larger range of $\Delta\omega_1$ as depicted in Figure III.4.

(b) The pulse sequence $(90)_0$-$(\alpha)_{90}$-$(90)_0$ works as a broadband inversion π pulse against $\Delta\omega_Q$ and $\Delta\omega_1$. It gives a better performance, for compensating $\Delta\omega_Q$ when α is anywhere between

150° and 300° and, for overcoming rf field inhomogeneity, may take values from 90° to 270°. It gives a uniform inversion over (i) positive $\Delta\omega_1$ when $\alpha = 90^{\circ}$ and (ii) negative $\Delta\omega_1$ when $\alpha = 270^{\circ}$.

(c) We could not construct composite $\pi/2$ pulse for compensating rf field inhomogeneity. But all those composite $\pi/2$ pulses which overcome $\Delta\omega_Q$ effect yield responses similar to that of a single $\pi/2$ pulse in the case of rf field inhomogeneity.

(d) The results presented here are independent of the efg asymmetry parameter (η), and hence these composite pulses should have a wide applicability.

(e) It is noteworthy that most of the sequences reported here for spin I = 1 NQR case are identical to those employed in NMR spectroscopy.[7-9] But it is not apparent <u>a priori</u> that all the NMR composite pulses behave in a similar fashion in the NQR case. For example, our $(90)_0$-$(300)_{90}$ is not a composite $\pi/2$ pulse in NMR, and the $(90)_0$-$(90)_{90}$ sequence, which is a composite $\pi/2$ pulse used in NMR, is not so in NQR spectroscopy.[6]

(f) One might think that the composite $\pi/2$ pulse $(385)_0$-$(320)_{180}$-$(25)_0$ is equivalent to $(25)_0$-$(320)_{180}$-$(25)_0$ (the flip angle 385 may be written as $(2\pi + 25)$ which is equivalent to 25) and that they would perform identically. To our surprise, however, the sequence $(25)_0$-$(320)_{180}$-$(25)_0$ is neither a composite $\pi/2$ nor even a $3\pi/2$ pulse sequence for compensating $\Delta\omega_Q$. This could be because in NQR one cannot treat the effect of an rf pulse to be a simple rotation.

A general difficulty faced by us during the course of designing the abovementioned composite pulses is the treatment of all the variables (θ_n and ϕ_n) to be entirely arbitrary. In the next section, we consider only the construction of phase alternating composite pulse sequences.

III.C Phase Alternating Composite Pulse Sequences (PACPS)

PACPS consists of rf pulses with phase values 0° and 180° only. The total number of variables defining an N pulse sequence is reduced from (2N-1) to N. We consider PACPS of the format $\bar{\theta}_1\ \theta_2\ \bar{\theta}_3$ and $\theta_1\ \bar{\theta}_2\ \theta_3$, where the overbar denotes a phase shift of π when compared to other rf pulses. The benefits of PACPS are:

(i) They can be easily implemented in an ordinary FT NQR instrument. However, in the case of composite pulses with arbitrarily phased rf pulses, it is often necessary to use sophisticated digital phase shifters.

(ii) With the reduced number of variables, the complexity in evaluating the Magnus expansion terms and the density matrix at different times would be simplified to a greater extent. Construction of new sequences therefore needs less computer time.

III.C.1 Derivation of PACPS through Magnus Expansion

It is a general property of all phase alternating sequences[10] that all even-order terms including the zeroth-order term, $V_1^{(0)}$, of the Magnus expansion can be represented as a linear combination

of I_{X2} and I_{X3}, whereas all odd-order terms are proportional to I_{X1}. The zeroth-order term, $V_1^{(0)}$ for a three-pulse PACPS can be derived based on Eqns. (III.29), (III.30) and (III.31). It is a general property of all phase alternating pulse sequences that the even-order terms including $V_1^{(0)}$ in the Magnus expansion will be a linear combination of I_{X2} and I_{X3} whereas the odd-order terms will be proportional to I_{X1}. The coefficients of I_{X1}, I_{X2} and I_{X3} operators in $V_1^{(0)}$ for $\bar{\theta}_1\ \theta_2\ \bar{\theta}_3$ are given below:

$$a \equiv 0 \qquad .. \quad \text{(III.64)}$$

$$b = 1-\cos\theta_1 + 2\cos(\theta_1-\theta_2) - \cos(\theta_1-\theta_2+\theta_3) \qquad .. \quad \text{(III.65)}$$

$$c = 2\sin\theta_1 - 2\sin(\theta_1-\theta_2) + \sin(\theta_1-\theta_2+\theta_3) \qquad .. \quad \text{(III.66)}$$

A zeroth-order composite pulse can be obtained if we can find θ_1, θ_2 and θ_3 with vanishing b and c. In fact, Eqns. (III.65) and (III.66) are the real and imaginary parts of a single complex equation and the following relationship holds.

$$b = c \tan\left[\frac{\theta_1 + \theta_3 - \theta_2}{2}\right]. \qquad .. \quad \text{(III.67)}$$

When $\theta_1 = \theta_3$ the sequence is called a symmetric phase alternating composite pulse sequence. For this case, the zeroth-order Magnus expansion term $V_1^{(0)}$ is similar to that of $V^{(0)}$ reported by Shaka and Pines[13] for resonance offset effects in the case of spin 1/2 NMR spectroscopy. Therefore, the analysis presented by Shaka and Pines[13] holds good for our case also.

There is a continuum of solutions as a function of the net flip angle on resonance, $\theta = \theta_2 - 2\theta_1$. Given θ, the solution is[13]

$$\theta = \arg\left[1-e^{-i\theta} \pm \left(1 + 14\, e^{-i\theta} + e^{-2i\theta}\right)^{1/2} \right] \qquad .. \text{(III.68)}$$

$$\theta_2 = 2\theta_1 + \theta \qquad .. \text{(III.69)}$$

where $\arg\left[re^{iD} \right] = D$ for real positive r. Hence, from Eqns. (III.65) and (III.66), we can construct composite pulses of any net flip angle θ so that a uniform excitation is obtained as a function of $\Delta\omega_Q$ to the zeroth-order in the Magnus expansion. Though the sequences reported in reference[13] are generally valid for the pure spin 1 NQR spectroscopy also, we prefer, among the sequences listed in Table III.3, the following, namely, $\overline{60}\ 300\ \overline{60}$ as a composite π pulse and $\overline{114.3}\ 318.6\ \overline{114.6}$ as composite $\pi/2$ pulse. Because of shorter T_2 in NQR, the longer time duration pulse sequences given in reference 13 will not be of interest to us here. For the sake of completeness, we reproduce the results for spin 1 NQR from literature[12] in Table III.4. Apart from these results, we have also derived some more composite $\pi/2$ and π pulses with smaller $V_1^{(0)}$ values and these are summarized in Table III.3. We have also considered other possible PACPS of the form $\theta_1\ \overline{\theta}_2\ \theta_3$. For such sequences $V_1^{(0)}$ is again given by Eqns. (III.64), (III.65) and (III.66) but with the reversed sign for 'b'.

We have explored the possibility of designing two pulse composite pulses which would tackle the problem of shorter T_2. Interestingly, if $\overline{\theta}_1\ \theta_2\ \overline{\theta}_1$ is a composite π pulse then

Table III.3 Zeroth-Order Magnus Expansion Terms, $\bar{V}^{(0)}$, for NQR Composite Pulses that Compensate efg Inhomogeneity in the Case of Spin I = 1

Composite pulse	$\bar{V}^{(0)}$
(a) Composite inversion π pulses:	
1) $260\ \overline{80}$	$[-0.0585\ I_{X2} - 0.332\ I_{X3}]\ \Delta\omega_Q$
2) $\overline{22.5}\ 225\ \overline{22.5}$	$-0.359\ I_{X2}\ \Delta\omega_Q$
3) $\overline{45}\ 270\ \overline{45}$	$[-0.132\ I_{X2}\ \Delta\omega_Q$
4) $\overline{60}\ 300\ \overline{60}$	0
5) $90\ \overline{180}\ 270$	$[-0.212\ I_{X2} + 0.424\ I_{X3}]\ \Delta\omega_Q$
6) $260\ \overline{160}\ 80$	$[-0.229\ I_{X2} - 0.451\ I_{X3}]\ \Delta\omega_Q$
7) $315\ \overline{225}\ 90$	$[-0.053\ I_{X2} - 0.310\ I_{X3}]\ \Delta\omega_Q$
(b) Composite π/2 pulses	
1) $\overline{22.5}\ 112.5$	$[0.359\ I_{X2} + 0.749\ I_{X3}]\ \Delta\omega_Q$
2) $\overline{45}\ 135$	$[0.132\ I_{X2} + 0.768\ I_{X3}]\ \Delta\omega_Q$
3) $\overline{60}\ 150$	$0.745\ I_{X3}\ \Delta\omega_Q$
4) $\overline{114.3}\ 318.6\ \overline{114.3}$	0

Table III.4 Phase Alternated NQR Composite Pulses for Broadband Excitation[12]

Angle	Bandwidth*	Length‡	Sequence
90	±0.20	542	$\overline{113}$ 316 $\overline{113}$
90	±0.35	698	24 $\overline{152}$ 346 $\overline{152}$ 24
90	±0.60	1218	$\overline{16}$ 300 $\overline{266}$ 54 $\overline{266}$ 300 $\overline{16}$
90	±0.80	1410	119 $\overline{183}$ 211 $\overline{384}$ 211 $\overline{183}$ 119
90	±1.0	2538	160 $\overline{324}$ 141 $\overline{204}$ 320 $\overline{84}$ 72 $\overline{84}$ 320 $\overline{204}$ 141 $\overline{324}$ 160
135	±0.15	471	$\overline{84}$ 303 $\overline{84}$
135	±0.35	713	39 $\overline{144}$ 347 $\overline{144}$ 39
135	±0.60	1251	$\overline{13}$ 320 $\overline{266}$ 53 $\overline{266}$ 320 $\overline{13}$
135	±0.80	1411	10 $\overline{105}$ 182 $\overline{214}$ 389 $\overline{214}$ 182 $\overline{105}$ 10
135	±1.1	2399	158 $\overline{308}$ 137 $\overline{178}$ 304 $\overline{80}$ 69 $\overline{80}$ 304 $\overline{178}$ 137 $\overline{308}$ 158
180	±0.15	416	$\overline{59}$ 298 $\overline{59}$
180	±0.35	740	58 $\overline{140}$ 344 $\overline{140}$ 58
180	±0.65	1232	325 $\overline{263}$ 56 $\overline{263}$ 325
180	±0.75	1352	$\overline{66}$ 180 $\overline{227}$ 406 $\overline{227}$ 180 $\overline{66}$
180	±0.85	1420	27 $\overline{99}$ 180 $\overline{211}$ 386 $\overline{211}$ 180 $\overline{99}$ 27
180	±1.2	2320	158 $\overline{294}$ 144 $\overline{152}$ 291 $\overline{89}$ 64 $\overline{89}$ 291 $\overline{152}$ 144 $\overline{294}$ 158

*In terms of the dimensionless offset parameter $\Delta\omega_Q/2\omega_1$; ‡Total rotation in degrees.

$\bar{\theta}_1$ ($\theta_{2/2}$) (that is, a pulse lasting for exactly half of the total time duration of the earlier one) is a composite $\pi/2$ pulse for uniform spin excitation over larger $\Delta\omega_Q$ range. For instance, $\overline{22.5}$ 225 $\overline{22.5}$ is a composite π pulse while $\overline{22.5}$ 112.5 is a composite $\pi/2$ pulse. Similarly, the composite $\pi/2$ pulses $\overline{45}$ 135 and $\overline{60}$ 150 have been derived from $\overline{45}$ 270 $\overline{45}$ and $\overline{60}$ 300 $\overline{60}$ composite π pulses. A two pulse composite π pulse also has been derived as 260 $\overline{80}$.

Computer simulations showing the function of various phase alternating composite pulses have been presented in Figures III.5-III.9. For comparison, the single pulse response has also been given along with those for the composite pulses.

III.C.2 Results and Discussion

It is apparent from the computer simulations that the compensation of efg inhomogeneity by composite pulses is much better than that by a single pulse. Differences in the performance of various zeroth-order composite pulses may be due to the contributions from higher order Magnus terms. We highlight some of the important observations that emerged from the construction of PACPS.

(i) Construction of only PACPS and symmetric PACPS simplifies the Magnus expansion approach. Design of symmetric π PACPS leads to the derivation of two-pulse composite $\pi/2$ pulses.

(ii) The sequence of the form $(\overline{60-x})$ $(300-2x)$ $(\overline{60-x})$ for x varying approximately from 0 to 15 is a composite π pulse. Similarly, $(\overline{115-x})$ $(320-2x)$ $(\overline{115-x})$ with x 0 to 10 is a

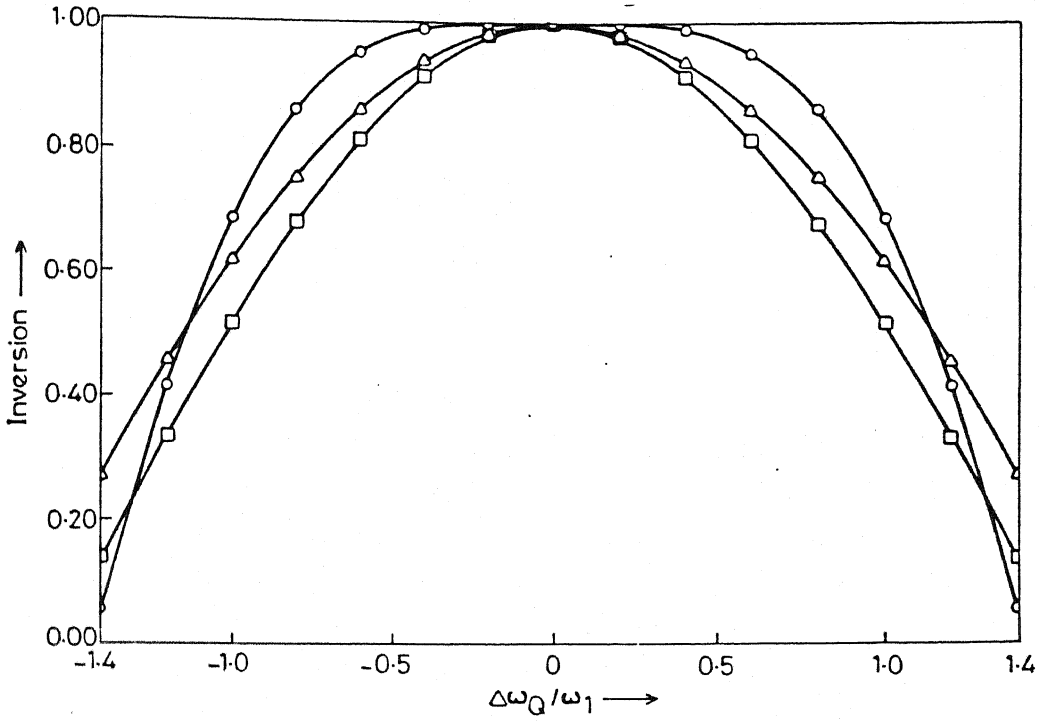

Figure III.6

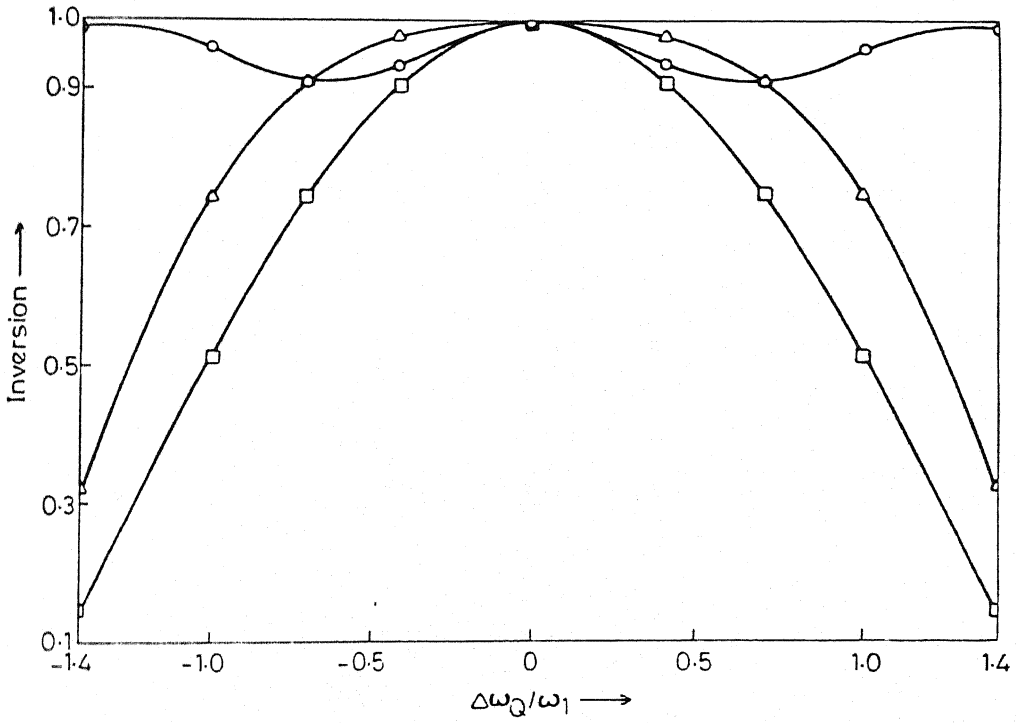

Figure III.5 Spin population inversion as a function of $\Delta\omega_Q/\omega_1$ due to a single π pulse (squares), symmetric zeroth-order $\overline{60}$ 300 $\overline{60}$ (circles) and $\overline{22.5}$ 225 $\overline{22.5}$ (triangles) composite pulses.

Figure III.6 Spin population inversion as a function of $\Delta\omega_Q/\omega_1$ due to a single π pulse (squares), zeroth-order $\overline{45}$ 270 $\overline{45}$ (triangles) and 90 $\overline{180}$ 270 (circles) composite pulses.

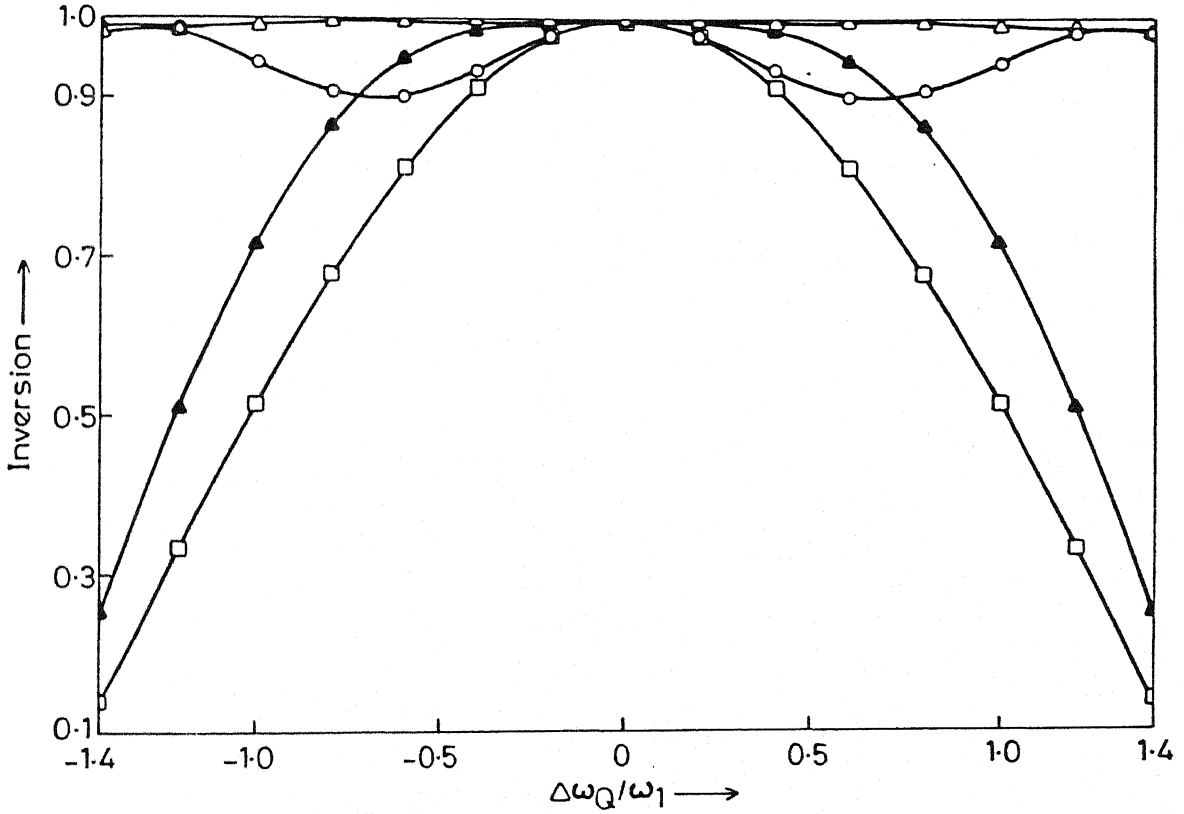

Figure III.7 Spin population inversion as a function of the ratio of efg inhomogeneity or resonance offset ($\Delta\omega_Q$) to the rf field strength (ω_1) due to a single π pulse (squares), zeroth-order 260 $\overline{80}$ (dark triangles), 260 $\overline{160}$ 80 (circles) and 315 $\overline{225}$ 90 (open triangles) composite pulses.

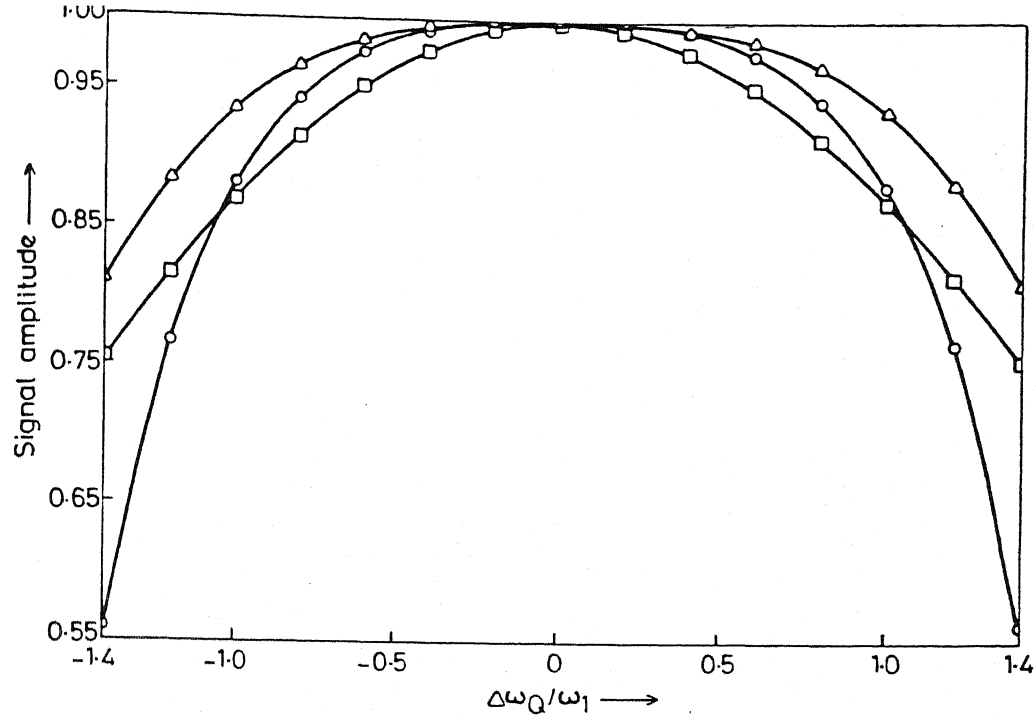

Figure III.9

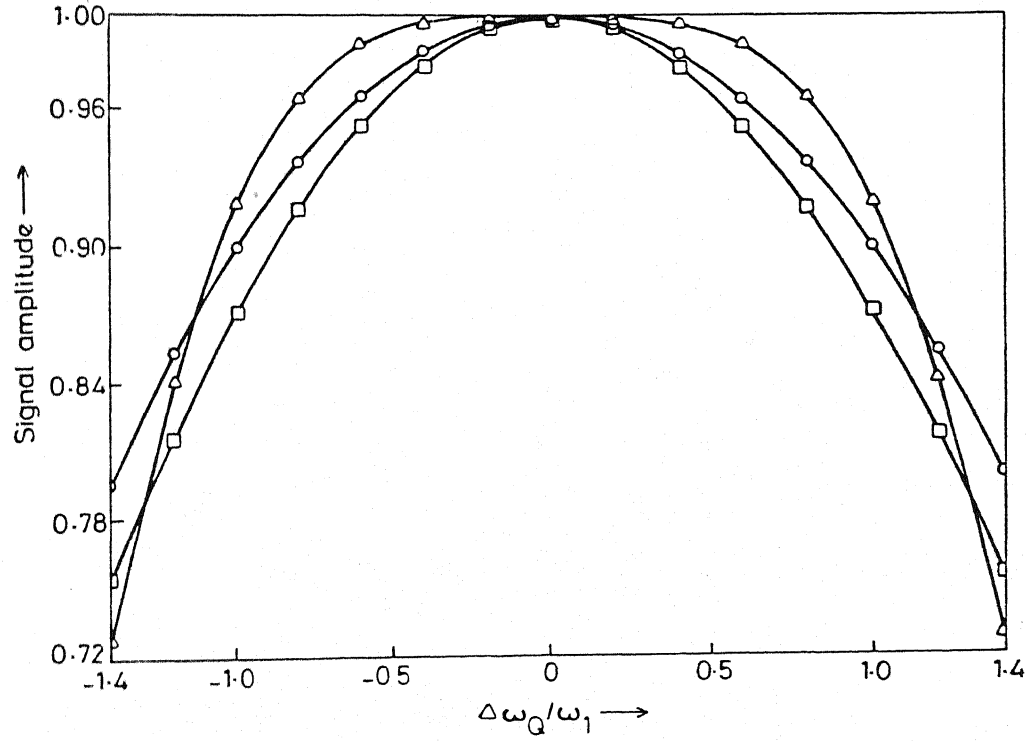

Figure III.8 The signal amplitude as a function of $\Delta\omega_Q/\omega_1$ due to a single $\pi/2$ pulse (squares), zeroth-order $\overline{45\ 135}$ (triangles) and $\overline{114.3\ 318.6\ 114.3}$ (circles) composite pulses.

Figure III.9 The signal amplitude as a function of $\Delta\omega_Q/\omega_1$ due to a single $\pi/2$ pulse (squares), zeroth-order $\overline{22.5\ 112.5}$ (circles) and $\overline{60\ 150}$ (triangles) composite pulses.

composite $\pi/2$ pulse for compensating efg inhomogeneity. This performance, which is insensitive to flip angle errors, shows that PACPS can also be used for overcoming rf field inhomogeneity problems.

(iii) The performance of the pulse sequence 315 $\overline{225}$ 90 is identical to that of its time-reversed sequence, namely, 90 $\overline{225}$ 315. This, however, is not the case with other non-symmetric PACPS.

(iv) The response of all NQR composite pulses which are proposed for broadband excitation over $\Delta\omega_Q$ is symmetric with respect to $\Delta\omega_Q$ as in NMR case.[14] This could be due to the bilinear nature[7] of the V_1 in NQR. This can be proved as given below. Let, U(+) be the propagator at some positive offset $\Delta\omega_Q$. U(+) will be given as

$$U(+) = \exp(i\beta I_{X2}) \exp(-i\alpha_n I_{X3}) \exp(-i\beta I_{X2}), \qquad .. \text{(III.70)}$$

and U(-), the propagator for the corresponding negative offset i.e., $-\Delta\omega_Q$, is then given by

$$U(-) = \exp(-i\beta I_{X2}) \exp(i\alpha_n I_{X3}) \exp(i\beta I_{X2}) \qquad .. \text{(III.71)}$$

The density matrix at the end of the pulse written as

$$\tilde{\rho}(t) = I_{X3}[\cos^2\beta + \sin^2\beta\cos\alpha_n] + \sin\beta\sin\alpha_n\, I_{X2} + \tfrac{1}{2}\sin 2\beta\,(\cos\alpha_n - 1)\, I_{X1} \qquad .. \text{(III.72)}$$

From this, one can easily show that

$$\langle I_z(+)\rangle = \langle I_z(-)\rangle \text{ for } \pi \text{ pulses} \qquad \text{.. (III.73)}$$

and $\langle I_x(+)\rangle = \langle I_x(-)\rangle$ for $\pi/2$ pulses.

This means that the population inversion by composite π pulses and spin excitation by composite $\pi/2$ pulses are independent of the sign of $\Delta\omega_Q$. This proof can be extended to other pulse sequences in NQR.

(v) In NQR of spin I = 1 quadrupolar nuclei, the in-phase (with respect to an applied rf pulse along the x-axis of QPAS) NQR signal is given by $\langle I_{X1}\rangle$ (Appendix D), whereas the 90° out-of-phase NQR signal is given by $\langle I_{X2}\rangle$. Therefore, for an on-resonance rf pulse, $\langle I_{X2}\rangle \gg \langle I_{X1}\rangle$, and the 90° out-of-phase signal is usually detected in an NQR experiment. In the present work, we have given the intensity of the 90° out-of-phase signal to examine composite $\pi/2$ pulses (Figures III.2, III.8 and III.9). The in-phase NQR signal has also been evaluated for all the NQR composite $\pi/2$ pulses. Now, the phase of the NQR signal can be defined by

$$\tan^{-1}\left[\frac{\langle I_{X2}\rangle}{\langle I_{X1}\rangle}\right].$$

For a single rf pulse, the phase is zero when $\Delta\omega_Q = 0$ while it is a linear function of $\Delta\omega_Q$. But for composite $\pi/2$ pulses the phase of the NQR signal is independent of the offset ($\Delta\omega_Q$) to an extent which is smaller than that of the response of composite $\pi/2$

pulses in NMR spectroscopy.[15] Therefore, it may be said that the responses of NQR composite pulses designed via the Magnus expansion approach are free from phase distortion to an appreciable extent.

(vi) There exists a one-to-one correspondence between the spin 1/2 NMR and spin 1 pure NQR spectroscopies. This is highlighted by our results on symmetric PACPS. Because of this similarity, all those PACPS designed for broadband excitation in spin 1/2 NMR[13] high field case appear to be valid for spin 1 NQR also. This similarity could be due to the 'two-level' behaviour of the spin 1 NQR. This can be explained as follows. If one applies an rf radiation along the x-axis of the QPAS then there will be a coherence between only two energy level i.e., $|0\rangle \longleftrightarrow \frac{1}{\sqrt{2}}[\,|+1\rangle + |-1\rangle\,]$(Figure III.1) without affecting the third eigen state. Similarly, an rf pulse considered along the y-axis of the QPAS induce only one transition, namely, $|0\rangle \longleftrightarrow \frac{i}{\sqrt{2}}[\,|+1\rangle - |-1\rangle\,]$ whereas a z-axis rf phase connects $\frac{1}{\sqrt{2}}[\,|+1\rangle + |-1\rangle\,]$ and $\frac{i}{\sqrt{2}}[\,|+1\rangle - |-1\rangle\,]$ energy levels. Thus an applied rf pulse always connects only two levels and hence the real three-level spin 1 problem reduces to a 'two-level' one. In fact, in 1977, Vega[16] has used this property of spin 1 NQR to determine efg axis system of a single crystal specimen.

(vii) It is noteworthy that composite $\pi/2$ pulses for a three-level case in NMR (e.g., spin-1 case) can be easily derived from our PACPS. If $\bar{\theta}_1\ \theta_2\ \bar{\theta}_3$ is a composite π pulse in NQR then $\bar{\theta}_1/2\ \theta_2/2\ \bar{\theta}_3/2$ is a composite $\pi/2$ pulse for compensating quadrupole and dipole-dipole interactions in spin 1 NMR.

It should be mentioned here that in a similar manner composite $\pi/2$ pulse for spin 1 NMR have been obtained from spin 1/2 NMR[17] and, in general, they can be derived from phase alternating composite pulses of a two-level problem. Symmetric $\pi/2$ PACPS thus constructed have been found to be giving broadband excitation and without any phase distortion in quadrupole echoes. We present the procedure of designing composite $\pi/2$ pulses for spin 1 NMR using the Magnus expansion approach with a proof for the above mentioned concept in Appendix E.

In the next chapter, we present the derivation of NQR composite pulses using the Magnus expansion approach for spin I = 3/2 nuclei. These results are then further generalized for an arbitrary spin I nucleus.

Summary

In this chapter, Magnus expansion approach has been employed to construct composite pulses for spin I = 1 NQR spectroscopy. The use of fictitious spin 1/2 operator formalism has reduced the complexity involved in the spin dynamics calculations to a significant extent. Composite π and $\pi/2$ pulses are found to compensate for efg and rf field inhomogeneities to a larger extent compared to a single rf pulse. It has been illustrated that consideration of PACPS simplifies the Magnus expansion approach, and better results suitable for experiments in NQR have been achieved. PACPS offers an easy way of synthesizing composite $\pi/2$ pulses for compensating quadrupole and dipole-dipole interactions in spin I = 1 NMR case. It is inferred that there exists an one-to-one correspondence between spin 1/2 NMR and spin 1 NQR spectroscopies.

REFERENCES

1. T. P. Das and E. L. Hahn, 'Nuclear Quadrupole Resonance Spectroscopy,' Academic Press, New York (1958).
2. S. Vega and A. Pines, J. Chem. Phys. 66, 5624 (1977).
3. R. S. Cantor and J. S. Waugh, J. Chem. Phys. 73, 1054 (1980).
4. M. Goldman, 'Spin Temperature and Nuclear Magnetic Resonance in Solids,' Oxford University Press, Oxford (1970), Chapter 1.
5. W. Magnus, Commun. Pure Appl. Math. 7, 649 (1954).
6. A. Ramamoorthy and P. T. Narasimhan, J. Molec. Struct. 192, 333 (1989).
7. R. Tycko, Phys. Rev. Lett. 51, 775 (1983);
   R. Tycko, E. Schneider and A. Pines, J. Chem. Phys. 81, 680 (1984).
8. M. H. Levitt, Prog. Nucl. Magn. Spectrosc. 18, 61 (1986).
9. R. Tycko, Ph.D. Thesis, University of California, Berkeley (1984).
10. (a) U. Haeberlen, 'High Resolution NMR in Solids: Selective Averaging,' Academic Press, New York (1976);
    (b) M. Mehring, 'Principles of High Resolution NMR in Solids,' second, revised and enlarged edition, Springer-Verlag, New York (1983).
11. (a) R. M. Wilcox, J. Math. Phys. 8, 962 (1967);
    (b) I. Bialynicki-Birula, B. Mielnik and J. Plebanski, Ann. Phys. 51, 187 (1969);
    (c) Ref. 10, Appendix B;
    (d) W. R. Salzman, J. Chem. Phys. 82, 822 (1985);
    W. R. Salzman, J. Chem. Phys. 85, 4605 (1986);

(e)W. R. Salzman, Chem. Phys. Lett. 124, 531 (1986);
S. Klarsfeld and J. A. Oteo, Phys. Rev. 39A, 3270 (1989).

12. M. M. Maricq, J. Chem. Phys. 85, 5167 (1986).

13. A. J. Shaka and A. Pines, J. Magn. Reson. 71, 495 (1987).

14. M. H. Levitt, J. Magn. Reson. 48, 234 (1982);
M. H. Levitt, J. Magn. Reson. 50, 95 (1982)

15. R. Tycko, H. M. Cho, E. Schneider and A. Pines, J. Magn. Reson. 61, 90 (1985).

16. S. Vega, J. Chem. Phys. 63, 3769 (1975).

17. M. H. Levitt, D. Suter and R. R. Ernst, J. Chem. Phys. 80, 3064 (1984).

CHAPTER IV

COMPOSITE PULSES FOR NQR OF SPIN I = 3/2 QUADRUPOLAR NUCLEI USING THE MAGNUS EXPANSION TECHNIQUE AND GENERALIZATION OF THE APPLICABILITY OF THE RESULTS TO SPIN I $\geq$ 1 NUCLEI

In the previous chapter, we presented the derivation of composite pulses using the Magnus expansion method for pure NQR spectroscopy of spin I = 1 nuclei.[1] Although these sequences will be of use in ^{2}D and ^{14}N NQR studies, the number of spin I = 1 quadrupolar nuclei that are of significance in nature are very few, namely ^{2}D, ^{6}Li and ^{14}N.[2,3] Most of the systems studied in NQR[2,3] consist of nuclei with half integral spins such as I = 3/2 (^{35}Cl, ^{37}Cl, ^{79}Br, ^{81}Br), I = 5/2 (^{27}Al, ^{55}Mn, ^{185}Re, ^{187}Re), I = 7/2 (^{51}V, ^{59}Co) and I = 9/2 (^{73}Ge, ^{209}Bi). It would, therefore, be valuable to design composite pulses for spin I > 1 systems in NQR. One might ask whether a strategy different from that for I = 1 is needed for the design of composite pulses for spins I>1. To answer this question, the following points may be noted:

i) Spins with I > 1 may have integral or half-integral values.

ii) Unlike spin I = 1, $\eta \neq 0$ case, all half-integral spins will have doubly degenerate energy levels.[2] The presence of η does not split the degenerate energy levels of half-integral

spins in the absence of a dc magnetic field (for integral spins with $I > 1$ all levels are doubly degenerate in the absence of a magnetic field except the $m_I = 0$ level). A schematic representation of the energy levels corresponding to a quadrupolar nucleus with spin $I > 1$ is given in Figure IV.1.

iii) By changing the rf coil axis direction in the laboratory frame it is possible to connect only a given pair of non-degenerate energy levels in the spin $I = 1$ case for a single crystal.[4] Such a clean selection is not possible for half integral quadrupolar spin systems.

iv) For half integral spin systems, the flip angle of an applied rf pulse depends on the η parameter whereas such is not the case in a spin $I = 1$ system. Thus the behaviour of half-integral quadrupolar spin systems would be different from that of spin $I = 1$ case.

Keeping these facts in mind, we decided to investigate the problem of design of composite pulses for half integral spin systems. The spin $I = 3/2$ case is an important one on account of its having a single quadrupolar frequency in the absence of a dc magnetic field. In order to study the spin dynamics of the spin $I = 3/2$ system we make use of the density matrix formalism and expand the density operator in terms of a suitably chosen set of base operators. The operators that we employ here are the irreducible spherical tensor operators.[5] Appendix B of this thesis summarizes the important definitions used in the tensor operator formalism.[6-8] Tensor operator formalism has the following

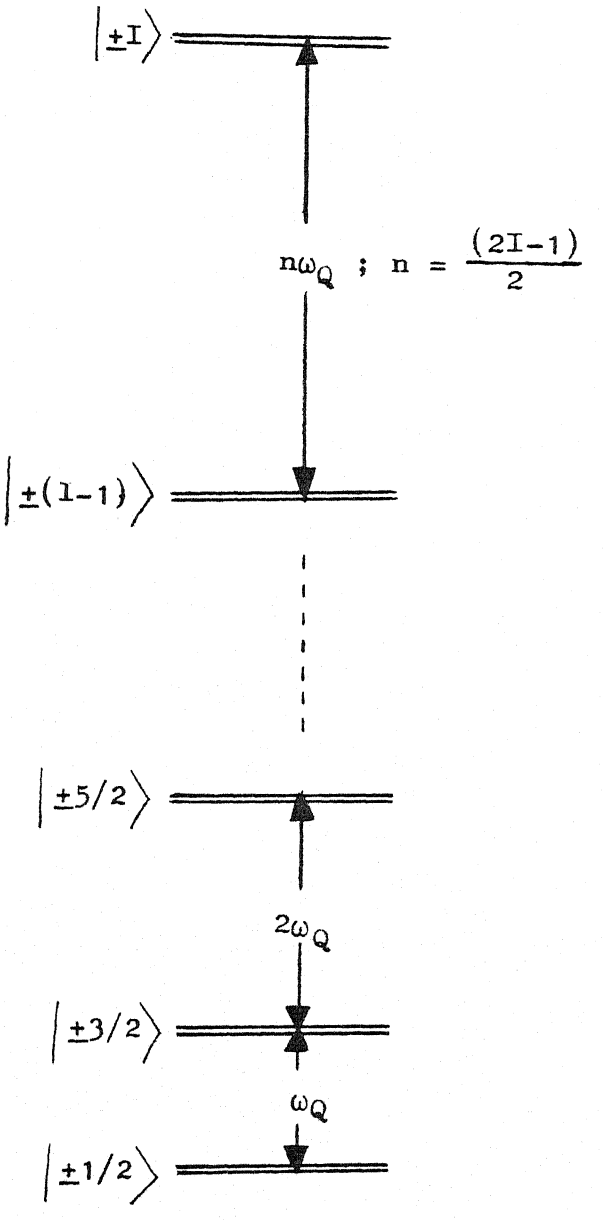

Figure IV.1 Energy level splitting (schematic) in the absence of Zeeman field for a half-integral spin I quadrupolar nucleus.

advantages over the fictitious spin-1/2 operator formalism:[9]

i) Tensor operators[6-8] form a complete basis set, whereas the fictitious spin-1/2 operators[9] do not.

ii) For spin I = 3/2, there are 18 fictitious spin-1/2 operators[9] compared with the 15 irreducible tensors.[8]

iii) Irreducible tensors obey well-known transformation laws, following rotations of the coordinate system.[5]

iv) Irreducible tensors carry information about the rank of the multipolar state and the order of multiple-quantum transitions.

Earlier tensor operators have been employed in electron paramagnetic resonance[10] and for the study of multiple quantum NMR,[6-8,11] to obtain analytical expressions for the eigenvalues of the NQR Hamiltonian for spins I = 1, 3/2 and 5/2 in terms of quadrupole coupling constant and η.[12] More recently, the use of tensor operators has been demonstrated for multiple quantum NQR studies also.[13]

In Section IV.A, we present the tensor operator representation of the various interaction energies that constitute the Hamiltonian of the system. The Magnus expansion method of designing composite pulses to compensate for efg and rf field inhomogeneities for the spin I = 3/2 case is outlined in Section IV.B. Comments on the applicability of the results to an arbitrary spin I quadrupolar nuclei are then made in Section IV.C.

IV.A Hamiltonians of the Spin System

We consider an ensemble of non-interacting spin I = 3/2 nuclei in a single crystal in a zero dc magnetic field. We assume that all the spins are physically equivalent,[2] whereby they can all be defined by a common quadrupole principal axis system (QPAS). We further assume that the QPAS coincides with the laboratory frame. We consider the following interactions to be present in our model: quadrupole interaction ($\mathcal{H}_Q$), efg inhomogeneity (V_1), the interaction of the applied rf pulse with the spin system ($\mathcal{H}_{rf}$) and the inhomogeneity in the applied rf field (V_2). In what follows, we present these Hamiltonians in terms of irreducible tensor operators in different frames, namely, (i) QPAS, (ii) a frame where $\mathcal{H}_Q$ is diagonal and (iii) QIF.[14]

IV.A.1 Quadrupole Hamiltonian

In QPAS, the quadrupole Hamiltonian, $\mathcal{H}_Q$, for a spin I = 3/2 nucleus is given as[2]

$$\mathcal{H}_Q = \frac{e^2qQ}{12}\left[3I_z^2 - I^2 + \eta(I_x^2 - I_y^2)\right] \qquad .. \text{(IV.1)}$$

Using the irreducible spherical tensor operator (T_q^n, where n is the rank and q is the order) formalism,[6-8] we can write

$$\mathcal{H}_Q = P' T_o^2 + P'' T_2^2(s) \qquad .. \text{(IV.2)}$$

$$P' = \frac{e^2qQ}{2\sqrt{6}} \qquad .. \text{(IV.3a)}$$

$$P'' = \frac{e^2qQ}{6\sqrt{2}}\,\eta \qquad .. \text{(IV.3b)}$$

The definition of tensor operators, commutation relationships and matrix representation of tensor operators for spin I = 3/2 case have been given in Appendix B.

$\mathcal{H}_Q$ can be also written in the following matrix form,

$$\mathcal{H}_Q = \frac{e^2qQ}{4} \begin{bmatrix} 1 & 0 & \frac{\eta}{\sqrt{3}} & 0 \\ 0 & -1 & 0 & \frac{\eta}{\sqrt{3}} \\ \frac{\eta}{\sqrt{3}} & 0 & -1 & 0 \\ 0 & \frac{\eta}{\sqrt{3}} & 0 & 1 \end{bmatrix} \qquad .. \text{(IV.4)}$$

The basis vectors used to represent the $\mathcal{H}_Q$ matrix follow the order $|+3/2\rangle$, $|+1/2\rangle$, $|-1/2\rangle$ and $|-3/2\rangle$ from left to right in the rows and top to bottom in the columns. In QPAS, $\mathcal{H}_Q$ as given above is not a diagonal matrix and it will be useful in spin dynamics calculations to have the diagonalized form of $\mathcal{H}_Q$. $\mathcal{H}_Q$ can be diagonalized by an unitary transformation by the operator T, defined by

$$T = \frac{1}{\sqrt{2}} \begin{bmatrix} X_1 & 0 & X_2 & 0 \\ 0 & -X_1 & 0 & X_2 \\ X_2 & 0 & -X_1 & 0 \\ 0 & X_2 & 0 & X_1 \end{bmatrix} \qquad .. \text{(IV.5)}$$

where $X_1 = (1 + 1/\lambda)^{1/2}$, .. (IV.6a)

$X_2 = (1 - 1/\lambda)^{1/2}$ .. (IV.6b)

and $\lambda = (1 + \eta^2/3)^{1/2}$ .. (IV.6c)

The diagonalised quadrupole Hamiltonian, $\mathcal{H}_Q$ can then be written as

$$\mathcal{H}_Q^d = T^{-1}\mathcal{H}_Q T = \frac{\omega_Q}{2}\begin{bmatrix} 1 & 0 & 0 & 0 \\ 0 & -1 & 0 & 0 \\ 0 & 0 & -1 & 0 \\ 0 & 0 & 0 & 1 \end{bmatrix} \quad .. \text{(IV.7)}$$

$$\omega_Q = \frac{e^2qQ}{2}(1 + \eta^2/3)^{1/2} \quad .. \text{(IV.8)}$$

where 'd' refers to the new representation defined by T and ω_Q is the quadrupole frequency corresponding to $|\pm 3/2\rangle \longleftrightarrow |\pm 1/2\rangle$ transition (see Figure IV.1). Using the matrix forms of different T_q^n given in Appendix B, we obtain

$$\mathcal{H}_Q^d = \frac{\omega_Q}{\sqrt{6}} T_o^2 \quad .. \text{(IV.9)}$$

IV.A.2 <u>EFG Inhomogeneity Hamiltonian</u>

In QPAS, the efg inhomogeneity Hamiltonian, V_1, is given by

$$V_1 = \Delta P' \; T_o^2 + \Delta P'' \; T_2^2(s) \quad .. \text{(IV.10a)}$$

with $\Delta P' = \frac{e^2(\delta q)Q}{2\sqrt{6}}$ .. (IV.10b)

and $\Delta P'' = \frac{e^2(\delta q)Q}{6\sqrt{2}}\eta$ .. (IV.10c)

δq is the inhomogeneity in efg. In a frame where $\mathcal{H}_Q$ is diagonal, V_1 becomes

$$V_1^d = T^{-1} V_1 T = \frac{\Delta\omega_Q}{\sqrt{6}} T_o^2 \qquad .. \text{(IV.11)}$$

$\Delta\omega_Q$ is the resonance offset term, or a term representing the distribution of quadrupole frequencies given in terms of δq as,

$$\Delta\omega_Q = \frac{e^2(\delta q)Q}{2} (1 + \eta^2/3)^{1/2} \qquad .. \text{(IV.12)}$$

In the observation frame of NQR i.e., QIF[14] defined by the unitary operator,

$$U_Q = \exp(-i \mathcal{H}_Q^d t) , \qquad .. \text{(IV.13)}$$

the efg inhomogeneity Hamiltonian is

$$\tilde{V}_1 = U_Q^{-1} V_1^d U_Q = V_1^d \qquad .. \text{(IV.14)}$$

In writing the above expression, we have used the commutation relationship $[U_Q, V_1^d] = 0$.

IV.A.3 RF Hamiltonian

A general form of the rf Hamiltonian, $\mathcal{H}_{rf}$, has been given in Chapter II (vide Eqn. (II.10)). Using tensor operators, $\mathcal{H}_{rf}$ in QPAS is written as

$$\mathcal{H}_{rf} = 2\omega_1 \cos(\omega_Q t + \phi(t)) T_1^1(a) \qquad .. \text{(IV.15)}$$

where ω_Q is the frequency of transition between $|\pm 3/2\rangle$ and $|\pm 1/2\rangle$ energy levels. The antisymmetric tensor operator $T_1^1(a)$ is explicitly given in Appendix B. $\mathcal{H}_{rf}$ in QPAS is given by the following matrix:

$$\mathcal{H}_{rf} = -D \begin{bmatrix} 0 & \sqrt{3} & 0 & 0 \\ \sqrt{3} & 0 & 2 & 0 \\ 0 & 2 & 0 & \sqrt{3} \\ 0 & 0 & \sqrt{3} & 0 \end{bmatrix} \qquad .. \text{(IV.16)}$$

$$\text{with } D = \omega_1 \cos(\omega_Q t + \phi(t)) . \qquad .. \text{(IV.17)}$$

In a frame defined by T, where $\mathcal{H}_Q$ is diagonal, $\mathcal{H}_{rf}^d$ is given by

$$\mathcal{H}_{rf}^d = T^{-1} \mathcal{H}_{rf} T = -D \begin{bmatrix} 0 & K_1 & 0 & K_2 \\ K_1 & 0 & K_3 & 0 \\ 0 & K_3 & 0 & K_1 \\ K_2 & 0 & K_1 & 0 \end{bmatrix} \qquad .. \text{(IV.18)}$$

$$\text{where } K_1 = -1/\lambda[\sqrt{3} + \eta/\sqrt{3}], \qquad .. \text{(IV.19a)}$$

$$K_2 = 1/\lambda[\sqrt{3}\ (\lambda^2-1)^{1/2} + \lambda - 1] \qquad .. \text{(IV.19b)}$$

$$\text{and } K_3 = 1/\lambda\ (1-\eta+\lambda) \qquad .. \text{(IV.19c)}$$

$\mathcal{H}_{rf}^d$ can be written in terms of tensor operators as

$$\mathcal{H}_{rf}^d = \frac{2D}{5}[\sqrt{3}\ K_1 + K_3]\ T_1^1(a) + \frac{2D}{3} K_2 T_3^3(a) + \frac{2D}{\sqrt{5}}\left[\frac{2}{3} K_1 - \frac{K_3}{\sqrt{3}}\right] T_1^3(a) \qquad .. \text{(IV.20)}$$

To eliminate the time dependency of $\mathcal{H}^{d}_{rf}$, we make a transformation to the QIF[14] defined by the unitary operator, U_Q (see Eqn. (IV.13)). Now, in QIF, the rf Hamiltonian becomes

$$\tilde{\mathcal{H}}_{rf} = U_Q^{-1}\, \mathcal{H}^{d}_{rf}\, U_Q \qquad .. \text{(IV.21)}$$

Using the transformation properties of various tensor operators under U_Q given in Table IV.1, we can write the rf Hamiltonian in QIF as

$$\begin{aligned}\tilde{\mathcal{H}}_{rf} = {} & T^1_1(a)\left[\frac{2\sqrt{3}}{5} K_1 D\cos(\omega_Q t) + \frac{2}{5} K_3 D + \frac{12D}{25\sqrt{3}} K_1(\sqrt{3}-1)\right] \\ & + T^3_3(a)\left[\frac{2}{3} D K_2\right] - \left[\frac{2i}{\sqrt{6}} D K_1 \sin(\omega_Q t)\right] T^2_1(s) \\ & + T^3_1(a)\left[\frac{4}{3\sqrt{5}} D K_1 \cos(\omega_Q t) - \frac{2}{\sqrt{15}} D K_3\right] \qquad .. \text{(IV.22)}\end{aligned}$$

After truncating the high frequency terms such as $\sin(n\omega_Q t)$ and $\cos(n\omega_Q t)$, with $n \gg 1$, integer, we get the time independent static rf Hamiltonian in QIF as

$$\begin{aligned}\tilde{\mathcal{H}}_{rf} = -K_1\omega_1 \Big\{ & \frac{\sqrt{3}}{5}\cos\phi(t)\, T^1_1(a) + \frac{2}{3\sqrt{5}}\cos\phi(t)\, T^3_1(a) \\ & + \frac{i}{\sqrt{6}}\sin\phi(t)\, T^2_1(s) \Big\} \qquad .. \text{(IV.23)}\end{aligned}$$

IV.A.4 RF Field Inhomogeneity Hamiltonian

Since the transformation property of the rf field inhomogeneity Hamiltonian, V_2, is similar to that of the rf Hamiltonian, $\mathcal{H}_{rf}$, we directly give the final form of $\tilde{V}_2$ in QIF as

Table IV.1 Transformation Properties of Tensor Operators $T_q^n(s,a)$ under the Quadrupole Interaction, $\mathcal{H}_Q^d = \frac{\omega_Q}{\sqrt{6}} T_o^2$ for spin $I = \frac{3}{2}$ after Bowden et al.[8]

$$U_Q^{-1}\, T_1^1(a)\, U_Q = \frac{1}{5} T_1^1(a)[2 + 3\cos(\omega_Q t)] + \frac{i}{\sqrt{2}} T_1^2(s)\sin(\omega_Q t) + \frac{2}{\sqrt{15}} T_1^3(a)[\cos(\omega_Q t) - 1]$$

$$U_Q^{-1}\, T_1^2(a)\, U_Q = \frac{3\sqrt{2}}{5} iT_1^2(s)\sin(\omega_Q t) + T_1^2(a)\cos(\omega_Q t) + \frac{2\sqrt{2}}{\sqrt{15}} iT_1^3(s)\sin(\omega_Q t)$$

$$U_Q^{-1}\, T_2^2(a)\, U_Q = T_2^2(a)\cos(\omega_Q t) + \frac{2i}{\sqrt{3}} T_2^3(s)\sin(\omega_Q t)$$

$$U_Q^{-1}\, T_1^3(a)\, U_Q = \frac{3}{5}\sqrt{\frac{3}{5}}\, T_1^1(a)[\cos(\omega_Q t) - 1] + \sqrt{\frac{3}{10}}\, iT_1^2(s)\sin(\omega_Q t) + \frac{1}{5} T_1^3(a)[3 + 2\cos(\omega_Q t)]$$

$$U_Q^{-1}\, T_2^3(a)\, U_Q = -\frac{\sqrt{3}}{2} iT_2^3(s)\sin(\omega_Q t) + T_2^3(a)\cos(\omega_Q t)$$

where $U_Q = \exp(-i\mathcal{H}_Q^d t)$; $\omega_Q = \frac{e^2qQ}{2}(1 + \eta^2/3)^{1/2}$. For the symmetric combinations, namely $T_q^n(s)$, replace a by s and s by a in the above expressions. T_o^1, T_o^2, $T_3^3(s)$ and $T_3^3(a)$ all commute with $\mathcal{H}_Q^d$.

$$\tilde{V}_2 = -K_1 \Delta\omega_1 \left\{ \frac{\sqrt{3}}{5} \cos\phi(t)\ T_1^1(a) + \frac{2}{3\sqrt{5}} \cos\phi(t)\ T_1^3(a) + \frac{i}{\sqrt{6}} \sin\phi(t)\ T_1^2(s) \right\} \quad .. \text{(IV.24)}$$

In the next section, we present the derivation of composite pulses for spin I = 3/2 NQR spectroscopy using a method based on the Magnus expansion approximation.

IV.B Design of NQR Composite Pulses for the Case of Spin I = 3/2

The total Hamiltonian for the spin system considered here may be written in QPAS as

$$\mathcal{H} = \mathcal{H}_Q + \mathcal{H}_{rf} + V_1 + V_2 \quad .. \text{(IV.25)}$$

Making use of the operator T and transforming to a frame where $\mathcal{H}_Q$ becomes diagonal, we get

$$\mathcal{H}^d = T^{-1}\mathcal{H}\ T = \mathcal{H}_Q^d + \mathcal{H}_{rf}^d + V_1^d + V_2^d \quad .. \text{(IV.26)}$$

To suppress the main interaction $\mathcal{H}_Q^d$, and to get a time independent rf field, we again go to the QIF.[14] Now the net Hamiltonian is given by

$$\tilde{\mathcal{H}}^d = U_Q^{-1}\mathcal{H}^d\ U_Q = \tilde{\mathcal{H}}_{rf}^d + \tilde{V}_1^d + \tilde{V}_2^d \quad .. \text{(IV.27)}$$

Henceforth we shall drop the superscript 'd' and write $\tilde{\mathcal{H}}^d$, $\tilde{\mathcal{H}}_{rf}^d$, $\tilde{V}_1^d$ and $\tilde{V}_2^d$ as $\tilde{\mathcal{H}}$, $\tilde{\mathcal{H}}_{rf}$, $\tilde{V}_1$ and $\tilde{V}_2$, respectively.

To achieve a composite pulse sequence during which the interactions $\tilde{V}_1$ and $\tilde{V}_2$ can be suppressed, we have to transfer $\tilde{\mathcal{H}}$ to the toggling frame[15] using the propagator $(U_{rf}(t))$ of the pulse sequence considered. We now consider a sequence of the type $(\theta_1)_0-(\theta_2)_{\phi_2}-(\theta_3)_{\phi_3}$, where θ_n is the flip angle of the nth-rf pulse of duration t_n and phase ϕ_n. The rf pulse sequence propagator, $U_{rf}(t)$, is given by

$$U_{rf}(t) = \begin{cases} \exp(-i\,\tilde{\mathcal{H}}_{1\ rf}\ t_1), & ..0 \leq t_1 \leq \dfrac{\theta_1}{\omega_{rf}} \\ \exp(-i\,\tilde{\mathcal{H}}_{2\ rf}\ t_2)\ \exp(-i\,\tilde{\mathcal{H}}_{1\ rf}\ t_1), & ..0 \leq t_2 \leq \dfrac{\theta_2}{\omega_{rf}} \\ \exp(-i\,\tilde{\mathcal{H}}_{3\ rf} t_3)\ \exp(-i\,\tilde{\mathcal{H}}_{2rf} t_2) \exp(-i\,\tilde{\mathcal{H}}_{1rf} t_1) & ..0 \leq t_3 \leq \dfrac{\theta_3}{\omega_{rf}} \end{cases} \quad .. \text{(IV.28)}$$

$$\text{where } \omega_{rf} = \frac{(3+\eta)\,\omega_1}{(3+\eta^2)^{1/2}} \quad .. \text{(IV.29a)}$$

$$\text{and } \theta_n = \omega_{rf}\ t_n \quad .. \text{(IV.29b)}$$

$\tilde{\mathcal{H}}_{n\ rf}$ is the Hamiltonian in QIF for the nth-rf pulse, and can be written as

$$\tilde{\mathcal{H}}_{n\ rf} = \omega_1\ K_1 \left\{ \frac{\sqrt{3}}{5} \cos\phi_n\ T_1^1(a) + \frac{2}{3\sqrt{5}} \cos\phi_n\ T_1^3(a) + \frac{i}{\sqrt{6}} \sin\phi_n\ T_1^2(s) \right\} \quad .. \text{(IV.30)}$$

In the following subsections, we consider the effects of V_1 and V_2 separately.

IV.B.1 Zeroth-Order Composite Pulses to Compensate for EFG Inhomogeneity

In the toggling frame, spins evolve under the transformed efg inhomogeneity Hamiltonian ($\tilde{\tilde{V}}_1(t)$) alone (neglecting the effects of V_2) (refer Appendix C) and the propagator is given by

$$U_v(t) = T \exp[-i \int_o^t \tilde{\tilde{V}}_1(t')\, dt'] \qquad .. \text{(IV.31)}$$

To get the effective time independent efg inhomogeneity Hamiltonian, we use the Magnus expansion[16] to write

$$\tilde{\tilde{V}}_1(t) = V_1^o + V_1^1 + \ldots \qquad .. \text{(IV.32)}$$

For the spin I = 3/2 system, the transformed Hamiltonian, $\tilde{\tilde{V}}_1(t)$, for a three-pulse scheme has been derived in the following way: first, the commutators between the rf Hamiltonian and different tensor operators, that is, $[\tilde{\mathcal{H}}_{nrf}, T_q^n]$ are evaluated, and these are listed in the Table IV.2. Then, using the nested commutation relationship (see Eqn. I.21), the transformation properties of different tensor operators under the effect of rf pulses have been derived, and these are summarized in the Table IV.3. Now using the results of Table IV.3 $\tilde{\tilde{V}}_1(t)$ is obtained as,

$$\tilde{\tilde{V}}_1(t) = \frac{\Delta\omega_Q}{\sqrt{6}} [a_1(t)T_o^2 + ia_2(t)T_1^2(s) + a_3(t)T_1^1(a) + a_4(t)T_1^3(a)] \qquad .. \text{(IV.33)}$$

Table IV.2 Commutation Relationships of few Selected Tensor Operators with the Hamiltonian, $\tilde{\mathcal{H}}$

$\tilde{\mathcal{H}} = \tilde{\mathcal{H}}_{nrf} + \tilde{V}_1 + \tilde{V}_2$

$$[\tilde{\mathcal{H}}, T_o^2] = -\sqrt{3}(\omega_1 + \Delta\omega_1)\, T_1^2(s)\cos\phi_n + \frac{6}{5}\sqrt{\frac{3}{2}}\, i(\omega_1 + \Delta\omega_1)\, T_1^1(a)\sin\phi_n + \frac{4}{\sqrt{10}}\, i(\omega_1 + \Delta\omega_1)\, T_1^3(a)\sin\phi_n$$

$$[\tilde{\mathcal{H}}, T_1^2(s)] = -\sqrt{3}(\omega_1 + \Delta\omega_1)\, T_o^2\cos\phi_n + \frac{\sqrt{18}}{5}\Delta\omega_Q T_1^1(a) + \frac{2}{3\sqrt{5}}\Delta\omega_Q\, T_1^3(a)$$

$$[\tilde{\mathcal{H}}, T_1^1(a)] = -\sqrt{\frac{3}{2}}\, i(\omega_1 + \Delta\omega_1)\, T_o^2\sin\phi_n - \frac{i}{\sqrt{2}}(\omega_1 + \Delta\omega_1)\, T_2^2(s)\sin\phi_n + \sqrt{\frac{2}{3}}(\omega_1 + \Delta\omega_1)\, T_2^3(a)\cos\phi_n + \frac{\Delta\omega_Q}{\sqrt{3}}\, T_1^2(s)$$

$$[\tilde{\mathcal{H}}, T_1^3(a)] = -\frac{3}{10}(\omega_1 + \Delta\omega_1)\, T_2^3(a)\cos\phi_n - \frac{3}{\sqrt{10}}\, i(\omega_1 + \Delta\omega_1)\, T_o^2\sin\phi_n + \frac{3\sqrt{3}}{\sqrt{40}}\, i(\omega_1 + \Delta\omega_1)\, T_2^2(s)\sin\phi_n + \sqrt{\frac{3}{5}}\,\Delta\omega_Q\, T_1^2(s)$$

$$[\tilde{\mathcal{H}}, T_2^2(s)] = \frac{6i}{5\sqrt{2}}(\omega_1 + \Delta\omega_1)\, T_1^1(a)\sin\phi_n - \sqrt{\frac{6}{5}}\, i(\omega_1 + \Delta\omega_1)\, T_1^3(a)\sin\phi_n - \sqrt{2}\, i(\omega_1 + \Delta\omega_1)\, T_3^3(a)\sin\phi_n + \frac{2}{\sqrt{3}}\,\Delta\omega_Q\, T_2^3(a)$$

$$[\tilde{\mathcal{H}}, T_2^3(a)] = -\sqrt{\frac{3}{2}}(\omega_1 + \Delta\omega_1)\, T_3^3(a)\cos\phi_n + \frac{3}{\sqrt{10}}(\omega_1 + \Delta\omega_1) T_1^3(a)\cos\phi_n + \frac{3}{5}\sqrt{\frac{3}{2}}(\omega_1 + \Delta\omega_1)\, T_1^1(a)\cos\phi_n + \frac{1}{2}\Delta\omega_Q\, T_2^2(s)$$

$$[\tilde{\mathcal{H}}, T_3^3(a)] = -\sqrt{\frac{3}{2}}(\omega_1 + \Delta\omega_1)\, T_2^3(a)\cos\phi_n + \frac{3i}{2\sqrt{2}}(\omega_1 + \Delta\omega_1)\, T_2^2(s)\sin\phi_n$$

...contd.

Table IV.2 (contd.)

where $\tilde{\mathcal{H}}_{nrf} = \omega_1 K_1 \left[\frac{\sqrt{3}}{5} \cos\phi_n \, T_1^1(a) + \frac{2}{3\sqrt{5}} \cos\phi_n \, T_1^3(a) + \frac{i}{\sqrt{6}} \sin\phi_n \, T_1^2(s) \right]$

$\tilde{V}_1 = \frac{\Delta\omega_Q}{\sqrt{6}} T_o^2$

and $\tilde{V}_2 = K_1 \, \omega_1 \left[\frac{\sqrt{3}}{5} \cos\phi_n \, T_1^1(a) + \frac{2}{3\sqrt{5}} \cos\phi_n \, T_1^3(a) + \frac{i}{\sqrt{6}} \sin\phi_n \, T_1^2(s) \right]$

Table IV.3 Evolution of Tensor Operators under the Effect of the Hamiltonian, $\tilde{\mathcal{H}}$.

$$\tilde{\mathcal{H}} = \tilde{\mathcal{H}}_{nrf} + \tilde{V}_1 + \tilde{V}_2$$

$$U\, T_o^2\, U^{-1} = T_o^2[\cos^2\beta + \sin^2\beta\cos\alpha_n] +$$

$$+ iT_1^2(s)\,\sin\beta[\cos\phi_n\sin\alpha_n + \sin\phi_n\cos\beta(\cos\alpha_n - 1)]$$

$$-[\tfrac{2}{3}\sqrt{\tfrac{6}{5}}\,T_1^3(a) + \tfrac{\sqrt{18}}{5}\,T_1^1(a)]\sin\beta[\cos\beta\cos\phi_n(\cos\alpha_n - 1) - \sin\alpha_n\sin\phi_n]$$

$$U\, T_1^1(a)\, U^{-1} = \sin\beta[\cos\beta\cos\phi_n(1-\cos\alpha_n) - \sin\alpha_n\sin\phi_n]\,\frac{T_o^2}{2}$$

$$+ \frac{i}{2\sqrt{2}}\,T_1^2(s)[\sin 2\phi_n\cos\alpha_n\sin^2\beta - \sin 2\phi_n\sin^2\beta - \cos\beta\sin\alpha_n]$$

$$- \frac{\sqrt{2}}{3}\,iT_2^3(a)[\sin\phi_n\cos\beta(\cos\alpha_n - 1) + \cos\phi_n\sin\alpha_n]\sin\beta$$

$$+ \frac{1}{\sqrt{6}}\,T_2^2(s)\,\sin\beta[\cos\beta\cos\phi_n(\cos\alpha_n - 1) - \sin\phi_n\sin\alpha_n]$$

$$+ \frac{1}{3}\,T_3^3(a)\,\sin^2\beta\,(1-\cos\alpha_n)$$

$$+ \frac{1}{5}\,T_1^1(a)[3\cos^2\phi_n(\sin^2\beta + \cos^2\beta\cos\alpha_n) + 3\sin^2\phi_n\cos\alpha_n + \sin^2\beta(1+\cos\alpha_n) + 2]$$

$$+ \frac{1}{\sqrt{15}}\,T_1^3(a)[2\cos^2\phi_n(\sin^2\beta + \cos^2\beta\cos\alpha_n) + 2\sin^2\phi_n\cos\alpha_n - \sin^2\beta(1+\cos\alpha_n) - 2]$$

...contd.

Table IV.3 (contd.)

$$U\,T_1^2(s)\,U^{-1} = -iT_o^2\sin\beta[\sin\phi_n\cos\beta(\cos\alpha_n-1)-\cos\phi_n\sin\alpha_n]$$
$$+[\tfrac{2}{3}\sqrt{\tfrac{6}{5}}\,iT_1^3(a)+\tfrac{\sqrt{18}}{5}\,iT_1^1(a)]\cdot$$
$$\cdot[\cos\phi_n(\sin\phi_n\sin^2\beta+\sin\phi_n\cos^2\beta\cos\alpha_n-\cos\phi_n\sin\alpha_n\cos\beta)$$
$$-\sin\phi_n(\cos\alpha_n\cos\phi_n+\sin\phi_n\cos\beta\sin\alpha_n)]$$
$$+T_1^2(s)[\sin^2\phi_n(\cos^2\beta\cos\alpha_n+\sin^2\beta)+\cos\alpha_n\cos^2\phi_n]$$

$$U\,T_1^3(a)\,U^{-1} = \tfrac{3}{\sqrt{30}}\,T_o^2\sin\beta[\cos\beta\cos\phi_n(1-\cos\alpha_n)-\sin\alpha_n\sin\phi_n]$$
$$+\tfrac{3i}{\sqrt{30}}\,T_1^2(s)[\tfrac{-1}{2}\sin2\phi_n(-\cos\alpha_n+\cos^2\beta\cos\alpha_n+\sin^2\beta)$$
$$-\sin\alpha_n\cos\beta]$$
$$+\sqrt{\tfrac{3}{10}}\,iT_2^3(a)\sin\beta[\sin\alpha_n\cos\phi_n+\sin\phi_n\cos\beta(1-\cos\alpha_n)]$$
$$+\tfrac{3}{2\sqrt{10}}\,T_2^2(s)\sin\beta[\sin\phi_n\sin\alpha_n+\cos\beta\cos\phi_n(1-\cos\alpha_n)]$$
$$+\tfrac{\sqrt{3}}{2\sqrt{5}}\,T_3^3(a)[\sin^2\beta(\cos\alpha_n-1)]$$
$$+\tfrac{3}{5}\sqrt{\tfrac{3}{5}}\,T_1^1(a)[-1-\tfrac{1}{2}\sin^2\beta(\cos\alpha_n-1)+\sin^2\phi_n\cos\alpha_n$$
$$+\cos^2\phi_n(\sin^2\beta+\cos^2\beta\cos\alpha_n)]$$
$$+\tfrac{3}{5}\,T_1^3(a)[1+\tfrac{1}{2}\sin^2\beta(\cos\alpha_n-1)+\tfrac{2}{3}\sin^2\phi_n\cos\alpha_n$$
$$+\tfrac{2}{3}\cos^2\phi_n(\sin^2\beta+\cos^2\beta\cos\alpha_n)]$$

...contd.

Table IV.3 (contd.)

$$U\,T_2^2(s)\,U^{-1} = -\frac{2i}{\sqrt{3}}T_2^3(a)\left[\frac{1}{2}\sin 2\phi_n(\sin^2\beta+\cos^2\beta\cos\alpha_n-\cos\alpha_n) + \cos\beta\sin\alpha_n\right]$$
$$+ T_2^2(s)\left[\cos\alpha_n(\sin^2\phi_n+\cos^2\phi_n\cos^2\beta) + \cos^2\phi_n\sin^2\beta\right]$$
$$+ \frac{\sqrt{6}}{5}T_1^1(a)\sin\beta\left[\cos\phi_n\cos\beta\cos\alpha_n + \sin\alpha_n\sin\phi_n - \cos\beta\cos\phi_n\right]$$
$$+ \sqrt{\frac{2}{5}}T_1^3(a)\sin\beta\left[\cos\phi_n\cos\beta(1-\cos\alpha_n) - \sin\alpha_n\sin\phi_n\right]$$
$$+ \sqrt{\frac{2}{3}}T_3^3(a)\sin\beta\left[\cos\phi_n\cos\beta(1-\cos\alpha_n) - \sin\alpha_n\sin\phi_n\right]$$

$$U\,T_2^3(a)\,U^{-1} = -\frac{3i}{5\sqrt{2}}T_1^1(a)\sin\beta\left[\cos\beta\sin\phi_n + \sin\alpha_n\cos\phi_n - \cos\beta\cos\alpha_n\sin\phi_n\right.$$
$$+ \frac{3i}{\sqrt{30}}T_1^3(a)\sin\beta\left[\cos\beta\sin\phi_n(1-\cos\alpha_n) + \sin\alpha_n\cos\phi_n\right]$$
$$+ \frac{i}{\sqrt{2}}T_3^3(a)\sin\beta\left[\cos\beta\sin\phi_n(1-\cos\alpha_n) + \sin\alpha_n\cos\phi_n\right]$$
$$+ T_2^3(a)\left[\cos\alpha_n\cos^2\phi_n + \sin^2\phi_n(\sin^2\beta + \cos\alpha_n\cos^2\beta)\right]$$
$$- \frac{\sqrt{3}}{2}iT_2^2(s)\left[\sin\alpha_n\cos\beta - \frac{1}{2}\sin 2\phi_n(-\cos\alpha_n + \sin^2\beta + \cos\alpha_n\cos^2\beta)\right]$$

$$U\,T_3^3(a)\,U^{-1} = \frac{3}{10}T_1^1(a)\sin^2\beta(1-\cos\alpha_n)$$
$$+ \frac{3}{2\sqrt{15}}T_1^3(a)\sin^2\beta(\cos\alpha_n-1)$$
$$+ T_3^3(a)\left[1 + \frac{1}{2}\sin^2\beta(\cos\alpha_n-1)\right]$$
$$+ \frac{\sqrt{3}}{2\sqrt{2}}T_2^2(s)\sin\beta\left[\cos\beta\cos\phi_n(1-\cos\alpha_n) + \sin\phi_n\sin\alpha_n\right]$$
$$+ \frac{i}{\sqrt{2}}T_2^3(a)\sin\beta\left[\cos\beta\sin\phi_n(-1+\cos\alpha_n) + \sin\alpha_n\cos\phi_n\right]$$

...contd.

where

$$a_1(t)=\begin{cases}\cos(\omega_{eff}t_1)\ , & \ldots\quad 0\le t_1\le \dfrac{\theta_1}{\omega_{rf}}\\ \cos\theta_1\cos(\omega_{eff}t_2)-\sin\theta_1\sin(\omega_{eff}t_2)\cos\phi_2\ , & \ldots\quad 0\le t_2\le \dfrac{\theta_2}{\omega_{rf}}\\ \left.\begin{array}{l}\cos\theta_1[\cos(\omega_{eff}t_3)\cos\theta_2-\sin\theta_2\sin(\omega_{eff}t_3)\cos(\phi_2-\phi_3)]\\ -\sin\theta_1(\cos\theta_2-1)\sin(\omega_{eff}t_3)[\frac{1}{2}\sin\phi_3\sin2\phi_2+\cos^2\phi_2\cos\phi_3]\\ -\sin\theta_1[\sin\theta_2\cos\phi_2\cos(\omega_{eff}t_3)+\sin(\omega_{eff}t_3)\cos\phi_3]\end{array}\right\} & \ldots\quad 0\le t_3\le \dfrac{\theta_3}{\omega_{rf}}\end{cases}$$

.. (IV.34)

$$a_2(t)=\begin{cases}\sin(\omega_{eff}t_1), & \ldots\quad 0\le t_1\le \dfrac{\theta_1}{\omega_{rf}}\\ \sin\theta_1\cos(\omega_{eff}t_2)+\cos\theta_1\sin(\omega_{eff}t_2)\cos\phi_3, & \ldots\quad 0\le t_2\le \dfrac{\theta_2}{\omega_{rf}}\\ \left.\begin{array}{l}-\sin\theta_1[\sin\theta_2\cos(\phi_2-\phi_3)\sin(\omega_{eff}t_3)-\cos\theta_2\cos(\omega_{eff}t_3)]\\ +\cos\theta_1(\cos\theta_2-1)\sin(\omega_{eff}t_3)[\cos^2\phi_2\cos\phi_3+\frac{1}{2}\sin2\phi_2\sin\phi_3]\\ +\cos\theta_1[\sin\theta_2\cos\phi_2\cos(\omega_{eff}t_3)+\cos\phi_3\sin(\omega_{eff}t_3)]\end{array}\right\} & \ldots\quad 0\le t_3\le \dfrac{\theta_3}{\omega_{rf}}\end{cases}$$

.. (IV.35)

$$a_3(t)=\begin{cases}0\ , & \ldots\quad 0\le t_1\le \dfrac{\theta_1}{\omega_{rf}}\\ \dfrac{-6}{5\sqrt{2}}\sin\phi_2\sin(\omega_{eff}t_2)\ , & \ldots\quad 0\le t_2\le \dfrac{\theta_2}{\omega_{rf}}\\ \left.\begin{array}{l}\dfrac{-6}{5\sqrt{2}}[\sin\theta_2\sin\phi_2\cos(\omega_{eff}t_3)+\sin\phi_3\sin(\omega_{eff}t_3)]\\ \dfrac{-3}{5\sqrt{2}}(\cos\theta_2-1)\sin(\omega_{eff}t_3)[\sin2\phi_2\cos\phi_3+\\ \qquad(1-\cos2\phi_2)\sin\phi_3]\end{array}\right\} & \ldots\quad 0\le t_3\le \dfrac{\theta_3}{\omega_{rf}}\end{cases}$$

.. (IV.36)

and

$$a_4(t) = \begin{cases} 0 \quad , & .. \; 0 \le t_1 \le \dfrac{\theta_1}{\omega_{rf}} \\ \dfrac{-4}{\sqrt{30}} \sin(\omega_{eff} t_2) \sin\phi_2 \quad , & .. \; 0 \le t_2 \le \dfrac{\theta_2}{\omega_{rf}} \\ \dfrac{-4}{\sqrt{30}} [\sin\theta_2 \sin\phi_2 \cos(\omega_{eff} t_3) + \sin\phi_3 \sin(\omega_{eff} t_3)] & \\ + \dfrac{2}{\sqrt{30}} (\cos\theta_2 - 1) \sin(\omega_{eff} t_3) [-\cos\phi_3 \sin 2\phi_2 & \\ \qquad + \sin\phi_3 (\cos 2\phi_2 - 1)] & .. \; 0 \le t_3 \le \dfrac{\theta_3}{\omega_{rf}} \end{cases}$$

.. (IV.37)

The zeroth-order Magnus expansion term, $V_1^{(0)}$ (vide Eqn. I.25) can be obtained by integrating Eqns. (IV.34), (IV.35), (IV.36) and (IV.37). Thus we get,

$$V_1^{(0)} = \frac{\Delta\omega_Q}{\sqrt{6}\omega_{rf}} [a_1 T_o^2 + i a_2 T_1^2(s) + a_3 T_1^1(a) + a_4 T_1^3(a)] \; .. \; (IV.38)$$

where $a_1 = \sin\theta_1 [1 + (\cos\theta_2 - 1)\cos\phi_2] + \cos\theta_1 [\sin\theta_2 + \cos\theta_2 \sin\theta_3]$

$$+ (\cos\theta_3 - 1)[\sin\theta_2 \cos\theta_1 \cos(\phi_2 - \phi_3) + \sin\theta_1 \cos\phi_3]$$

$$- \sin\theta_1 \sin\theta_2 \sin\theta_3 \cos\phi_2 + (\cos\theta_2 - 1)(\cos\theta_3 - 1)\sin\theta_1 \cdot$$

$$\cdot [\tfrac{1}{2} \sin\phi_3 \sin 2\phi_2 + \cos^2\phi_2 \cos\phi_3]$$

.. (IV.39)

$$a_2 = \cos\theta_1 [1 + \cos\phi_2(\cos\theta_2 - 1) - \sin\theta_2 \sin\theta_3 \cos\phi_2 + \cos\phi_3(\cos\theta_3 - 1)]$$

$$- \sin\theta_1 [\sin\theta_2 + \cos\theta_2 \sin\theta_3 + \sin\theta_2(\cos\theta_3 - 1)\cos(\phi_2 - \phi_3)]$$

$$+ \cos\theta_1 (\cos\theta_2 - 1)(\cos\theta_3 - 1) [\tfrac{1}{2} \sin 2\phi_2 \sin\phi_3 + \cos^2\phi_2 \cos\phi_3] - 1$$

.. (IV.40)

$$a_3 = \frac{-3}{5\sqrt{2}}(\cos\theta_2-1)[2\sin\phi_2 + \cos\phi_3\sin 2\phi_2(\cos\theta_3-1) + \sin\phi_3(1-\cos 2\phi_2)(\cos\theta_3-1)] + \frac{6}{5\sqrt{2}}[\sin\theta_2\sin\theta_3\sin\phi_3 - \sin\phi_3(\cos\theta_3-1)] \quad .. \text{(IV.41)}$$

and

$$a_4 = \frac{-4}{\sqrt{30}}(\cos\theta_2-1)[\sin\phi_2 + \frac{\cos\phi_3}{2}\sin 2\phi_2(\cos\theta_3-1) - \frac{\sin\phi_3}{2}(\cos 2\phi_2-1)(\cos\theta_3-1)] + \frac{4}{\sqrt{30}}[\sin\theta_2\sin\theta_3\sin\phi_2 - \sin\phi_3(\cos\theta_3-1)] \quad .. \text{(IV.42)}$$

The condition that a zeroth-order composite pulse sequence should satisfy $V_1^{(0)} = 0$,[17] demands that all the coefficients a_1, a_2, a_3 and a_4 have to be individually zero. But the condition that $[V_1^{(0)}, \rho(0)] = 0$[18] needs only a_2, a_3 and a_4 to be zero. Using these conditions, we have arrived at many sequences for spin I = 3/2 case. These sequences with their zeroth-order terms, $V_1^{(0)}$, are given in Table IV.4. It should be mentioned here that all these sequences which compensate for efg inhomogeneity in the case of spin I = 3/2 have been discussed in Chapter III in the context of spin I = 1 nuclei (see Tables III.1 and III.3). The underlying similarity between these two cases now emerges.

IV.B.2 Zeroth-Order Composite Pulses to Compensate rf Field Inhomogeneity

The time dependent rf field inhomogeneity Hamiltonian in the toggling frame[10] of a three-pulse sequence has been derived

Table IV.4 Zeroth-Order Magnus Expansion Terms, $V_1^{(0)}$, for NQR Composite Pulses that Compensate for efg inhomogeneity Effects in the Case of Spin I = 3/2 Quadrupole Nuclei

Composite Pulse	$V_1^{(0)}(\sqrt{6}\,\omega_{rf}/\Delta\omega_Q)$
(a) Composite $\pi/2$ pulses	
$\overline{22.5}$ 112.5	$1.765\,T_o^2 + 0.848\,iT_1^2(s)$
$\overline{45}$ 135	$2.41\,T_o^2 + 0.414\,iT_1^2(s)$
$\overline{60}$ 150	$2.73\,T_o^2 - 0.149\,iT_1^2(s)$
$(90)_0\text{-}(300)_{90}$	$T_o^2 - 0.134\,iT_1^2(s) + 0.424\,T_1^1(a) + 0.365\,T_1^3(a)$
$\overline{114.3}$ 318.6 $\overline{114.3}$	0
385 $\overline{320}$ 25	$0.033\,T_o^2 - 0.033\,iT_1^2(s)$
(b) Composite π pulses	
260 $\overline{80}$	$-1.97\,T_o^2 - 0.35\,iT_1^2(s)$
$\overline{22.5}$ 225 $\overline{225}$	$1.67\,iT_1^2(s)$
$\overline{45}$ 270 $\overline{45}$	$0.83\,iT_1^2(s)$
$\overline{60}$ 300 $\overline{60}$	0
90 $\overline{180}$ 270	$4.0\,T_o^2 - 2.0\,iT_1^2(s)$
260 $\overline{160}$ 80	$-3.939\,T_o^2 - 2.0\,iT_1^2(s)$
90 $\overline{225}$ 315	$3.414\,T_o^2 - 0.586\,iT_1^2(s)$
315 $\overline{225}$ 90	$-3.414\,T_o^2 - 0.586\,iT_1^2(s)$
$(90)_0\text{-}(270)_{90}\text{-}(90)_0$	0

where $\omega_{rf} = (3+\eta)\omega_1/(3+\eta^2)^{1/2}$.

using the results of Tables IV.2 and IV.3 to be

$$\tilde{\tilde{V}}_2(t) = \Delta\omega_1[b_1(t)T_o^2 + b_2(t)T_1^1(a) + b_3(t)T_1^2(s) + b_4(t)T_1^3(a)] \quad .. \text{(IV.43)}$$

$$b_1(t) = \begin{cases} 0 \ , & .. \ 0 \le t_1 \le \dfrac{\theta_1}{\omega_{rf}} \\ -\frac{1}{2}\sin\theta_1\sin\phi_2 \ , & .. \ 0 \le t_2 \le \dfrac{\theta_2}{\omega_{rf}} \\ \frac{1}{2}\cos\theta_1\sin\theta_2\cos\phi_2(\cos\phi_3-\sin\phi_3) & \\ + \frac{1}{\sqrt{2}}\sin\theta_1(\cos\theta_2-1)\left[\frac{3}{10}\cos\phi_3\sin2\phi_2-\cos^2\phi_2\sin\phi_3\right. & \\ \qquad \left. + \frac{1}{5}\sin2\phi_2\sin\phi_3\right] & .. \ 0 \le t_3 \le \dfrac{\theta_3}{\omega_{rf}} \end{cases} \quad .. \text{(IV.44)}$$

$$b_2(t) = \begin{cases} \frac{3}{5} \ , & 0 \le t_1 \le \dfrac{\theta_1}{\omega_{rf}} \\ \frac{3}{5}\cos\phi_2 \ , & 0 \le t_2 \le \dfrac{\theta_2}{\omega_{rf}} \\ \frac{3}{5}\cos\phi_3 + \frac{3}{10}(\cos\theta_2-1)[\cos\phi_3(1-\cos2\phi_2)-\sin\phi_3\sin2\phi_2] & 0 \le t_3 \le \dfrac{\theta_3}{\omega_{rf}} \end{cases} \quad .. \text{(IV.45)}$$

$$b_3(t) = \begin{cases} 0 \ , & .. \ 0 \le t_1 \le \dfrac{\theta_1}{\omega_{rf}} \\ \frac{i}{2}\cos\theta_1\sin\phi_2 \ , & .. \ 0 \le t_2 \le \dfrac{\theta_2}{\omega_{rf}} \\ \frac{-i}{2}\sin\theta_1\sin\theta_2\cos\phi_2(\cos\phi_3-\sin\phi_3) & \\ \frac{-i}{5\sqrt{2}}\cos\theta_1(\cos\theta_2-1)\left[\frac{3}{2}\cos\phi_3\sin2\phi_2 - 5\cos^2\phi_2\sin\phi_3\right. & \\ \qquad \left. +\sin2\phi_2\cos\phi_3\right] & .. \ 0 \le t_3 \le \dfrac{\theta_3}{\omega_{rf}} \end{cases} \quad .. \text{(IV.46)}$$

and

$$b_4(t) = \begin{cases} \frac{2}{\sqrt{15}}\,, & .. \; 0 \le t_1 \le \frac{\theta_1}{\omega_{rf}} \\ \frac{2}{\sqrt{15}}\cos\phi_2\,, & .. \; 0 \le t_2 \le \frac{\theta_2}{\omega_{rf}} \\ \frac{1}{\sqrt{15}}(\cos\theta_2 - 1)[\cos\phi_3(1-\cos 2\phi_2) - \sin\phi_3 \sin 2\phi_2] \\ + \frac{2}{\sqrt{15}}\cos\phi_3 & .. \; 0 \le t_3 \le \frac{\theta_3}{\omega_{rf}} \end{cases}$$

.. (IV.47)

Using the Magnus expansion,[16] we write

$$\approx\!\!\!\!\!\!\sim \quad V_2(t) = V_2^{(0)} + V_2^{(1)} + \ldots \qquad .. \text{ (IV.48)}$$

To get an effective time independent Hamiltonian, $\approx\!\!\!\!\!\!\sim V_2$, in the toggling frame,[15] we truncate all higher order terms ($V_2^{(n)}$; $n \geq 1$) in the series. By integrating Eqns. (IV.44) - (IV.47), we get the zeroth-order term, $V_2^{(0)}$ as

$$V_2^{(0)} = \frac{\Delta\omega_1}{\omega_{rf}} [b_1 T_0^2 + b_2 T_1^1(a) + b_3 T_1^2(s) + b_4 T_1^3(a)] \qquad .. \text{ (IV.49)}$$

where $b_1 = -\frac{\theta_2}{\sqrt{2}} \sin\theta_1 \sin\phi_2 + \frac{\theta_3}{\sqrt{2}} \cos\theta_1 \sin\theta_2 \cos\phi_2 (\cos\phi_3 - \sin\phi_3)$

$$+ \frac{\theta_3}{5\sqrt{2}} \sin\theta_1 (\cos\theta_2 - 1) \left\{ \frac{3}{2} \cos\phi_3 \sin 2\phi_2 - 5\cos^2\phi_2 \sin\phi_3 \right.$$

$$\left. + \sin\phi_3 \sin 2\phi_2 \right\} \qquad .. \text{ (IV.50)}$$

$$b_2 = \frac{3}{5}\left\{\begin{array}{l}\theta_1 + \theta_2\cos\phi_2 + \theta_3\cos\phi_3 \\ + \theta_3(\cos\ _2-1)\left[\frac{1}{2}\cos\phi_3(1-\cos2\phi_2) - \sin\phi_3\sin2\phi_2\right]\end{array}\right\} \quad .. \text{(IV.51)}$$

$$b_3 = \frac{i}{2}\left\{\begin{array}{l}\theta_2\cos\theta_1\sin\phi_2 + \theta_3\sin\theta_1\sin\theta_2\cos\phi_2(\cos\phi_3-\sin\phi_3) - \\ \theta_3\cos\theta_1(\cos\theta_2-1)\left[\frac{1}{2}\cos\phi_3\sin2\phi_2-\cos^2\phi_2\sin\phi_3\right. \\ \qquad\qquad \left. + \frac{1}{5}\sin2\phi_2\cos\phi_3\right]\end{array}\right\} \quad .. \text{(IV.52)}$$

and

$$b_4 = \frac{1}{\sqrt{15}}\left\{\begin{array}{l}2(\theta_1 + \theta_2\cos\phi_2 + \theta_3\cos\phi_3) \\ \qquad + \theta_3(\cos\theta_2-1)[1-\cos2\phi_2-\sin\phi_3\sin2\phi_2]\end{array}\right\} \quad .. \text{(IV.53)}$$

Using the conditions $V_2^{(0)} = 0$[17] and $[V_2^{(0)}, \rho(0)]$,[18] we obtain expressions for some of the zeroth-order composite π pulses for comensating the rf field inhomogeneity. These sequences are given in Table IV.5 along with their zeroth-order Magnus expansion terms. To our surprise, these sequences are exactly the same as that for spin I = 1 composite pulses[12] presented in Chapter III.

IV.B.3 Efficiency of Composite Pulses

The degree of compensation of a composite pulse against efg and rf field inhomogeneities can be obtained by following the time-evolution of the spin density matrix under the action of the applied pulse sequence (see Appendix D). The

Table IV.5 Zeroth-Order Magnus Expansion Terms, $V_2^{(0)}$, for NQR Composite Pulses that Compensate for rf Field Inhomogeneity in the Case of Spin I = 3/2 Quadrupole Nuclei

Composite π Pulses	$V_2^{(0)}$ $\omega_{rf}/\Delta\omega_1$
$(90)_0-(180)_{90}-(90)_0$	$-1.57\ T_o^2 + 0.94\ T_1^1(a) + 0.81\ T_1^3(a)$
$(180)_0-(180)_{120}-(180)_0$	$0.85\ T_1^1(a) - 1.92\ iT_1^2(s)$
$(90)_0-(360)_{120}-(90)_0$	$-2.72\ T_o^2 - 1.41\ T_1^1(a) - 1.22\ T_1^3(a)$

where $\omega_{rf} = (3+\eta)\omega_1/(3+\eta^2)^{1/2}$

reduced thermal equilibrium density matrix in QIF is given by

$$\tilde{\rho}(0) \approx \pi_Q^d \qquad \text{.. (IV.54)}$$

The state of the spin system at the end of a composite pulse sequence can be defined by the density matrix, $\tilde{\rho}(t)$, as

$$\tilde{\rho}(t) = U(t)\, \tilde{\rho}(0)\, U(t)^{-1} \qquad \text{.. (IV.55)}$$

where $U(t) = T \exp\left[-i \int_0^t \tilde{\mathcal{H}}(t')\, dt'\right]$ .. (IV.56)

The effective Hamiltonian in QIF during an nth-rf pulse in the composite pulse sequence is

$$\tilde{\mathcal{H}} = \tilde{\mathcal{H}}_{nrf} + \tilde{V}_1 + \tilde{V}_2 \qquad \text{.. (IV.57)}$$

$\tilde{\rho}(t)$ can be evaluated using the nested commutation (see Eqn. (I.21)) between $\tilde{\mathcal{H}}$ and $\tilde{\rho}(t)$. We have evaluated the commutation relationships between the Hamiltonian $\tilde{\mathcal{H}}$ and different irreducible tensor operators $T_q^n(s,a)$, and the results are given in Table IV.2. Substituing the results of Table IV.2 in the nested commutation relationship, the transformation of various tensors under the effect of $\tilde{\mathcal{H}}$ have been derived and they are summarized in Table IV.3. Now, using the results of Table IV.3, one can easily calculate the spin density matrix $\tilde{\rho}(t)$ for any type of pulse sequences in NQR spectroscopy. For a three-pulse composite pulse, we present in the following $\tilde{\rho}(t)$ at different time

intervals of the sequence. The density matrix $\tilde{\rho}(t_1)$, after the first pulse, namely, $(\theta_1)_o$ in the composite pulse sequence, is derived as

$$\tilde{\rho}(t_1) = T_o^2 [\cos^2\beta + \sin^2\beta \cos\alpha_1] + iT_1^2(s) \sin\beta \sin\alpha_1 - T_1^1(a) \frac{\sqrt{18}}{10} \sin 2\beta (\cos\alpha_1 - 1) - T_1^3(a) \frac{2}{\sqrt{30}} \sin 2\beta (\cos\alpha_1 - 1) \quad .. \text{(IV.58)}$$

where $\beta = \tan^{-1}\left[\frac{K_1(\omega_1 + \Delta\omega_1)}{\sqrt{6}\,\Delta\omega_Q} \right]$, .. (IV.59a)

$$\alpha_1 = [\Delta\omega_Q \sqrt{6} \cos\beta + K_1(\omega_1 + \Delta\omega_1)\sin\beta] t_1 \quad .. \text{(IV.59b)}$$

and

$$K_1 = \sqrt{3} \cos\lambda + \sin\lambda \quad .. \text{(IV.59c)}$$

α_1 is the effective flip angle of the rf pulse when V_1 and V_2 are not negligible whereas θ_1 is the flip angle of the same rf pulse when the effects of V_1 and V_2 are not considered. Now, after the application of a second rf pulse, namely, $(\theta_2)_{\phi_2}$, the density matrix in QIF becomes

$$\tilde{\rho}(t_2) = A_1 T_o^2 + iB_1 T_1^2(s) + C_1 T_1^1(a) + D_1 T_1^3(a) \quad .. \text{(IV.60)}$$

where $A_1 = \cos^4\beta + \sin^4\beta \cos\alpha_1 \cos\alpha_2 + \cos^2\beta \sin^2\beta (\cos\alpha_1 + \cos\alpha_2)$

$$- \frac{1}{2} \sin 2\beta \sin\beta (\cos\alpha_1 - 1)[\cos\beta \cos\phi_2 - \sin\alpha_2 \sin\phi_2 - \cos\beta \cos\phi_2 \cos\alpha_2]$$

$$- \sin\alpha_1 \sin^2\beta [\sin\phi_2 \cos\beta (1 - \cos\alpha_2) + \sin\alpha_2 \cos\phi_2] \quad .. \text{(IV.61)}$$

$$B_1 = \sin\beta[\cos^2\beta + \sin^2\beta\cos\alpha_1]\,[\cos\phi_2\sin\alpha_2 + \sin\phi_2\cos\beta\,(\cos\alpha_2-1)]$$

$$+ \tfrac{1}{4}\sin 2\beta\,(\cos\alpha_1-1)[-\sin 2\phi_2\,\cos\alpha_2\sin^2\beta + \sin 2\phi_2\sin^2\beta + 2\cos\beta\,\sin\alpha_2]$$

$$+\sin\alpha_1\sin\beta[\sin^2\phi_2(\sin^2\beta + \cos^2\beta\cos\alpha_2) + \cos\alpha_2\cos^2\phi_2] \quad .. \text{ (IV.62)}$$

$$C_1 = \frac{-\sqrt{18}}{5}\sin\beta(\cos^2\beta + \sin^2\beta\cos\alpha_1)[\cos\beta\cos\phi_2(\cos\alpha_2-1) - \sin\alpha_2\sin\phi_2]$$

$$- \frac{\sqrt{18}}{10}\sin 2\beta(\cos\alpha_1-1)\left[\cos^2\phi_2(\sin^2\beta + \cos^2\beta\cos\alpha_2) + \sin^2\phi_2\cos\alpha_2\right]$$

$$- \frac{\sqrt{18}}{5}\sin\beta\sin\alpha_1[\cos\phi_2(\sin\phi_2\sin^2\beta + \sin\phi_2\cos^2\beta\cos\alpha_2 - \cos\phi_2\sin\alpha_2\cos\beta)$$

$$-\sin\phi_2(\sin\phi_2\cos\beta\sin\alpha_2 + \cos\alpha_2\cos\phi_2)] \quad .. \text{ (IV.63)}$$

$$D_1 = -\frac{2}{3}\sqrt{\frac{6}{5}}\,[\cos^2\beta + \cos\alpha_1\sin^2\beta]\sin\beta[\cos\beta\cos\phi_2(\cos\alpha_2-1) - \sin\phi_2\sin\alpha_2]$$

$$-\sin 2\beta(\cos\alpha_1-1)\sqrt{\frac{2}{15}}\,[\cos^2\phi_2(\sin^2\beta + \cos^2\beta\cos\alpha_2) + \sin^2\phi_2\cos\alpha_2]$$

$$- \frac{2}{3}\sqrt{\frac{6}{5}}\sin\beta\sin\alpha_1[\cos\phi_2(\sin\phi_2\sin^2\beta + \sin\phi_2\cos^2\beta\cos\alpha_2 - \cos\phi_2\sin\alpha_2\cos\beta)$$

$$-\sin\phi_2(\sin\phi_2\cos\beta\sin\alpha_2 + \cos\alpha_2\cos\phi_2)] \quad .. \text{ (IV.64)}$$

and

$$\alpha_2 = [\Delta\omega_Q\sqrt{6}\,\cos\beta + K_1(\omega_1 + \Delta\omega_1)\sin\beta]t_2 \quad .. \text{ (IV.65)}$$

The density matrix after the third pulse, $\tilde{\rho}(t_3)$ is given by

$$\tilde{\rho}(t_3) = A_2 T_o^2 + iB_2 T_1^2(s) + C_2 T_1^1(a) + D_2 T_1^3(a) \qquad .. \text{(IV.66)}$$

$$\begin{aligned} A_2 = {} & A_1[\cos^2\beta + \sin^2\beta\cos\alpha_3] \\ & + B_1\sin\beta[\sin\phi_3\cos\beta(1-\cos\alpha_3) - \cos\phi_3\sin\alpha_3] \\ & + \frac{C_1}{\sqrt{2}}\sin\beta[\cos\beta\cos\phi_3 + \sin\alpha_3\sin\phi_3 - \cos\beta\cos\alpha_3\cos\phi_3] \\ & + D_1\sqrt{\frac{3}{10}}\sin\beta[\cos\beta\cos\phi_3 + \sin\alpha_3\sin\phi_3 - \cos\beta\cos\phi_3\cos\alpha_3] \end{aligned} \qquad .. \text{(IV.67)}$$

$$\begin{aligned} B_2 = {} & A_1\sin\beta[\cos\phi_3\sin\alpha_3 - \sin\phi_3\cos\beta(\cos\alpha_3-1)] \\ & + iB_1\left\{\sin^2\phi_3[\sin^2\beta + \cos^2\beta\cos\alpha_3] + \cos\phi_3\cos(\alpha_3+\phi_3)\right\} \\ & + \frac{C_1}{2\sqrt{2}}\left\{\sin 2\phi_3\sin^2\beta(1-\cos\alpha_3) - 2\cos\beta\sin\alpha_3\right\} \\ & + D_1\sqrt{\frac{3}{10}}\left\{\frac{\sin 2\phi_3}{2}(\sin^2\beta - \cos\alpha_3 + \cos^2\beta\cos\alpha_3) - \sin\alpha_3\cos\beta\right\} \end{aligned} \qquad .. \text{(IV.68)}$$

$$\begin{aligned} C_2 = {} & \frac{3C_1}{5}[\cos^2\phi_3(\cos^2\beta\cos\alpha_3 + \sin^2\beta) + \sin^2\phi_3\sin\alpha_3] \\ & + \frac{C_1}{5}[\sin^2\beta(-1+\cos\alpha_3) + 2] \\ & - \frac{\sqrt{18}}{5}B_1[-\cos\phi_3(\sin\phi_3\sin^2\beta + \sin\phi_3\cos^2\beta\cos\alpha_3 \\ & \qquad + \cos\phi_3\sin\alpha_3\cos\beta) \\ & \qquad + \sin\phi_3(\cos\alpha_3\cos\phi_3 - \sin\phi_3\cos\beta\sin\alpha_3)] \\ & - \frac{\sqrt{18}}{5}A_1\left[\frac{\sin 2\beta}{2}\cos\phi_3(\cos\alpha_3-1) + \sin\alpha_3\sin\beta\sin\phi_3\right] \\ & + \frac{3}{5}\sqrt{\frac{3}{5}}D_1\left[-1 - \frac{\sin^2\beta}{2}(\cos\alpha_3-1) + \sin^2\phi_3\cos\alpha_3\right. \\ & \qquad \left. + \cos^2\phi_3(\sin^2\beta + \cos^2\beta\cos\alpha_3)\right] \end{aligned} \qquad .. \text{(IV.69)}$$

and

$$D_2 = -\sqrt{\frac{8}{15}}\sin\beta\, A_1[\cos\beta\cos\phi_3(\cos\alpha_3-1) + \sin\alpha_3\sin\phi_3]$$
$$+\sqrt{\frac{8}{15}} B_1[\cos\phi_3(\sin\phi_3\sin^2\beta + \sin\phi_3\cos^2\beta\cos\alpha_3 + \cos\phi_3\sin\alpha_3\cos\beta) + \sin\phi_3(\sin\phi_3\cos\beta\sin\alpha_3 - \cos\alpha_3\cos\phi_3)]$$
$$+\frac{C_1}{\sqrt{15}}[2\cos^2\phi_3(\sin^2\beta + \cos^2\beta\cos\alpha_3) + 2\sin^2\phi_3\cos\alpha_3 + \sin^2\beta(1-\cos\alpha_3) - 2]$$
$$+\frac{3}{5} D_1\left[1+\frac{\sin^2\beta}{2}(\cos\alpha_3-1) + \frac{2}{3}\sin^2\phi_3\cos\alpha_3 + \frac{2}{3}\cos^2\phi_3(\sin^2\beta + \cos^2\beta\cos\alpha_3)\right] \quad .. \text{(IV.70)}$$

where $\alpha_3 = t_3[\Delta\omega_Q\sqrt{6}\cos\beta + (\omega_1 + \Delta\omega_1)K_1\sin\beta]$ .. (IV.71)

Now, the efficiency of a composite $\pi/2$ pulse can be judged by measuring the signal intensity, W_1' (refer to Appendix D) as a function of $\Delta\omega_Q$ or $\Delta\omega_1$. W_1' is given as (see Eqn.(II.27)).

$$W_1' = \frac{\mathrm{Tr}\left[\frac{-i}{2\sqrt{2}} T_1^2(s)^\dagger \tilde{\rho}(t_3)\right]}{\mathrm{Tr}\left[\left(\frac{-i}{2\sqrt{2}} T_1^2(s)\right)^2\right]} \quad .. \text{(IV.72)}$$

where $iT_1^2(s)$ is the tensor operator corresponding to the observable spin magnetization in QIF. Similarly, the extent of spin inversion by a composite π pulse is given by (see Eqn. (II.28)):

$$W_2' = \frac{-\mathrm{Tr}[T_o^{2\dagger}\tilde{\rho}(t_3)]}{\mathrm{Tr}[(T_o^2)^2]} \quad .. \text{(IV.73)}$$

where $(T_q^n)\dagger$ is the adjoint of T_q^n expressed as

$$(T_q^n) = (-1)^q T_{-q}^n \qquad .. (IV.74)$$

Analytical expressions for W_1' and W_2' have been derived and, interestingly, these expressions are similar to those for W_1 (Eqn. III.41) and W_2 (Eqn. III.42). However, W_n and W_n' differ only in the definitions of α_n (effective flip angle of an nth-rf pulse in the composite pulse sequence) and β (i.e. the angle which defines the direction of the effective rf field). It has been proved through computer simulations of W_1' and W_2' (as functions of $\Delta\omega_Q$ and $\Delta\omega_1$) that W_1' and W_2' behave in a manner similar to W_1 and W_2, respectively. Therefore, all those composite $\pi/2$ and π pulses reported in Tables IV.4 and IV.5 for spin $I = 3/2$ case, perform in a manner similar to that of spin $I = 1$ composite pulses as shown in Figures III.2 - III.9.

In the next section, we will discuss the applicability of these composite pulses to spin I quadrupolar nuclei in general.

IV.C Comments on the Applicability of Composite Pulses for NQR of any Spin I Quadrupole Nuclei

Usually in the theoretical analysis of magnetic resonance experiments, one is interested in knowing the expectation values of angular momentum operators I_x, I_y and I_z. This is because the effects of any kind of interactions on the spin system can be completely defined by $\langle I_x \rangle$, $\langle I_y \rangle$ and $\langle I_z \rangle$. For example, in the present work, the efficiency of a composite pulse is judged by $\langle I_x \rangle$, $\langle I_y \rangle$ and $\langle I_z \rangle$. Generally the analytical expressions for $\langle I_x \rangle$, $\langle I_y \rangle$ and $\langle I_z \rangle$ can be given in terms of

effective flip angles (α_n), rf pulse phases (ϕ_n) and the angle (β) which defines the direction of the rf radiation. Expressions for α_n and β depend upon the spin value I and the asymmetry parameter (η). Apart from the difference in the definition of α_n and β, analytical expressions for $\langle I_x \rangle$, $\langle I_y \rangle$ and $\langle I_z \rangle$ are very similar irrespective of the spin value. This has been proved for spin I = 3/2 and I = 1 problems in the last section. By mathematical induction, the proof follows for any value of I. Therefore the expression for testing composite pulses, namely, W_1 and W_2 (see Chapter III), are valid for a general spin I. Hence composite pulses reported in Chapter III will be applicable to an arbitrary spin I case. The general expressions for α_n and β are given below:

$$\alpha_n = t_n[\Delta\omega_Q \cos\beta + K' \sin\beta] \qquad .. \text{(IV.75)}$$

and $$\beta = \tan^{-1}\left[\frac{K'}{\Delta\omega_Q}\right] \qquad .. \text{(IV.76)}$$

Explicit expressions of $\Delta\omega_Q$ and K' for different spin I values have been summarized in Table IV.6.

In this context, it is worthwhile to understand the two-level nature of higher spin systems in the absence of Zeeman field. Though higher spin systems ($I \geq 3/2$) possess multilevel, an applied rf radiation connects only two doubly degenerate energy levels. For example, in (i) I = 3/2: $|\pm 1/2\rangle \leftrightarrow |\pm 3/2\rangle$, (ii) I = 5/2: $|\pm 1/2\rangle \leftrightarrow |\pm 3/2\rangle$ or $|\pm 3/2\rangle \leftrightarrow |\pm 5/2\rangle$ and similarly the single quantum coherences in I = 7/2 and I = 9/2 case (see

Table IV.6 Expressions for efg Inhomogeneity ($\Delta\omega_Q$) and the Effective rf field strength (K') for Different Spin Values

Spin of the Quadrupole Nuclei, I	$\Delta\omega_Q$	K'
1	$\frac{(3+\eta)}{4} e^2(\delta q)Q$	$2\ (\omega_1 + \Delta\omega_1)$
3/2	$\frac{(1+\eta^2/3)^{1/2}}{2} e^2(\delta q)Q$	$\frac{(3+\eta)}{(3+\eta^2)^{1/2}}\ (\omega_1+\Delta\omega_1)$
5/2 $\eta = 0$	(i) $\frac{3}{20} e^2(\delta q)Q$ for $\lvert\pm 1/2\rangle \leftrightarrow \lvert\pm 3/2\rangle$	$\sqrt{8}\ (\omega_1+\Delta\omega_1)$
	(ii) $\frac{3}{10} e^2(\delta q)Q$ for $\lvert\pm 3/2\rangle \leftrightarrow \lvert\pm 5/2\rangle$	$\sqrt{5}\ (\omega_1+\Delta\omega_1)$
7/2 $\eta = 0$	(i) $\frac{e^2(\delta q)Q}{14}$ for $\lvert\pm 1/2\rangle \leftrightarrow \lvert\pm 3/2\rangle$	$\sqrt{15}\ (\omega_1+\Delta\omega_1)$
	(ii) $\frac{e^2(\delta q)Q}{7}$ for $\lvert\pm 3/2\rangle \leftrightarrow \lvert\pm 5/2\rangle$	$\sqrt{12}\ (\omega_1+\Delta\omega_1)$
	(iii) $\frac{3}{14} e^2(\delta q)Q$ for $\lvert\pm 5/2\rangle \leftrightarrow \lvert\pm 7/2\rangle$	$\sqrt{7}\ (\omega_1+\Delta\omega_1)$

Figure IV.1). This could be the reason for the similarities noticed in the analytical expressions of I_p (where p = x, y, z) for different spin I cases. However, this may be no longer true if one does not considers non-interacting spins in the system. We may therefore propose spin I = 1 pure NQR composite pulses for higher spin systems in pure NQR spectroscopy.

In the next chapter, we discuss the procedure for pulse response studies of NQR powder specimen and present a powder averaging method for general spin I nuclei. We also present a numerical procedure for designing composite $\pi/2$ pulses to enhance the intensity of NQR signals from powder specimen.

Summary

Details of construction of composite $\pi/2$ and π pulses for compensating efg and rf field inhomogeneities have been presented for spin I = 3/2 case in pure NQR. The irreducible spherical tensor operator formalism and the Magnus expansion approach have been used for constructing composite pulses. Transformation properties of the various tensor operators involved have been tabulated, and these results could be used for constructing higher order sequences and also for studying the time evolution of the spin systems under different kinds of pulse sequences. Comments on the applicability of composite pulses for arbitrary spin I quadrupolar nuclei are made on thebasis ofthe similarity in the performance of composite pulses for spin I = 1 and I = 3/2 cases.

REFERENCES

1. A. Ramamoorthy and P. T. Narasimhan, J. Molec. Struct. 192, 333 (1989).
2. T. P. Das and E. L. Hahn, 'Nuclear Quadrupole Resonance Spectroscopy,' Academic Press, New York (1958).
3. (a) E. A. C. Lucken, 'Nuclear Quadrupole Coupling Constants,' Academic Press, New York (1969).
   (b) G. K. Semin, T. A. Babushkina and G. G. Yakobson in 'Nuclear Quadrupole Resonance in Chemistry,' translated from Russian by A. Barauch, Ed. A. J. Pick, John Wiley and Sons, New York (1975).
4. S. Vega, J. Chem. Phys. 63, 3769 (1975).
5. (a) M. E. Rose, 'Elementary Theory of Angular Momentum,' John Wiley and Sons, Inc., New York (1957).
   (b) A. R. Edmonds, 'Angular Momentum in Quantum Mechanics,' Princeton University Press, Princeton, New Jersey (1957).
   (c) U. Fano and G. Racah, 'Irreducible Tensorial Sets,' Academic Press, New York (1959).
6. G. J. Bowden and W. D. Hutchison, J. Magn. Reson. 67, 403 (1986).
7. G. J. Bowden and W. D. Hutchison, J. Magn. Reson. 70, 361 (1986);
   G. J. Bowden and W. D. Hutchison, J. Magn. Reson. 72, 61 (1987);
   G. J. Bowden, W. D. Hutchison and F. Separovic, J. Magn. Reson. 79, 413 (1988);
   G. J. Bowden, J. Khachan and J. P. D. Martin, J. Magn. Reson. 83, 79 (1989);

W. D. Hutchison, Ph.D. Thesis, University of New South Wales, NSW, Australia (1987).

8. G. J. Bowden, W. D. Hutchison and J. Khachan, J. Magn. Reson. 67, 415 (1986);
G. J. Bowden and W. D. Hutchison, J. Magn. Reson. 71, 1 (1987).

9. (a) A. Wokaun and R. R. Ernst, J. Chem. Phys. 67, 1752 (1977).
(b) S. Vega, J. Chem. Phys. 68, 5518 (1978).

10. H. A. Buckmaster, Can. J. Phys. 40, 1670 (1962);
H. A. Buckmaster, R. Chatterjee and Y. H. Shing, Phys. Status Solidi 13, 9 (1972).

11. B. C. Sanctuary, Mol. Phys. 48, 1155 (1983);
B. C. Sanctuary, T. K. Halstead and P. A. Osment, Mol. Phys. 49, 753 (1983).

12. M. S. Krishnan and B. C. Sanctuary, Z. Naturforsch. 41a, 353 (1986).

13. R. Reddy and P. T. Narasimhan, J. Molec. Struct. 192, 309 (1989).

14. M. Goldman, 'Spin Temperature and Nuclear Magnetic Resonance in Solids,' Oxford University Press, Oxford (1970), Chapter 1.

15. (a) U. Haeberlen, 'High Resolution NMR in Solids: Selective Averaging,' Academic Press, New York (1976).
(b) M. Mehring, 'Principles of High Resolution NMR in Solids,' second, revised and enlarged edition, Springer-Verlag, New York (1983).

16. W. Magnus, Commun. Pure Appl. Math. 7, 649 (1954).

17. R. Tycko, Phys. Rev. Lett. 51, 775 (1983).

18. R. Tycko, E. Schneider and A. Pines, J. Chem. Phys. 81, 680 (1984).

CHAPTER V

DESIGN OF COMPOSITE $\pi/2$ PULSES USING A NUMERICAL APPROACH TO ENHANCE THE NQR SIGNAL INTENSITY IN POWDER SPECIMENS

Large single crystals of most inorganic and organic compounds are not easily available. Smaller sized single crystals do not fill up the rf coil used in NQR spectrometers and the poor filling factor leads to a poor signal intensity.[1] Polycrystalline materials are therefore commonly used instead of single crystals in NQR. In this thesis, we have so far considered composite pulse sequences for single crystals and developed the theory accordingly. The validity of such sequences for powders can be demonstrated theoretically only if powder averaging is carried out taking into account the random orientation of the efg axes of the crystallites constituting the powder specimen.

NQR signal intensities observed for most polycrystalline samples by the application of a single rf pulse are generally poor[1] and in some cases it may not be even possible to detect the signals. This is because the strength of the rf pulse felt by the quadrupolar nuclear spins in different crystallites varies and only those nuclei whose moments precess perpendicular to the rf coil axis produce the maximum signal. It would be therefore worthwhile to design composite $\pi/2$ pulses to excite all the crystallites

uniformly in order to achieve better signal intensity. In Section V.A of this chapter, we present a theoretical model for calculating the rf pulse responses. Section V.B introduces a numerical approach to the synthesis of composite $\pi/2$ pulse sequences for use with powder specimens.

V.A.1 Model for the Spin System

In a polycrystalline sample consisting of quadrupolar nuclei, the QPAS of each crystallite is randomly oriented. Hence, unlike in the case of a single crystal, a common QPAS cannot be employed. Instead, we consider an ensemble of isolated non-interacting quadrupolar nuclei whose QPAS's are randomly oriented with respect to the laboratory frame. The angles α and β (see Figure V.1) define the orientation of V_{xx} in a given crystallite with respect to the laboratory frame in which the coil axis is the x-axis. Here it is assumed that the laboratory frame coincides with the rf principal axis system (RFPAS). We consider only the following two terms in the spin Hamiltonian, namely, the quadrupolar Hamiltonian ($\mathcal{H}_Q$), and the pulsed rf interaction with the spin system ($\mathcal{H}_{rf}$). Admittedly, this is not a good model to mimic exactly the nature of the powder specimen. A similar model has been used by Peterson[2] in his calculations of rf pulse responses in powder NQR and by Cantor and Waugh[3] in their work on pulsed spin-locking phenomenon in pure NQR spectroscopy of spin I = 1 nuclei.

In what follows, we present the details of the calculation of the response of powder samples to rf pulses using the model proposed here in order to design appropriate composite $\pi/2$ pulses

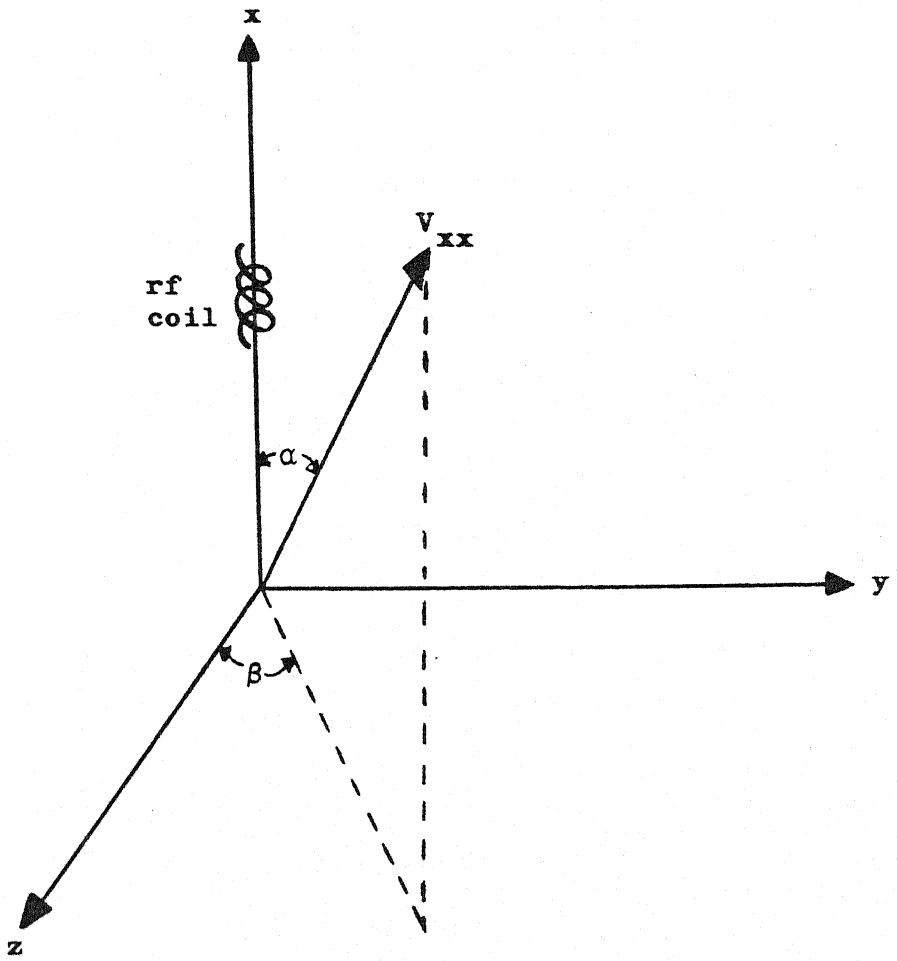

Figure V.1 Diagram showing the random orientation of QPAS's of crystallites in NQR powders with respect to the RFPAS.

for NQR spectroscopy.

V.A.2 Calculation of the System's Response to Pulsed RF

V.A.2(i) Spin I = 1 Case

Assuming that the rf pulse is applied along the x-axis of the laboratory frame with a frequency ω_Q and phase ϕ, the rf Hamiltonian in this frame is given as

$$\mathcal{H}_{rf} = -2\omega_1 \cos(\omega_Q t + \phi)[I_z \sin\alpha\cos\beta + I_y \sin\alpha\sin\beta + I_x \cos\alpha] \quad .. (V.1)$$

The frequency of the rf pulse corresponds to one of the three transitions, namely, $|0\rangle \leftrightarrow \frac{1}{\sqrt{2}}\left[|+1\rangle + |-1\rangle\right]$ (see Figure III.1). Using the fictitious spin-1/2 operator formalism,[4] Eqn. (V.1) can be written as

$$\mathcal{H}_{rf} = -4\omega_1 \cos(\omega_Q t + \phi)\left[I_{Z1} \sin\alpha\cos\beta + I_{Y1} \sin\alpha\sin\beta + I_{X1} \cos\alpha\right] \quad .. (V.2)$$

The time development of the model system will be described by following the time evolution of the reduced thermal equilibrium density matrix, $\rho(0)$ (see Eqn. (I.10)), in QIF.[5] In QIF which is defined by U_Q (see Eqn. (II.12)), the net Hamiltonian defining the spin system is given by

$$\begin{aligned}\tilde{\mathcal{H}} &= U_Q^{-1} \mathcal{H} U_Q = \tilde{\mathcal{H}}_{rf}(t) \\ &= -4\omega_1 \cos(\omega_Q t + \phi)\, \sin\alpha\cos\beta\left[I_{Z1}\cos\left(\frac{\omega_Q t}{2}\right) - I_{Z2}\sin\left(\frac{\omega_Q t}{2}\right)\right] \\ &\quad + \sin\alpha\sin\beta\left[I_{Y1}\cos\left(\frac{\omega_Q t}{2}\right) - I_{Y2}\sin\left(\frac{\omega_Q t}{2}\right)\right] \\ &\quad + \cos\alpha\left[I_{X1}\cos\left(\frac{\omega_Q t}{2}\right) + I_{X2}\sin\left(\frac{\omega_Q t}{2}\right)\right] \quad .. (V.3)\end{aligned}$$

After truncating high frequency terms in $\tilde{\mathcal{H}}_{rf}(t)$, we get the time independent rf Hamiltonian as

$$\tilde{\mathcal{H}}_{rf} = -2\omega_1 \cos\alpha [I_{X1}\cos\phi - I_{X2}\sin\phi] \qquad .. \text{(V.4)}$$

In deriving the above equation, we have made use of the time evolution of fictitious spin-1/2 operators[4] under $\mathcal{H}_Q$ given in Table V.1. These results have been obtained from the commutation relations of fictitious spin-1/2 operators given in Appendix A. Though the rf components along all the three axes (x, y and z) of the laboratory frame are present in QIF, only the x-component (see Eqn. (V.4)) is effective in inducing a transition between $|0\rangle$ and $\frac{1}{\sqrt{2}}[\,|+1\rangle + |-1\rangle\,]$ energy levels. It is important to note that the rf field felt by the spin system (see Eqn. (V.4)) is independent of the polar coordinate β whereas it depends on α. Now, at the end of an applied rf pulse with time-duration, t_1, the density matrix, $\tilde{\rho}(t_1)$, is given by

$$\tilde{\rho}(t_1) = U_{rf}\,\tilde{\rho}(0)\,U_{rf}^{-1} = \exp(-i\tilde{\mathcal{H}}_{rf}t_1)\,\rho(0)\,\exp(i\tilde{\mathcal{H}}_{rf}t_1)$$

$$= \omega_Q[I_{X3}\cos(2\omega_1\cos\alpha t_1) - I_{X2}\sin(2\omega_1\cos\alpha t_1)] \qquad .. \text{(V.5)}$$

Now , for a particular value of α we can get the 90° out-of-phase single pulse response (refer to Appendix D) as the expectation value of I_X at the end of the rf pulse

$$I_x = Tr\left\{\tilde{\rho}(t_1)\,\tilde{I}_x\sin(\omega_Q t)\right\}$$

$$= \omega_Q \sin(2\omega_1\cos\alpha t_1) \qquad .. \text{(V.6)}$$

Table V.1 Time Evolution of a few Selected Fictitious Spin-1/2 Operators under the Influence of the Quadrupole Hamiltonian, $\mathcal{H}_Q$

$U_Q\, I_{X1}\, U_Q^{-1} = I_{X1} \cos(\omega_Q t) + I_{X2} \sin(\omega_Q t)$
$U_Q\, I_{Y1}\, U_Q^{-1} = I_{Y1} \cos(\frac{\omega_Q t}{2}) - I_{Y2} \sin(\frac{\omega_Q t}{2})$
$U_Q\, I_{Z1}\, U_Q^{-1} = I_{Z1} \cos(\frac{\omega_Q t}{2}) - I_{Z2} \sin(\frac{\omega_Q t}{2})$

where $U_Q = \exp(-i \mathcal{H}_Q t)$

and $\mathcal{H}_Q = \frac{e^2 qQ}{2} (I_{X3} - I_{Y3} - I_{Z3})$.

We now perform the powder averaging. The fraction of crystallites with their x-axes pointing at an angle between α and $\alpha+d\alpha$ with respect to the rf coil axis is

$$\frac{2\pi \sin\alpha\, d\alpha}{4\pi} = \frac{-d\cos\alpha}{2} \qquad .. (V.7)$$

The NQR signal from a polycrystalline sample at the end of the rf pulse can be obtained by averaging over all possible α values.

$$\overline{\langle I_{coil} \rangle} = -\frac{\omega_Q}{2} \int_0^{\alpha=\pi} \cos\alpha \sin(2\omega_1 \cos\alpha)\, d(\cos\alpha)$$

$$= \omega_Q \left[\frac{\sin(\theta_1)}{\theta_1^2} - \frac{\cos(\theta_1)}{\theta_1} \right] \qquad .. (V.8)$$

where θ_1 is the flip angle of the rf pulse defined as $\theta_1 = 2\omega_1 t_1$. The quantity in square brackets in Eqn. (V.8) is $J_1(\theta_1)$, the first-order Bessel function. The dependence of $\overline{\langle I_{coil} \rangle}$ on θ_1 is given in Figure V.2. The value of θ_1 corresponding to the global maximum is 119° (0.66π). This means that the application of an rf pulse with a flip angle of 119° gives a maximum signal intensity in the NQR of powder specimens. This is the equivalent of a '$\pi/2$ pulse' for a powder specimen. The 'π pulse' for a powder specimen is not simply twice the time duration of $\pi/2$ pulse but it is 256° (1.43π), since this is the pulse that gives a zero signal intensity. This powder averaging procedure[2] is equivalent to calculating the rf pulse response in a single crystal first and then averaging over all possible values of α, the orientation of this crystal with respect to the rf coil axis. In the next

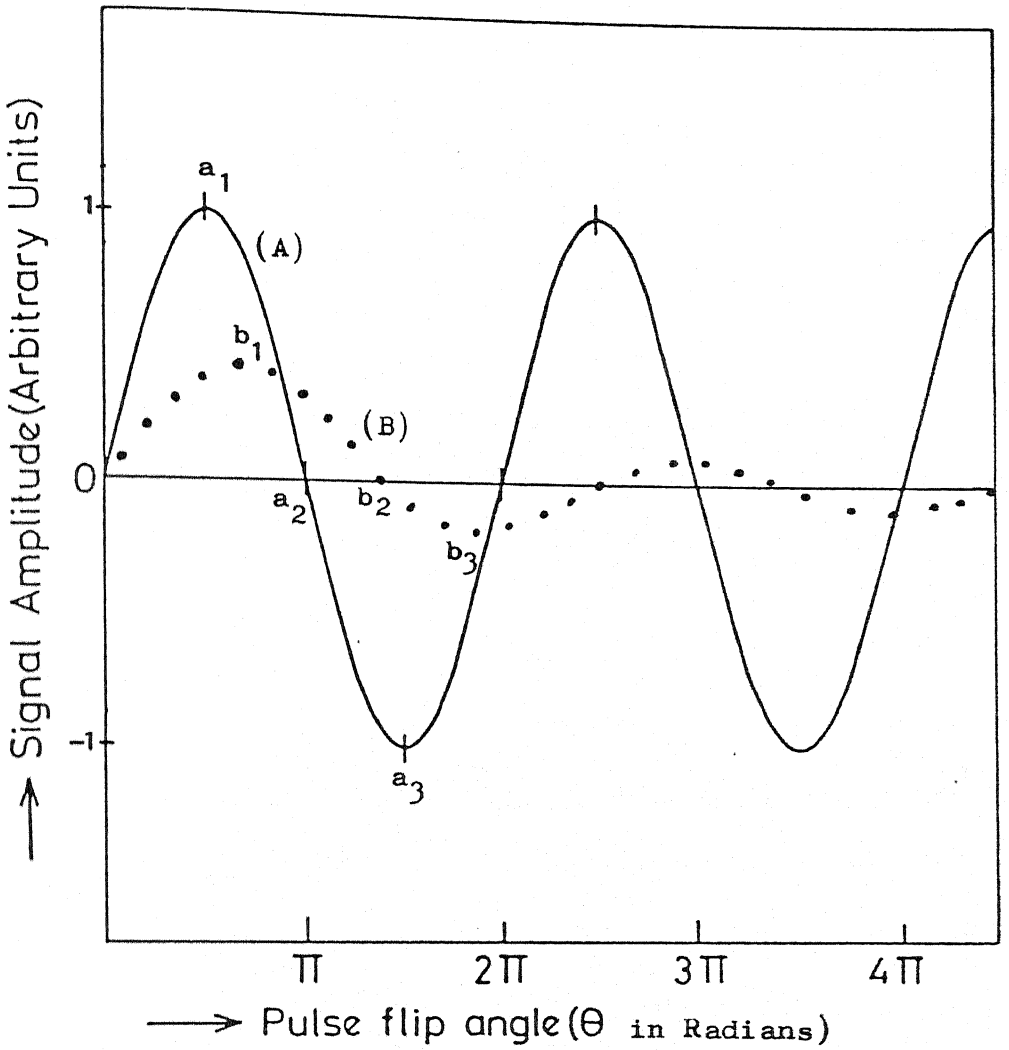

Figure V.2 Response to a single resonant rf pulse of spin I quadrupole nuclei constituting (A) single crystal and (B) powder systems.

a_1: $(\pi/2, 1)$; a_2: $(\pi, 0)$; a_3: $(3\pi/2, -1)$

b_1: $(0.66\pi, 0.436)$; b_2: $(1.43\pi, 0)$; b_3: $(1.88\pi, -0168)$

subsection, the response of a polycrystalline sample containing spin I = 3/2 nuclei to an rf pulse is discussed.

V.A.2(ii) The Case of Spin I = 3/2

We now consider an ensemble of non-interacting quadrupole nuclei with spin I = 3/2, with $\eta \neq 0$ and in the absence of a dc magnetic field. The diagonal quadrupole Hamiltonian, $\mathcal{H}_Q^d$, and the rf Hamiltonian, $\tilde{\mathcal{H}}_{rf}$, in QIF, using the tensor operator formalism[6] have been derived in Chapter IV (see Eqns. (IV.9) and (IV.23)). Now the density matrix after the application of an rf pulse with time duration t_1 is given by

$$\tilde{\rho}(t_1) = \exp(-i\tilde{\mathcal{H}}_{rf}t_1)\ \rho(0)\ \exp(i\tilde{\mathcal{H}}_{rf}t_1) \qquad .. \text{(V.9)}$$

$\tilde{\rho}(t_1)$ may be evaluated using the transformation properties of tensor operators given in Table IV.3, and is given by

$$\tilde{\rho}(t_1) = \frac{\omega_Q}{\sqrt{6}}\left[T_o^2 \cos\theta_1 + iT_1^2(s) \sin\theta_1\right] \qquad .. \text{(V.10)}$$

Now the signal intensity at the end of a single rf pulse in a single crystal case is

$$\langle I_x \rangle = \mathrm{Tr}\left\{\frac{-i}{2\sqrt{2}}\, T_1^2(s)\ \tilde{\rho}(t_1)\right\}$$

$$= \frac{\sqrt{3}\omega_Q}{8} \sin\theta_1 \qquad .. \text{(V.11)}$$

where θ_1 is the flip angle of an rf pulse in the case of a single

crystal, and is given by

$$\theta_1 = \frac{(3+\eta)\omega_1 t_1}{(3+\eta^2)^{1/2}} . \qquad .. (V.12)$$

Now assuming that the axis of the rf coil is oriented with respect to the crystallite's efg x-axis by an angle α, we get

$$\langle I_x \rangle = \frac{\sqrt{3}\omega_Q}{8} \sin(\theta_1 \cos\alpha) . \qquad .. (V.13)$$

Averaging over all possible orientations of the x-axis of the crystallites as shown for spin I = 1 case, we get the NQR signal intensity to be

$$\overline{\langle I_{coil} \rangle} = \frac{\sqrt{3}\omega_Q}{8}\left[\frac{\sin\theta_1}{\theta_1^2} - \frac{\cos\theta_1}{\theta_1}\right] . \qquad .. (V.14)$$

Generalizing, we see that when we consider the NQR allowed transition between a pair of energy levels, the response to a single pulse for a powder system containing quadrupole nuclei of spin I can be written as

$$\text{signal intensity} = C\left[\frac{\sin\theta_1}{\theta_1^2} - \frac{\cos\theta_1}{\theta_1}\right]$$

$$= C\, J_1(\theta_1) . \qquad .. (V.15)$$

The expressions for C and θ_1 are given in Table V.2 for different spin systems. This generalization is expected to be of much use in the NQR spectroscopy of powder and amorphous samples.

Table V.2 Expressions for C and θ_1 in Eqn. (V.15) for Various Values of the Spin I

Spin I	C	θ_1
1	$\frac{e^2qQ}{4}(3+\eta)$	$2\omega_1 t_1$
3/2	$\frac{\sqrt{3}e^2qQ}{16}(1+\eta^2/3)^{1/2}$	$\frac{(3+\eta)}{(3+\eta^2)^{1/2}}\omega_1 t_1$
5/2 $\eta=0$	(i) $\frac{e^2qQ}{40}$ for $\lvert\pm\frac{1}{2}\rangle \leftrightarrow \lvert\pm 3/2\rangle$	$\sqrt{8}\,\omega_1 t_1$
	(ii) $\frac{\sqrt{5}e^2qQ}{20}$ for $\lvert\pm 3/2\rangle \leftrightarrow \lvert\pm 5/2\rangle$	$\sqrt{5}\,\omega_1 t_1$
7/2 $\eta=0$	(i) $\frac{9\sqrt{15}}{56}e^2qQ$ for $\lvert\pm 1/2\rangle \leftrightarrow \lvert\pm 3/2\rangle$	$\sqrt{15}\,\omega_1 t_1$
	(ii) $\frac{3\sqrt{12}}{7}e^2qQ$ for $\lvert\pm 3/2\rangle \leftrightarrow \lvert\pm 5/2\rangle$	$\sqrt{12}\,\omega_1 t_1$
	(iii) $\frac{11\sqrt{7}}{28}e^2qQ$ for $\lvert\pm 5/2\rangle \leftrightarrow \lvert\pm 7/2\rangle$	$\sqrt{7}\,\omega_1 t_1$

V.B Numerical Design of Composite Pulses to Enhance the NQR Signal Intensity of Powder Samples

As seen in the last section, the flip angle of an rf pulse which gives a maximum NQR signal in the case of powders is 0.66π, unlike in single crystals where it is 0.5π. It should be possible to enhance the signal intensity from powder materials by using composite $\pi/2$ pulses that correspond to the optimum single $\pi/2$ pulse for powders. Such pulse sequences have to be synthesized so that they can uniformly excite different crystallites and thus yield good signal intensity. For this purpose, we shall use a general numerical approach for designing composite $\pi/2$ pulses.

Consider a cluster of N number of rf pulses, without any time delay between them and with constant rf amplitude (ω_1) and frequency (ω_Q) of the type $(\theta_1)_{\phi_1}-(\theta_2)_{\phi_2}\ldots.(\theta_N)_{\phi_N}$. Assuming that $\phi_1 = 0$ as the reference phase of the sequence, we can define the complete pulse sequence by (2N-1) variables. Now, using the density matrix approach, we can find out the signal intensity at the end of the pulse sequence for NQR powders by applying the powder averaging procedure given in the last section. The analytical expression thus derived for the NQR signal intensity is a function of (2N-1) variables. Now one has to find out the optimum values of the variables corresponding to the global maximum of the function, $\overline{\langle I_{coil} \rangle}_{max}$.

In the present work, we assume a three-pulse sequence, $(\theta_1)_0-(\theta_2)_{\phi_2}-(\theta_3)_{\phi_3}$. The reasons for limiting ourselves to a three-pulse sequence are:

(i) Sequences with a large number of rf pulses, have a larger time duration and hence will not be useful in NQR on account of the shorter T_2. As the pulse time-duration approaches T_2, the signal intensity decreases.

(ii) Constructing a pulse sequence with large number of rf pulses needs enormous computer time to maximize the function on account of the larger number of variables. Moreover, the spin dynamics calculation becomes cumbersome as we increase the number of rf pulses in the sequence.

V.B.1 Spin I = 1 Case

We first consider an ensemble of spin I = 1 nuclei, in a single crystal specimen. Using the fictitious spin-1/2 operator formalism, we can study the evolution of the spin system under the effect of the three-pulse sequence. At the end of the composite pulse we have

$$\begin{aligned}
\text{signal intensity} &= \langle I_x \rangle \\
&= \omega_Q(-\sin\phi_3)\left\{\frac{\sin\theta_1}{2}\sin(2\phi_2)\cos\phi_3(1-\cos\theta_2) + \cos\theta_1\sin\theta_2\sin(\phi_3-\phi_2)\right. \\
&\qquad \left. + \sin\theta_1\sin\phi_3(\sin^2\phi_2 + \cos^2\phi_2\cos\theta_2)\right\} \\
&+ \omega_Q\cos\phi_3\left\{\frac{\sin\theta_1}{2}\sin(2\phi_2)\sin\phi_3\cos\theta_3(1-\cos\theta_2)\right. \\
&\qquad - \cos\theta_1\sin\theta_2\cos\theta_3\cos(\phi_1-\phi_2) \\
&\qquad - \sin\theta_1\cos\theta_3\cos\phi_3(\sin^2\phi_2 + \cos\theta_2\cos^2\phi_2) \\
&\qquad \left. + \sin\theta_3(\sin\theta_1\sin\theta_2\cos\phi_2 - \cos\theta_1\cos\theta_2)\right\} \qquad \ldots (V.16)
\end{aligned}$$

where $\theta_n = 2\omega_1 t_n$.

The signal from the powder sample can be obtained in terms of the single crystal results using the powder averaging procedure,

$$\overline{\langle I_{coil} \rangle} = -\frac{\omega_Q}{2} \int_0^{\alpha=\pi} \cos\alpha \, \langle I_x \rangle_{powder} \, d(\cos\alpha) \; . \qquad .. \; (V.17)$$

The analytical expression for $\langle I_x \rangle_{powder}$ is similar to that for $\langle I_x \rangle$ (see Eqn. (V.16)) but with θ_n' instead of θ_n, where $\theta_n' = \theta_n \cos\alpha$. $\overline{\langle I_{coil} \rangle}$ is derived to be

$$\overline{\langle I_{coil} \rangle} = \omega_Q [\, X + Y \,] \qquad .. \; (V.18)$$

where $X = 2 \sin\phi_3 \sin\phi_2 \cos(\phi_3 - \phi_2) \left[\frac{-\sin\theta_1}{\theta_1^2} + \frac{\cos\theta_1}{\theta_1} \right]$

$$+ \left\{ \begin{array}{l} -\frac{1}{2} \sin 2\phi_3 \sin\phi_2 \, [\cos\phi_2 + \sin\phi_2] \\ + \sin^3\phi_3 \cos\phi_2 (1 + \cos\phi_2) \end{array} \right\} \left[\frac{\cos(R)}{R} - \frac{\sin(R)}{R^2} \right]$$

$$+ \sin\phi_3 (\cos\phi_2 - 1) \sin(\phi_3 - \phi_2) \left[\frac{\cos(S)}{S} - \frac{\sin(S)}{S^2} \right]$$

$$.. \; (V.19)$$

and

$$Y = \frac{e_1}{2} \left[\frac{\cos G}{G} - \frac{\sin G}{G^2} + \frac{\cos H}{H} - \frac{\sin H}{H^2} \right]$$

$$+ (e_2 + e_3 - 2e_4) \left[\frac{\cos A}{A} - \frac{\sin A}{A^2} \right]$$

$$+ (e_3 - e_2) \left[\frac{\cos B}{B} - \frac{\sin B}{B^2} + \frac{\cos D}{D} - \frac{\sin D}{D^2} \right]$$

$$+ (e_2 + e_3 + 2e_4) \left[\frac{\cos C}{C} - \frac{\sin C}{C^2} \right] \qquad .. \; (V.20)$$

with

$$A = \theta_1 + \theta_2 + \theta_3,$$
$$B = \theta_1 - \theta_2 + \theta_3,$$
$$C = \theta_1 + \theta_2 - \theta_3,$$
$$D = \theta_1 - \theta_2 - \theta_3,$$
$$E = \theta_1 + \theta_2,$$
$$F = \theta_1 - \theta_2,$$
$$G = \theta_1 + \theta_3,$$
$$H = \theta_1 - \theta_3,$$
$$e_1 = \cos\phi_3 \sin\phi_2 \sin(\phi_2 - \phi_3),$$
$$e_2 = \tfrac{1}{2}\cos\phi_3 \cos(\phi_3 - \phi_2),$$
$$e_3 = \tfrac{1}{2}\cos\phi_2 \cos\phi_3 \cos(\phi_3 - \phi_2),$$

and $e_4 = \tfrac{1}{2}\cos\phi_3$.

The problem of maximizing the function $\overline{\langle I_{coil} \rangle}$ is a non-linear one, and it is highly time-consuming. We have developed a computer programme (in FORTRAN language) and numerically evaluated this function by varying the flip angles and phases in steps of 3°. If we use a two-pulse sequence and maximize $\overline{\langle I_{coil} \rangle}$ using Eqns. (V.18) - (V.20), we get the sequence:

$(126)_0$-$(300)_{80}$ with relative intensity 0.44.

For a three-pulse sequence, we get

$(90)_0$-$(70)_{45}$-$(20)_{25}$ with relative intensity 0.64.

It is clear from these results that as the number of rf pulses in the composite $\pi/2$ pulse sequence increases the signal intensity

from the powder specimen increases. This could be due to the fact that the flexibility available with a two-pulse sequence is less than with a three-pulse sequence. However, at the same time the duration of the total pulse sequence should be much less than T_2.

V.B.2 General Spin I Case

It would be useful if one constructs composite $\pi/2$ pulses for spin I = 3/2 and for other spins also. We have followed a similar numerical approach for spin I = 3/2 nuclei using the irreducible spherical tensor operators to design a composite $\pi/2$ pulse to maximize the NQR signal intensity from powder specimens in the absence of a Zeeman field. We have derived the analytical expression for $\overline{\langle I_{coil} \rangle}$ for the spin I = 3/2 case and found that this function is similar to that of spin I = 1 case. The definition of flip angle, however, is altered depending on the spin of the nucleus (refer Table V.2). For example, in the spin I = 3/2 case we have $\theta_n = \frac{(3+\eta)\omega_1 t_n}{(3+\eta^2)^{1/2}}$, in comparison to $\theta_n = 2\omega_1 t_n$ in the I = 1 case. Keeping this in mind, we may conclude that the values of the variables defining the pulse sequence are the same. Hence, a $(90)_0$-$(70)_{45}$-$(20)_{25}$ composite $\pi/2$ pulse sequence can also be used for spin I = 3/2 nuclei in the absence of a magnetic field. Arguments similar to those given in Chapter IV can be used to generalize the applicability of this composite $\pi/2$ pulse sequence to an arbitrary spin I quadrupolar nucleus.

In the next chapter we present some experimental results using composite pulses for broadband excitation in NQR spectroscopy.

Summary

A numerical approach has been presented for constructing composite $\pi/2$ pulses for powder specimens to improve the signal-to-noise ratio. Using the fictitious spin-1/2 operator formalism for spin I = 1 and the tensor operator formalism for spin I = 3/2, the expectation values, namely, $\langle I_x \rangle$ and thus $\overline{\langle I_{coil} \rangle}$ have been formulated and the duration and phase of rf pulses constituting the composite $\pi/2$ pulses have been optimized. Thus, it has been found that the pulse sequence $(126)_0$-$(300)_{80}$ and $(90)_0$-$(70)_{45}$-$(20)_{25}$ can yield optimum signals and could serve as good $\pi/2$ pulses for powder materials. If the pulse flip angles are defined taking into account its variation with respect to the spin than these composite $\pi/2$ pulses can be employed, in general, for an allowed NQR transition.

REFERENCES

1. T. P. Das and E. L. Hahn, 'Nuclear Quadrupole Resonance Spectroscopy,' Academic Press, New York (1958).
2. G. L. Peterson, Ph.D. Thesis, Brown University, Providence, Rhode Island, U.S.A. (1975).
3. R. S. Cantor and J. S. Waugh, J. Chem. Phys. 73, 1054 (1980).
4. S. Vega and A. Pines, J. Chem. Phys. 66, 5624 (1977).
5. M. Goldman, 'Spin Temperature and Nuclear Magnetic Resonance in Solids,' Oxford University Press, Oxford (1970).
6. G. J. Bowden, W. D. Hutchison and J. Khachan, J. Magn. Reson. 67, 415 (1986);
   G. J. Bowden and W. D. Hutchison, J. Magn. Reson. 71, 1 (1987);
   W. D. Hutchison, Ph.D. Thesis, University of New South Wales, NSW, Australia (1987).

CHAPTER VI

EXPERIMENTAL DEMONSTRATION OF THE PERFORMANCE OF COMPOSITE PULSES IN PURE NQR SPECTROSCOPY

In Chapters III and IV, we have derived composite pulses for use in pure NQR spectroscopy via the Magnus expansion approach. This chapter deals with the experimental verification of the functioning of composite pulses in pure NQR spectroscopy. The composite pulses we have earlier derived pertain to single crystal specimens consisting of physically equivalent nuclei. Nevertheless, as general tests of performance, we have chosen to observe the ^{35}Cl pure nuclear quadrupole resonance of mercuric chloride powder and sodium chlorate (both powder and single crystal), at room temperature. In Section A of this chapter, the experimental set up used for testing composite pulses is described. Section B outlines the procedure for evaluating the performance of composite pulses, while Section C presents the experimental results showing the performance of composite pulses in mercuric chloride and sodium chlorate samples.

VI.A Experimental Set-up

This section briefly highlights the instrumental set up used for the experimental verification of NQR composite pulses.

For the present experimental work, we need to have an instrument with the following facilities. Pulse programmer with atleast $\pi/2$ phase shifts, a high-power transmitter, a receiver with large bandwidth and short dead time, fast digitizer and the spectrometer frequency going down to a few MHz. The non-availability of a pulsed FT NQR spectrometer with the abovementioned facilities in our laboratory necessitated the use of a commercial Bruker CXP 90 FT NMR spectrometer elsewhere.* The following features of the spectrometer have been used in our experimental study.

(1) High power, single solenoid coil, solid state NMR probes.

(2) High power transmitter including broadband driver amplifier and rf power amplifier.

(3) Pulse programmer, which is capable of producing rf pulses of shortest duration equal to 0.5 μs with a minimum duration step of 10.0 ns and with phases selectable in $\pi/2$ steps.

(4) Broadband receiver with direct detection (no intermediate frequency stages).

(5) Quadrature phase detection is used which allows one to place the transmitter frequency in the middle of the multiple line NQR frequency spectrum; in this manner, an efficient use of transmitter power is achieved.

(6) BC-130 fast digitizer for large NQR spectral widths having a minimum dwell time of 0.1 μs in steps of 0.1 μs.

---

*Chemical Physics Laboratory, Central Leather Research Institute, Madras, India

(7) ASPECT 2000 computer to control the spectrometer.

VI.B Experimental Verification of Composite Pulses

In any FT NQR experiment, the very first thing one has to do is to establish the relation between the flip angle and the time duration of the applied rf pulse. As has been explained in the last chapter, this relation is not a general one but varies from sample to sample. In the present work, we first performed a "$\pi/2$" pulse width calibration by pulsing close to resonance and determining the pulse width resulting in maximum signal intensity. For this, the time duration of the rf pulse width was varied and the signal intensities compared for different pulse width values. Similarly, the "π" pulse width, which gives zero signal on resonance, has also been calibrated. From these $\pi/2$ and π pulse widths, we have derived the time durations of rf pulses that constitute the composite pulse.

Now to judge the compensation of efg inhomogeneity or resonance offset effects by composite pulses, the response of the system to a single pulse was compared with its response to composite pulses at different transmitter offsets. The quality of a composite $\pi/2$ pulse may then be assessed by the extent to which it overcomes resonance offset and efficiently produces transverse magnetization resulting in improved signal intensity, as compared to the response to a single pulse excitation. Similarly, a better composite π pulse is one which gives minimum NQR signal by inverting spin population over a wider offset range when compared to the single π pulse. Important results proving

the compensation of efg inhomogeneity by composite pulses are given in the next section.

VI.C Experimental Results Showing the Performance of Composite Pulses

VI.C.1 Mercuric Chloride ($HgCl_2$)

The two ^{35}Cl NQR lines at 22.23 MHz and 22.05 MHz were first observed in $HgCl_2$ powder sample at room temperature in an unpublished work by Buyle-Bodin and Monfils, which has been quoted by Bassompiere[1] in 1953; later Buyle-Bodin and Monfils[2] studied the temperature dependence of these two lines. In 1954, Dehmelt et al.[3] assigned these two different NQR lines to the chemically inequivalent chlorines in the $HgCl_2$ molecule in the solid state. Barnes and Hultsch[4] measured the line widths in a powder sample of $HgCl_2$ and reported a value of 1.2 kHz. The asymmetry in efg has been measured in the single crystal[5] and polycrystalline material[6] of $HgCl_2$ through the Zeeman perturbed NQR spectroscopy. The asymmetry parameter (η) values for the two different ^{35}Cl sites and their efg values are summarized in Table VI.1. The crystal structure of $HgCl_2$ is given in detail in well-known book by Wyckoff,[7] and the relevant data on the crystal structure of this compound are presented in Table VI.2. Dehmelt measured the frequency of ^{37}Cl quadrupole nuclei at 303 K to be 17.5197±0.9 MHz. In the present work, we focus attention on the ^{35}Cl NQR spectroscopy. This two-line spectrum (line separation 180 kHz) would be an important system for testing the compensation of efg inhomogeneity by composite pulses.

Table VI.1 NQR Frequency, Asymmetry Parameter and Electric Field Gradients in $HgCl_2$ (300 K)

Frequency (MHz)		Electric Field Gradients (q's), in units of e
22.23	0.30±0.01	$q_{xx} = + 5.58 \times 10^{24}$ $q_{yy} = +10.36 \times 10^{24}$ $q_{zz} = -15.94 \times 10^{24}$
22.05	0.28±0.01	$q_{xx} = + 5.70 \times 10^{24}$ $q_{yy} = +10.14 \times 10^{24}$ $q_{zz} = -15.84 \times 10^{24}$

Table VI.2 Crystal Structure and Molecular Dimension Data on $HgCl_2$

Orthorhombic Unit Cell

a_o = 4.325 Å

b_o = 12.735 Å

c_o = 5.963 Å

Space group is V_h^{16} .

There are four molecules in the unit cell.

Each unit cell has two planes, which contain two molecules each, at a distance of (1/4) c_o and (3/4) c_o. The nearest distance between the two chlorine atoms in the adjacent layers is 3.35 Å.

$HgCl_2$ is a linear molecule, and the two molecules in a plane are such that their molecular axes make an angle of 77°. The molecular axis (Cl-Hg-Cl) makes an angle of 38°30' from b_o axis. The Hg-Cl bond distances are 2.23 Å and 2.27 Å.

The ionic radii of Hg^{++} and Cl^- are 1.1 Å and 1.86 Å, respectively.

A well-powdered specimen of pure $HgCl_2$ was taken in a 10 mm flat-bottomed sample tube. First, the CXP 90 Bruker spectrometer was tuned (all parts of the spectrometer, namely, probe, preamplifier, and transmitter, were tuned and receiver quadrature balance adjusted) to a frequency 22.053 MHz which is very close by one of the two NQR lines at room temperature (297 K). Fixing the transmitter gain corresponds to an rf pulse power of approximately 500 Watts; such an rf pulse was applied and the intensity of the low frequency line alone measured as a function of pulse width. Thus the powder '$\pi/2$' pulse was determined to have a width of 7.5 microseconds (μs) and the powder 'π' pulse a width of 15.0 μs. The same measurement was repeated for the transmitter frequency re-tuned to 22.233 MHz, which is near the higher frequency ^{35}Cl NQR line, and the duration times of $\pi/2$ andπ pulses have been confirmed. For different frequencies of irradiation (from one end of the spectrum to the other) by single pulse and by composite $\pi/2$ pulses, NQR signals have been recorded after Fourier transforming the FID and then phase correcting the frequency domain signal. A few of them for single $\pi/2$ pulse and for $\overline{45}$ 135 composite $\pi/2$ pulse are shown in Figure VI.1-VI.10. From these figures, it is apparent that the $\overline{45}$ 135 composite $\pi/2$ pulse excites both the NQR lines significantly more uniformly when compared to the single $\pi/2$ pulse. Therefore, it may be stated that $\overline{45}$ 135 pulse is a broadband composite $\pi/2$ pulse in NQR spectroscopy. In a similar manner, the response to all other composite $\pi/2$ pulses at different resonance offset frequencies have been found to be better than the response to the single $\pi/2$ pulse. One typical NQR spectrum

Figures VI.1 — VI.10

^{35}Cl pure quadrupole resonance spectrum of $HgCl_2$ powder specimen obtained by the application of single and composite rf pulses at various offset ($\Delta\omega_Q$) values at room temperature (297 K).

Common spectral parameters

Synthesizer frequency	=	22.14 MHz
Frequency of irradiation	=	22.14 + offset
Spectral width	=	455.0 kHz
Number of scans	=	20
Pulse time duration	=	$\pi/2$ pulse corresponds to 7.5 μs and π pulse corresponds to 15.0 μs.
Normalization constant (NC)	=	-2 unless otherwise mentioned in the figure

Zero Hertz in the x-axis scale corresponds to the irradiation frequency.

Figure VI.1(a) Single $\pi/2$

$\Delta\omega_Q$ = 50 kHz

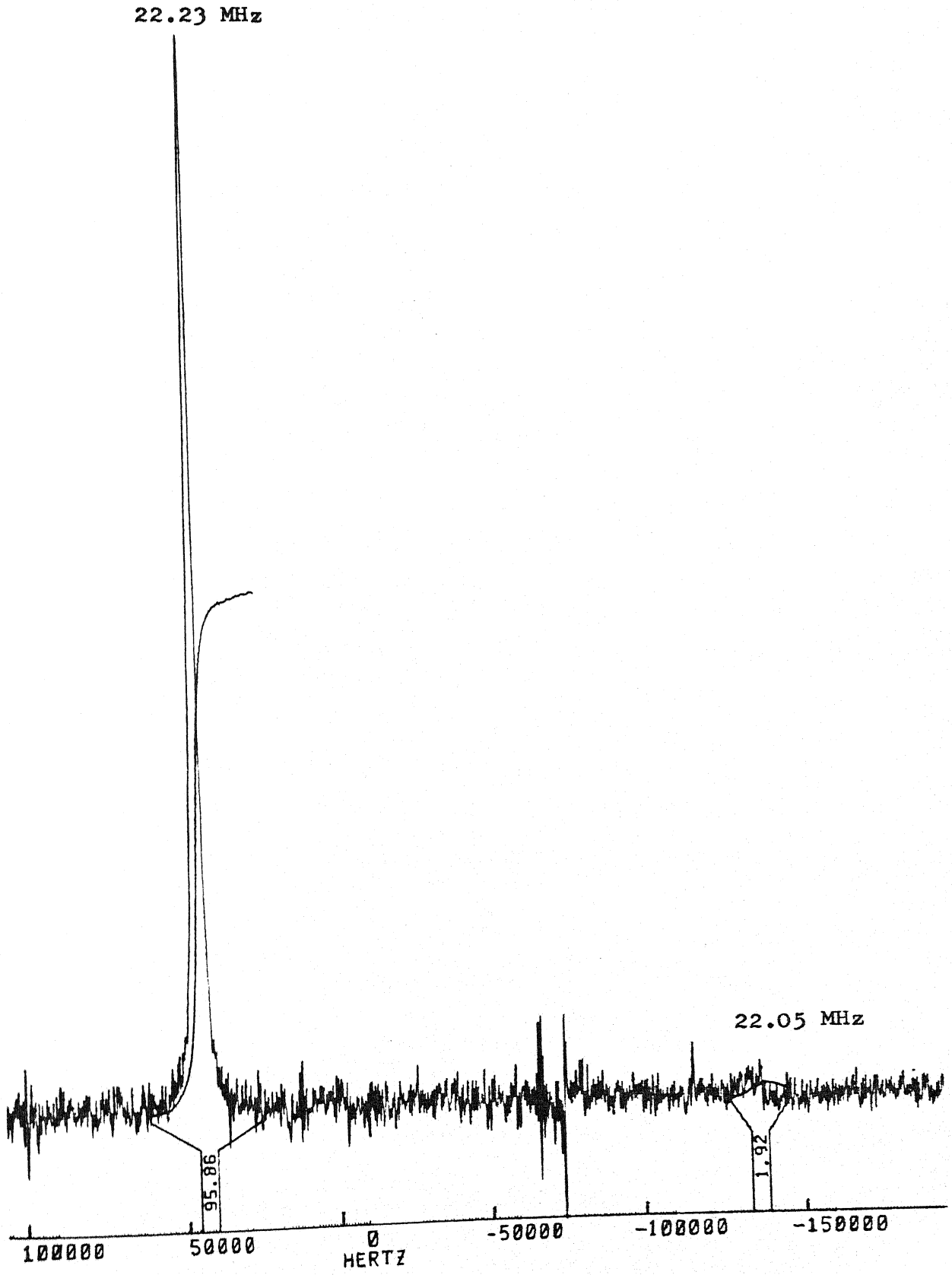

Figure VI.1(b) $\overline{45}$ 135

$\Delta\omega_Q$ = 50 kHz

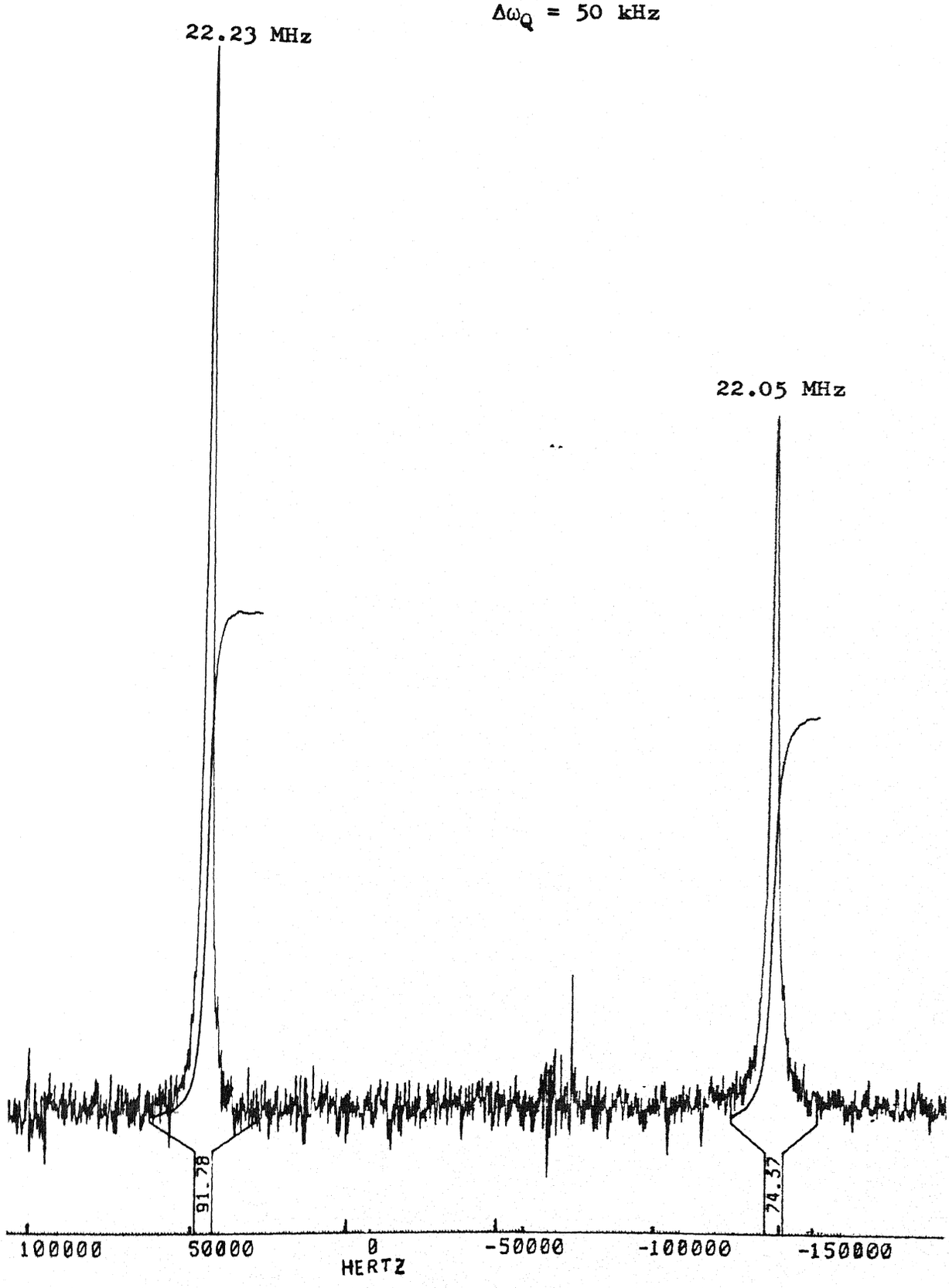

Figure VI.2(a) Single $\pi/2$

$\Delta\omega_Q$ = 40 kHz

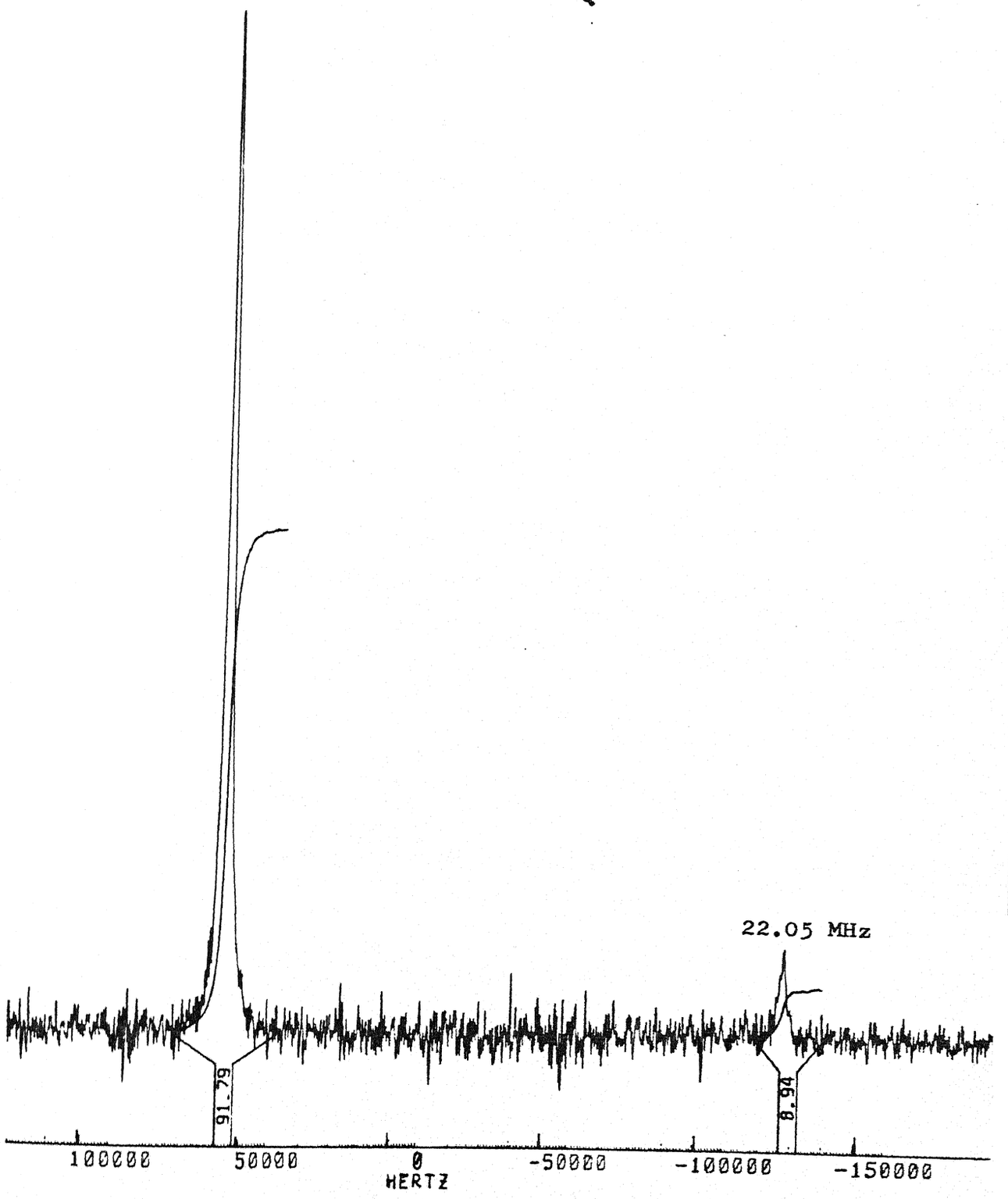

Figure VI.2(b) $\overline{45}$ 135

$\Delta\omega_Q$ = 40 kHz

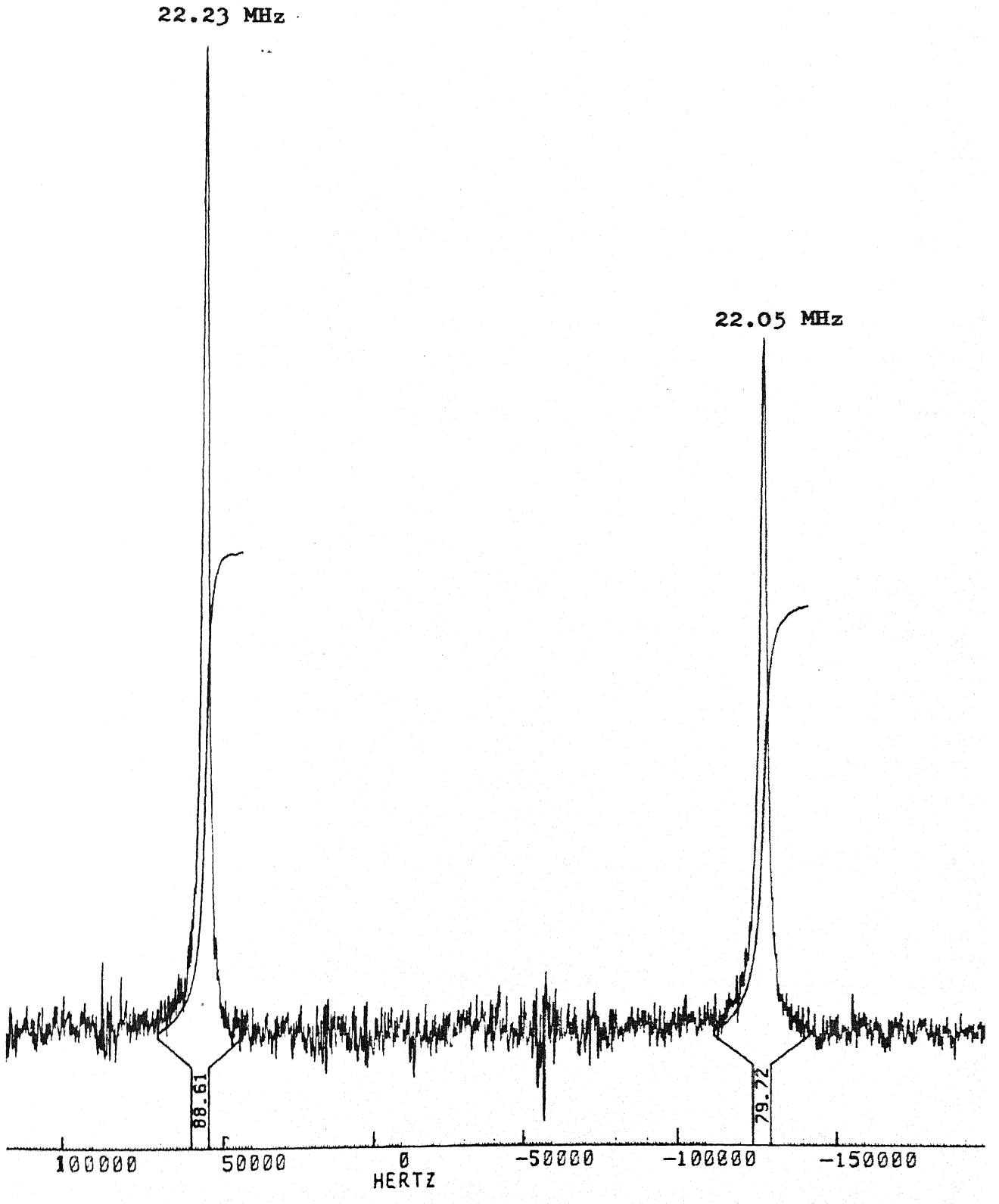

Figure VI.3(a) Single $\pi/2$

$\Delta\omega_Q$ = 30 kHz

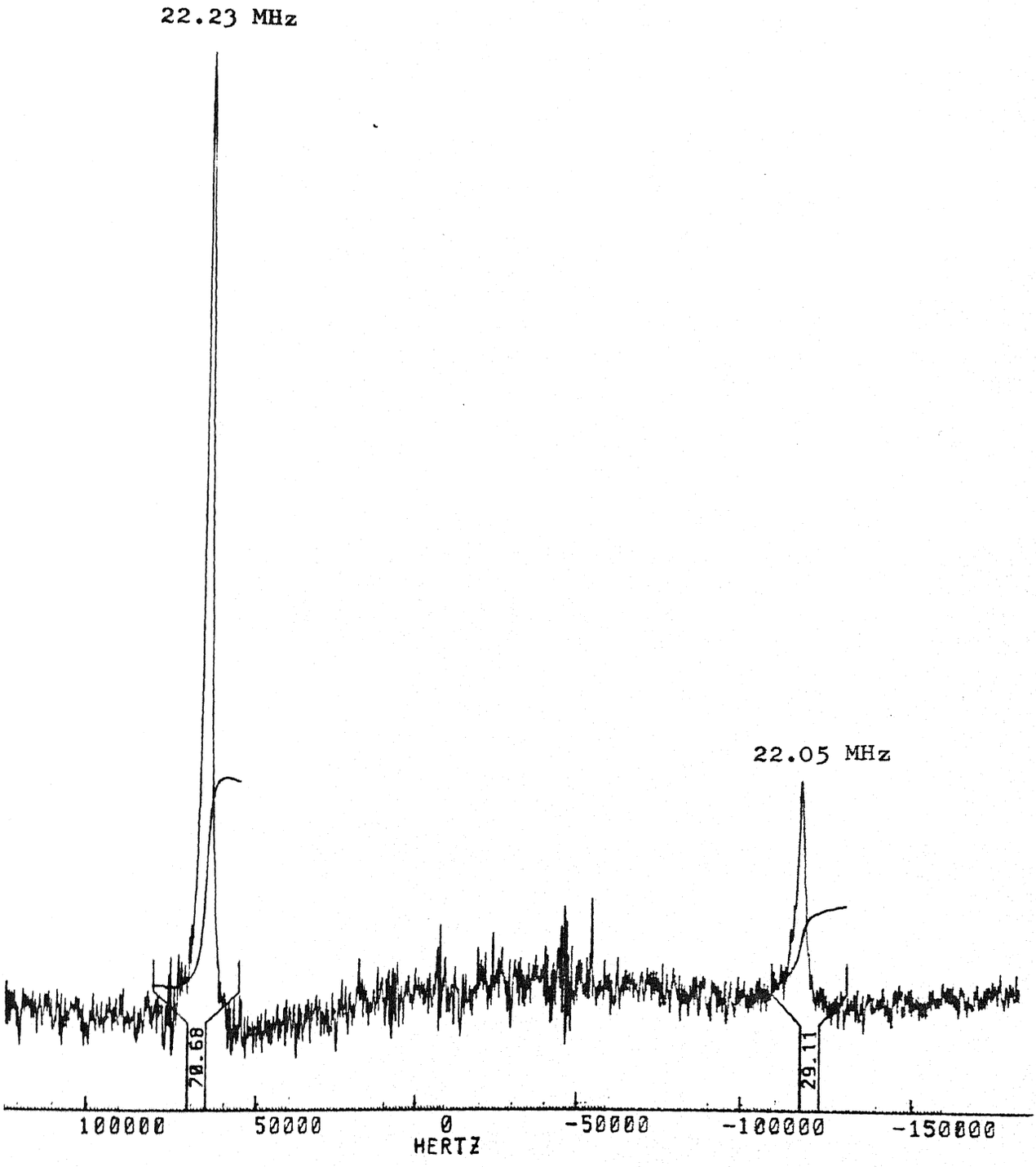

Figure VI.3(b) $\overline{45}$ 135

$\Delta\omega_Q$ = 30 kHz

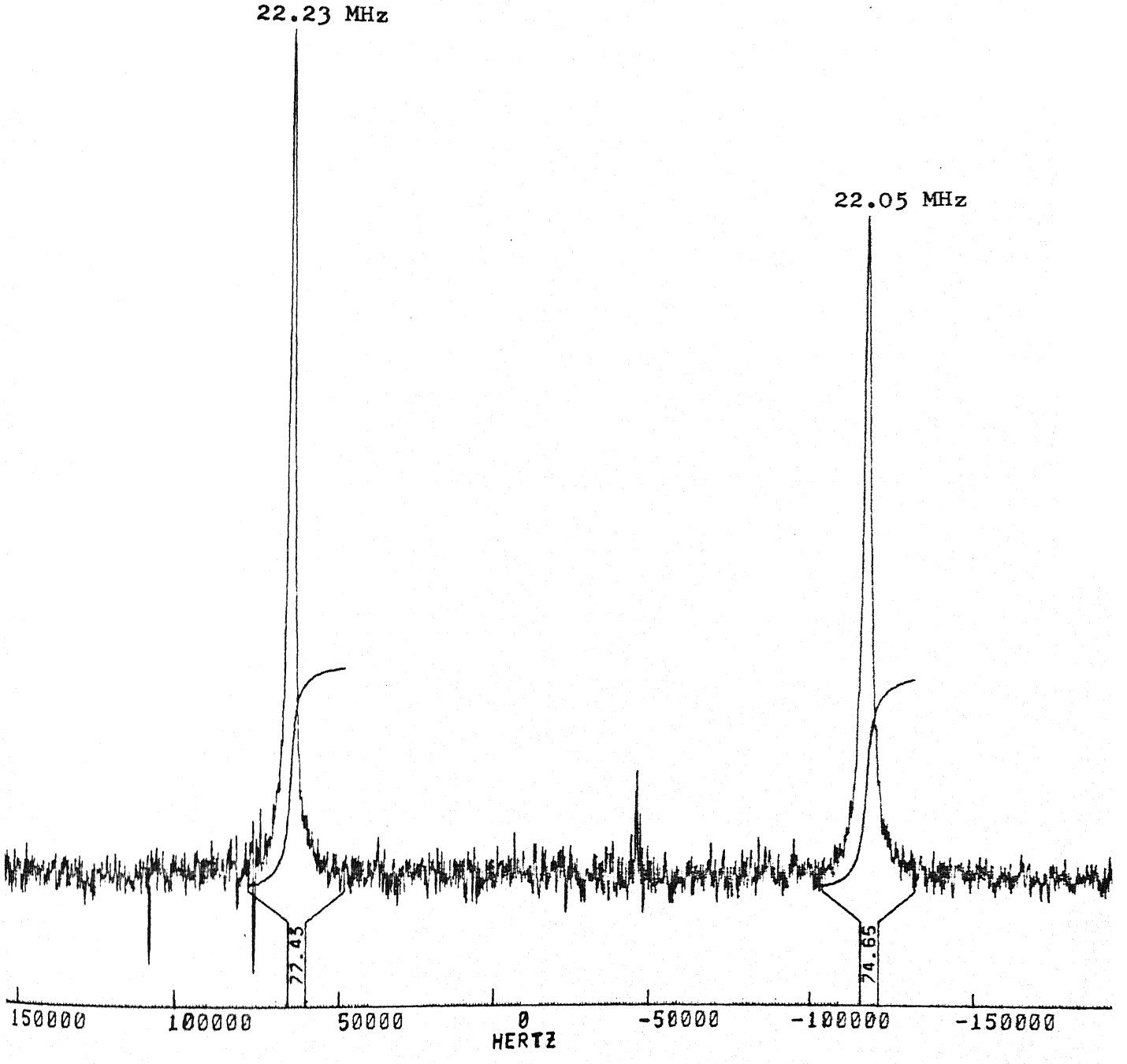

Figure VI.4(a) Single $\pi/2$

$\Delta\omega_Q$ = 20 kHz

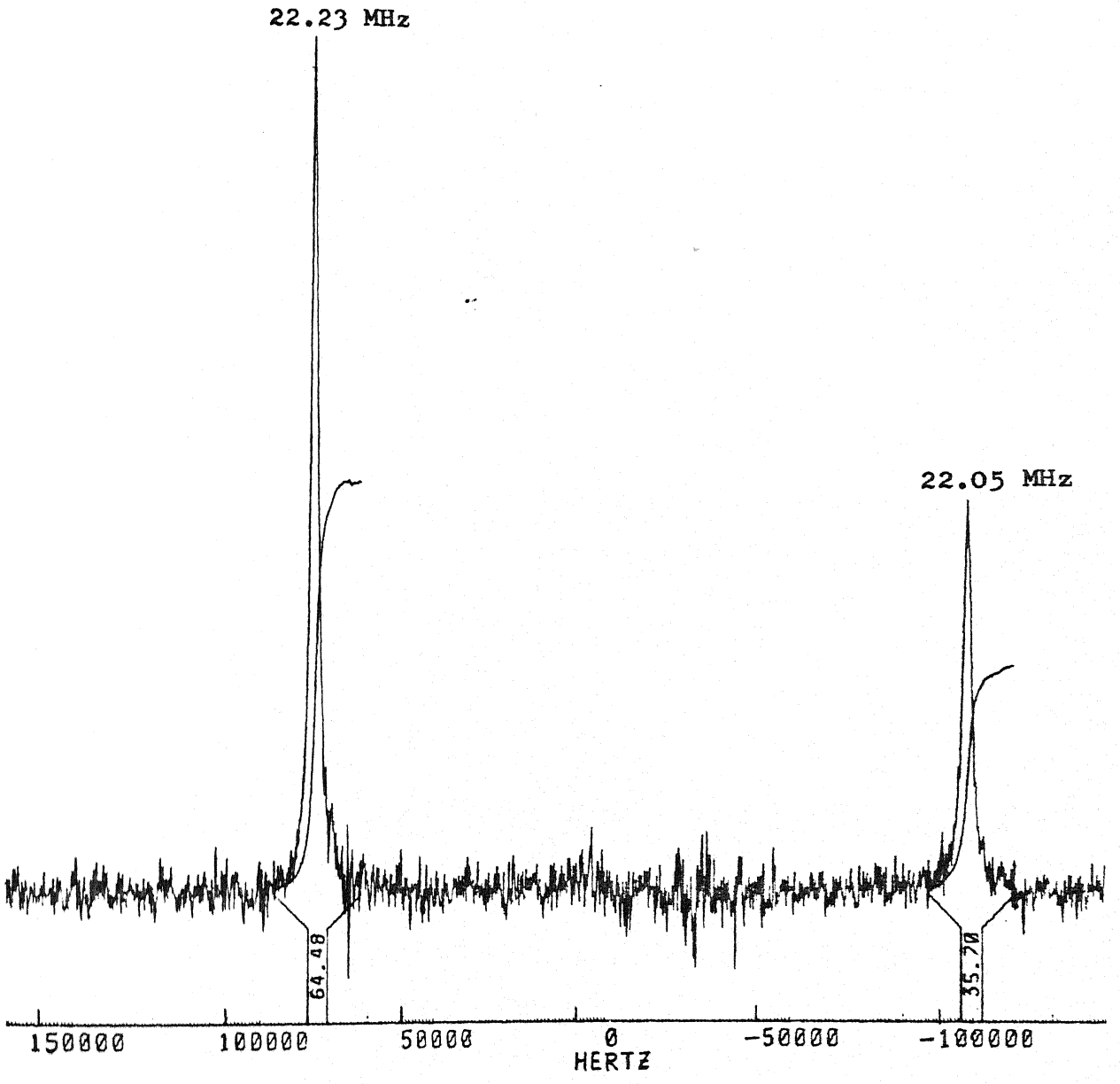

Figure VI.4(b) $\overline{45}$ 135

$\Delta\omega_Q$ = 20 kHz

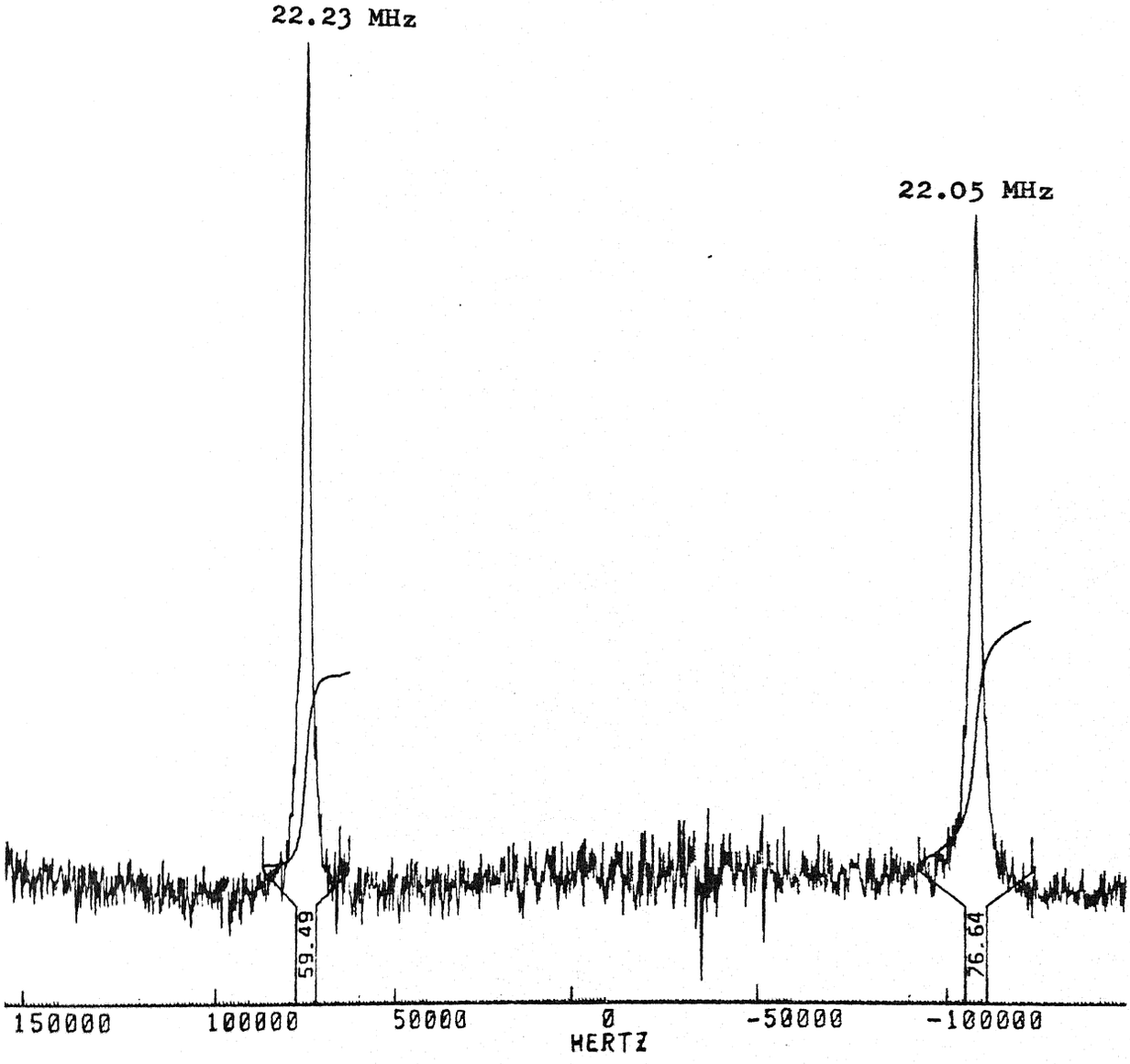

Figure VI.5(a) Single $\pi/2$

$\Delta\omega_Q = 0$

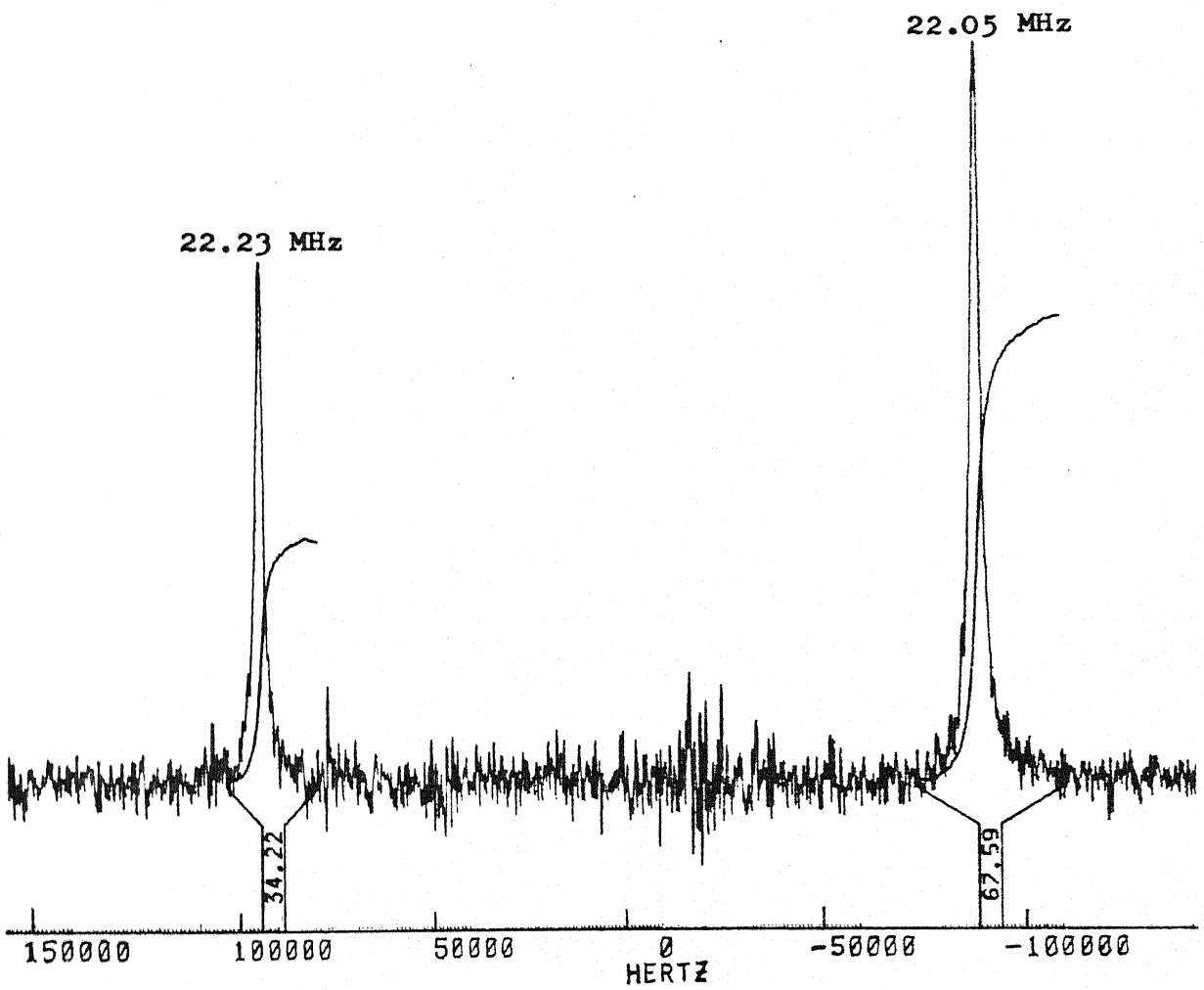

Figure VI.5(b) $\overline{45}$ 135

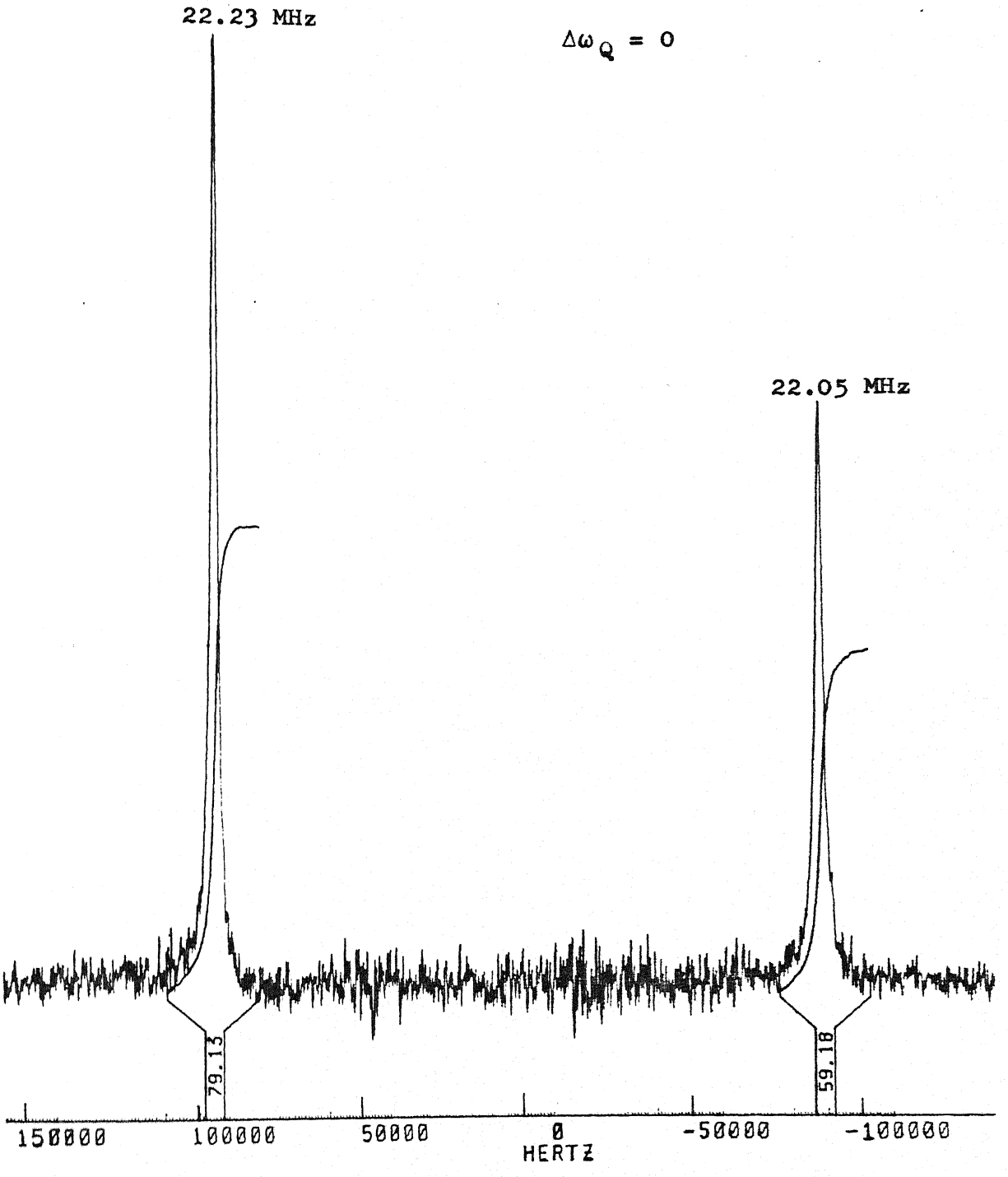

Figure VI.6(a) Single $\pi/2$

$\Delta\omega_Q = -10$ kHz

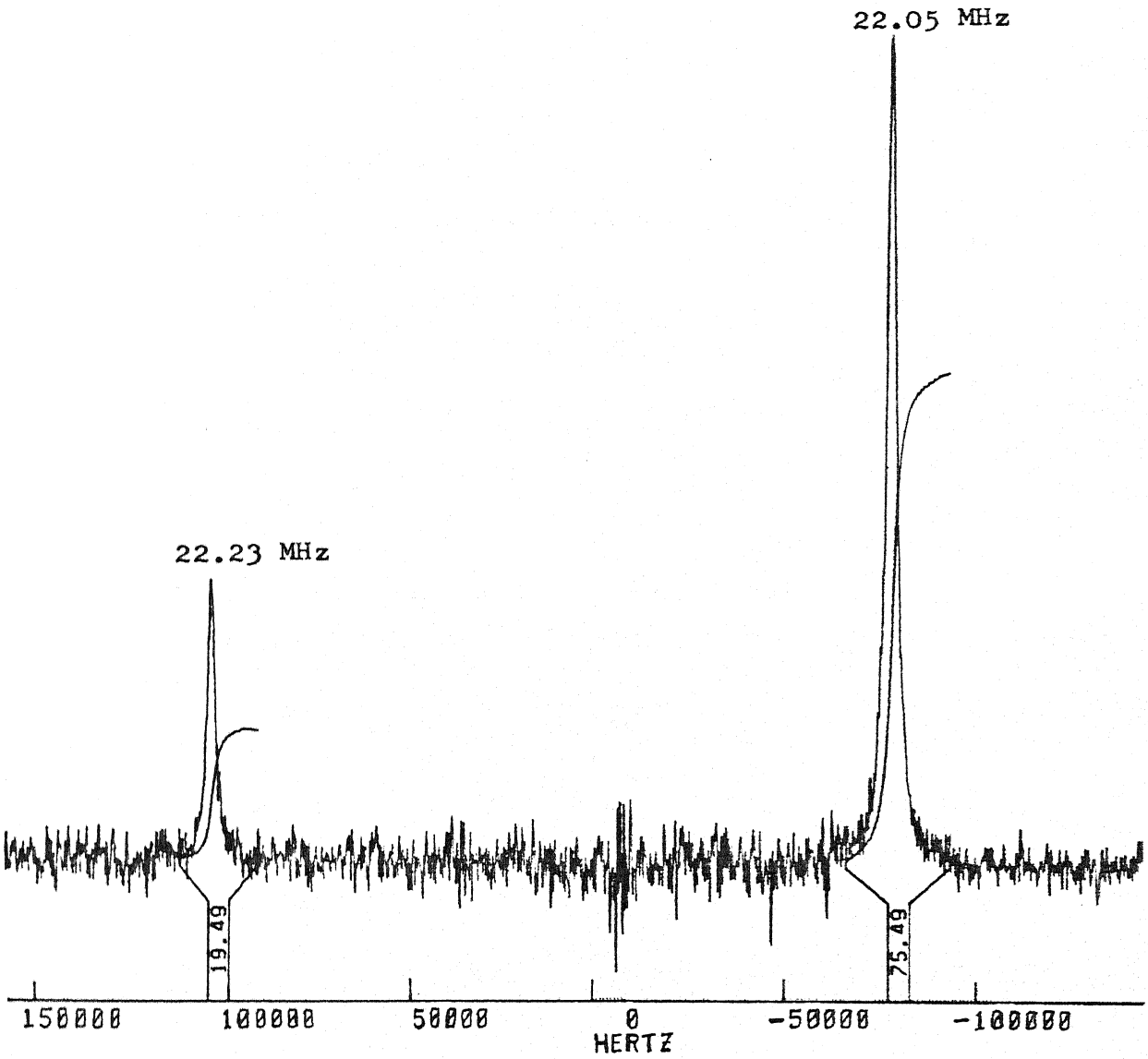

Figure VI.6(b) $\overline{45}$ 135

$\Delta\omega_Q$ = -10 kHz

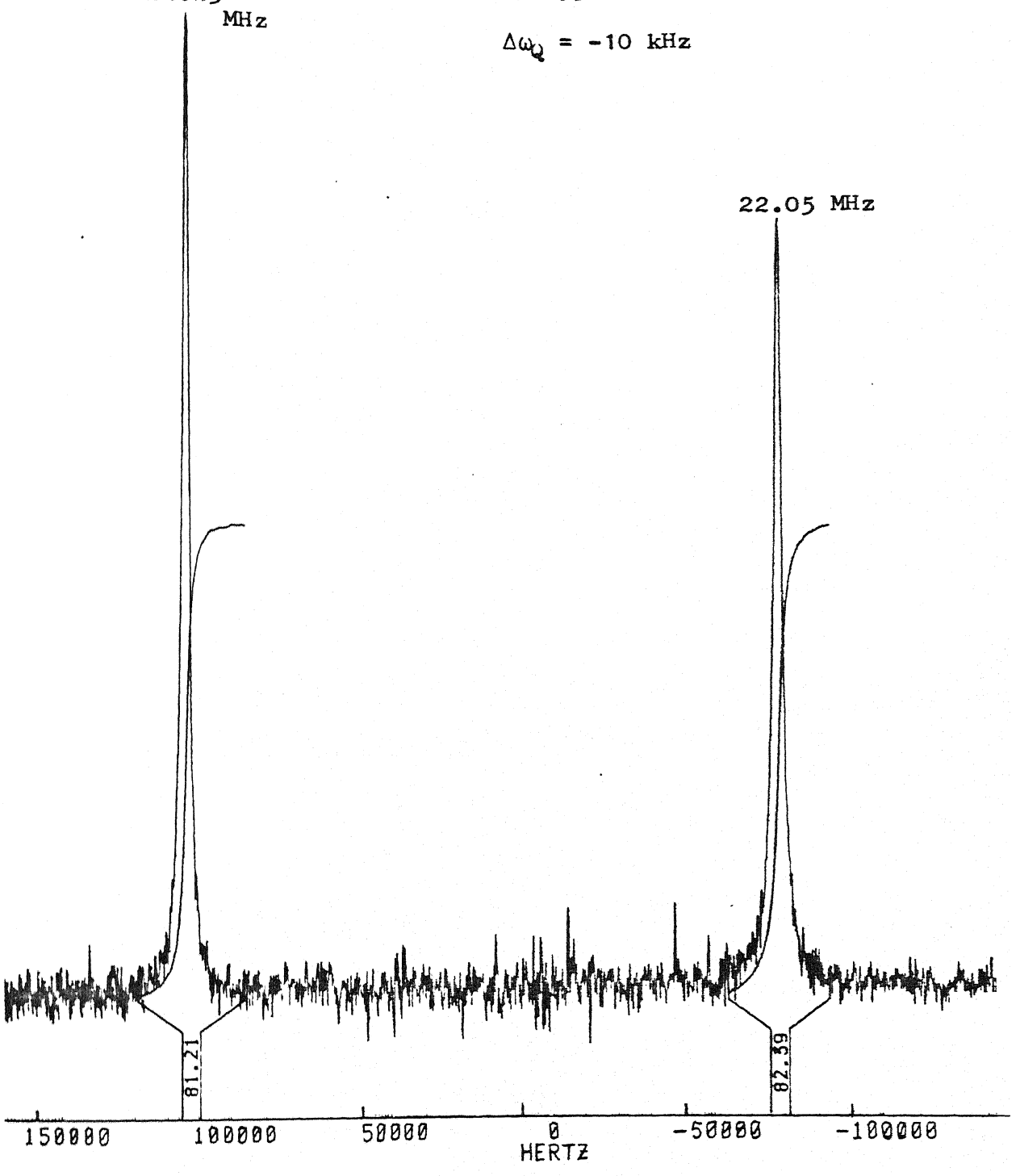

Figure VI.7(a) Single $\pi/2$

$\Delta\omega_Q$ = -20 kHz

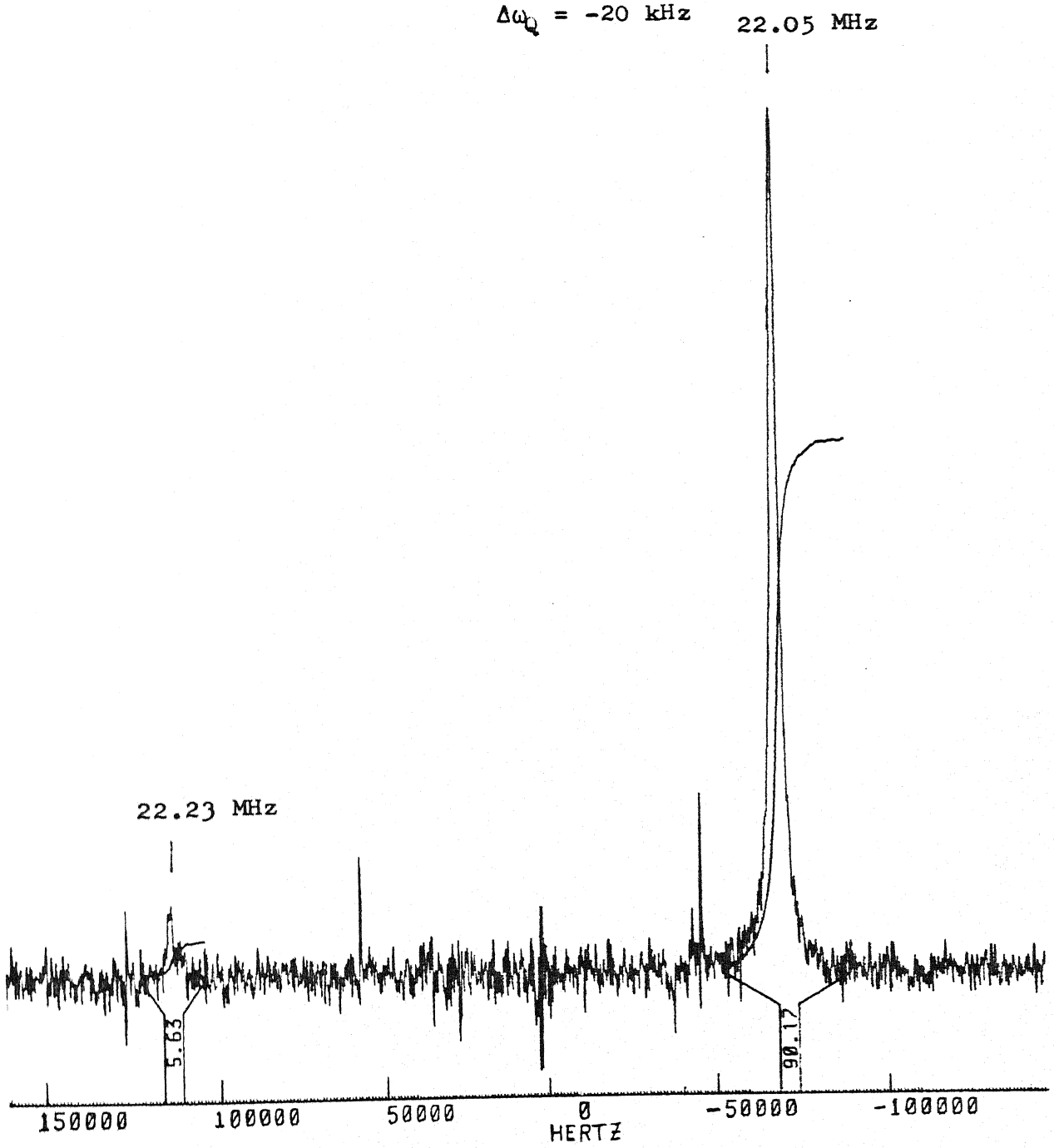

Figure VI.7(b) $\overline{45}$ 135

$\Delta\omega_Q$ = -20 kHz

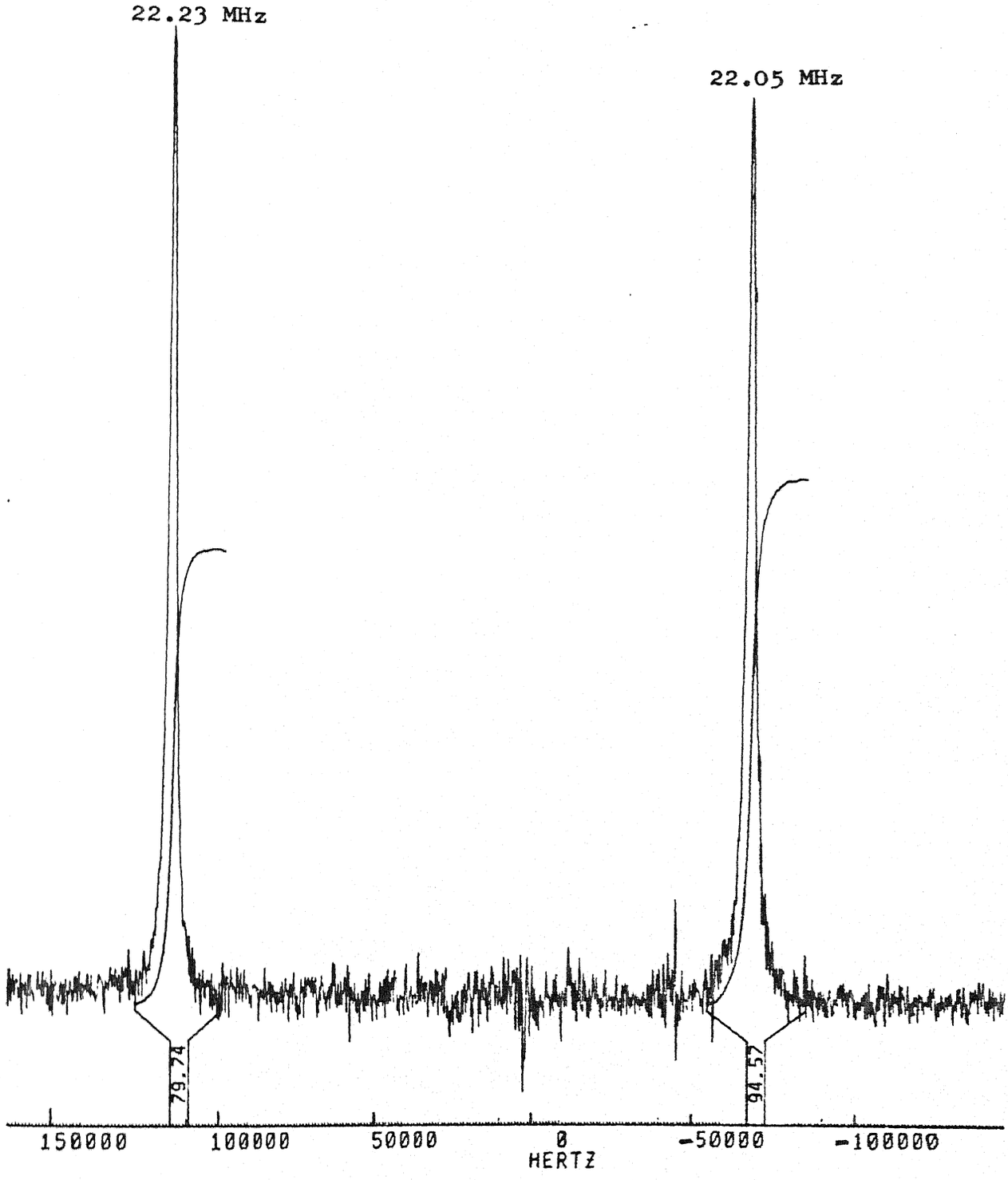

Figure VI.8(a) Single $\pi/2$

$\Delta\omega_Q$ = -30 kHz

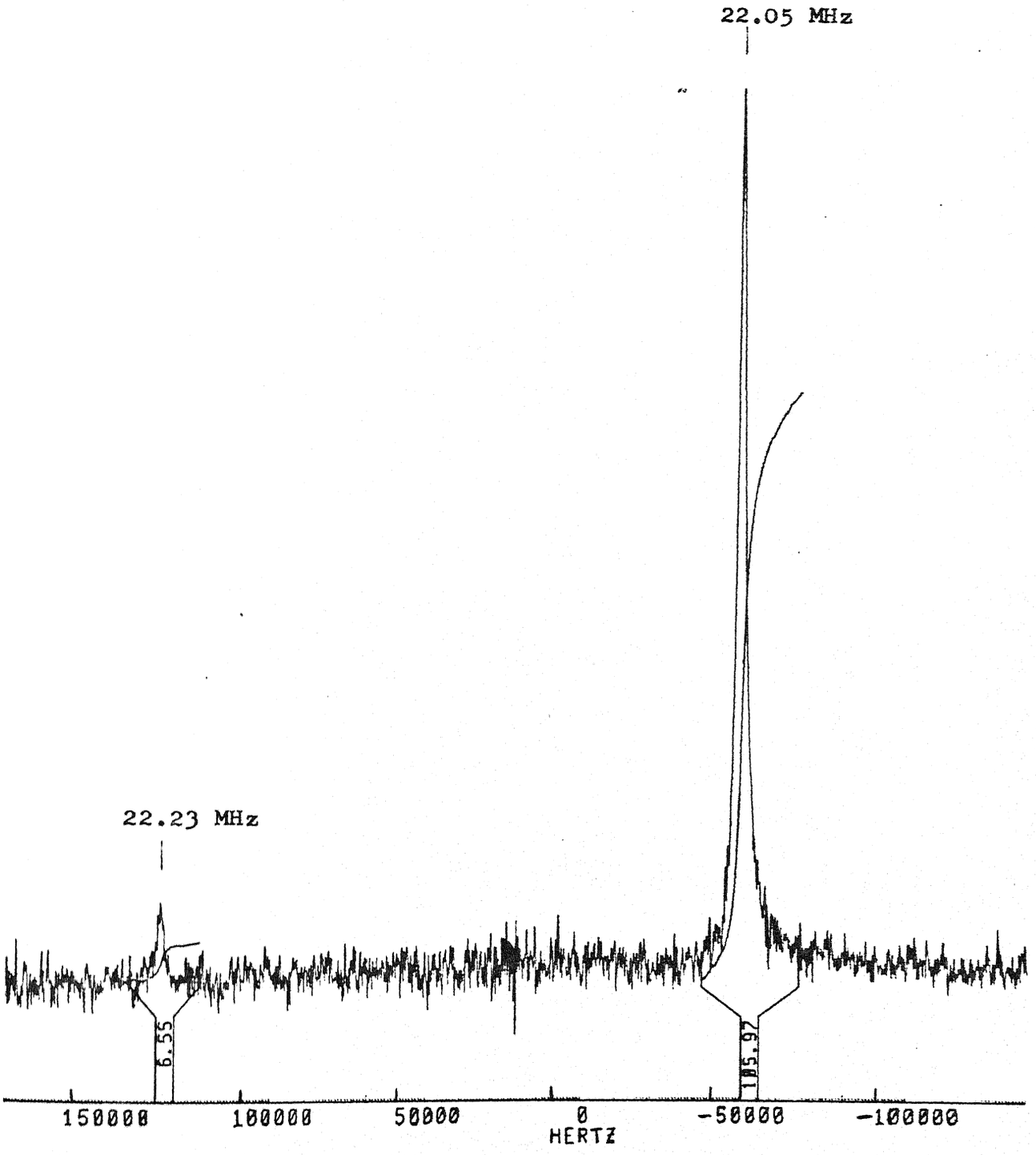

Figure VI.8(b) $\overline{45}$ 135

$\Delta\omega_Q$ = -30 kHz

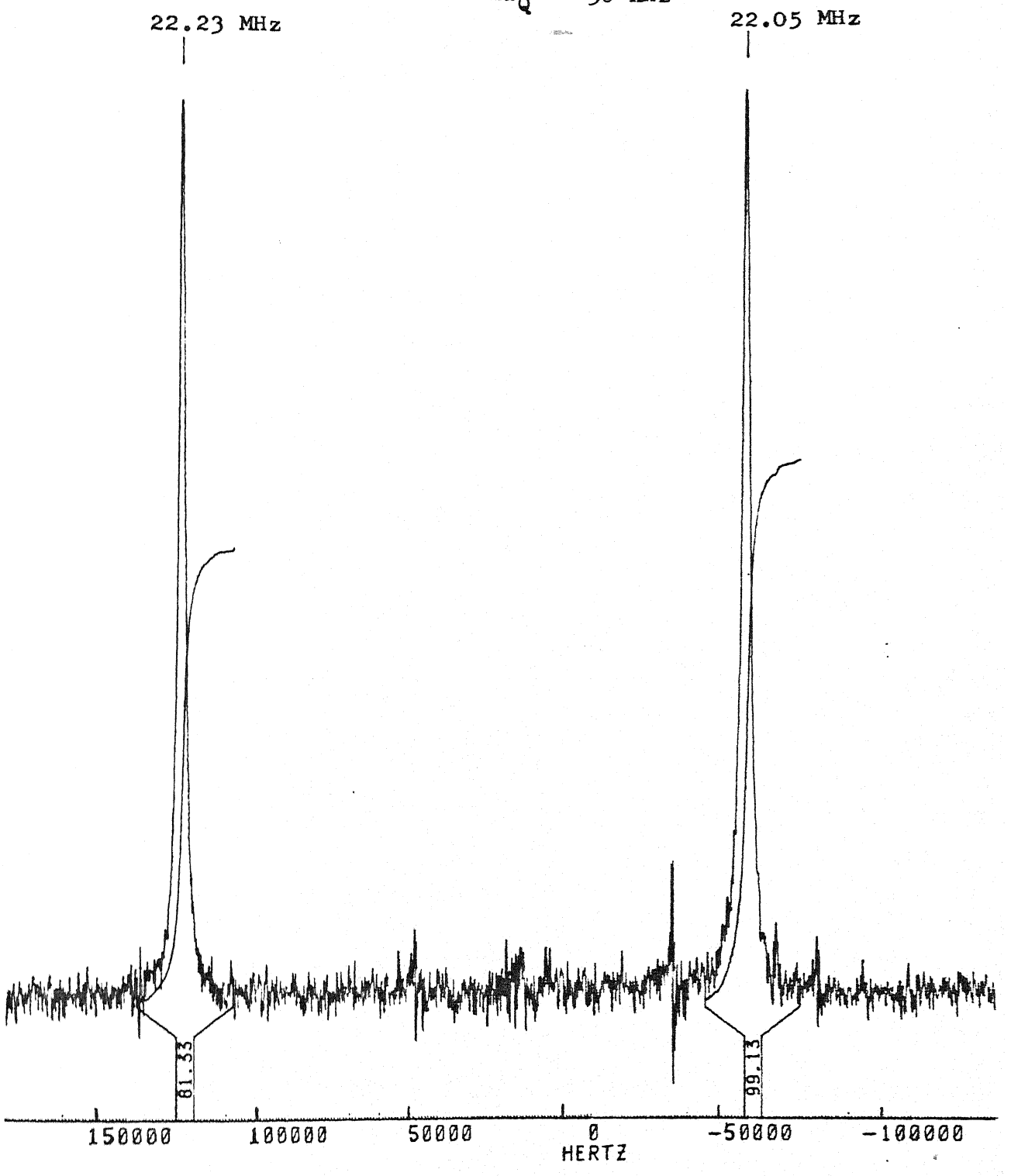

Figure VI.9(a) Single $\pi/2$

$\Delta\omega_Q$ = -40 kHz

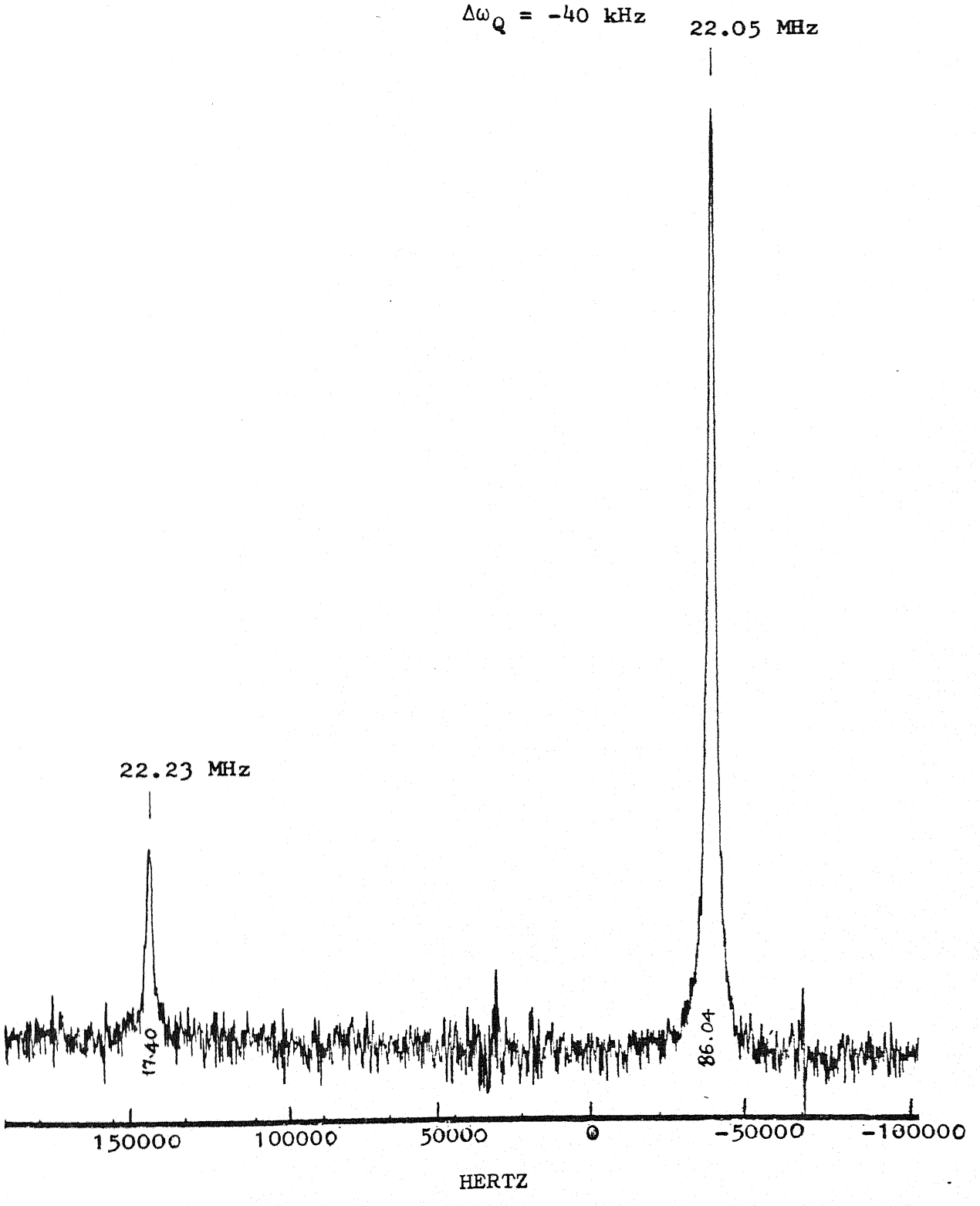

Figure VI.9(b) $\overline{45}$ 135

$\Delta\omega_Q$ = -40 kHz

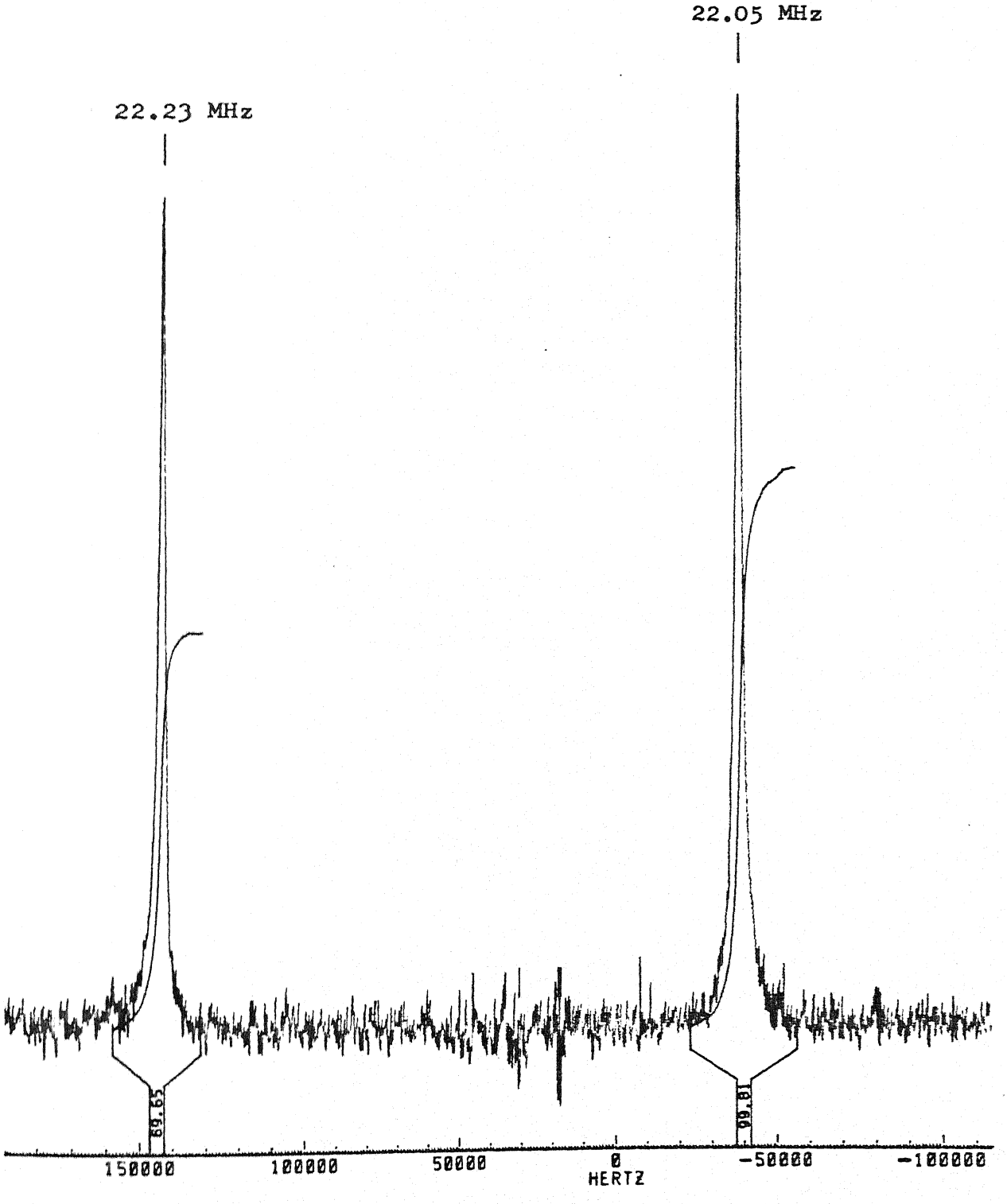

Figure VI.10(a) Single $\pi/2$

$\Delta\omega_Q$ = -50 kHz

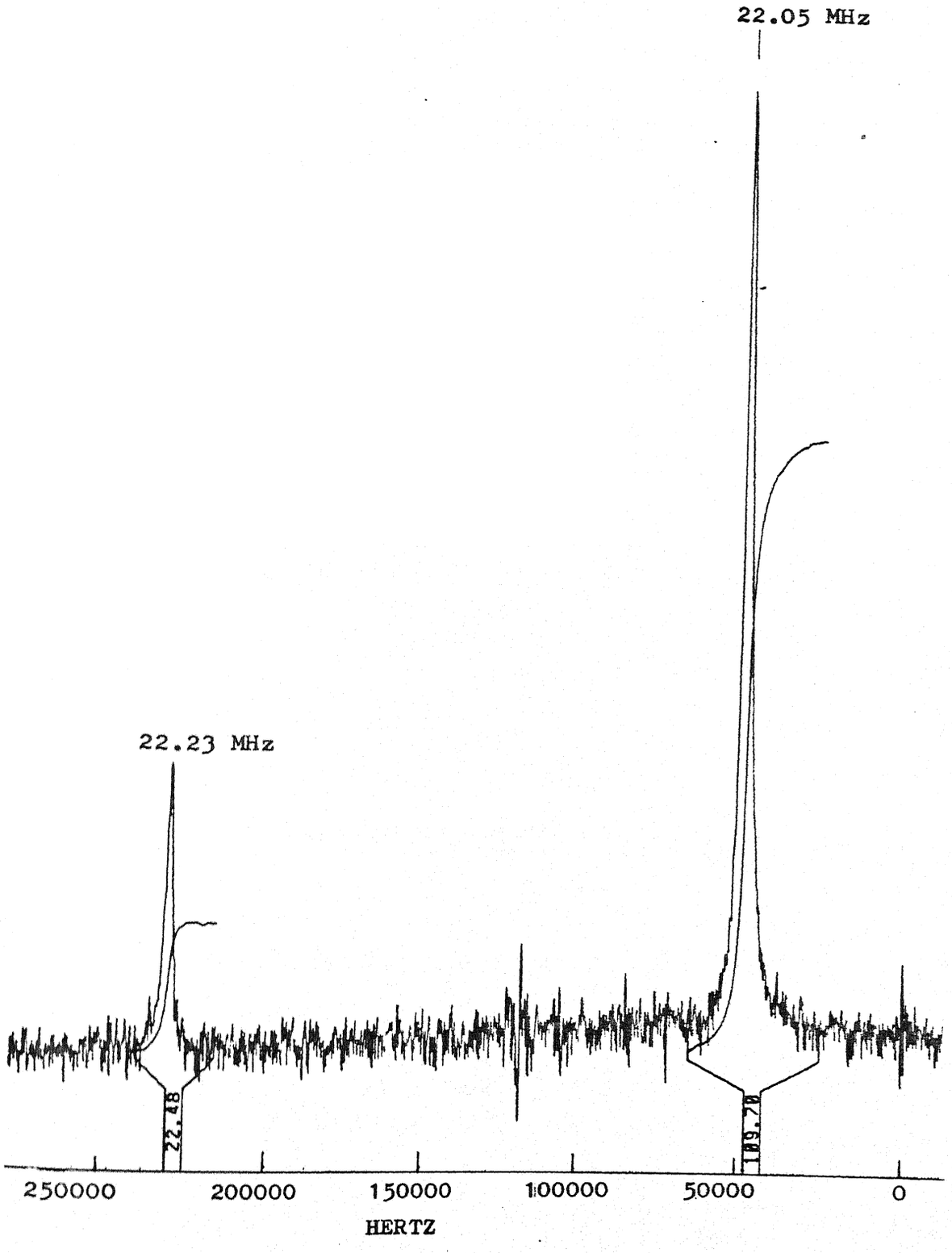

Figure VI.10(b) $\overline{45}$ 135

$\Delta\omega_Q$ = -50 kHz

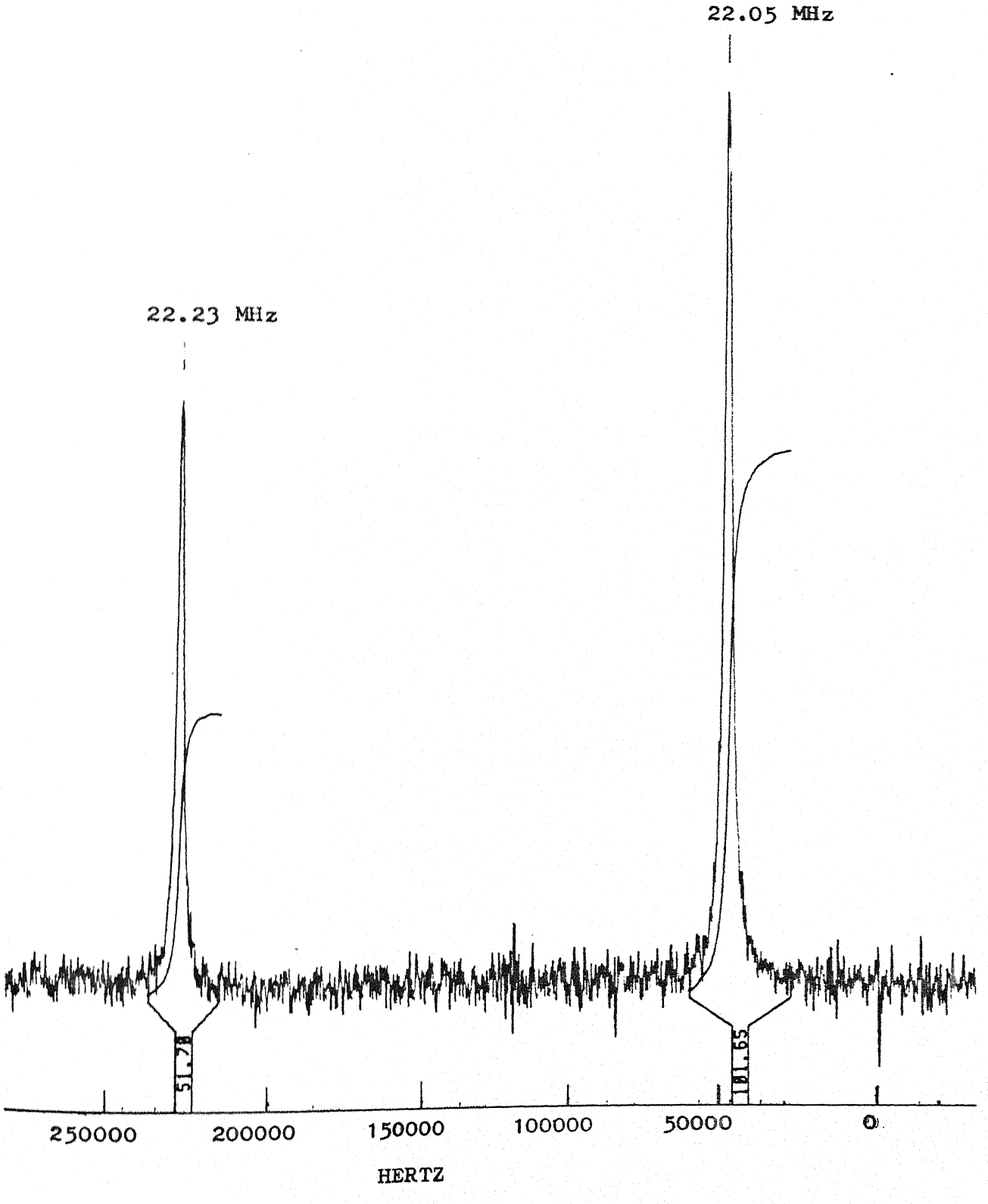

of each composite $\pi/2$ pulse for the transmitter frequency at 22.14 MHz (i.e. at the centre of the spectrum) has been given (Figure VI.11). It is clear that with increase of overall pulse train duration its performance deteriorates beyond a point, i.e. the NQR signal intensity goes down (refer Fig. VI.11(g)). This is due to the fact that, when the excitation time period approaches T_2, the spin magnetization dephases in the transverse plane and hence less signal intensity is observed. Therefore, a composite pulse duration time must be much shorter than T_2 of the sample but it should be long enough to nullify the errors of individual rf pulses to give a broadband excitation.

In a separate experiment, the time duration of the $\pi/2$ pulse was deliberately misset, that is, it was decreased in value by 30 percent. With this error, both single $\pi/2$ and composite $\pi/2$ pulses have been applied. The observed results have shown that composite $\pi/2$ pulse gives a uniform broadband excitation even when flip angle errors of this magnitude are involved. But the overall signal intensity in this case, when compared to the response by a composite $\pi/2$ pulse without error, is less. We conclude that "our composite pulse is tolerant of mis-settings in the flip angle θ".

The response of single π and composite π pulse $(90)_0\text{-}(270)_{90}\text{-}(90)_0$ at different frequencies have been given in Figures VI.12 and VI.13. All these signals have been phase corrected with respect to a single $\pi/2$ pulse NQR spectrum. The less intense and almost absorption free dispersion signals resulting with $(90)_0\text{-}(270)_{90}\text{-}(90)_0$ composite π pulse, as compared to

Figure VI.11(a) $\overline{22.5}$ 112.5

$\Delta\omega_Q = 0$

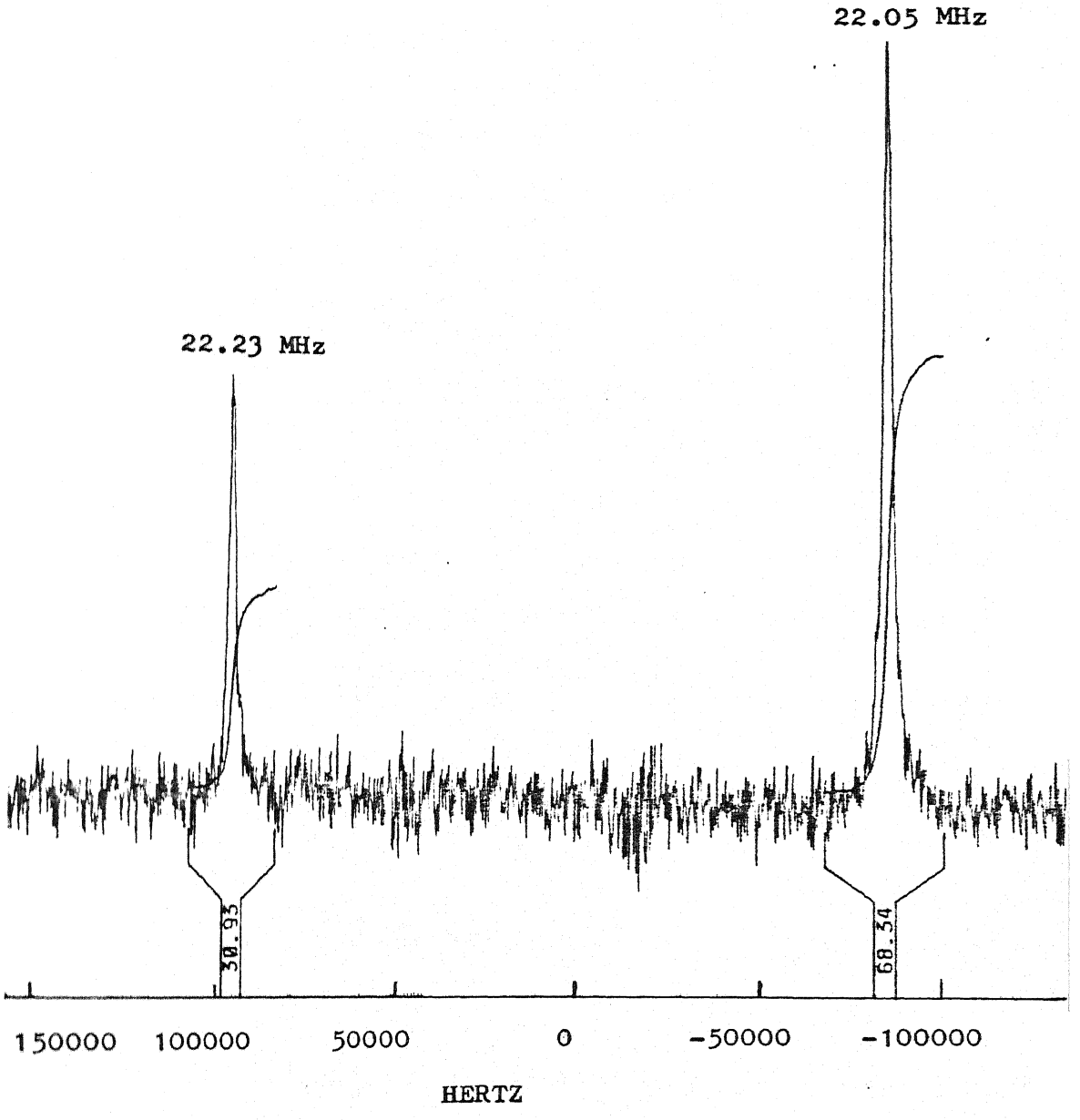

This figure and all the following figures upto Figure VI.13 are having the same common spectral parameters given in page 167.

Figure VI.11(b) $\overline{60}$ 150

$\Delta\omega_Q = 0$

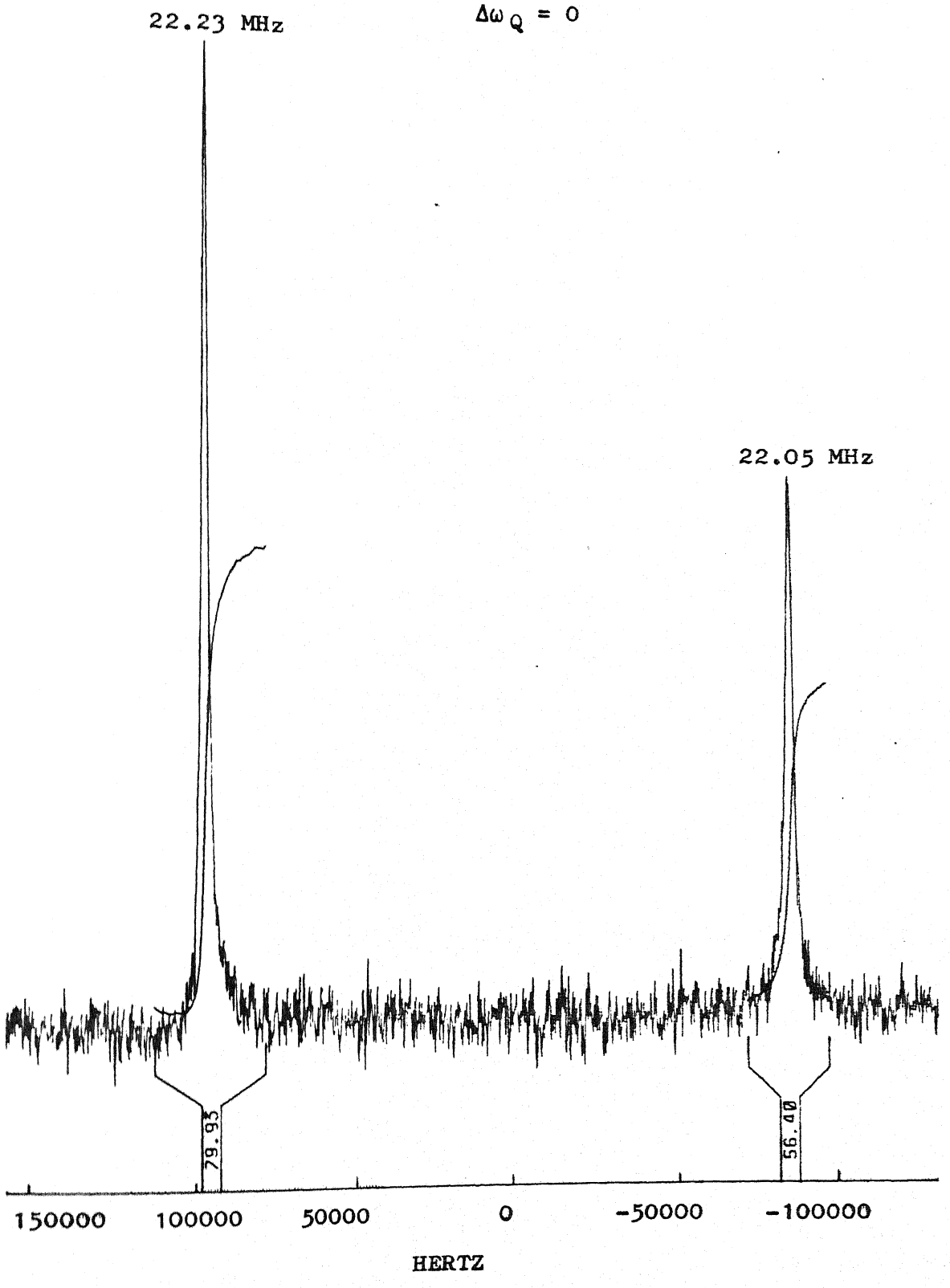

Figure VI.11(c) $385\ \overline{320}\ 25$

$\Delta\omega_Q = 0$

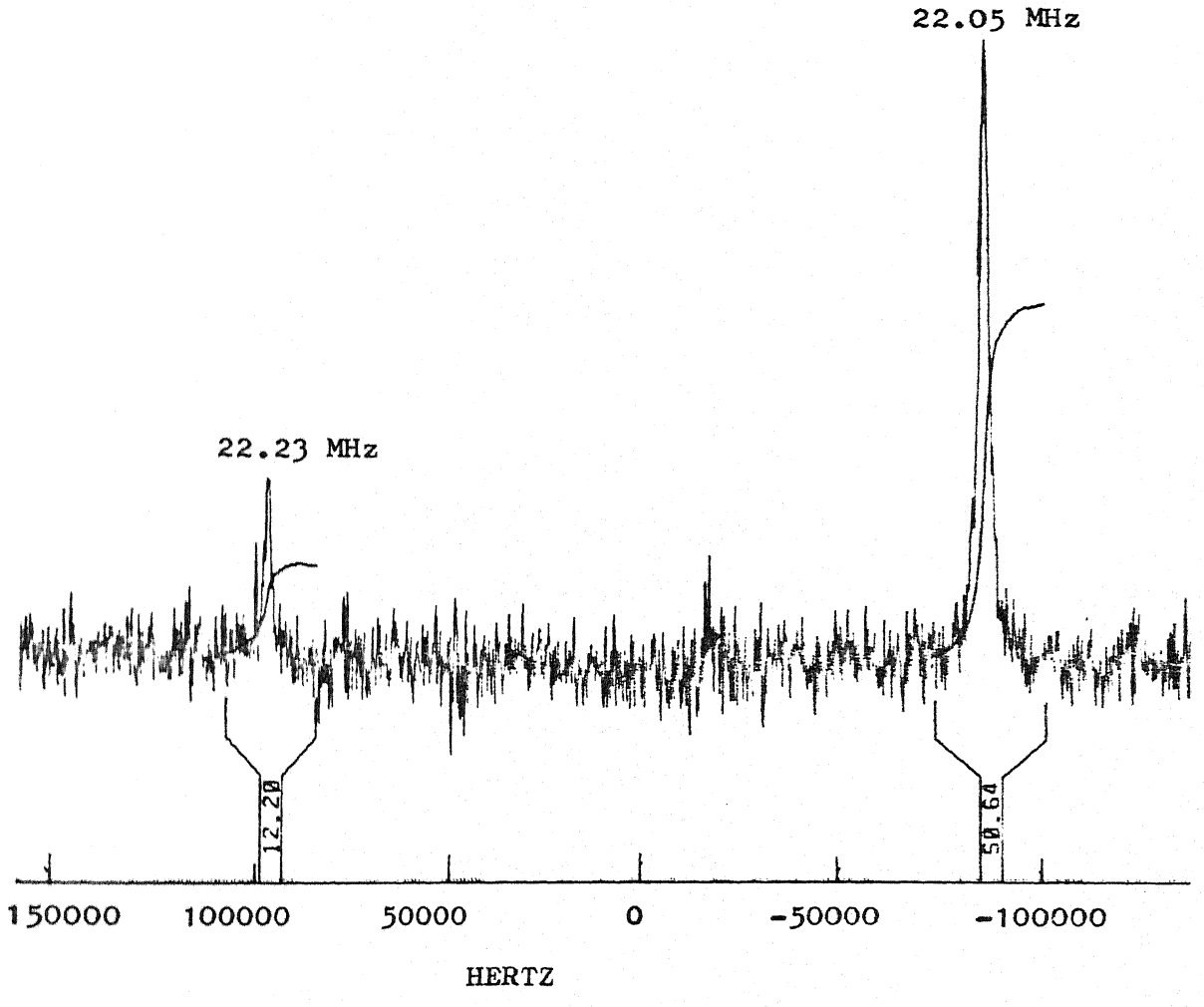

Figure VI.11(d) Single $\pi/2$

$\Delta\omega_Q = 0$

NC = -3

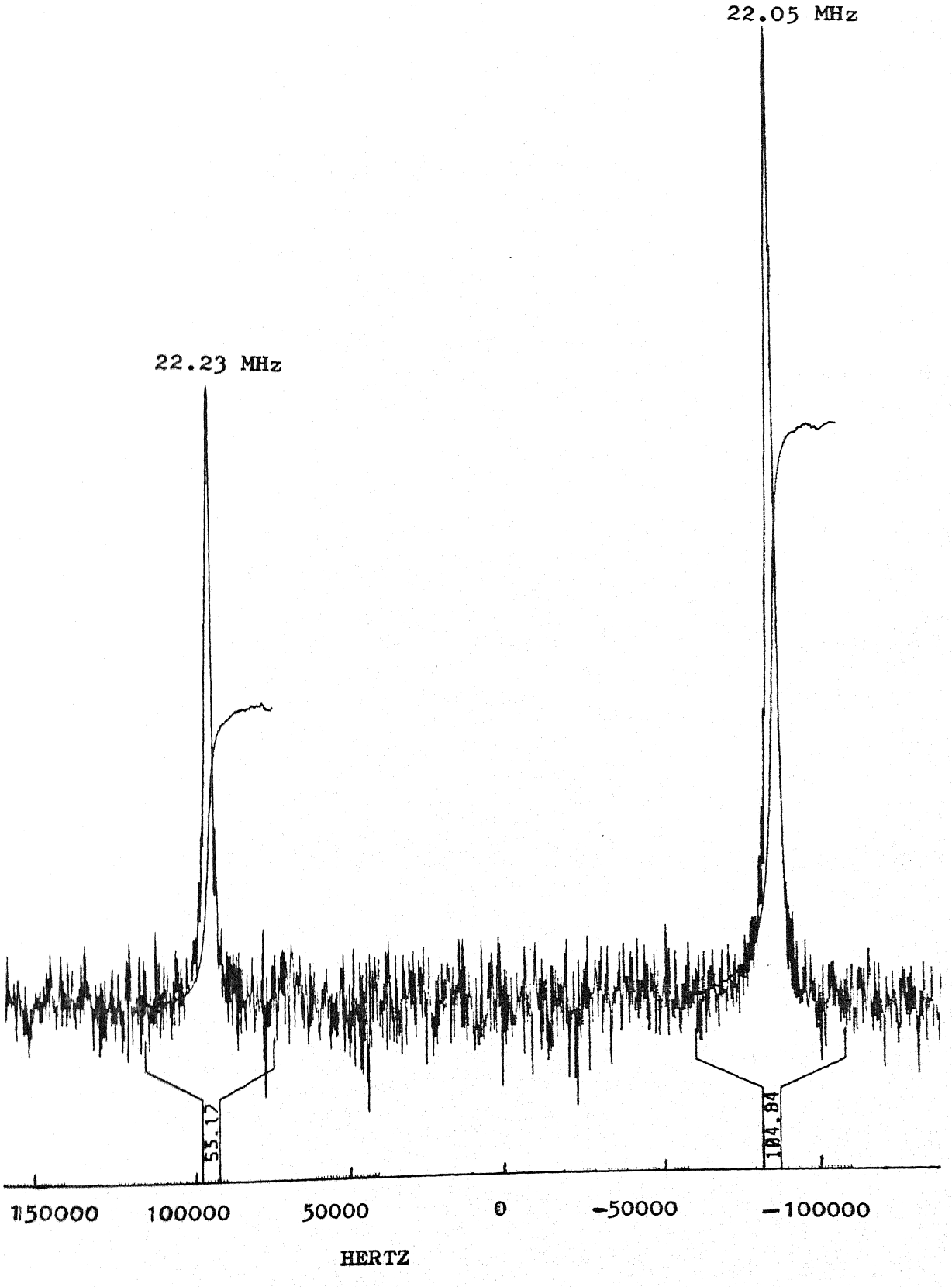

Figure VI.11(e) $\overline{45}$ 135

$\Delta\omega_Q = 0$

NC = -3

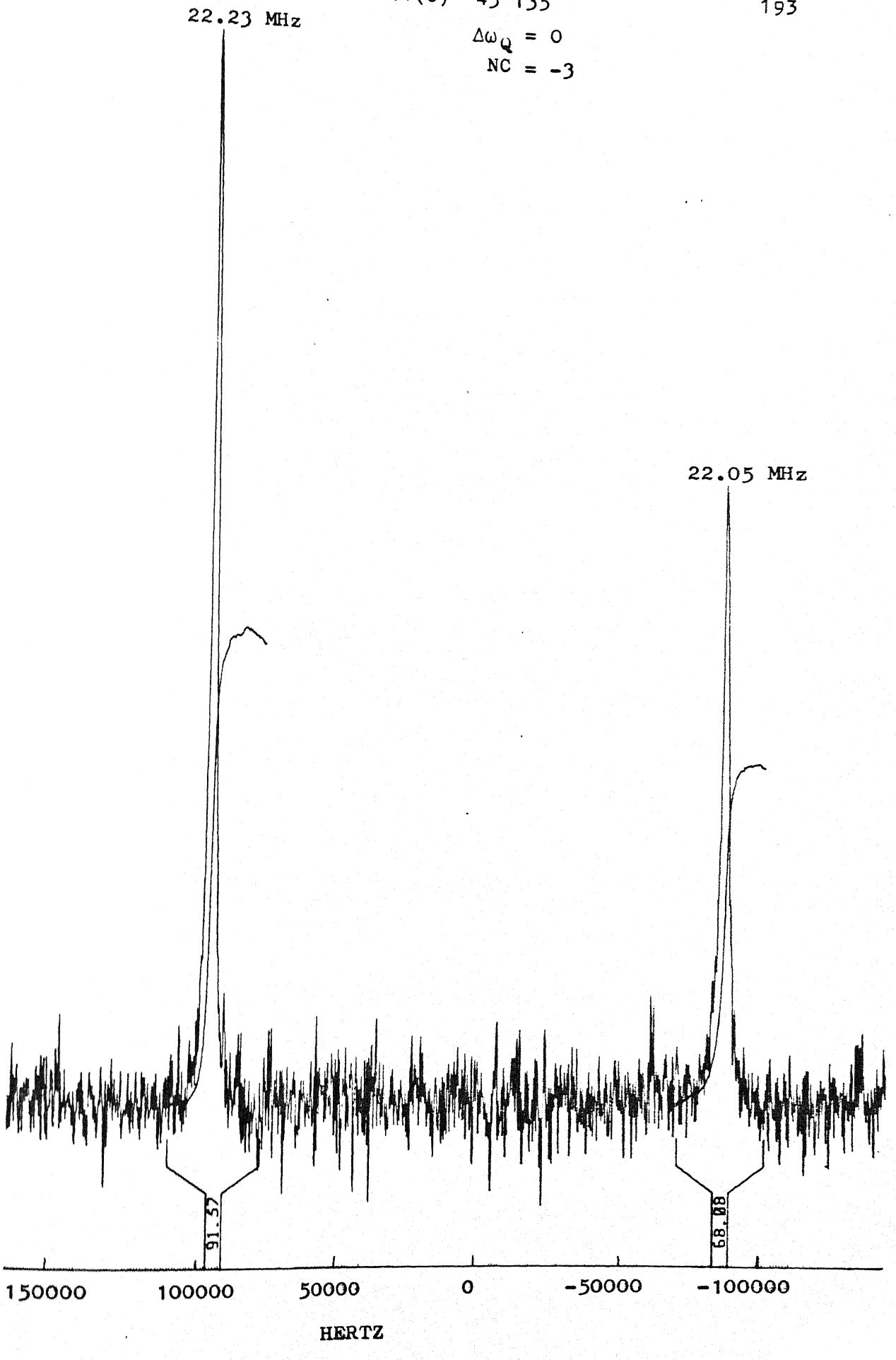

Figure VI.11(f) $\overline{113}$ 316 $\overline{113}$

$\Delta\omega_Q = 0$

NC = -3

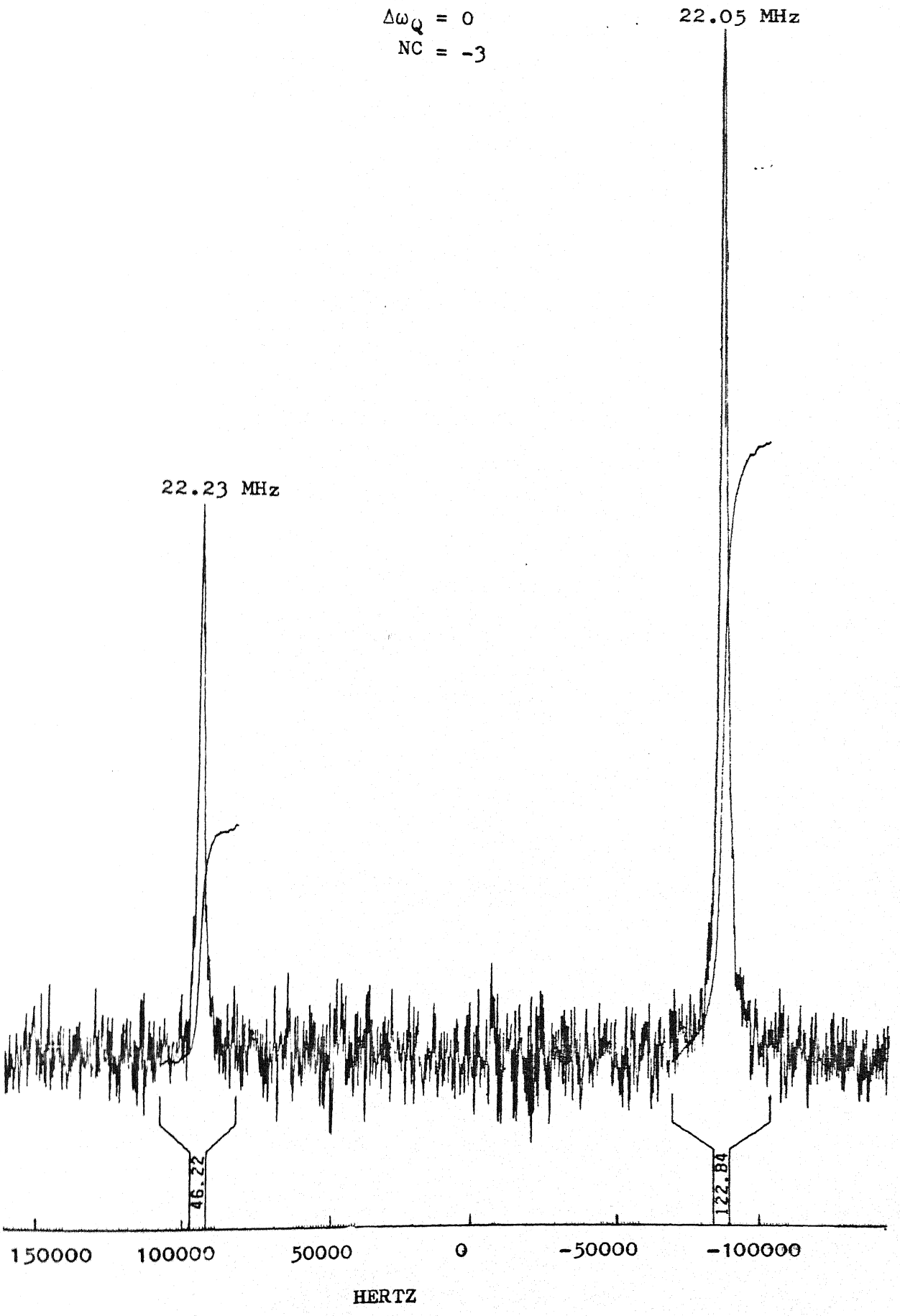

Figure VI.11(g)

160 $\overline{324}$ 141 $\overline{204}$ 320 $\overline{84}$ 72 $\overline{84}$ 320 $\overline{204}$ 141 $\overline{324}$ 160

$\Delta\omega_Q$ = 0

NC = -3

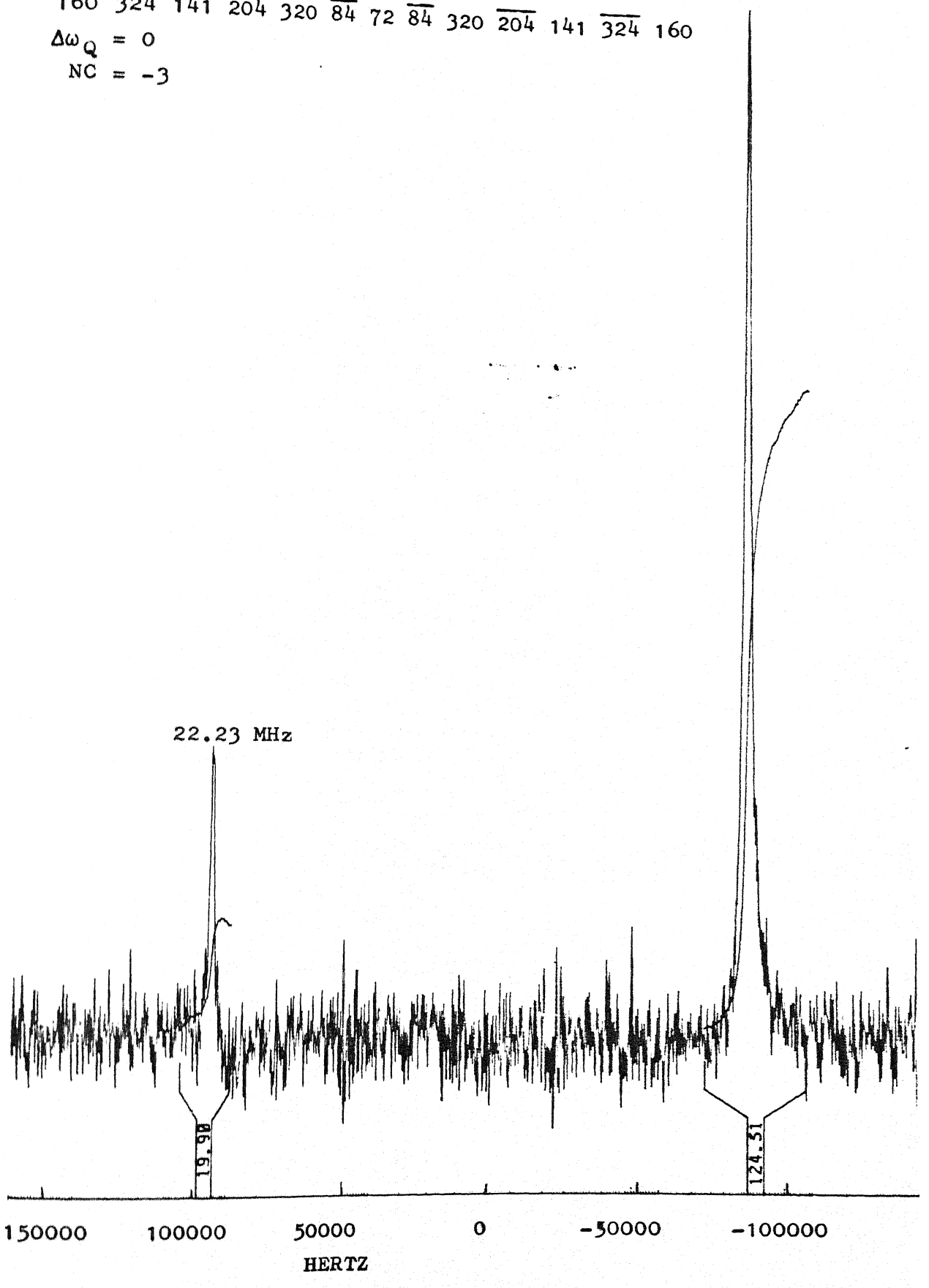

Figure VI.12(a)

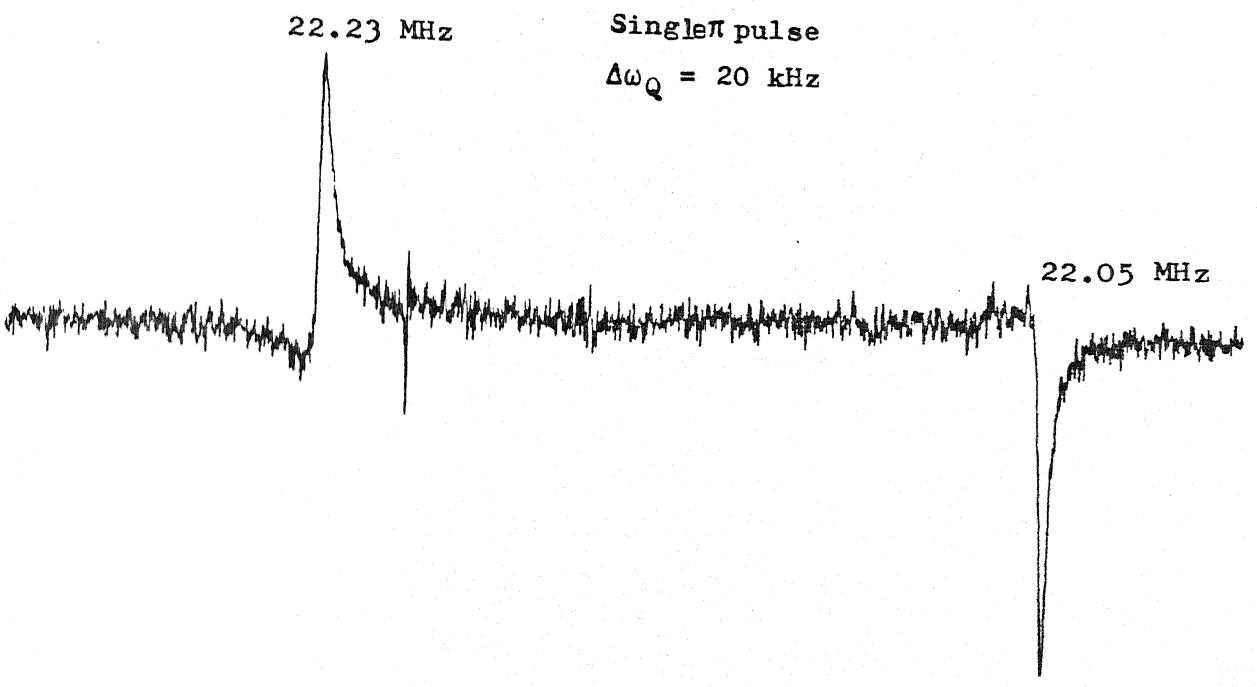

Figure VI.12(b)

$(90)_0$-$(270)_{90}$-$(90)_0$

$\Delta\omega_Q$ = 20 kHz

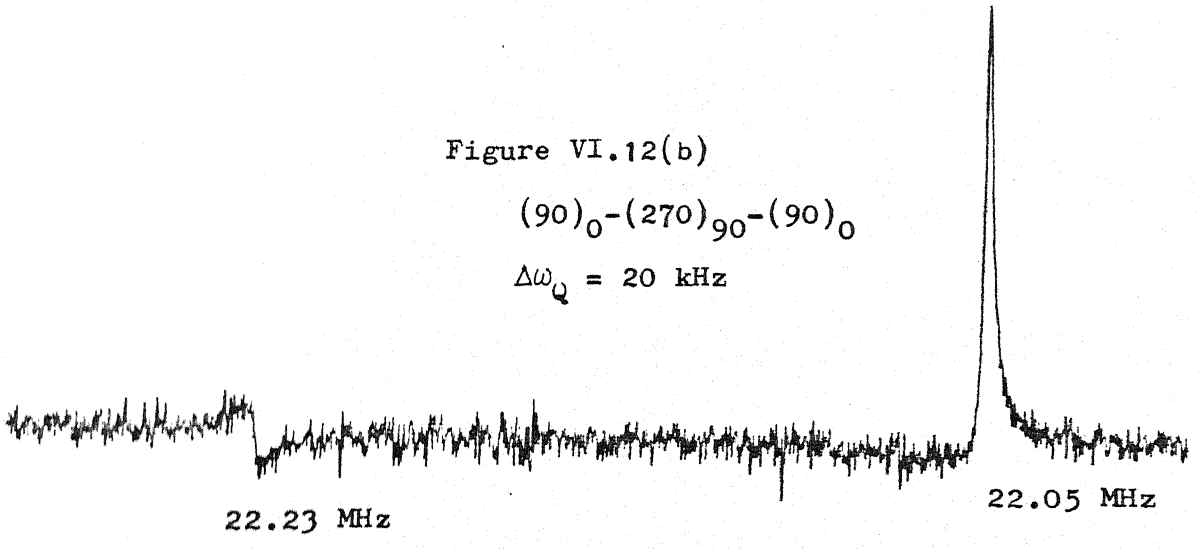

Figure VI.13(a)

Single π pulse

$\Delta\omega_Q = 0$

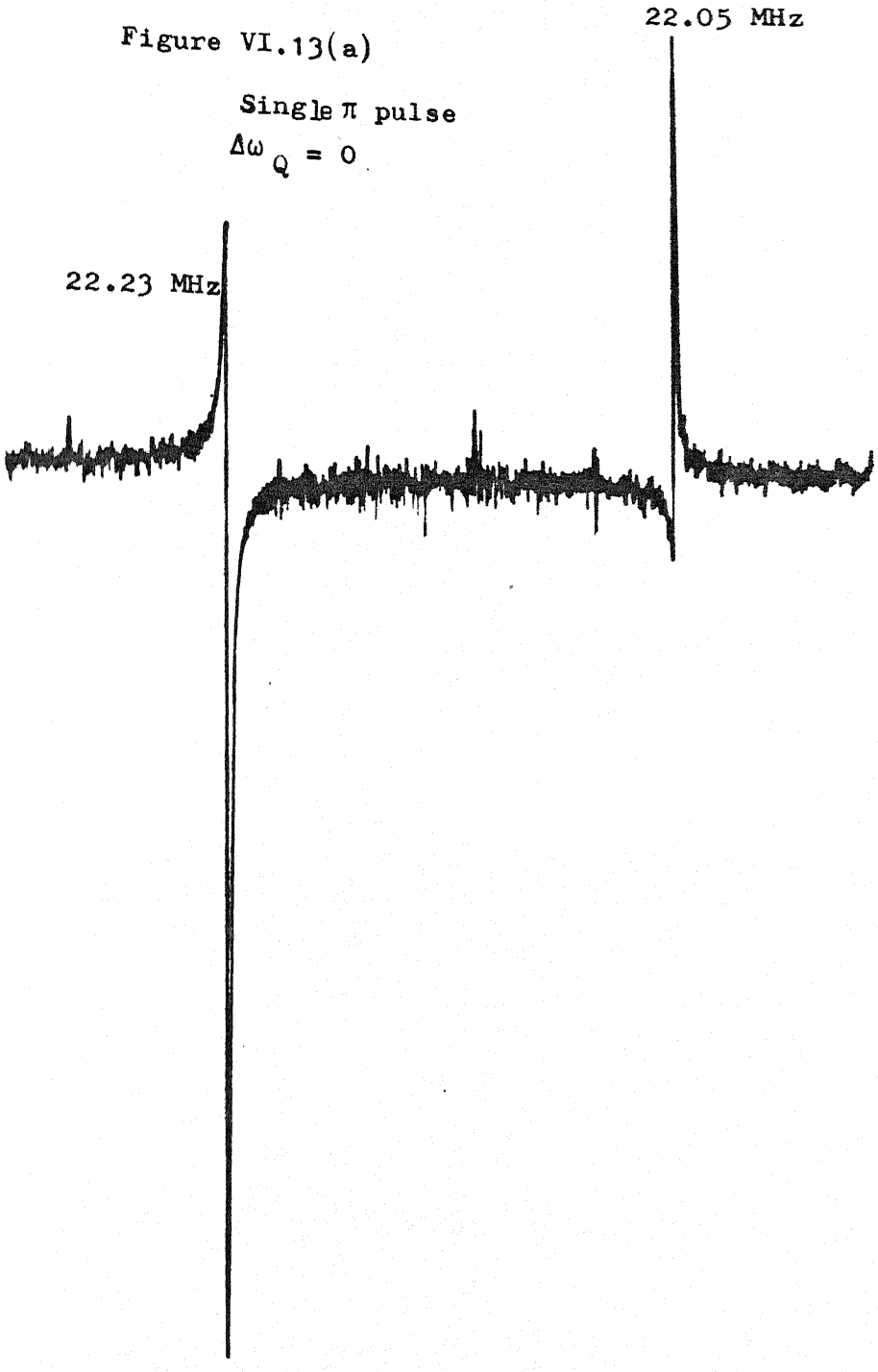

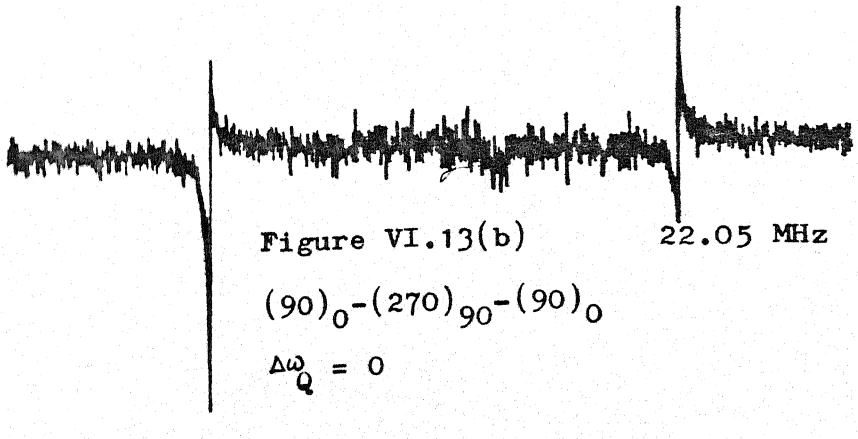

Figure VI.13(b)

$(90)_0-(270)_{90}-(90)_0$

$\Delta\omega_Q = 0$

Figure VI.13 (c),(d) & (e)

$\Delta\omega_Q = 0$

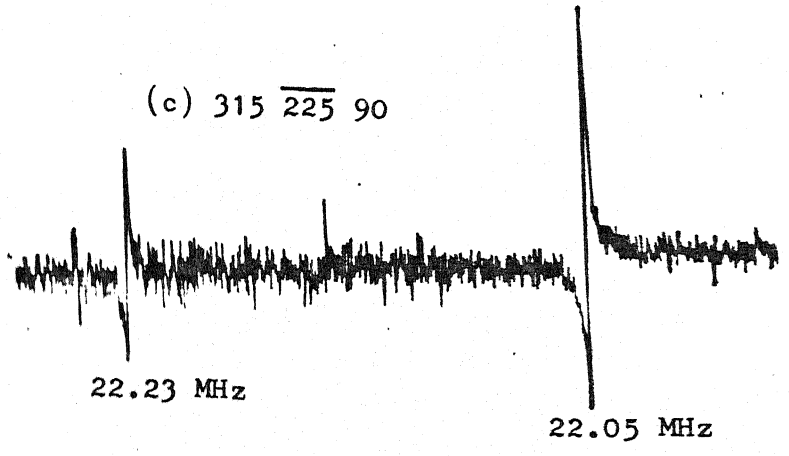

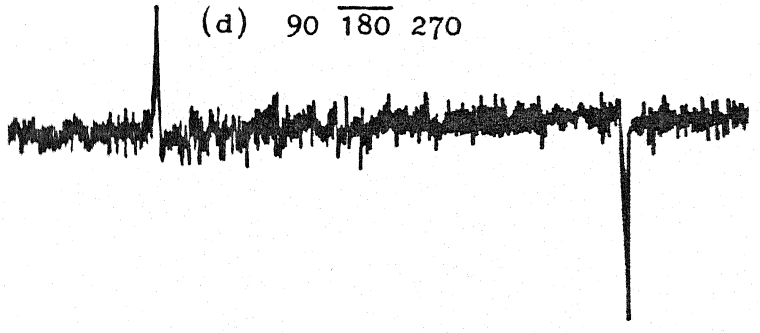

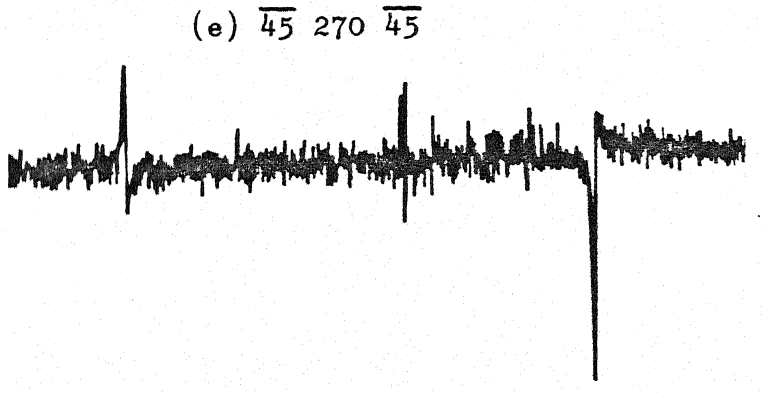

single π pulse response, confirms that the composite π pulse gives an efficient broadband spin population inversion. Similarly, all other composite π pulses have been tested and one typical NQR spectrum of each composite π pulse at 22.14 MHz is given in Figure VI.13.

VI.C.2 Sodium Chlorate ($NaClO_3$)

This is a standard system and has often been studied by various ^{35}Cl pure quadrupole resonance.[8] The pure NQR spectrum of $NaClO_3$ consists of a single NQR line at 29.9125 MHz at room temperature. The line width is of the order of a kHz. The unit cell of this system is cubic, with length of each side 6.57 Å and consists of four molecules. The ClO_3^- ion forms a pyramid with the Cl atom at the apex and its three-fold axis of symmetry renders the system axially symmetric, with $\eta=0$. Each molecular axis is parallel to the body diagonal of the unit cell. In the present work, we have analyzed the performance of composite pulses in both single crystalline and powder specimens of $NaClO_3$. The single crystal was grown by the slow evaporation of a saturated solution of $NaClO_3$.

The powder $\pi/2$ pulse width has been measured to be 10 μs and powder π pulse to be 20 μs. Similarly, the single crystal $\pi/2$ pulse has been identified as 9 μs and π pulse as 18 μs. Now in both the samples, the responses to composite $\pi/2$ pulse and single $\pi/2$ pulse have been compared at different transmitter frequencies. Surprisingly, responses are identical irrespective of the kind of pulse applied i.e., single or composite. This

suggests that the composite $\pi/2$ pulses are not compensating the efg inhomogeneity in $NaClO_3$ system. However, composite π pulses produced much better population inversion for a wider offset range than a single π pulse in single crystalline and powder samples. These results of spin inversion after phase correcting with respect to a single $\pi/2$ pulse NQR spectrum are shown in Figures VI.14 - VI.24 for both single crystal and powder samples of $NaClO_3$.

VI.C.3 Discussion

The theoretically predicted band width of uniform excitation by the $\overline{45}$ 135 composite $\pi/2$ pulse is approximately 60 kHz but the experimental results in $HgCl_2$ show that it gives a uniform excitation over 180 kHz. This could be due to the excitation by the side lobes of the 'Magnus' response (which is the extent of excitation against the offset values, see Chapter III).

The failure of composite $\pi/2$ pulses in the $NaClO_3$ system as against its remarkable efficiency in $HgCl_2$ is a phenomenon which we do not understand at present. We surmise that the presence of more than one physically inequivalent site and/powder specimens leads to behaviour that is not adequately modelled by our single site/single crystal theory. It is all the more intriguing that, nevertheless, our composite $\pi/2$ pulses work well for $HgCl_2$, and the composite π pulses work for all the samples we have investigated. Finally, because of the practical difficulties, including availability of suitable samples, growing single crystals, getting spectrometer time in a distant host laboratory etc.,

Figure VI.14 - VI.24

^{35}Cl pure NQR spectrum of $NaClO_3$ sample obtained by the application of single and composite π pulses at various offset ($\Delta\omega_Q$) values at room temperature (297 K).

Common Spectral Parameters

Synthesizer frequency = 29.9130 MHz

Frequency of irradiation = 29.9130 + offset

Spectral width = 100 kHz

Pulse time durations:

i) for $NaClO_3$ powder case

$\pi/2$ pulse width is 10.0 μs

and π pulse width is 20.0 μs

ii) for $NaClO_3$ single crystal case

$\pi/2$ pulse corresponds to 9.0 μs

and π pulse corresponds to 18.0 μs

Normalization constant = -2.

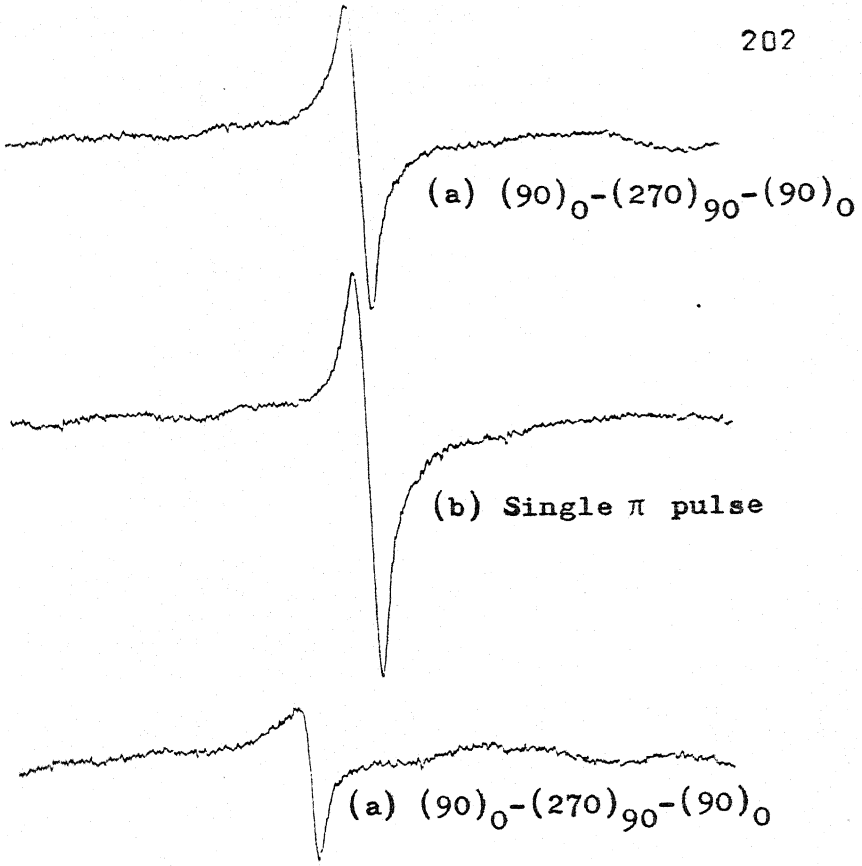

Figure VI.14
$\Delta\omega_Q$ = 20 kHz

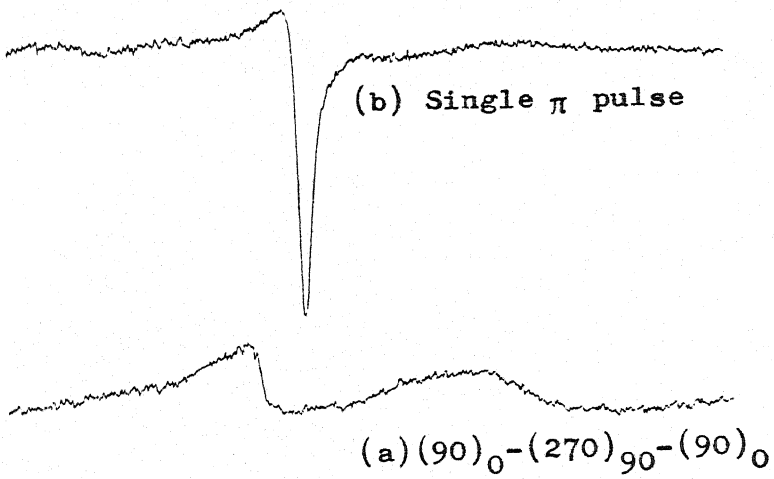

Figure VI.15
$\Delta\omega_Q$ = 15 kHz

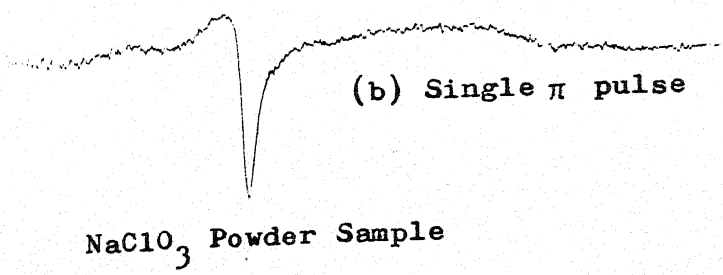

Figure VI.16
$\Delta\omega_Q$ = 10 kHz

$NaClO_3$ Powder Sample

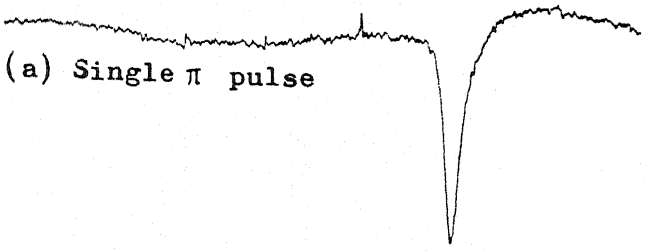

Figure VI.17
$\Delta\omega_Q$ = -5 kHz

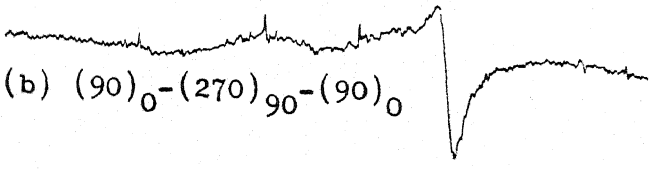

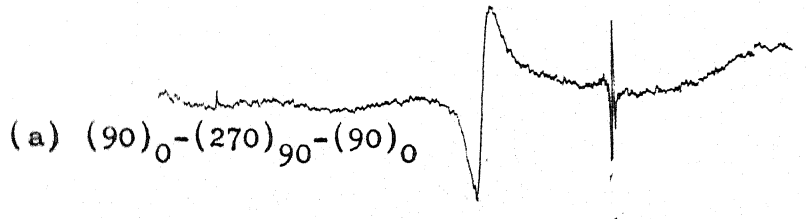

Figure VI.18
$\Delta\omega_Q$ = -10 kHz

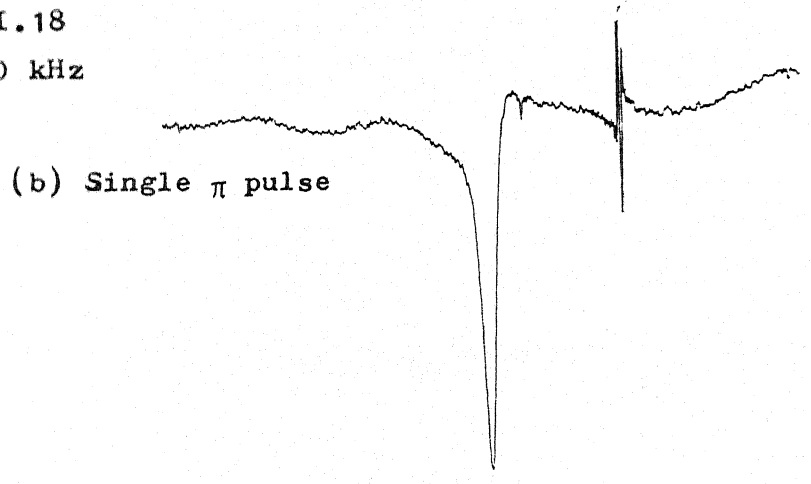

$NaClO_3$ Powder Sample

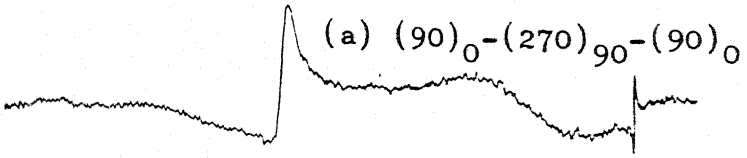

Figure VI.19
$\Delta\omega_Q$ = -20 kHz

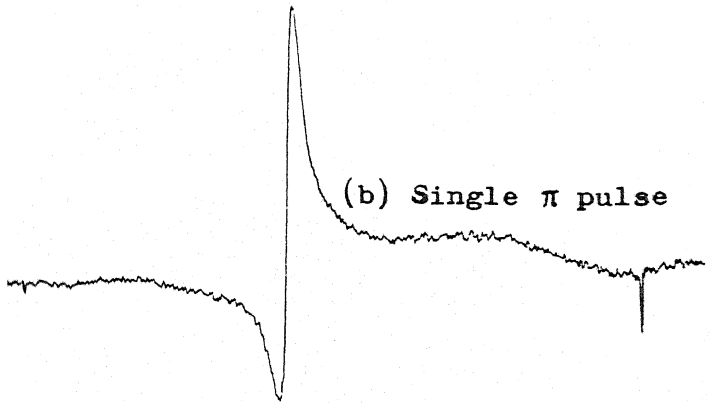

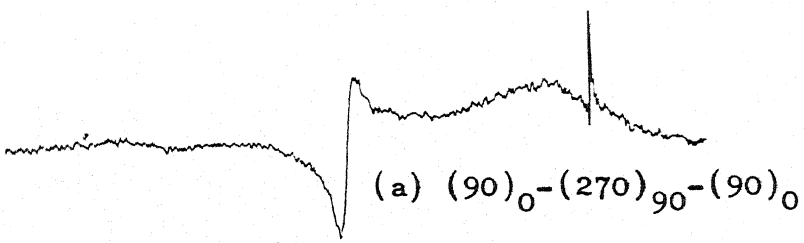

Figure VI.20
$\Delta\omega_Q$ = -15 kHz

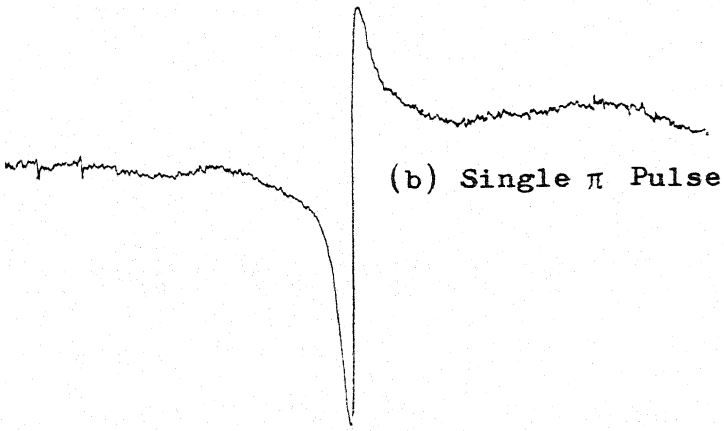

$NaClO_3$ Powder Sample

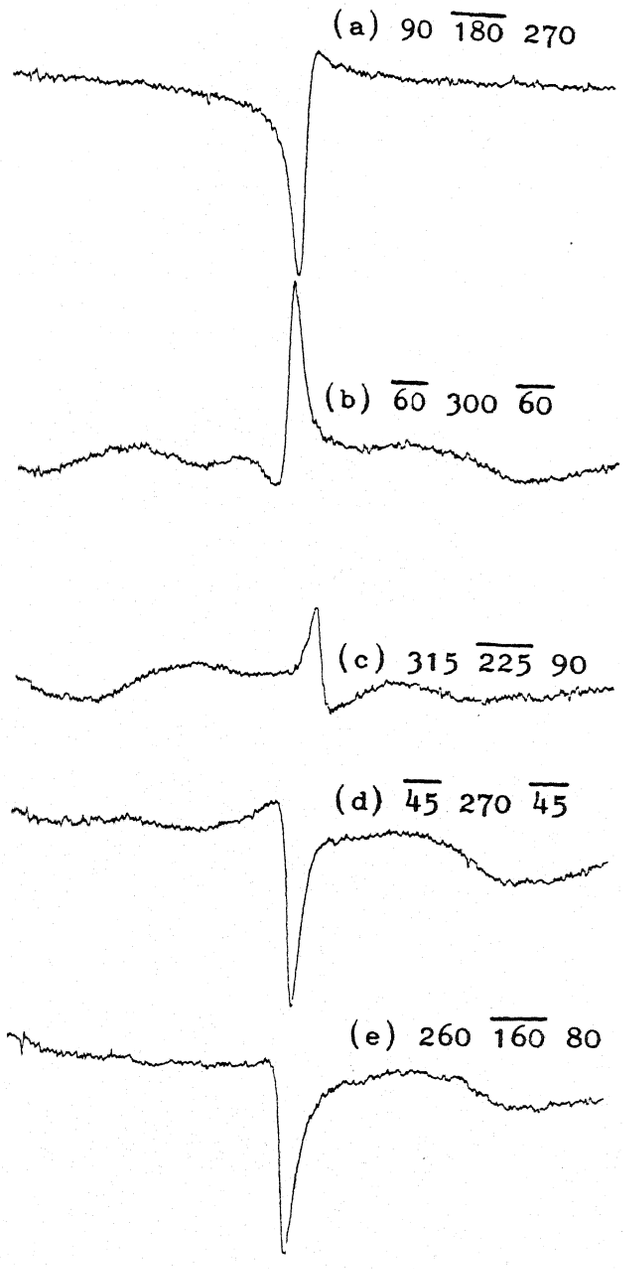

Figure VI.21 $NaClO_3$ Powder Sample
$\Delta\omega_Q$ = 10 kHz

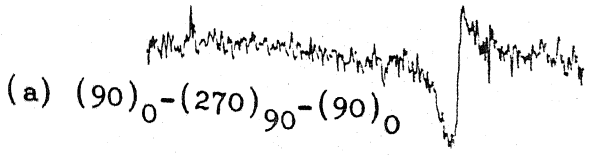

(a) $(90)_0-(270)_{90}-(90)_0$

Figure VI.22

$\Delta\omega_Q$ = -10 kHz

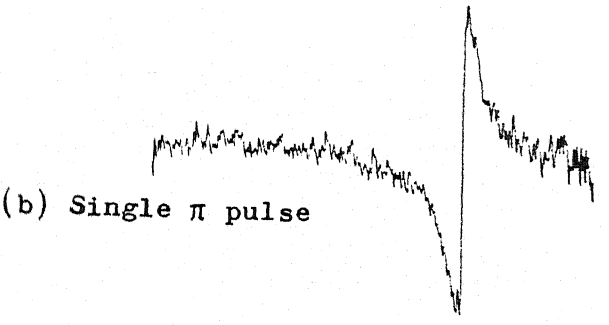

(b) Single π pulse

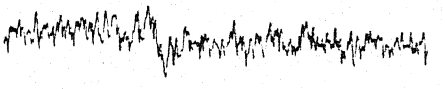

(a) $(90)_0-(270)_{90}-(90)_0$

Figure VI.23

$\Delta\omega_Q$ = 5 kHz

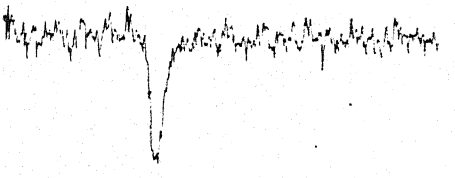

(b) Single π pulse

$NaClO_3$ Single Crystal

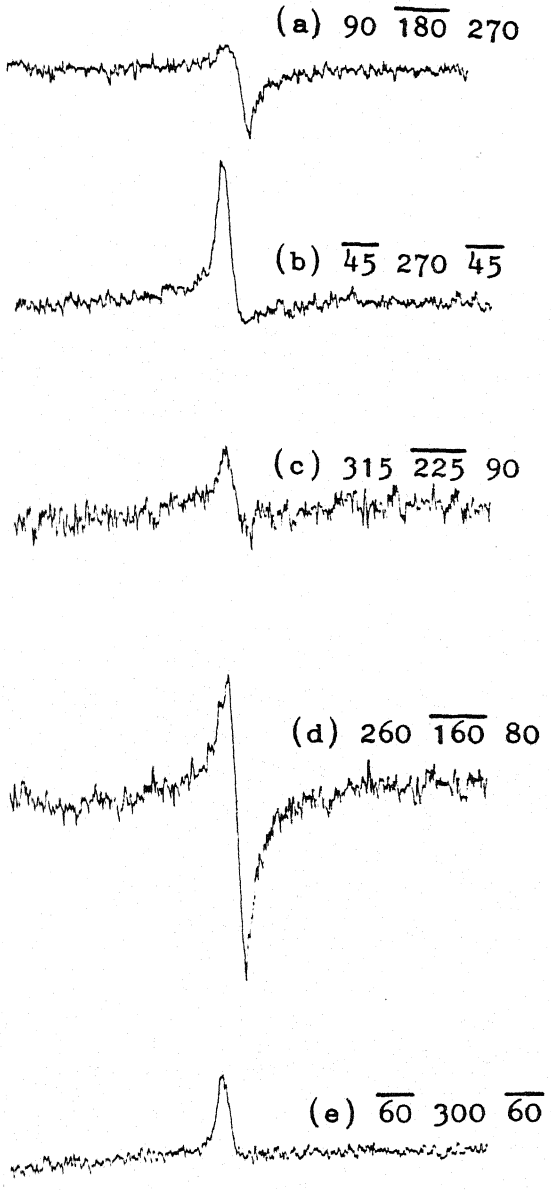

Figure VI.24 $NaClO_3$ Single Crystal
$\Delta\omega_Q$ = 10 kHz

a more elaborate study could not be pursued in the present work.

Summary

In this chapter, the experimental demonstration of the behaviour of composite pulses has been presented. It is inferred that composite π pulses work well in all the systems we have tested, whereas composite $\pi/2$ pulses do not. The excellent performance of composite $\pi/2$ pulses in the case of $HgCl_2$ is worth pointing out. From our experimental studies, we suggest that $\overline{45\ 135}$ for composite $\pi/2$ pulse and $(90)_0$-$(270)_{90}$-$(90)_0$ for composite π pulse are superior excitation trains in pure NQR spectroscopy.

REFERENCES

1. M. A. Massompiere, Compt. Rend. 236, 596 (1953).
2. Buyle-Bodin and A. Monfils, Compt. Rend. 236, 1157 (1953).
3. H. G. Dehmelt, H. G. Robinson and W. Gordy, Phys. Rev. 93, 480 (1954).
4. R. G. Barnes and R. A. Hultsch, Phys. Rev. Lett. 1, 227 (1958).
5. J. Ramakrishna, Phil. Mag. 14, 589 (1966);
   H. Negita, T. Tanaka, T. Okuda and H. Shimada, Inorg. Chem. 5, 2126 (1966).
6. Dinesh and P. T. Narasimhan, J. Chem. Phys. 45, 2170 (1966).
7. R. W. G. Wyckoff, 'Crystal Structures,' Vol. I, Interscience Publishers, Inc., New York (1963).
8. T. P. Das and E. L. Hahn, 'Solid State Physics,' Supplement 1, Academic Press, New York (1958).

CHAPTER VII

SUMMARY AND SCOPE FOR FURTHER WORK

VII.1 Summary

A general Magnus expansion approach has been developed and effectively employed in the problem of designing NQR composite pulses. This approach is shown to be successful in the context of broadband excitation problem for any quadrupole spin system, irrespective of the spin quantum number. Composite pulses are obtained to compensate for efg and rf field inhomogeneities via the Magnus expansion approach. These sequences are shown to behave as a single rf pulse, namely, $(\theta)_{\phi}$ with a net flip angle of θ and phase ϕ.

Our main efforts at constructing NQR composite pulses have brought out many interesting results related to the fundamental properties of the spin system. Particularly, our design of PACPS has led us to infer that the two separate cases, namely, spin I = 1 pure NQR and spin I = 1/2 NMR, are closely related. This has also led to the construction of composite $\pi/2$ pulses to compensate for quadrupolar and dipole-dipole interactions in the case of spin I = 1 NMR spectroscopy (refer Appendix E). Furthermore, NQR composite pulses that have been designed for spin I = 1 and 3/2 cases, are also applicable for any general quadrupole spin I nucleus. These results predict that the study of the system of non-interacting quadrupole nuclei in the absence of a Zeeman field

is basically a two-level problem.

Composite pulses designed using the Magnus expansion method have been examined experimentally by studying the ^{35}Cl NQR of $HgCl_2$ and $NaClO_3$ samples. Our experimental results support rather well the applicability of composite pulses for the uniform spin excitation and inversion in pure NQR spectroscopy.

Apart from this, composite $\pi/2$ pulses have also been synthesized using a numerical method to enhance the NQR signal intensity in powder samples (Chapter V).

In the next section, we point out the future scope of this work.

VII.2 Scope for Further Work

To improve the performance of composite pulses, one may consider higher-order terms in the Magnus expansion (Chapters II - IV). However, this would entail increasing the number of rf pulses constituting a given composite pulse. We should keep in mind that the total time duration of a composite pulse should be much less than T_2. Construction of composite pulses which compensate for two or more parameters (such as efg, rf field inhomogeneities and dipole-dipole interaction) would be welcome from the point of view of several important experimental studies in NQR. These goals could be attained using computer programs for solving complicated analytical expressions in the framework of the Magnus expansion technique. It might be possible to evaluate higher-order terms in the Magnus expansion following some recent approaches.[1] In particular convergence problems with the

Magnus expansion may also be overcome by Maricq's approach.[2] The evaluation of the rf interaction frame Hamiltonian could be simplified by using recursive evaluation procedures.[3]

The transformation properties of irreducible spherical tensor operators given in Chapter IV would be useful in evaluating the performance of any kind of pulse sequences in spin I = 3/2 NQR spectroscopy. As an additional exercise to simplify the complexity involved in spin dynamics studies in magnetic resonance, one can develop a computer program for an easy evaluation of unitary transformations of base operators constituting the spin density matrix.

In this work, we have designed NQR composite pulses for single crystals. These composite pulses, when actually produced as shown in Chapter VI, perform well in powder $HgCl_2$ also, even-though one cannot assume a priori that pulse sequence designed for single crystals will work for powders also. Therefore, it may be important, and more worthwhile, to design NQR composite pulses via the Magnus expansion approach for powders separately. Also, it would be desirable to test the composite pulses designed explicitly for powders in the present work (Chapter V). Experimental work with such composite pulses would point the way to improve their applicability further. It would be thus necessary to employ pulses with phases other than 0°, 90° or integral multiples of 90° also.

An exciting area of further research is the use of composite pulses for investigating NQR of high-T_c superconductivity

samples whose spectra are very broad (~MHz).[4] Composite $\pi/2$ pulses designed using the numerical approach in Chapter V may be employed in order to get better NQR signal intensity in these samples. Application of these NQR composite pulses might also benefit zero field NQR and NMR spectroscopy.[5] Relaxation times, T_1 and T_2, can be measured with better accuracy using composite π and $\pi/2$ pulses in spin-inversion recovery or saturation recovery and spin echo methods. In this context, it would be worthwhile to study the problem of designing composite π pulses specifically for the purpose of refocussing in NQR spin echo experiments.

REFERENCES

1. W. R. Salzman, J. Chem. Phys. 82, 822 (1985);
   W. R. Salzman, J. Chem. Phys. 85, 4605 (1986);
   W. R. Salzman, Chem. Phys. Lett. 124, 531 (1986);
   S. Klarsfeld and J. A. Oteo, Phys. Rev. 39A, 3270 (1989).
2. M. M. Maricq, J. Chem. Phys. 86, 5647 (1987).
3. D. Suter and A. Pines, J. Magn. Reson. 75, 509 (1987).
4. I. Furo, A. Janossy, L. Mihaly, P. Banki, I. Pocsik, I. Bakonyi, I. Heinmaa, E. Joon and E. Lippmaa, Phys. Rev. 36B, 5690 (1987);
   W. W. Warren, R. E. Walstedt, G. F. Brennert, R. F. Bell, R. J. Cava and G. P. Espinosa, J. Appl. Phys. 64, 6081 (1988).
5. D. B. Zax, A. Bielecki, K. W. Zilm, A. Pines and D. P. Weitakamp, J. Chem. Phys. 83, 4877 (1985).

APPENDIX A

FICTITIOUS SPIN-1/2 OPERATOR FORMALISM

In the case of spin $I \geq 1$, the density matrix of the spin system cannot be completely described by only three spin angular momentum operators and for this it is necessary to have a set of $(2I+1)^2-1$ base operators.[1] For spin I = 1 case, Vega and Pines have developed an operator formalism[2,3] which is very compact and convenient in studying the time evolution of the density matrix for spin I = 1 quadrupolar system.[2,4] They are traceless, independent, Hermitian operators and they form the generators of the group SU(3) These operators in terms of three cartesian linear angular momentum operators are given by[2]

$$I_{X1} = \frac{I_x}{2} \quad ; \quad I_{Y1} = \frac{I_y}{2} \quad ; \quad I_{Z1} = \frac{I_z}{2} \quad ;$$

$$I_{X2} = \frac{1}{2}\,(I_yI_z+I_zI_y) \quad ; \quad I_{Y2} = \frac{1}{2}\,(I_zI_x+I_xI_z) \quad ; \quad I_{Z2} = \frac{1}{2}\,(I_xI_y+I_yI_x) \quad ,$$

$$I_{X3} = \frac{1}{2}\,(I_z^2-I_y^2) \quad ; \quad I_{Y3} = \frac{1}{2}\,(I_x^2-I_z^2) \quad ; \quad I_{Z3} = \frac{1}{2}\,(I_y^2-I_x^2) \quad .$$

The two indices p, i in I_{pi} denote that for each p, we have a subspace i = 1, 2, 3 with spin 1/2 transformation properties and hence the name fictitious spin-1/2 operators.[1] I_{p1}, I_{p2} and I_{p3}

behave like the cartesian angular momentum operators I_x, I_y and I_z for all three possible p's; p = X, Y, Z. Only 8 of these operators are linearly independent and this dependence is expressed by $I_{X3} + I_{Y3} + I_{Z3} = 0$.

To simplify the spin dynamics calculation in NQR spectroscopy, some more operators have been defined as[4] given below:

$$I_{X4} = I_{Y3} - I_{Z3} \; ; \; I_{Y4} = I_{Z3} - I_{X3} \; ; \; I_{Z4} = I_{X3} - I_{Y3} \; .$$

It is necessary to know various commutation relations[3,5] among these operators for evaluating the time evolution of the spin systems and these have been summarized in Table A.1. We have employed this operator formalism for studying the spin dynamics of spin 1 NQR spectroscopy[6] in Chapters III and V of this thesis.

References

1. A. Abragam, 'Principles of Nuclear Magnetism,' Oxford University Press, Oxford (1961), Chapter II.
2. S. Vega, J. Chem. Phys. 63, 3769 (1975).
3. S. Vega and A. Pines, J. Chem. Phys. 66, 5624 (1977).
4. R. S. Cantor and J. S. Waugh, J. Chem. Phys. 73, 1054 (1980).
5. T. W. Shattuck, Ph.D. Thesis, University of California, Berkeley (1976).
6. A. Ramamoorthy and P. T. Narasimhan, J. Molec. Struct. 192, 333 (1989).

A

B \ A	I_{X1}	I_{X2}	I_{X3}	I_{Y1}	I_{Y2}	I_{Y3}	I_{Z1}	I_{Z2}	I_{Z3}	I_{X4}	I_{Y4}	I_{Z4}
I_{X1}	0	I_{X3}	$-I_{X2}$	$1/2\ I_{Z1}$	$-1/2\ I_{Z2}$	$1/2\ I_{X2}$	$-1/2\ I_{Y1}$	$1/2\ I_{Y2}$	$1/2\ I_{X2}$	0	$3/2\ I_{X2}$	$-3/2\ I_{X2}$
I_{X2}	$-I_{X3}$	0	I_{X1}	$-1/2\ I_{Z2}$	$-1/2\ I_{Z1}$	$-1/2\ I_{X1}$	$1/2\ I_{Y2}$	$1/2\ I_{Y1}$	$-1/2\ I_{X1}$	0	$-3/2\ I_{X1}$	$3/2\ I_{X1}$
I_{X3}	I_{X2}	$-I_{X1}$	0	$-1/2\ I_{Y2}$	$1/2\ I_{Y1}$	0	$-1/2\ I_{Z2}$	$1/2\ I_{Z1}$	0	0	0	0
I_{Y1}	$-1/2\ I_{Z1}$	$1/2\ I_{Z2}$	$1/2\ I_{Y2}$	0	I_{Y3}	$-I_{Y2}$	$1/2\ I_{X1}$	$-1/2\ I_{X2}$	$1/2\ I_{Y2}$	$-3/2\ I_{Y2}$	0	$3/2\ I_{Y2}$
I_{Y2}	$1/2\ I_{Z2}$	$1/2\ I_{Z1}$	$-1/2\ I_{Y1}$	$-I_{Y3}$	0	I_{Y1}	$-1/2\ I_{X2}$	$-1/2\ I_{X1}$	$-1/2\ I_{Y1}$	$3/2\ I_{Y1}$	0	$-3/2\ I_{Y1}$
I_{Y3}	$-1/2\ I_{X2}$	$1/2\ I_{X1}$	0	I_{Y2}	$-I_{Y1}$	0	$-1/2\ I_{Z2}$	$1/2\ I_{Z1}$	0	0	0	0
I_{Z1}	$1/2\ I_{Y1}$	$-1/2\ I_{Y2}$	$1/2\ I_{Z2}$	$-1/2\ I_{X1}$	$1/2\ I_{X2}$	$1/2\ I_{Z2}$	0	I_{Z3}	$-I_{Z2}$	$3/2\ I_{Z2}$	$-3/2\ I_{Z2}$	0
I_{Z2}	$-1/2\ I_{Y2}$	$-1/2\ I_{Y1}$	$-1/2\ I_{Z1}$	$1/2\ I_{X2}$	$1/2\ I_{X1}$	$-1/2\ I_{Z1}$	$-I_{Z3}$	0	I_{Z1}	$-3/2\ I_{Z1}$	$3/2\ I_{Z1}$	0
I_{Z3}	$-1/2\ I_{X2}$	$1/2\ I_{X1}$	0	$-1/2\ I_{Y2}$	$1/2\ I_{Y1}$	0	I_{Z2}	$-I_{Z1}$	0	0	0	0
I_{X4}	0	0	0	$3/2\ I_{Y2}$	$-3/2\ I_{Y1}$	0	$-3/2\ I_{Z2}$	$3/2\ I_{Z1}$	0	0	0	0
I_{Y4}	$-3/2\ I_{X2}$	$3/2\ I_{X1}$	0	0	0	0	$3/2\ I_{Z2}$	$-3/2\ I_{Z1}$	0	0	0	0
I_{Z4}	$3/2\ I_{X2}$	$-3/2\ I_{X1}$	0	$-3/2\ I_{Y2}$	$3/2\ I_{Y1}$	0	0	0	0	0	0	0

$$[A,B] = iC$$

Table A.1. Commutation relationships between fictitious spin-1/2 operators for spin I = 1 case

APPENDIX B

TENSOR OPERATOR FORMALISM

For spin I = 3/2, a basis set of 15 operators is required to define the density matrix of the spin system. Here, we have used the irreducible tensor operators[1-3] for studying the time evolution of the density matrix in the case of pure NQR of spin I = 3/2 nuclei (vide Chapters IV and V). Irreducible tensor operators T_q^n of rank n and order q have been defined by Buckmaster et al.[1] via the Wigner-Eckart theorem[4] as

$$\langle Im | T_q^n | Im' \rangle = (-1)^{I-m} \begin{pmatrix} I & n & I \\ -m & q & m' \end{pmatrix} \langle I \| T^n \| I \rangle$$

$$= (2I+1)^{-1/2} \langle Im'nq | Im \rangle \langle I \| T^n \| I \rangle$$

where $\begin{pmatrix} I & n & I \\ -m & q & m' \end{pmatrix}$ and $\langle Im'nq | Im \rangle$ are the well-documented 3j and Clebsch-Gordan coefficients,[5] respectively, and the reduced matrix element is given by[4]

$$\langle I \| T^n \| I \rangle = \left[\frac{n!\ n!\ (2I+n+1)}{2^n (2n)!\ (2I-n)!} \right]^{1/2} .$$

Irreducible tensor operators T_q^n thus defined are given in the Table B.1 for $n \leq 5$. Later Bowden and Hutchison,[2] introduced the symmetric and antisymmetric combinations of $T_{\pm q}^n$ explicitly as

Table B.1 Tensor Operators for $n \leq 5$ After Buckmaster et al.[1]

$$T^0_0 = 1 \quad ; \quad T^2_0 = \left(\tfrac{1}{6}\right)^{1/2} \left[3 I_z^2 - I(I+1)\right] ;$$

$$T^1_0 = I_z \quad ; \quad T^2_{\pm 1} = \mp \tfrac{1}{2} \left[I_z, I_\pm\right]_+ ;$$

$$T^1_{\pm 1} = \mp \left(\tfrac{1}{2}\right)^{1/2} I_\pm \quad ; \quad T^2_{\pm 2} = \tfrac{1}{2} I_\pm^2$$

$$T^3_0 = \left(\tfrac{1}{10}\right)^{1/2} \left[5 I_z^3 - \left\{3 I(I+1) - 1\right\} I_z\right]$$

$$T^3_{\pm 1} = \mp \tfrac{1}{4} \left(\tfrac{3}{10}\right)^{1/2} \tfrac{1}{2} \left[\left\{5 I_z^2 - I(I+1) - \tfrac{1}{2}\right\}, I_\pm\right]_+$$

$$T^3_{\pm 2} = \left(\tfrac{3}{4}\right)^{1/2} \tfrac{1}{2} \left[I_z, I_\pm^2\right]_+$$

$$T^3_{\pm 3} = \mp \tfrac{1}{2} \left(\tfrac{1}{2}\right)^{1/2} I_\pm^3$$

$$T^4_0 = \tfrac{1}{2} \left(\tfrac{1}{70}\right)^{1/2} \left[35 I_z^4 - \left\{30 I(I+1) - 25\right\} I_z^2 + 3 I^2(I+1)^2 - 6I(I+1)\right]$$

$$T^4_{\pm 1} = \mp \left(\tfrac{1}{14}\right)^{1/2} \left[\left\{7 I_z^3 - \left[3 I(I+1) + 1\right] I_z\right\}, I_\pm\right]_+$$

$$T^4_{\pm 2} = \tfrac{1}{4} \left(\tfrac{1}{7}\right)^{1/2} \left[\left\{7 I_z^2 - I(I+1) - 5\right\}, I_\pm^2\right]_+$$

$$T^4_{\pm 3} = \mp \left(\tfrac{1}{2}\right)^{1/2} \tfrac{1}{2} \left[I_z, I_\pm^3\right]_+$$

$$T^4_{\pm 4} = \tfrac{1}{4} I_\pm^4$$

$$T^5_0 = \tfrac{1}{6} \left(\tfrac{1}{14}\right)^{1/2} \left[63 I_z^5 + 35\left\{3 - 5I(I+1)\right\} I_z^3 + \left\{12 - 50 I(I+1) + 15 I^2(I+1)^2\right\} I_z\right]$$

$$T^5_{\pm 1} = \mp \left(\tfrac{5}{21}\right)^{1/2} I_\pm \left[21 I_z^4 \pm 42 I_z^3 + 7\left\{9 - 2 I(I+1)\right\} I_z^2 \pm 14\left\{3 - I(I+1)\right\} I_z + \left\{12 - 8 I(I+1) + I^2(I+1)^2\right\}\right]$$

$$T^5_{\pm 2} = \tfrac{1}{2} \left(\tfrac{5}{3}\right)^{1/2} I_\pm^2 \left[3 I_z^3 \pm 9 I_z^2 + \left\{12 - I(I+1)\right\} I_z \pm \left\{6 - I(I+1)\right\}\right]$$

$$T^5_{\pm 3} = \mp \tfrac{1}{12} \left(\tfrac{5}{2}\right)^{1/2} I_\pm^3 \left[9 I_z^2 \pm 27 I_z + \left\{24 - I(I+1)\right\}\right]$$

$$T^5_{\pm 4} = \tfrac{1}{4} \left(\tfrac{5}{1}\right)^{1/2} I_\pm^4 \left[I_z \pm 2\right]$$

$$T^5_{\pm 5} = \mp \tfrac{1}{4} \left(\tfrac{1}{2}\right)^{1/2} I_\pm^5$$

$$T_q^n(s) = \sqrt{1/2}\ (T_q^n + T_{-q}^n)$$

and $T_q^n(a) = \sqrt{1/2}\ (T_q^n - T_{-q}^n)$ with $q \neq 0$.

These T_q^n are called non-unit irreducible tensors and they are orthogonal but not orthonormal. But the unit tensors T_q^n are orthonormal and are given by[2]

$$T_q^n = \frac{(2n+1)^{1/2}}{\langle I \| T^n \| I \rangle} T_q^n$$

and $\mathrm{Tr}\left[(T_q^n)^\dagger T_{q'}^{n'} \right] = \delta_{nn'} \delta_{qq'}$

where the adjoint is

$$(T_q^n)^\dagger = (-1)^q T_{-q}^n \ .$$

Since the unit tensors form a complete orthonormal basis set, any operator can be expressed in terms of the T_q^n. For example, the density matrix σ may be written as

$$\sigma = \sum_{n,q} \rho_q^n T_q^n$$

where the coefficients ρ_q^n are referred to as Fano statistical tensors, given by

$$\rho_q^n = \mathrm{Tr}\left[(T_q^n)^\dagger \sigma \right].$$

The non-unit tensors are more convenient to use because they hold for all spin I. We have used the non-unit irreducible tensor operators in this thesis. Because T_q^n form a basis set, the product of any two tensor operators can be written as follows:

$$T_q^n \; T_{q'}^{n'} = \sum_{NQ} a\,(n,\, n',\, N,\, I)\, \langle NQ|n,q,n',q'\rangle \; T_Q^N$$

where $a\,(n,\, n',\, N,\, I) = (2N+1)^{1/2}\,(-1)^{N+2I}$

$$\begin{Bmatrix} n & n' & N \\ I & I & I \end{Bmatrix} \frac{\langle I \| T^n \| I\rangle \langle I \| T^{n'} \| I\rangle}{\langle I \| T^N \| I\rangle}$$

and $\begin{Bmatrix} n & n' & N \\ I & I & I \end{Bmatrix}$ is a Wigner 6j coefficient.

The commutation relations can be given as

$$[T_q^n,\, T_{q'}^{n'}] = T_q^n \; T_{q'}^{n'} - T_{q'}^{n'} \; T_q^n$$

$$= \sum_{NQ} a\,(n,\, n',\, N,\, I)\, [I-(-1)^{n+n'-N}]\, \langle NQ|n,q,n',q'\rangle \; T_Q^N$$

In Table B.2, we present the commutation relationships[3] between different tensor operators which have been used in Chapters IV and V in designing composite pulses for I = 3/2 case. In Table B.3, we present the matrix representation of a few selected tensor operators which have been useful in Chapters IV and V for representing various spin Hamiltonians in different interaction frames.

Table B.2 Commutation Relationships for I = 3/2, with Symmetric and Anti-symmetric Combinations[3]

$[T_o^1, T_1^1(s)] = T_1^1(a)$

$[T_o^1, T_1^1(a)] = T_1^1(s)$

$[T_o^1, T_1^2(s)] = T_1^2(a)$

$[T_o^1, T_1^2(a)] = T_1^2(s)$

$[T_o^1, T_2^2(s)] = 2T_2^2(a)$

$[T_o^1, T_2^2(a)] = 2T_2^2(s)$

$[T_o^1, T_1^3(s)] = T_1^3(a)$

$[T_o^1, T_1^3(a)] = T_1^3(s)$

$[T_o^1, T_2^3(s)] = 2T_2^3(a)$

$[T_o^1, T_2^3(a)] = 2T_2^3(s)$

$[T_o^1, T_3^3(s)] = \sqrt{3}T_3^3(a)$

$[T_o^1, T_3^3(a)] = 3T_3^3(s)$

$[T_1^1(s), T_1^1(a)] = T_o^1$

$[T_1^1(s), T_o^2] = -\sqrt{3}T_1^2(a)$

$[T_1^1(s), T_1^2(s)] = -T_2^2(a)$

$[T_1^1(s), T_1^2(a)] = \sqrt{3}T_o^2 - T_2^2(s)$

$[T_1^1(s), T_2^2(s)] = T_1^2(a)$

$[T_1^1(s), T_2^2(a)] = T_1^2(s)$

$[T_1^1(s), T_o^3] = -\sqrt{6}T_1^3(a)$

$[T_1^1(s), T_1^3(s)] = -\sqrt{\frac{5}{2}}T_2^3(a)$

$[T_1^1(s), T_1^3(a)] = -\sqrt{6}T_o^3 - \sqrt{\frac{5}{2}}T_2^3(s)$

$[T_1^1(a), T_1^3(a)] = -\sqrt{\frac{5}{2}}T_2^3(a)$

$[T_1^1(a), T_2^3(s)] = -\sqrt{\frac{5}{2}}T_1^3(s) - \sqrt{\frac{3}{2}}T_3^3(s)$

$[T_1^1(a), T_2^3(a)] = -\sqrt{\frac{5}{2}}T_1^3(a) - \sqrt{\frac{3}{2}}T_3^3(a)$

$[T_1^1(a), T_3^3(s)] = -\sqrt{\frac{3}{2}}T_2^3(s)$

$[T_1^1(a), T_3^3(a)] = -\sqrt{\frac{3}{2}}T_2^3(a)$

$[T_o^2, T_1^2(s)] = \frac{6\sqrt{3}}{5}T_1^1(a) + \frac{4}{\sqrt{5}}T_1^3(a)$

$[T_o^2, T_1^2(a)] = \frac{6\sqrt{3}}{5}T_1^1(s) + \frac{4}{\sqrt{5}}T_1^3(s)$

$[T_o^2, T_2^2(s)] = 2\sqrt{2}T_2^3(a)$

$[T_1^1(s), T_1^3(s)] = -\sqrt{6}T_o^3 - \sqrt{\frac{5}{2}}T_2^3(s)$

$[T_1^1(s), T_1^3(a)] = -\sqrt{\frac{5}{2}}T_2^3(a)$

$[T_1^1(a), T_1^3(a)] = -\sqrt{6}T_1^3(s)$

$[T_1^1(a), T_o^3] = -\sqrt{6}T_1^3(s)$

$[T_1^1(a), T_1^3(s)] = -\sqrt{6}T_o^3 - \sqrt{\frac{5}{2}}T_2^3(s)$

$[T_1^1(a), T_1^3(a)] = -\sqrt{\frac{5}{2}}T_2^3(a)$

$[T_1^1(a), T_2^3(s)] = -\sqrt{\frac{5}{2}}T_1^3(s) - \sqrt{\frac{3}{2}}T_3^3(s)$

$[T_1^1(a), T_2^3(a)] = -\sqrt{\frac{5}{2}}T_1^3(a) - \sqrt{\frac{3}{2}}T_3^3(a)$

$[T_1^1(a), T_3^3(s)] = -\sqrt{\frac{3}{2}}T_2^3(s)$

$[T_1^1(a), T_3^3(a)] = -\sqrt{\frac{3}{2}}T_2^3(a)$

$[T_o^2, T_1^2(s)] = \frac{6\sqrt{3}}{5}T_1^1(a) + \frac{4}{\sqrt{5}}T_1^3(a)$

$[T_o^2, T_1^2(a)] = \frac{6\sqrt{3}}{5}T_1^1(s) + \frac{4}{\sqrt{5}}T_1^3(s)$

$[T_o^2, T_2^2(s)] = 2\sqrt{2}T_2^3(a)$

Table B.2 (contd.)

$$[T_o^2 \ , \ T_2^2(a)] = 2\sqrt{2}T_2^3(s)$$

$$[T_o^2 \ , \ T_1^3(s)] = \frac{3}{\sqrt{5}}T_1^2(a)$$

$$[T_o^2 \ , \ T_1^3(a)] = \frac{3}{\sqrt{5}}T_1^2(s)$$

$$[T_o^2 \ , \ T_2^3(s)] = \frac{3}{\sqrt{2}}T_2^2(a)$$

$$[T_o^2 \ , \ T_2^3(a)] = \frac{3}{\sqrt{2}}T_2^2(s)$$

$$[T_1^2(s), \ T_1^2(a)] = \frac{6}{5}T_o^1 + \frac{4\sqrt{2}}{\sqrt{5}}T_o^3$$

$$[T_1^2(s), \ T_2^2(s)] = -\frac{6}{5}T_1^1(a) + \frac{2\sqrt{3}}{\sqrt{5}}T_1^3(a) + 2T_3^3(a)$$

$$[T_1^2(s), \ T_2^2(a)] = -\frac{6}{5}T_1^1(s) + \frac{2\sqrt{3}}{\sqrt{5}}T_1^3(s) + 2T_3^3(s)$$

$$[T_1^2(s), \ T_3^3(s)] = -\frac{3}{2}T_2^2(a)$$

$$[T_1^2(s), \ T_o^3 \ ] = -\frac{3\sqrt{2}}{\sqrt{5}}T_1^2(a)$$

$$[T_1^2(s), \ T_1^3(s)] = -\frac{3\sqrt{3}}{\sqrt{20}}T_2^2(a)$$

$$[T_1^2(s), \ T_1^3(a)] = \frac{3}{\sqrt{5}}T_o^2 - \frac{3\sqrt{3}}{\sqrt{20}}T_2^2(s)$$

$$[T_1^2(s), \ T_3^3(a)] = -\frac{3}{2}T_2^2(s)$$

$$[T_1^2(a), \ T_2^2(s)] = \frac{6}{5}T_1^1(s) - \frac{2\sqrt{3}}{\sqrt{5}}T_1^3(s) + 2T_3^3(s)$$

$$[T_1^2(a), \ T_2^2(a)] = \frac{6}{5}T_1^1(a) - \frac{2\sqrt{3}}{\sqrt{5}}T_1^3(a) + 2T_3^3(a)$$

$$[T_1^2(a), \ T_o^3 \ ] = -\frac{3\sqrt{2}}{\sqrt{5}}T_1^2(s)$$

$$[T_1^2(a), \ T_1^3(s)] = -\frac{3}{\sqrt{5}}T_o^2 - \frac{3\sqrt{3}}{\sqrt{20}}T_2^2(s)$$

$$[T_1^2(a), \ T_1^3(a)] = -\frac{3\sqrt{3}}{\sqrt{20}}T_2^2(a)$$

$$[T_1^2(a), \ T_3^3(s)] = \frac{3}{2}T_2^2(s)$$

$$[T_1^2(a), \ T_3^3(a)] = \frac{3}{2}T_2^2(a)$$

$$[T_2^2(s), \ T_2^2(a)] = -\frac{12}{5}T_o^1 + \frac{2\sqrt{2}}{\sqrt{5}}T_o^3$$

$$[T_2^2(s), \ T_o^3 \ ] = \frac{3}{\sqrt{10}}T_2^2(a)$$

$$[T_2^2(s), \ T_1^3(s)] = \frac{3\sqrt{3}}{2\sqrt{5}}T_1^2(a)$$

$$[T_2^2(s), \ T_1^3(a)] = -\frac{3\sqrt{3}}{2\sqrt{5}}T_1^2(s)$$

$$[T_2^2(s), \ T_2^3(a)] = \frac{-3}{\sqrt{2}}T_o^2$$

$$[T_2^2(s), \ T_3^3(s)] = -\frac{3}{2}T_1^2(a)$$

$$[T_2^2(s), \ T_3^3(a)] = -\frac{3}{2}T_1^2(s)$$

$$[T_2^2(a), \ T_o^3 \ ] = \frac{3}{\sqrt{10}}T_2^2(s)$$

$$[T_2^2(a), \ T_1^3(s)] = \frac{3\sqrt{3}}{2\sqrt{5}}T_1^2(s)$$

$$[T_2^2(a), \ T_1^3(a)] = -\frac{3\sqrt{3}}{2\sqrt{5}}T_1^2(a)$$

$$[T_2^2(a), \ T_2^3(s)] = \frac{3}{\sqrt{2}}T_o^2$$

$$[T_2^2(a), \ T_3^3(s)] = \frac{3}{2}T_1^2(s)$$

$$[T_2^2(a), \ T_3^3(a)] = \frac{3}{2}T_1^2(a)$$

$$[T_o^3 \ , \ T_1^3(s)] = \frac{9\sqrt{3}}{5\sqrt{2}}T_1^1(a) - \frac{3}{\sqrt{10}}T_1^3(a)$$

$$[T_o^3 \ , \ T_1^3(a)] = \frac{9\sqrt{3}}{5\sqrt{2}}T_1^1(s) - \frac{3}{\sqrt{10}}T_1^3(s)$$

$$[T_o^3 \ , \ T_2^3(s)] = -\frac{3}{\sqrt{10}}T_2^3(a)$$

$$[T_o^3 \ , \ T_2^3(a)] = -\frac{3}{\sqrt{10}}T_2^3(s)$$

$$[T_o^3 \ , \ T_3^3(s)] = \frac{3}{\sqrt{10}}T_3^3(a)$$

$$[T_o^3 \ , \ T_3^3(a)] = \frac{3}{\sqrt{10}}T_3^3(s)$$

$$[T_1^3(s), \ T_1^3(a)] = \frac{9}{10}T_o^1 - \frac{3}{\sqrt{10}}T_o^3$$

...contd.

Table B.2 (contd.)

$$[T_1^3(s),\ T_2^3(s)] = -\frac{9}{2\sqrt{10}}T_1^1(a) - \frac{3}{\sqrt{10}}T_3^3(a)$$

$$[T_1^3(s),\ T_3^3(s)] = \frac{3}{\sqrt{10}}T_2^3(a)$$

$$[T_1^3(s),\ T_3^3(a)] = \frac{3}{\sqrt{10}}T_2^3(s)$$

$$[T_1^3(a),\ T_2^3(s)] = \frac{9}{2\sqrt{10}}T_1^1(s) - \frac{3}{\sqrt{10}}T_3^3(s)$$

$$[T_1^3(a),\ T_2^3(a)] = \frac{9}{2\sqrt{10}}T_1^1(a) - \frac{3}{\sqrt{10}}T_3^3(a)$$

$$[T_1^3(a),\ T_3^3(s)] = -\frac{3}{\sqrt{10}}T_2^3(s)$$

$$[T_1^3(a),\ T_3^3(a)] = -\frac{3}{\sqrt{10}}T_2^3(a)$$

$$[T_2^3(s),\ T_2^3(a)] = -\frac{9}{5}T_o^1 + \frac{3}{\sqrt{10}}T_o^3$$

$$[T_2^3(s),\ T_3^3(s)] = \frac{9\sqrt{3}}{10\sqrt{2}}T_1^1(a) + \frac{3}{\sqrt{10}}T_1^3(a)$$

$$[T_2^3(s),\ T_3^3(a)] = \frac{9\sqrt{3}}{10\sqrt{2}}T_1^1(s) + \frac{3}{\sqrt{10}}T_1^3(s)$$

$$[T_2^3(a),\ T_3^3(s)] = -\frac{9\sqrt{3}}{10\sqrt{2}}T_1^1(s) - \frac{3}{\sqrt{10}}T_1^3(s)$$

$$[T_2^3(a),\ T_3^3(a)] = -\frac{9\sqrt{3}}{10\sqrt{2}}T_1^1(a) - \frac{3}{\sqrt{10}}T_1^3(a)$$

$$[T_3^3(s),\ T_3^3(a)] = \frac{27}{10}T_o^1 + \frac{3}{\sqrt{10}}T_o^3$$

$$[T_1^3(s),\ T_2^3(a)] = -\frac{3}{\sqrt{10}}T_3^3(s) - \frac{9}{2\sqrt{10}}T_1^1(s)$$

Table B.3 Matrix Representation of few Selected Tensor Operators T_q^n (s,a)

$$T_o^2 = 3/2 \quad \begin{bmatrix} 1 & 0 & 0 & 0 \\ 0 & -1 & 0 & 0 \\ 0 & 0 & -1 & 0 \\ 0 & 0 & 0 & 1 \end{bmatrix}$$

$$T_1^1(a) = -1/2 \quad \begin{bmatrix} 0 & \sqrt{3} & 0 & 0 \\ \sqrt{3} & 0 & 2 & 0 \\ 0 & 2 & 0 & \sqrt{3} \\ 0 & 0 & \sqrt{3} & 0 \end{bmatrix}$$

$$T_1^2(s) = \sqrt{3}/2 \quad \begin{bmatrix} 0 & -1 & 0 & 0 \\ 1 & 0 & 0 & 0 \\ 0 & 0 & 0 & 1 \\ 0 & 0 & -1 & 0 \end{bmatrix}$$

$$T_1^3(a) = \frac{3}{2\sqrt{5}} \quad \begin{bmatrix} 0 & -1 & 0 & 0 \\ -1 & 0 & \sqrt{3} & 0 \\ 0 & \sqrt{3} & 0 & -1 \\ 0 & 0 & -1 & 0 \end{bmatrix}$$

$$T_2^2(s) = \sqrt{3}/2 \quad \begin{bmatrix} 0 & 0 & 1 & 0 \\ 0 & 0 & 0 & 1 \\ 1 & 0 & 0 & 0 \\ 0 & 1 & 0 & 0 \end{bmatrix}$$

Table B.3 (contd.)

$$T_2^3(a) = \frac{3}{2\sqrt{2}} \begin{bmatrix} 0 & 0 & 1 & 0 \\ 0 & 0 & 0 & -1 \\ -1 & 0 & 0 & 0 \\ 0 & 1 & 0 & 0 \end{bmatrix}$$

$$T_3^3(a) = -3/2 \begin{bmatrix} 0 & 0 & 0 & 1 \\ 0 & 0 & 0 & 0 \\ 0 & 0 & 0 & 0 \\ 1 & 0 & 0 & 0 \end{bmatrix}$$

References

1. H. A. Buckmaster, Can. J. Phys. 40, 1670 (1962);
H. A. Buckmaster, R. Chatterjee and Y. H. Shing, Phys. Stat. Sol. 13, 9 (1972).

2. G. J. Bowden and W. D. Hutchison, J. Magn. Reson. 67, 403 (1986);
G.J. Bowden and W.D. Hutchison, J. Magn. Reson. 70, 361 (1986);
G.J. Bowden and W.D. Hutchison, J. Magn. Reson. 71, 1 (1987);
G.J. Bowden and W.D. Hutchison, J. Magn. Reson. 72, 61 (1987);
G. J. Bowden, W. D. Hutchison and F. Separovic, J. Magn. Reson. 79, 413 (1988);
G. J. Bowden, J. Khachan and J. P. D. Martin, J. Magn. Reson. 83, 79 (1989).

3. G. J. Bowden, W. D. Hutchison and J. Khachan, J. Magn. Reson. 67, 415 (1986);
W. D. Hutchison, Ph.D. Thesis, University of New South Wales, NSW, Australia (1987).

4.(a) M. E. Rose, 'Elementary Theory of Angular Momentum,' John Wiley and Sons, Inc., New York (1957);

(b) A. R. Edmonds, 'Angular Momentum in Quantum Mechanics,' Princeton University Press, Princeton, New Jersey (1957);

(c) U. Fano and G. Racah, 'Irreducible Tensorial Sets,' Academic Press, New York (1959);

(d) L. C. Biedenharn and J. D. Louck, 'The Racah-Wigner Algebra in Quantum Theory,' Encyclopedia of Mathematics and its

Applications (G. C. Rota, ed.), Vol. 9, Addison-Wesley Publishing Company, Inc., Massachusetts (1981).

5. M. Rotenberg, R. Bivins, N. Metropolis and J. K. Wooten, 'The 3-j and 6-j Symbols,' MIT Press, Cambridge, Massachusetts (1959).

APPENDIX C

IMPORTANCE OF 'INTERACTION FRAMES' IN NQR SPECTROSCOPY

This Appendix explains how an uninteresting interaction can be largely removed by properly introducing the interaction representation.[1] We consider a general case with the complete spin Hamiltonian, $\mathcal{H}$, in the laboratory frame as given by

$$\mathcal{H} = \mathcal{H}_{big} + \mathcal{H}_{small} \qquad .. (C.1)$$

where the 'big' and 'small' suffixes denote the strength of the respective interactions present in the spin system.

$$\frac{d\rho(t)}{dt} = -i[\mathcal{H}, \rho(t)] . \qquad .. (C.2)$$

Generally, the time evolution of the spin system due to the action of the large interaction ($\mathcal{H}_{big}$) is well known and may not give any new information, but investigations on the effects of $\mathcal{H}_{small}$ would produce much structural information about the spin system.[2] So, one is interested in suppressing $\mathcal{H}_{big}$. This can be achieved by the appropriate incorporation of an interaction representation which is defined by $\mathcal{H}_{big}$. Now, the equation of motion is written as

$$\frac{d\tilde{\rho}(t)}{dt} = -i[\tilde{\mathcal{H}}, \tilde{\rho}(t)] \qquad .. (C.3)$$

where the tilde (~) represents the new frame.

$$\tilde{\rho}(t) = U_{big}^{-1}\, \rho(t)\, U_{big} \qquad .. \text{(C.4)}$$

$$\tilde{\mathcal{H}} = U_{big}^{-1}\, \mathcal{H}\, U_{big} \qquad .. \text{(C.5)}$$

$$U_{big} = \exp(-i\, \mathcal{H}_{big}\, t) \qquad .. \text{(C.6)}$$

Eqn. (C.4) can be rearranged as

$$\rho(t) = U_{big}\, \tilde{\rho}(t)\, U_{big}^{-1} \qquad .. \text{(C.7)}$$

This leads to

$$\frac{d\rho(t)}{dt} = \left(\frac{d\, U_{big}}{dt}\right) \tilde{\rho}(t)\, U_{big}^{-1} + U_{big} \left(\frac{d\tilde{\rho}(t)}{dt}\right) U_{big}^{-1} + U_{big}\, \tilde{\rho}(t) \left(\frac{d\, U_{big}^{-1}}{dt}\right) \qquad .. \text{(C.8)}$$

Using Eqn. (C.7), we write

$$\frac{d\rho(t)}{dt} = (-i\, \mathcal{H}_{big})\, \rho(t) + U_{big} \left(\frac{d\tilde{\rho}(t)}{dt}\right) U_{big}^{-1} + \rho(t)\, (i\, \mathcal{H}_{big}) \qquad .. \text{(C.9)}$$

Equating Eqns. (C.2) and (C.9), we get after cancelling out the commutators with $\mathcal{H}_{big}$,

$$-i[\mathcal{H}_{small}, \rho(t)] = U_{big} \left(\frac{d\tilde{\rho}(t)}{dt}\right) U_{big}^{-1} \qquad .. \text{(C.10)}$$

Multiplying Eqn. (C.10) from the left with U_{big}^{-1} and from the right with U_{big} gives

$$-i[\tilde{\mathcal{H}}_{small}, \tilde{\rho}(t)] = \frac{d\tilde{\rho}(t)}{dt} \qquad .. (C.11)$$

It is apparent from this equation that the total spin populations evolve only under the transformed Hamiltonian ($\tilde{\mathcal{H}}_{small}$) in an interaction representation. The effect of $\mathcal{H}_{big}$ has therefore been removed by this procedure. However, it should be remembered that the $\mathcal{H}_{big}$ is partly transferred to the small Hamiltonian. This procedure is widely used in magnetic resonance, for example, QIF[3] in NQR, rotating frame in NMR[2] and toggling frame in AHT.[2] In the present thesis, we have used the idea of QIF and toggling frame in designing composite pulses.

References

1. K. Blum, 'Density Matrix Theory and Applications,' Plenum Press, New York (1981), Chapter 2.
2. U. Haeberlen, 'High Resolution NMR in Solids: Selective Averaging,' Academic Press, New York (1976), Chapter IV.
3. M. Goldman, 'Spin Temperature and Nuclear Magnetic Resonance in Solids,' Clarendon Press, Oxford (1970), Chapter 1.

APPENDIX D

CALCULATION OF THE RESPONSE TO AN ON-RESONANCE RF PULSE IN NQR SPECTROSCOPY

At thermal equilibrium, the spin system is defined by the reduced density matrix $\rho(0)$ (vide Eqn. (I.10)). Effects of applied rf pulses can be analyzed by solving the von Neumann equation.[1] In QIF, during an rf pulse whose time duration is t_w, the spin system evolves only under $\tilde{\mathcal{H}}_{rf}$ ($\because \tilde{\mathcal{H}}_{rf} \gg \tilde{\mathcal{H}}_{int}$). In the absence of rf pulse, only internal interactions are operative in bringing out changes on the state of the spin system. Therefore, at time t, the density matrix $\tilde{\rho}(t)$ in QIF is given by

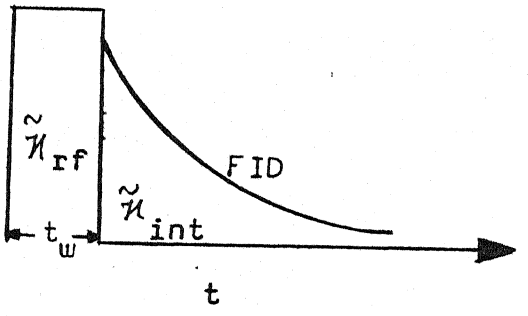

$$\tilde{\rho}(t) = \exp(-i\,\tilde{\mathcal{H}}_{int}t)\ \exp(-i\,\tilde{\mathcal{H}}_{rf}t_w)\ \rho(0)\ \exp(i\,\tilde{\mathcal{H}}_{rf}t_w)\ \exp(i\,\tilde{\mathcal{H}}_{int}t) \qquad .. \text{ (D.1)}$$

This can be explicitly evaluated for different spin values using the nested commutation relationship with an appropriate basis set of traceless independent Hermitian operators. Now, the phase sensitively detected NQR signal (FID) in an experiment can be mathematically expressed by the expectation values of the observable spin angular momentum operator, i.e.,

always out-of-phase NQR signal is detected in an NQR experiment. In the present work, while testing the performance of composite pulses, we have considered only $\tilde{M}_{x90}$ component. Similarly, responses of any kind of rf pulse sequences can be analyzed in NQR spectroscopy.

Reference

1. U. Haeberlen, 'High Resolution NMR in Solids: Selective Averaging,' Academic Press, New York (1976).

APPENDIX E

PHASE ALTERNATED COMPOSITE $\pi/2$ PULSES TO COMPENSATE FOR QUADRUPOLE INTERACTION IN THE CASE OF SPIN I = 1 NMR SPECTROSCOPY

In solid state NMR spectroscopy, spectral lines are generally broad because of the presence of nuclear dipole-dipole (ω_D) and nuclear quadrupole (ω_Q) interactions in the case of spin I = 1 nuclei.[1] In addition to this, the influence of the quadrupole interaction during rf pulses of finite duration and limited power leads to severe distortions in the powder line shape.[2] This problem may be overcome by the application of short length rf pulses with either high rf power or smaller flip angle. Increasing the rf power indefinitely is not possible because of technical problems, affecting the pulse transmitter and rf probe, whereas small flip angles lead to poor signal intensity. Therefore, the task of achieving uniform excitation over the range of line broadening interactions, quadrupole interaction in particular, is difficult using a single rf pulse. To some extent, these distortions have been overcome by replacing single rf pulses with composite pulses.[3] First, Tycko and coworkers[4,5] constructed composite π pulses using the Magnus expansion approximation[6] for broadband population inversion over larger range of ω_Q and ω_D. It should be mentioned here that composite $\pi/2$ pulses are important in quadrupole echo experiments.[8,9] The purpose of using quadrupole

echo technique is to circumvent the dead-time problem associated with single pulse experiments. Furthermore, quadrupole echo technique especially in ^{2}H-NMR, has become a powerful means for probing dynamic processes in polymers[9-13] and biological materials.[13-15] It would therefore be very useful to construct composite $\pi/2$ pulses for achieving quadrupole echo without phase distortions. For this purpose, Siminovitch et al.[16] examined several composite pulses experimentally and they concluded that these sequences also introduce additional distortions with the reduction of finite pulse width effects. Recently, Dongsheng et al.[17] constructed higher-order composite $\pi/2$ pulses for quadrupole echo without phase distortions but only at the expense of increasing the excitation period. These sequences will not be of much use because effects of chemical exchange during composite pulses introduce additional complications in the interpretation and analysis of lineshapes in solid state NMR.[16,18] The purpose of this work is to construct short duration composite $\pi/2$ pulse sequences by the Magnus expansion approach[4] for quadrupole echo without phase distortions in spin I = 1 NMR case. Here the irreducible spherical tensor operators[19] are employed to simplify the derivation of Magnus expansion terms. In the following section, Hamiltonians of different interactions present in the spin system have been given.

Hamiltonian of the System of Spin I = 1 Nuclei

Consider an ensemble of spin I = 1 nuclei in the presence of magnetic field. The total spin system in the rotating frame

of NMR is given by the net Hamiltonian $\mathcal{H}$ as

$$\mathcal{H} = \mathcal{H}_{rf} + \mathcal{H}_D + \mathcal{H}_Q \qquad .. \quad (E.1)$$

where $\mathcal{H}_{rf}$ represents the interaction of rf radiation of strength ω_1 (rad/sec) and phase $\phi(t)$ with the spin system. It can be written as

$$\mathcal{H}_{rf} = \omega_1 [I_x \cos\phi(t) + I_y \sin\phi(t)]. \qquad .. \quad (E.2)$$

Using the tensor operator formalism,[19] $\mathcal{H}_{rf}$ is given by

$$\mathcal{H}_{rf} = -\omega_1 [T_1^1(a) \cos\phi(t) - iT_1^1(s) \sin\phi(t)] \quad .. \quad (E.3)$$

The term $\mathcal{H}_D$ denotes the dipole-dipole interaction, which can be expressed as

$$\mathcal{H}_D = \sum_{i>j} d_{ij} (I_{Zi} I_{Zj} - \frac{1}{3} \vec{I}_i . \vec{I}_j) \qquad .. \quad (E.4)$$

where d_{ij} is the dipole-dipole coupling constant between spins i and j. The quadrupole coupling seen by a given spin can in first order be replaced by its part $\mathcal{H}_Q$ that commutes with the Zeeman Hamiltonian $\mathcal{H}_Z = -\omega_o I_Z$, ω_o is the Larmor frequency.

$$\mathcal{H}_Q = \omega_Q (I_Z^2 - I^2/3) \qquad .. \quad (E.5)$$

where ω_Q is the quadrupole coupling constant and it is expressed as

$$\omega_Q = \frac{e^2 qQ}{4I(2I-1)} \left[\frac{1}{2}(3\cos^2\alpha - 1) + \eta\cos 2\beta \sin^2\alpha\right] \quad .. (E.6)$$

α and β are the spherical polar angles which define the direction of the Zeeman field with respect to the crystal frame. η describes the asymmetry present in the electric field gradient surrounding the quadrupole nuclei. The transformation properties of $\mathcal{H}_Q$ and $\mathcal{H}_D$ are similar to those of the irreducible tensor operator T_o^2 with rank 2 and order zero. Therefore, one of them here (i.e., $\mathcal{H}_Q$) is considered, but the result will be the same for both the cases. In the next section, a brief discussion of the Magnus expansion technique to design composite pulses is given. Detailed procedure of designing composite pulses have been given elsewhere.[4]

Derivation of Zeroth-Order Composite Pulses Using the Magnus Expansion Approach

The net evolution operator in the rotating frame can be given as[4]

$$U(t) = U_{rf}(t)\, U_Q(t) \quad .. (E.7)$$

$$U_Q(t) = T \exp\left[-i \int_o^t \tilde{\mathcal{H}}_Q(t')\, dt'\right] \quad .. (E.8)$$

where T is the Dyson time-ordering operator and $\tilde{\mathcal{H}}_Q(t)$ is the total Hamiltonian in the rf interaction frame[20] which is defined by $U_{rf}(t)$, i.e.,

$$\tilde{\mathcal{H}}_Q(t) = U_{rf}(t)^{-1}\, \mathcal{H}_Q\, U_{rf}(t)$$

Here, only the phase alternating pulse sequences of the type $\bar{\theta}_1\ \theta_2\ \bar{\theta}_3$ are considered which can be implemented in an experiment easily without the need for a sophisticated digital phase shifter. The overbar in our notation indicates that the corresponding rf pulse in 180° phase shifted with respect to other pulses in the sequence. θ_n is the flip angle of an nth rf pulse with time duration t_n as given by $\theta_n = \omega_1 t_n$.

The rf propagator $U_{rf}(t)$ can be written for an n-pulse sequence as

$$U_{rf}(t) = U_{rf_n}\ U_{rf_{n-1}} \cdots\cdots\ U_{rf_2}\ U_{rf_1} \qquad .. \text{(E.10)}$$

$$U_{rf_n} = \exp\left[-iT_1^1(a)\ \cos\phi_n t_n\right] \qquad .. \text{(E.11)}$$

$\tilde{\mathcal{H}}_Q(t)$ can be obtained from the transformation properties of tensor operators under the effect of $U_{rf}(t)$ which are given in the reference 19. The time dependent $\tilde{\mathcal{H}}_Q(t)$ can be written using the Magnus expansion[6] as

$$\tilde{\mathcal{H}}_Q(t) = \mathcal{H}_Q^{(0)} + \mathcal{H}_Q^{(1)} + \mathcal{H}_Q^{(2)} + \ldots \qquad .. \text{(E.12)}$$

where $\mathcal{H}_Q^{(i)}$ is the ith order term in the Magnus expansion. Here, only the zeroth-order term in the Magnus expansion is considered and it is given as,

$$\mathcal{H}_Q^{(0)} = \frac{1}{t}\int_0^t dt'\ \tilde{\mathcal{H}}_Q(t') \qquad .. \text{(E.13)}$$

For a pulse sequence of the type $\bar{\theta}_1\ \theta_2\ \bar{\theta}_3$, one can derive $\mathcal{H}_Q^{(0)}$ to be

$$\mathcal{H}_Q^{(0)} = \frac{\sqrt{2}\omega_Q}{\sqrt{3}\omega_1 t}\left[a\, T_o^2 + ib\, T_1^2(s) + c\, T_2^2(s)\right] \quad .. \text{(E.14)}$$

where

$$a = \frac{3}{4}\left[\frac{(\theta_1+\theta_2+\theta_3)}{3} + \sin 2\theta_1 + \sin(2\theta_2-2\theta_1) + \frac{1}{2}\sin(2\theta_3-2\theta_2+2\theta_1)\right] \quad .. \text{(E.15)}$$

$$b = \frac{\sqrt{3}}{4}\left[1-2\cos 2\theta_1 + 2\cos(2\theta_1-2\theta_2) - \cos(2\theta_1+2\theta_3-2\theta_2)\right] \quad .. \text{(E.16)}$$

and

$$c = \frac{\sqrt{3}}{8}\left[-(\theta_1+\theta_2+\theta_3) + 2\sin 2\theta_1 + 2\sin(2\theta_2-2\theta_1) + \sin(2\theta_1+2\theta_3-2\theta_2)\right] \quad .. \text{(E.17)}$$

According to the Magnus expansion technique[4,5] a zeroth-order composite pulse can be obtained by selecting flip angle values in such a way that the sequence should satisfy the condition $\mathcal{H}_Q^{(0)} = 0$. For this sequence, $U_Q = \mathbb{1}$; thus, one can achieve uniform excitation over larger range of ω_Q. From Eqns. (E.15)-(E.17) one can say that it is not possible to satisfy this condition with a three pulse phase alternated sequence. So, the condition is relaxed to

$$[\mathcal{H}_Q^{(0)}, \rho(0)] = 0 \quad .. \text{(E.18)}$$

where $\rho(0) = \omega_o I_Z$ is the thermal equilibrium density matrix. This condition demands only 'b' given by Eqn. (E.16) to be equal to zero because in $\mathcal{H}_Q^{(0)}$, T_o^2 and $T_2^2(s)$ commute with $\rho(0)$ but $[T_1^2(s), \rho(0)] \neq 0$. A set of zeroth-order composite $\pi/2$ pulses derived with b = 0 and with smaller size 'b' have been summarized in Table E.1 along with the corresponding zeroth-order Magnus

Table E.1 Composite $\pi/2$ Pulses with Their Zeroth-Order Magnus Expansion Terms and Their Bandwidth of Uniform Excitation Over ω_Q or ω_D

Composite pulse	Bandwidth[a]	$\omega_1 t \, \mathcal{H}_Q^{(0)}/\omega_Q$
1. 130 $\overline{80}$ 40	± 1.4	$-0.315\ T_o^2 + 0.707\ iT_1^2(s) - 1.468\ T_2^2(s)$
2. 157.5 $\overline{112.5}$ 45	± 0.8	$0.077\ T_o^2 + 0.207\ iT_1^2(s) - 2.73\ T_2^2(s)$
3. 130 $\overline{40}$	± 0.4	$0.003\ T_o^2 - 0.123\ iT_1^2(s) - 0.873\ T_2^2(s)$
4. $\overline{22.5}$ 112.5	± 0.25	$0.914\ T_o^2 - 0.15iT_1^2(s) - 0.167\ T_2^2(s)$
5. $\overline{60}$ 150	± 0.25	$1.278\ T_o^2 + 0.354\ iT_1^2(s) - 0.342\ T_2^2(s)$
6. $\overline{30}$ 150 $\overline{30}$	± 0.4	$0.748\ T_o^2 - 0.648\ T_2^2(s)$
7. $\overline{11.25}$ 112.5 $\overline{11.25}$	± 0.25	$0.481\ T_o^2 - 0.599\ iT_1^2(s) - 0.417\ T_2^2(s)$

[a] In terms of the dimensionless quadrupole interaction parameter $\Delta\omega_Q/2\omega_1$.

terms. Interestingly, when the duration of individual rf pulses in the sequences given in Table E.1, are doubled, one gets a set of composite π pulse for NQR spectroscopy of spin I = 1 nuclei[21] which compensate for the efg inhomogeneity. It is noteworthy that any pulse sequence involving phase shifts only in multiples of π radians and which generates a broadband population inversion in two-level systems will provide a broadband excitation in the anharmonic three-level system if the pulse duration is halved.[7] Since halving the individual pulse durations in an composite π pulse of spin 1 NQR case leads to a composite $\pi/2$ pulse in spin 1 NMR case, the spin 1 NQR system must be a two-level problem. In the next section the performance of composite $\pi/2$ pulses have been illustrated.

Performance of Composite Pulses

To test the performance of composite $\pi/2$ pulses, the analytical expressions for the amplitude and phase of the quadrupole echo reported by Barbara[22] have been used for a three pulse sequence of the type $\bar{\theta}_1\,\theta_2\bar{\theta}_3$. They can be given as follows:

$$\text{Echo amplitude, } A = (A_1^2 + A_2^2)^{3/2} \qquad \ldots (E.19)$$

$$\text{Phase } \phi = \tan^{-1}(A_2/A_1) \qquad \ldots (E.20)$$

where

$$A_1 = \sin K[\cos\theta_1\cos\theta_2\sin\theta_3 - \cos\theta_3\sin(\theta_2-\theta_1)] - \sin\theta_1\sin\theta_2\sin\theta_3\sin 3K \qquad \ldots (E.21)$$

$$A_2 = \sin 2K \sin\theta_2 \sin(\theta_3 - \theta_1) \quad .. \text{(E.22)}$$

$$K = \tan^{-1}(2\omega_1/\omega_Q) \quad . \quad .. \text{(E.23)}$$

When $\theta_1 = \theta_3$, that is, for a symmetric phase alternating sequence of the form $\bar{\theta}_1\ \theta_2\ \bar{\theta}_1$, $A_2 = 0$ and hence $\phi = 0$, irrespective of the strength of the quadrupole interaction, ω_Q. Hence, symmetric phase alternating composite $\pi/2$ pulses can be used for getting quadrupole echo without phase distortions. The performance of different composite $\pi/2$ pulses has been tested by evaluating the amplitude of quadrupole echo with respect to ω_Q and their bandwidth of uniform excitation is summarized in Table E.1. Admittedly, the degree of compensation of ω_Q by these sequences is not very good. But one can construct symmetric sequences with a larger number of rf pulses so as to enhance the degree of compensation against ω_Q as well as to suppress phase distortions. Some of the composite $\pi/2$ sequences obtained for this purpose from two-level NMR broadband inversion sequences[23] are given in Table E.2.

Summary

Construction of phase alternated composite $\pi/2$ pulses for use in solid state NMR spectroscopy using the Magnus expansion procedure is presented. It is important to note that the application of symmetric phase alternated composite $\pi/2$ pulses gives quadrupole echo with no phase distortions. Furthermore, these sequences behave like single rf pulses with a constant net flip angle of $\pi/2$ radians over larger range of ω_Q. The irreducible

Table E.2 Symmetric Phase Alternating Composite $\pi/2$ Pulses for Compensating Quadrupole Interactions in the case of Spin I = 1 NMR Spectroscopy

1)	171.5	$\overline{140}$	27	$\overline{140}$	171.5					
2)	29	$\overline{70}$	172	$\overline{70}$	29					
3)	162.5	$\overline{131.5}$	28	$\overline{131.5}$	162.5					
4)	$\overline{33}$	90	$\overline{113.5}$	203	$\overline{113.5}$	90	$\overline{33}$			
5)	13.5	$\overline{49.5}$	90	$\overline{105.5}$	193	$\overline{105.5}$	90	$\overline{49.5}$	13.5	
6)	79	$\overline{147}$	72	$\overline{76}$	145.5	$\overline{44.5}$	32	$\overline{44.5}$	145.5	$\overline{76}$
								72	$\overline{147}$	79

spherical tensor operator formalism employed here simplifies the derivation of Magnus expansion terms and hence the design of composite pulses to a greater extent. It has been shown that phase alternating composite $\pi/2$ pulses for a three-level case can be derived from NQR phase alternating composite inversion pulses which combat the effects of efg inhomogeneity in the case of spin I = 1 quadrupolar nuclei. Hence, the design of composite pulses for spin 1 nuclei in NMR and in pure NQR spectroscopies need not to be considered separately.

References

1. A. Abragam, 'Principles of Nuclear Magnetism,' Oxford University Press, Oxford (1961).
2. M. Bloom, J. H. Davis and M. I. Valic, Can. J. Phys. 58, 1510 (1980).
3. M. H. Levitt, Prog. NMR Spectrosc. 18, 61 (1986).
4. R. Tycko, Phys. Rev. Lett. 51, 775 (1983).
5. R. Tycko, E. Schneider and A. Pines, J. Chem. Phys. 81, 680 (1984).
6. W. Magnus, Commun. Pure Appl. Math. 7, 649 (1954).
7. M. H. Levitt, D. Suter and R. R. Ernst, J. Chem. Phys. 80, 3064 (1984).
8. I. Solomon, Phys. Rev. 110, 61 (1958).
9. J. H. Davis, K. R. Jeffrey, M. Bloom, M. I. Valic and T. P. Higgs, Chem. Phys. Lett. 42, 390 (1976).
10. R. Hentschel and H. W. Spiess, J. Magn. Reson. 35, 157 (1979).

11. H. W. Spiess, Colloid. Polym. Sci. 261, 193 (1983).

12. J. Seelig, Q. Rev. Biophys. 10, 353 (1977).

13. R. G. Griffin, Methods Enzymol. 72, 108 (1981).

14. J. H. Davis, Biochim. Biophys. Acta, 737, 117 (1983).

15. D. A. Torchia, Ann. Rev. Biophys. Bioeng. 13, 125 (1984).

16. D. J. Siminovitch, D. P. Raleigh, E. T. Olejniczak and R.G. Griffin, J. Chem. Phys. 84, 2556 (1986).

17. W. Dongsheng, L. Gengying and W. Xuewen, J. Magn. Reson. 74, 464 (1987).

18. T. M. Barbara, M. S. Greenfield, R. L. Vold and R. R. Vold, J. Magn. Reson. 69, 311 (1986).

19. G. J. Bowden and W. D. Hutchison, J. Magn. Reson. 67, 403 (1986).

20. U. Haeberlen, 'High Resolution NMR in Solids : Selective Averaging,' Academic Press, New York (1976).

21. A. Ramamoorthy and P. T. Narasimhan, J. Molec. Struct. 192, 333 (1989).

22. T. M. Barbara, J. Magn. Reson. 67, 491 (1986).

23. A. J. Shaka and A. Pines, J. Magn. Reson. 71, 495 (1987).